

UNIVERSITA' DEGLI STUDI DI NAPOLI FEDERICO II



FACOLTA' DI SCIENZE MATEMATICHE FISICHE E NATURALI

DOTTORATO DI RICERCA IN SCIENZE CHIMICHE XXIV CICLO

2008-2011

DESIGN AND SYNTHESIS OF NEW SELECTIVE  
CHEMOTHERAPEUTIC AGENTS

CONCETTA PAOLELLA

TUTORE: DR ANNALISA GUARAGNA

CO-TUTORE: PROF. GIOVANNI PALUMBO

COORDINATORE: PROF. LUCIO PREVITERA



*Ad Amedeo*

## LIST OF ABBREVIATIONS

A	adenine
ABC	abacavir
Ac	acetyl group
Ac <sub>2</sub> O	acetic anhydride
AcOH	acetic acid
ALA	aminolevulinic acid
ALAS	ALA synthase
ALAD	aminolevulinate dehydratase
ANA	altritol nucleic acid
AZT	3'-azidothymidine
BBB	blood-brain barriers
Bn	benzyl group
BnBr	benzyl bromide
BnOH	Benzyl alcohol
Boc	<i>t</i> -butoxycarbonyl group
BSA	<i>N,N</i> -bis-dimethylsilylacetamide
BuLi	butyllithium
Bz	benzoyl group
BzCl	benzoyl chloride
C	cytosine
CeNA	cyclohexenyl nucleic acid
CH <sub>2</sub> Cl <sub>2</sub>	dichloromethane
CHCl <sub>3</sub>	chloroform
CH <sub>3</sub> CN	acetonitrile
CH <sub>3</sub> OH	methanol
CLB	chloroambucil
CLL	chronic lymphocytic leukemia
CNA	cyclohexyl nucleic acid
CoA	coenzyme A
COSY	correlation spectroscopy

CPO	coproporphyrinogen oxidase
<i>m</i> -CPBA	<i>m</i> -chloroperbenzoic acid
d4T	stavudine
DBU	1,8-diazobicyclo[5.4.0]undec-7-ene
DCC	<i>N,N'</i> -dicyclohexylcarbodiimide
DCU	dicyclohexylurea
DCM	dichloromethane
ddC	2',3'-dideoxycytidine
ddI	2',3'-dideoxyinosine
DDQ	2,3-dichloro-5,6-dicyano-1,4-benzoquinone
DEAD	diethyl azodicarboxylate
DET	diethyl tartrate
DIBAL-H	diisobutylaluminium hydride
DIPA	diisopropylamine
DIPEA	diisopropylethylamine
DMAP	4- <i>N,N</i> -dimethylaminopyridine
DMDO	dimethyldioxirane
DMF	<i>N,N</i> -dimethylformamide
DMSO	dimethyl sulfoxide
DNA	deoxyribonucleic acid
dNTP	2'-deoxynucleoside 5'-triphosphate
dr	diastereomeric ratio
ds	double strand
EC <sub>50</sub>	half maximal effective concentration
EDTA	ethylenediaminetetraacetic acid
<i>ee</i>	enantiomeric excess
EFdA	2'-deoxy-4'-C-ethynyl-2-fluoroadenosine
EPR	enhanced permeability and retention
Et <sub>2</sub> O	diethyl ether
EtOAc	ethyl acetate
FA	folic acid
FDA	food and drug administration
FECH	ferrochelatase

## List of Abbreviations

FR	folate receptor
FTC	5-fluoro- $\beta$ -L-thiocytidine
G	guanine
GPI	glycosylphosphatidylinositol
HBV	hepatitis B virus
HCl	hydrogen chloride
Him	imidazole
HIV	human immunodeficiency virus
HNA	hexitol nucleic acid
HOBT	hydroxybenzotriazole
HMB	hydroxymethylbilane
Homo-DNA	hexopyranosyl-(4'→6') DNA
HP	hematoporphyrin
HPD	hematoporphyrin derivative
I <sub>2</sub>	iodine
iBu	isobutyl
IC <sub>50</sub>	half maximal inhibitory concentration
ISC	inter system crossing
<i>J</i>	coupling constant
KHMDS	potassium hexamethyldisilazide
KOH	potassium hydroxide
LDA	lithium diisopropylamide
LiAlH <sub>4</sub>	lithium aluminum hydride
LiBH <sub>4</sub>	lithium borohydride
Li(MeO) <sub>3</sub> AlH	trimethoxy lithium aluminum hydride
LiH	lithium hydride
MAbs	monoclonal antibodies
MeONa	sodium methoxide
MeOH	methanol
MMT	monomethoxy trityl
MNA	mannitol nucleic acid
Mos	modified oligonucleotides
mRNA	messenger ribonucleic acid

m-THPP	meso-tetra(hydroxyphenyl) porphyrin
Na(AcO) <sub>3</sub> BH	sodium triacetoxymborohydride
NaBH <sub>4</sub>	sodium borohydride
NAs	nucleoside analogues
NaH	sodium hydride
NaOH	sodium hydroxide
NH <sub>3</sub>	ammonia
NH <sub>4</sub> Cl	ammonium chloride
NHS	<i>N</i> -hydroxy succinimide
Ni/Ra	raney Nickel
NMO	4-methylmorpholine <i>N</i> -oxide
NMP	<i>N</i> -methyl-2-pyrrolidone
NMR	nuclear magnetic resonance
NNRTIs	non-nucleosides reverse transcriptase inhibitors
NRTIs	nucleoside reverse transcriptase inhibitors
NtRTIs	nucleotide reverse transcriptase inhibitors
PEG	polyethylene glycol
PBG	porphobilinogen
PBDG	porphobilinogen deaminase
PBR	peripheral-type benzodiazepine receptors
PDT	photodynamic therapy
PPh <sub>3</sub>	triphenylphosphine
PLP	pyridoxal-5-phosphate
PNA	peptide nucleic acid
PpIX	protoporphyrin IX
PPO	protoporphyrinogen oxidase
PS	photosensitizer
PTFE	polytetrafluoroethylene
PTSA	<i>p</i> -toluenesulfonic acid
Py	pyridine
PyBOP	benzotriazol-1-yl-oxytripyrrolidinophosphonium hexafluorophosphate
Red-Al	sodium bis(2-methoxyethoxy)aluminumhydride

## List of Abbreviations

RISC	RNA-induced silencing complex
RNA	ribonucleic acid
RT	reverse transcriptase
SdNs	substituted nucleosides
siRNA	small interfering RNA
T	thymine
TBAF	tetrabutylammonium fluoride
TBDPS	<i>t</i> -butyldiphenylsilyl group
<i>t</i> -BuOOH	tert-butyl hydroperoxide
3TC	$\beta$ -L-thiocytidine
TEA	triethylamine
TFA	trifluoroacetic acid
TFDO	methyl(trifluoromethyl)dioxirane
TfOH	triflic acid
TFV	tenofovir
THF	tetrahydrofuran
Ti( <i>O</i> -Pr) <sup><i>i</i></sup> <sub>4</sub>	titanium tetraisopropoxide
TLC	thin layer chromatography
T <sub>m</sub>	melting temperature
TMSCl	chlorotrimethylsilane
TMSOTf	trimethylsilyl trifluoromethanesulfonate
TPA	12- <i>O</i> -tetradecanoylphorbol-13-acetate
TPP	tetraphenylporphyrin
TS	tumor-specific
TS	talaporfin sodium
TIS	triisopropylsilane
TTM	tumor-targeting module
WC	<i>Watson-Crick</i>
XTT	2,3-bis-(2- methoxy-4- nitro-5-sulfophenyl)-2H-tetrazolium-5-carboxanilide
UHP	hydrogen peroxide urea
UROD	uroporphyrinogen decarboxylase

## TABLE OF CONTENTS

<i>Preface</i> .....	1
<i>Chapter 1</i> .....	3
1.1 <i>Introduction</i> .....	4
1.1.1    Carrier-Linked Prodrug Strategies.....	7
1.1.1.1  Passive Targeting.....	7
1.1.1.2  Active Targeting.....	8
Unit 1: Ligand.....	9
Folic Acid.....	9
Unit 2: Linker.....	12
Unit 3: Cleavable Bond.....	13
Unit 4: Anticancer Agents.....	14
FDA-approved Anticancer Drugs.....	14
1.2 <i>Results and Discussion</i> .....	19
1.2.1    Synthesis of CLB-Delivery System <b>1</b> .....	21
1.2.2    Synthesis of CLB-Delivery System <b>2</b> .....	23
1.2.3    Biological Assays.....	26
1.3 <i>Conclusion</i> .....	35
1.4 <i>Experimental Section</i> .....	36
Chemistry.....	36
Synthetic Procedures and Characterization Data for Intermediates and Conjugates.....	36
Biology.....	44
<i>Chapter 2</i> .....	49
2.1 <i>Introduction</i> .....	50
2.1.1    History of Photodynamic Therapy.....	50
2.1.2    Mechanism of Photodynamic Therapy.....	53
2.1.3    Photosensitizers.....	56
2.1.3.1  First and Second Generation Photosensitizers.....	56
5-Aminolevulinic Acid.....	57
2.1.3.2  Third Generation Photosensitizers.....	62
2.2 <i>Results and Discussion</i> .....	69
2.2.1    Synthesis of FA-5-ALA Conjugates <b>1</b> and <b>2</b> .....	70
2.2.2    Synthesis of Conjugate 3.....	73
2.3 <i>Conclusion</i> .....	77
2.4 <i>Experimental Section</i> .....	78

2.4.1	Solution-Phase Synthesis .....	78
2.4.2	Solid-Phase Synthesis .....	82
Chapter 3.....		85
3.1	<i>Introduction</i> .....	86
3.1.1	Anti-HIV Chemotherapy.....	87
3.1.1.1	Nucleoside Reverse Transcriptase Inhibitors.....	88
3.1.1.2	Antiviral and Antitumor Nucleosides .....	89
3.1.2	HIV Drug Resistance .....	90
3.1.2.1	4'-Substituted Nucleoside Analogues .....	91
3.2.	<i>Results and Discussion</i> .....	98
3.2.1	Synthesis of 2,3-Dihydro-1,4-Dithiaryl Nucleosides.....	98
3.2.1.1	Conclusion .....	105
3.2.1.2	Experimental Section.....	106
3.2.2	Synthesis of 2',3'-Didehydro-2',3'-Dideoxy-4'-Methoxy Nucleosides.....	110
3.2.2.1	Conclusion .....	119
3.2.2.2	Experimental Section.....	120
Chapter 4.....		127
4.1	<i>Introduction</i> .....	128
4.1.1	Features of Synthetic Oligonucleotides. ....	129
4.1.2	Stability <i>in vivo</i> of Synthetic Oligonucleotides: Sugar-Modified Nucleic Acids....	130
4.1.3	The Critical Role of Sugar Conformation in the Therapeutic Potential of Oligonucleotide Analogues.....	134
4.1.4	Six-Membered Nucleic Acids .....	135
4.2	<i>Results and Discussion</i> .....	143
4.2.1	Synthesis of Nucleoside Units. ....	144
	Synthesis of (2 <i>R</i> )-2-(Hydroxymethyl) Cyclohexan-1-one ( <b>17</b> ) .....	144
	Synthesis of (2 <i>R</i> )-2-(Benzyloxymethyl) Cyclohexan-1-one ( <b>6</b> ) .....	146
	Synthesis of (6 <i>R</i> )-6-(Benzyloxymethyl)-2-Cyclohexen-1-one ( <b>20</b> ) .....	146
	Synthesis of (1 <i>aS</i> , 2 <i>R</i> , 3 <i>R</i> , 5 <i>aS</i> )-2-Hydroxy-3-(Benzyloxymethyl) Perhydro-1- Benzoxirene [ <i>syn</i> -( <i>anti</i> - <b>5</b> )] .....	147
	Synthesis of Carbocyclic Nucleoside Analogues <b>1</b> and <b>2</b> .....	149
4.2.2	Oligonucleotide Synthesis.....	151
4.3	<i>Conclusion</i> .....	153
4.4	<i>Experimental Section</i> .....	154

## PREFACE

The chemotherapy, a branch of pharmacology that develops drugs for therapeutic purposes can be divided into antiviral and antitumor chemotherapy. In both case the primary requirement for a chemotherapeutic agent must be the selectivity for the diseased cells in order to preserving healthy ones, so preventing the occurrence of possible side effects.

Inspired by postulate of Paul Ehrlich, the pioneer of selective chemotherapy, which is based on the creation of a ‘magic bullets’ to be used in the fight against human diseases, scientists have pointed a lot of attention on the development of powerful molecular therapeutics. In particular, in the antitumor chemotherapy field, current efforts are devoted to the construction of new and efficient targeted-drug delivery systems which allow a controlled drug release once reached cancerous tissue. This approach has been realized thanks to the use of controlled release carriers which include liposomes, monoclonal antibody, drug loaded biodegradable microspheres and drug polymer conjugates.

On the other side, the antiviral chemotherapy has take advantage of the advent of gene silencing strategies based on the development of synthetic MOs that promise to achieve the specificity and efficacy that Ehrlich thought. This strategies for regulating the expression of a gene results completely selective, and of universal applicability, compared to traditional therapies. Strong motivations for this research have been the promising results obtained with antisense, antigene, aptamer, and, in more recent times, RNAi and miRNA strategies.



The background features a white page with abstract pink graphics. Three circles of varying sizes are arranged vertically, each composed of concentric rings of different shades of pink. Two thin pink lines intersect at the top left and extend diagonally across the page, framing the circles. The text is positioned on the left side of the page.

# **Synthesis and Evaluation of Folate- based Chlorambucil Delivery Systems for Tumor-Targeted Chemotherapy**

*CHAPTER 1*

## 1.1 INTRODUCTION

With the exception of coronary and heart diseases, cancer remains the major cause of death in the Western world. Despite the significant progress in the development of cancer detection, prevention, surgery, and therapy, there is still no efficient cure for patients with malignant diseases. The greater part of clinically approved anticancer drugs are characterized by a narrow therapeutic window that results mainly from a high systemic toxicity of the drugs in combination with an evident lack of tumor selectivity causing undesirable severe side effects, such as hair loss and damage to the liver, kidney, and bone marrow.

One strategy aimed at providing substantial increases in the clinical efficacy of such drugs, is the development of relatively non-toxic prodrug forms of these cytotoxins that can be selectively activated in tumor tissue. The term prodrug was first introduced in 1958 by Adrien Albert<sup>1</sup> to describe compounds that undergo biotransformation prior to eliciting their pharmacological effects. In accordance with this definition, prodrugs are derivatives of drugs that are metabolized or activated after administration in the body to release or generate the pharmacologically active species; if possible at the site of action. They could be designed to overcome pharmaceutical, pharmacokinetic, or pharmacodynamic barriers such as insufficient chemical stability, poor solubility, unacceptable taste or odor, irritation or pain, insufficient oral absorption, inadequate blood-brain barrier permeability, marked presystemic metabolism, and toxicity.<sup>2</sup>

Inadequate aqueous solubility is an important factor limiting parenteral, percutaneous, and oral bioavailability of common drugs. In such cases, a prodrug strategy may bring great pharmaceutical and pharmacokinetic benefit. Charged promoieties (esters: phosphates, hemisuccinates, aminoacyl conjugates, dimethylamino acetates) and neutral promoieties (poly(ethylene glycol)s, PEG) can be used. Some examples of this prodrugs are reported in **Figure 1** such as Fosphenytoin,<sup>3</sup> a hydrophilic phosphate prodrug of the anticonvulsant phenytoin which is rapidly hydrolyzed by phosphatases. Another example is Parecoxib Sodium, a water soluble and injectable prodrug of Valdecoxib that is a selective inhibitor COX-2 (enzyme responsible for inflammation or pain). It can be used when patients are unable to take oral drug.

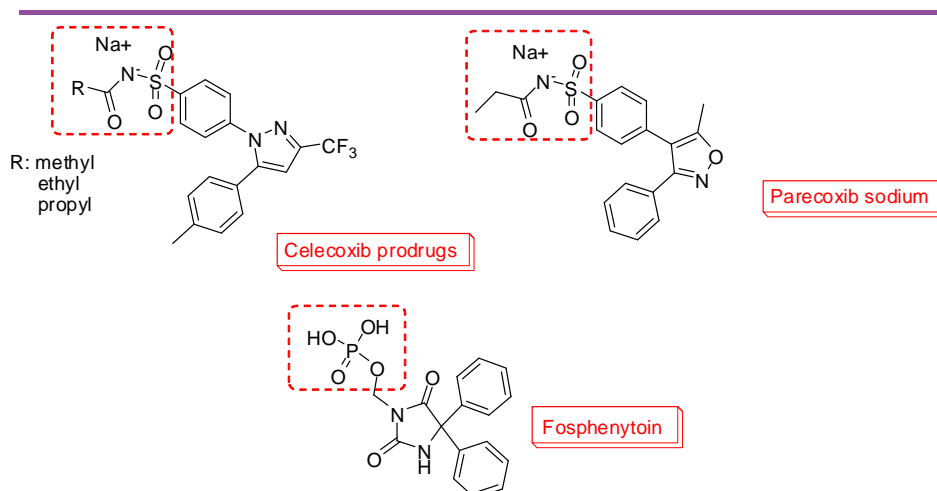


**Figure 1.** Examples of prodrug designed to improve aqueous solubility.

A classic and clinically successful example of such a prodrug is *N*4-pentyloxycarbonyl-5'-deoxy-5-fluorocytidine (**Figure 2**), more commonly known as Capecitabine or Xeloda, a cytotoxic agent orally administered and preferentially activated in tumor cells. This carbamate of fluoropyrimidine was synthesized<sup>4</sup> in the 1990s as an oral formulation designed to circumvent the unacceptable toxicity of 5'-deoxy-5-fluorouridine. The main limitation of the latter derives from its gastrointestinal toxicity, attributed to liberation of 5-fluoruracil in the small intestine under the action of thymidine phosphorylase, a tumor-associated angiogenesis factor. Capecitabine was thus designed to be not metabolized by thymidine phosphorylase; indeed, after oral administration, it crosses the gastrointestinal barrier intact and is rapidly and almost completely absorbed. It is subsequently converted into 5-fluoruracil in a three-step process involving several enzymes (**Figure 2**). In theory, this prodrug of 5-fluoruracil should have two main advantages, which may translate into an improved therapeutic index. First, it should increase the concentration of the active principle at the tumor site, and so, should have greater activity; second, it should decrease the concentration of drug in healthy tissues with a consequent reduction in systemic toxicity.

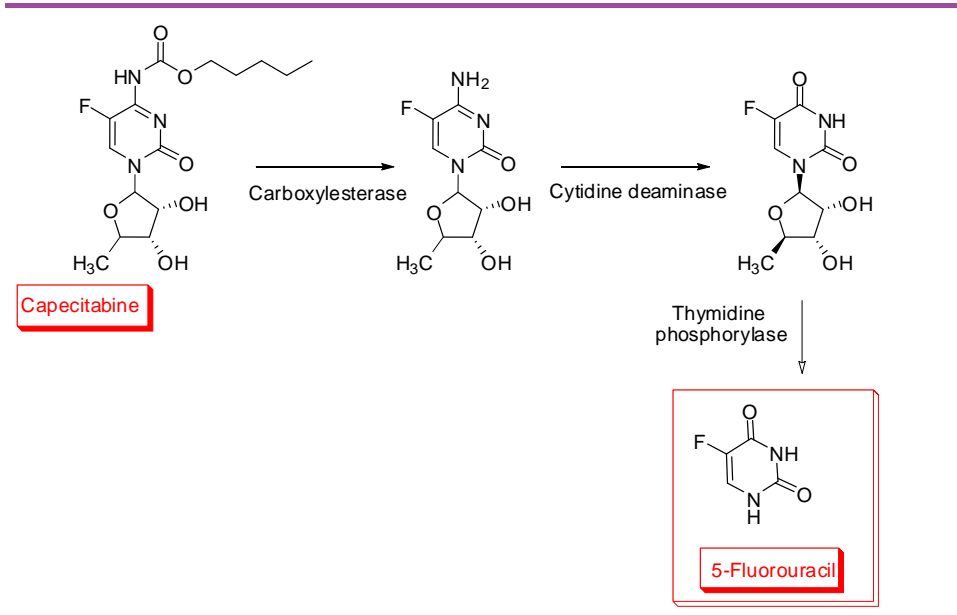


**Figure 2.** Structure of a Capecitabine prodrug converted by three enzymes to 5-fluorouracil.

Another well-known example of an enzyme-activated prodrug is L-Dopa. This agent is a precursor of the dopamine neurotransmitter and so has been the mainstay of Parkinson's disease therapy since its discovery in the early 1960s. It has the usefulness to cross the protective blood-brain barriers (BBB) by amino acid transporters, whereas dopamine itself cannot. After brain entry, L-Dopa is decarboxylated by aromatic L-amino acid decarboxylase to dopamine (**Figure 3**), which can act locally, being no longer a substrate for neutral amino acid transporter.<sup>5</sup>

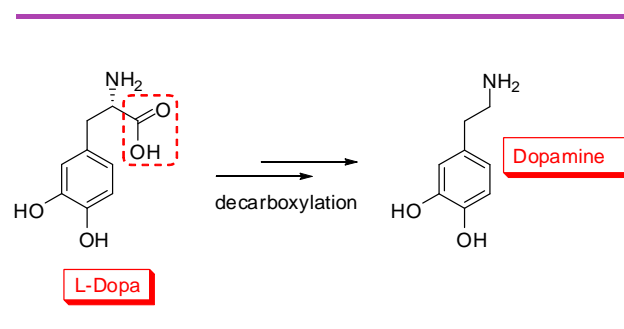


**Figure 3.** L-Dopa: example of prodrug targeting the brain.

### 1.1.1 CARRIER-LINKED PRODRUG STRATEGIES

One approach that has now been validated by clinical success aimed at improving selectivity of anticancer agents is currently being pursued:<sup>6</sup> it is mostly based on the subtle biochemical differences discriminating healthy from malignant cells. This approach involved the conjugation of the drug to tumor-specific ligands, and was called “magic bullet” by pioneer of chemotherapy Paul Ehrlich on 1900.<sup>7</sup>

Carrier-linked prodrug strategy is based on passive or active targeting. Differences in the biochemical and physiological characteristics of healthy and malignant tissue are responsible for the passive tumor accumulation of macromolecules. Active targeting relies on the interaction of the carrier-linked prodrug with a tumor-associated cell surface marker such as a receptor or antigen.

#### 1.1.1.1 PASSIVE TARGETING

Passive targeting exploits anomalies of malignant tissue at vasculolymphatic level that result from the tumor’s pathophysiology. Indeed, it’s know that at a size of 2–3 mm, tumor cell clusters induce angiogenesis to satisfy their increasing demands for nutrition and oxygen. During this process newly formed blood vessels often greatly differ from those of normal tissue. Neovasculature generated by the tumor is characterized by an irregular shape and dilated, leaky or defective vessels. The endothelial cells are poorly aligned or disorganized with large fenestrations. Other differences affect the perivascular cells, the basement membrane, and the smooth-muscle layer which are frequently absent or abnormal. These anatomical features make the vasculature of tumor tissue permeable to macromolecules or even larger nanometer-scale particles, whereas in the blood vessels of healthy tissue only small molecules can pass the endothelial barrier. Furthermore, whereas smaller molecules were shown to be rapidly cleared from the tumor interstitium, large molecules are retained, thus showing high intratumor concentrations even after 100h post-application. This enhanced retention of macromolecules in tumor tissue is primarily caused by a lack of lymphatic drainage due to an impaired or absent lymphatic system. Hence, it is the combination of both

enhanced permeability and retention (EPR)<sup>6</sup> that is responsible for the accumulation of macromolecules in solid tumors, as illustrated in **Figure 5**.

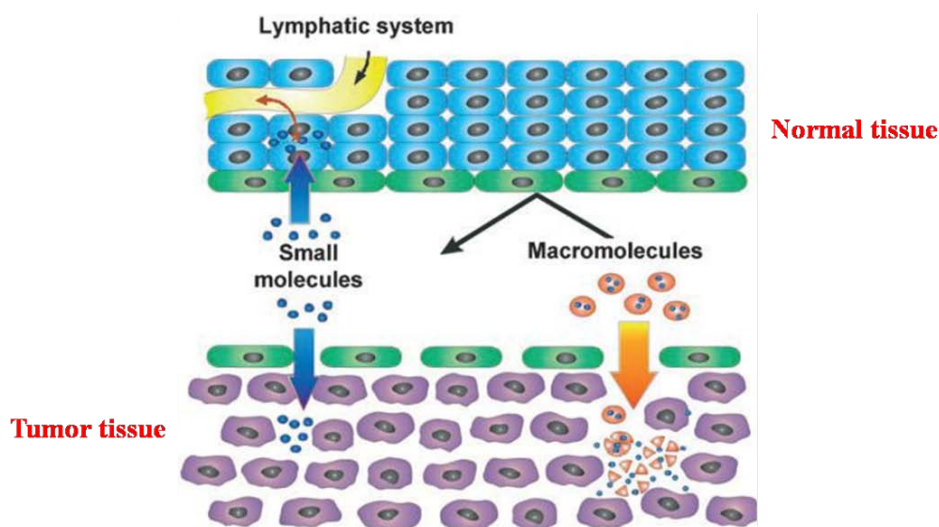


**Figure 5.** Representation of the anatomical and physiological characteristics of normal and tumor tissue and EPR effect.<sup>i</sup>

Thus, an accumulation of drugs in tumor tissue is simply achieved by employing large molecules (synthetic or biopolymers) or nanoparticles (liposomes, nanospheres)<sup>8</sup> as inert carriers that do not necessarily interact with tumor cells but strongly influence the drug's biodistribution.

Appropriate carrier molecule has to fulfill following requirements: it should be sufficiently water soluble, nontoxic, nonimmunogenic and should ideally be biodegradable and have low polydispersity.

### 1.1.1.2 ACTIVE TARGETING

Active targeting is based on differences in cell surface antigen or receptor expression between normal and cancer tissue. The aim of active targeting is to develop drug conjugates with tumor-specific ligands that interact specifically with their cellular target. Among such approaches, so called “guided molecular missiles” or “molecular Trojan horses” have been widely and successfully reported over the last years.<sup>9,10</sup> A

<sup>i</sup>Figure adapted from “Prodrug Strategies in Anticancer Chemotherapy”, *ChemMedChem* **2008**, 3, 20–53.

typical structure of a tumor-targeting drug-delivery system is characterized by four modules as shown in **Figure 6**:<sup>11</sup>

- ✚ a ligand capable of detecting cancer cells
- ✚ a linker that functions as a spacer and helps to improve the pharmacokinetics and pharmacodynamics of antitumor agent resulting
- ✚ a cleavable bond, located between the spacer and the drug that would allow the release of the latter
- ✚ an antitumor agent.

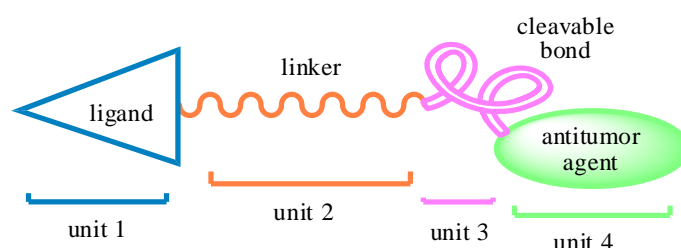


**Figure 6.** Typical structure of antitumor *carrier-linked prodrug*.

## UNIT 1: LIGAND

A rapidly growing tumor requires various nutrients and vitamins. Thus, tumor cells overexpress many tumor-specific receptors, which can be used as targets to deliver cytotoxic agents into tumors.

Ligands that have been exploited for this approach to tumor targeting include monoclonal antibodies and low molecular weight receptor-binding molecules such as peptide hormones, receptor antagonists and agonists, oligosaccharides, oligopeptides, and vitamins. (vitamin B12,<sup>12</sup> biotin<sup>13</sup> and riboflavin<sup>14</sup>). Moreover, it has long been recognized that folate receptors (FRs) are excellent biomarkers to this end.<sup>15</sup>

## FOLIC ACID

Folic acid is an important member of water-soluble B-group vitamins functioning as co-factors in one-carbon transfer reactions including *de novo* biosynthesis of nucleotides and plays a key role in metabolic processes involved in DNA and RNA synthesis,

epigenetic processes, cellular proliferation and survival. The human membrane FR has three main isoforms, namely FR- $\alpha$ , FR- $\beta$  and FR- $\gamma$ . These receptors belong to a special class of glycopolypeptides of apparent Mr in the range of 38-45 kDa and are attached to the plasma membrane by a GPI anchor. FRs are expressed in a limited number of normal tissues but are overexpressed in a large number of epithelial malignancies.

Since folic acid enters cells by receptor-mediated endocytosis (**Figure 7**), a striking consequence is that those FRs expressed by cancer cells can be exploited to selectively convey specific anticancer drugs.

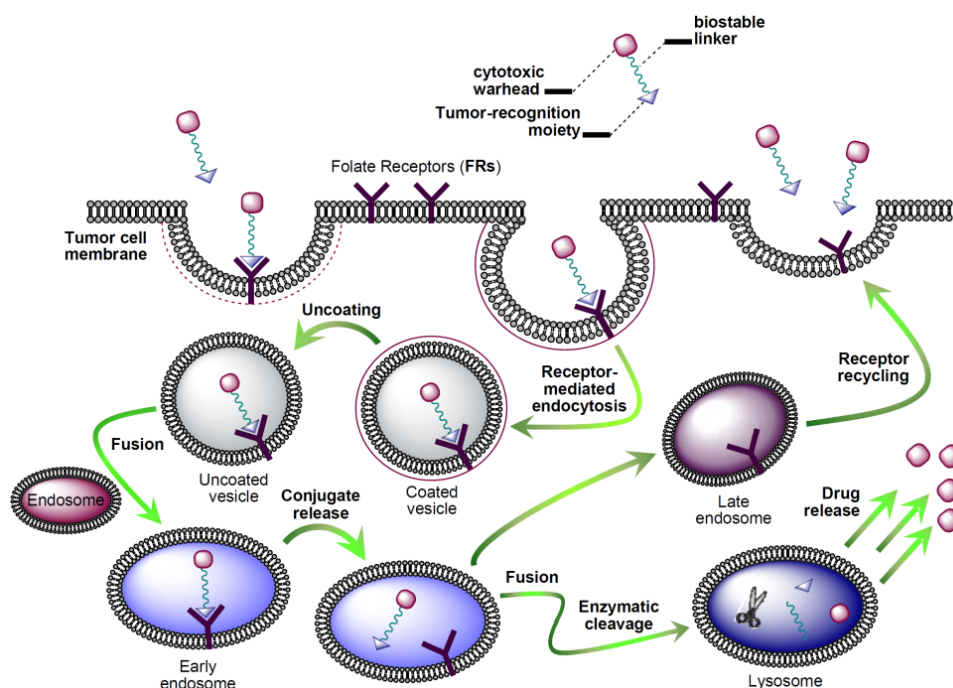


**Figure 7.** FR-mediated endocytosis of a folic acid drug conjugate.

Tumor-targeting folic acid conjugates, covalently linked via folate's  $\gamma$ -carboxyl moiety, maintain a high affinity for the FRs,<sup>16</sup> and the mechanism of cellular uptake of folic acid conjugates by FRs is as effective as that displayed by folic acid in its free form.<sup>17</sup> Despite their molecular complexity, folic acid conjugates can still enter cells by FR-mediated endocytosis<sup>18</sup> and move through many organelles supplying transported materials to cell cytoplasm. The drug is then released in the endosomes/lysosomes mainly by enzymatic cleavage or owing to the acidic environment occurring in lysosomes. The uptake process can be reiterated because of the recycling of the unligated FR back to the cell surface, allowing continuous supplies of folate-linked

drugs into the cell<sup>19</sup> (**Figure 7**). Folate as a targeting ligand offers many potential advantages over macromolecules such as monoclonal antibodies; these include:

- ✦ small size ( $M$  441.4) of the targeting ligand, which often leads to favorable pharmacokinetic properties of the folate conjugates and reduced probability of immunogenicity thus allowing for repeated administration;
- ✦ convenient availability and low cost;
- ✦ relatively simple and defined conjugation chemistry;
- ✦ high binding affinity for the FRs ( $K_D \sim 0.1$ - $1.0$  nmol/L) even after conjugation to its therapeutic/diagnostic cargo;
- ✦ the receptor/ligand complex can be induced to internalize via endocytosis, which may facilitate the cytosolic delivery of therapeutic agents;
- ✦ high frequency of overexpression among human tumors thus a wide range of tumor targets.

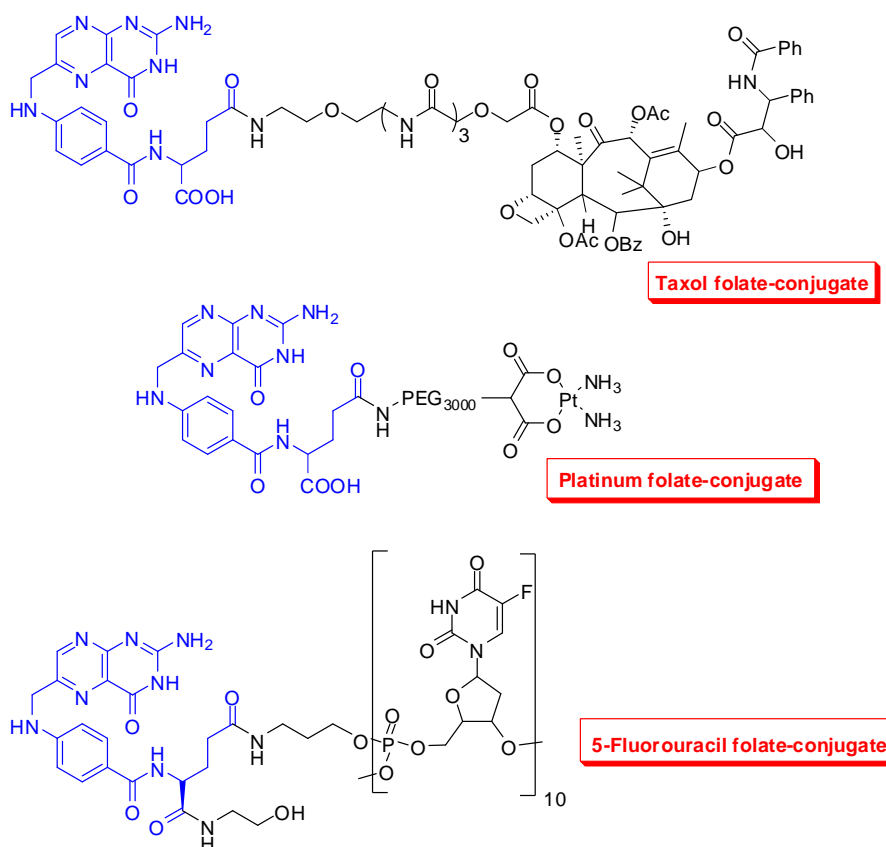


**Figure 8.** Examples of drug folate-conjugates.

The conjugation of folic acid with various anticancer agents, such as taxol<sup>20</sup>, platinum compounds<sup>21</sup> or fluorouracil,<sup>22</sup> has been the subject of recent researches; some examples

were reported in **Figure 8**. Preliminary experimental studies in animal models confirmed the regression of tumor<sup>23</sup>.

## UNIT 2: LINKER

Direct conjugation of the drug to folic acid has been observed to affect the affinity of resultant derivative. Experimental data reported in the literature<sup>24</sup> have shown that for folate conjugates, the linker (unit 2), which allows to anchor the drug to the ligand, plays an important role. For this purpose the use of polymeric linker is often frequent in this type of prodrugs. However, it is unknown the requested length of the linker able to determine an effective recognition of these molecular systems by receptor. The choice of macromolecular systems working as spacer units is also dictated by the fact that these compounds are not efficiently eliminated by the kidneys, thus showing a better retention of prolonged half-life in plasma. Although the permeability of a molecule depends on several factors as size, shape, charge and deformability of the molecule,<sup>24</sup> a general rule that can be applied to most of the macromolecular carrier, provides that: neutral or negatively charged molecules with weight greater than 40 kDa are able to avoid renal clearance.<sup>25</sup> Oligomeric or polymeric spacers with these prerequisites are already widely used in prodrug formation, mainly as carriers. **Table 1** shows an overview of various synthetic polymers used for this purpose. Usually, an ideal carrier must meet following requirements:

- ✚ to be non-toxic or immunogenic,
- ✚ to possess good biodegradability and low polydispersity,
- ✚ to be sufficiently soluble to be administered.

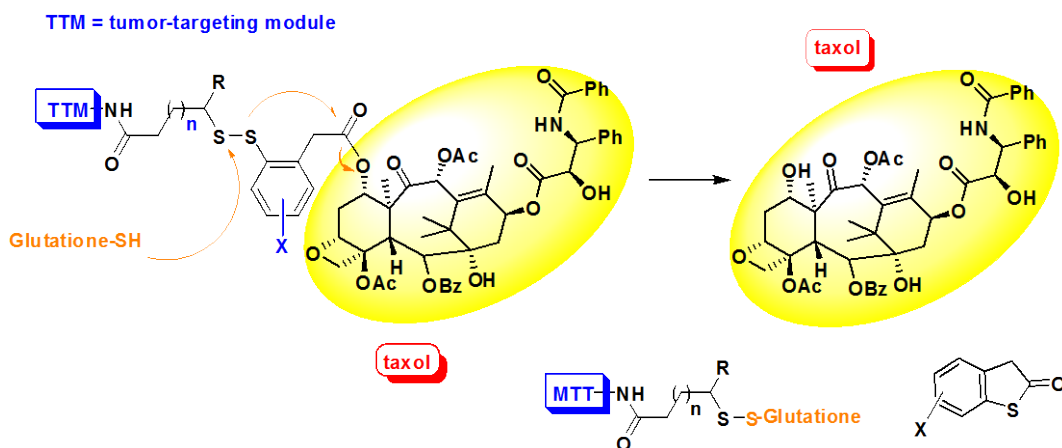
Polyether and peptide spacers meet these requirements and indeed are frequently used as a polymeric carriers.<sup>26</sup>

Name	Structure
polyethylene glycol (PEG)	
methoxypolyethylene glycol (mPEG)	
polyglutamic acid (PG)	
copolymer of <i>N</i> -(2-hydroxypropyl) methacrylamide (HPMA).	
Dextran	

**Table 1.** Some synthetic polymers used in prodrug strategies.

### UNIT 3: CLEAVABLE BOND

Following endocytosis of the drug in the cell membrane the next phase involves the release of the drug in its active form, due to some intracellular event so that it can effectively exhibit its antitumor activity. The release is usually performed by inserting a cleavable bond between the drug and the carrier. The concept of “programming” molecular separation to occur between the ligand and the “drug” is not new. In fact, this process occurs naturally with many bacterial, plant and fungal protein toxins that bind to receptors on target cells through specialized domains. For many toxins (ricin, diphtheria toxin) this bond consists of a disulfide one. Linkers containing disulfide bonds are common in carrier-linked prodrug systems due to their stability in blood circulation; moreover they are efficiently cleaved by glutathione-S-transferase enzyme, particularly overexpressed in tumor cells allowing the release of the active therapeutic agent.<sup>27</sup> As an example, an efficacious tumor-targeting drug conjugate is reported in **Scheme 1**, which exhibited extremely promising results in human cancer xenografts in SCID mice. The glutathione-triggered cascade drug release takes place to generate the free anticancer agent, taxol via thiolactone formation and ester bond cleavage.



**Scheme 1.** Release of drug by glutathione.

However, cellular environment of tumors offers a wide choice of intervention as it is characterized by a lot of specific enzymes and intense lysosomal activity. To this regard it was found a more high content of specific lysosomal glycosidases such as  $\beta$ -galactosidase,  $\beta$ -glucuronidase and  $\beta$ -*N*-acetylglucosaminidase, specific esterase, reductase inhibitors and protease inhibitors, than in healthy cells.<sup>28</sup>

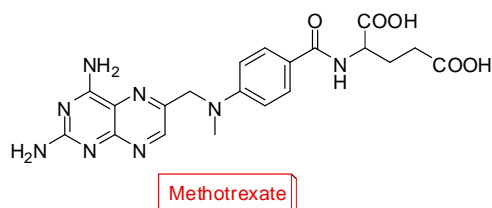
## UNIT 4: ANTICANCER AGENTS

The available anticancer drugs have distinct mechanisms of action which can differentiate in their effects on different normal and cancer cells types. There are about 50 drugs approved by the Food and Drug Administration; some examples are following reported.

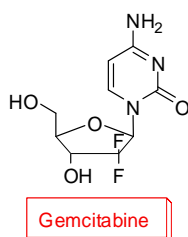
### FDA-APPROVED ANTICANCER DRUGS

**Methotrexate**<sup>29</sup> is used as maintenance therapy for childhood acute lymphoblastic leukemia, where it can be given intrathecally for central nervous system prophylaxis. It is also useful in choriocarcinoma, non-Hodgkin's lymphoma, and a number of solid tumors. Methotrexate competitively inhibits dihydrofolate reductase which is responsible for the conversion of folic acid to tetrahydrofolic acid. At two stages in the biosynthesis of purines and at one stage in the synthesis of pyrimidines, one-carbon

transfer reactions occur which require specific coenzymes synthesized in the cell from tetrahydrofolic acid. Methotrexate acts specifically during DNA and RNA synthesis, and thus it is cytotoxic during the S-phase of the cell cycle. Logically, it therefore has a greater toxic effect on rapidly dividing cells (such as malignant and myeloid cells, and gastrointestinal and oral mucosa), which replicate their DNA more frequently, and thus inhibits the growth and proliferation of these noncancerous cells.



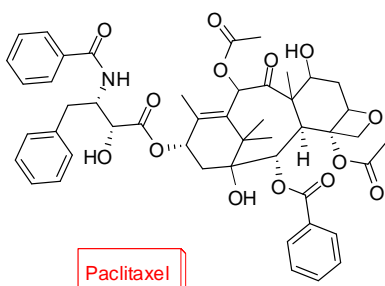
**Gemcitabine**<sup>30</sup> (Gemzar) is a pyrimidine nucleoside analogue. In comprehensive preclinical and clinical studies, it has shown activity against a wide spectrum of human solid tumors including non small cell lung, pancreatic, colon, breast, bladder, ovarian, head and neck, cervical and hepatocellular tumours. It exerts its antiproliferative activity via multiple mechanisms of action. Gemcitabine is phosphorylated intracellularly by deoxycytidine kinase and subsequently by nucleotide kinases to its active metabolites, diphosphate and triphosphate gemcitabine. The triphosphate is then incorporated into DNA, blocking DNA synthesis and inducing apoptosis.



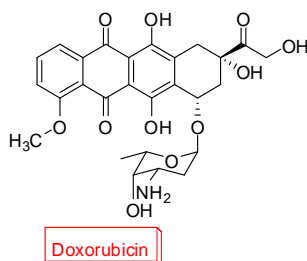
**Paclitaxel**<sup>31</sup> (Taxol) is a highly complex tetracyclic diterpene found in the needles and bark of *Taxus brevifolia*, the Pacific yew tree. The cytotoxic nature of extracts of *Taxus brevifolia* was first demonstrated in 1964 through a screening program coordinated by the National Cancer Institute; pure paclitaxel was isolated in 1966 and its structure published in 1971. Together with docetaxel, it forms the drug category of the taxanes.

Taxol is now used to treat patients with lung, ovarian, breast cancer, head and neck cancer, advanced forms of Kaposi's sarcoma and for the prevention of restenosis.

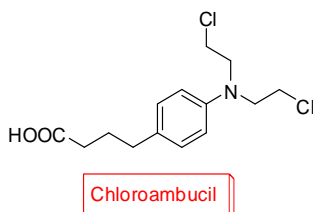
Paclitaxel is a mitotic inhibitor, it stabilizes microtubules and as a result, interferes with the normal breakdown of microtubules during cell division.



**Doxorubicin**<sup>32</sup> (Adriamycin) is a type of anthracycline antibiotic, made from the bacterium *Streptomyces*. Adriamycin can be used to treat early-stage or node-positive breast cancer, HER2-positive breast cancer, and metastatic disease. It is sometimes combined with cytoxan and 5-fluorouracil to make a cocktail of breast-cancer fighting chemotherapy drugs.



**Chloroambucil**<sup>32</sup> (Leukeran) is a bifunctional alkylating chemotherapeutic agent of the mustards type, clinically used for the treatment of chronic lymphatic leukemia, lymphomas, and advanced ovarian and breast carcinomas. Like all alkylating agents, CLB toxicity stands on its oxidative stress-inducing properties that are exerted equally toward healthy and cancer tissues.



- 
- <sup>1</sup> Albert, A. *Nature* **1958**, *182*, 421-422
- <sup>2</sup> Ettmayer, P.; Amidon, G. L.; Clement, B.; Testa, B. *J. Med. Chem.* **2004**, *47*, 2393-2404
- <sup>3</sup> Gerber, N.; Mays, D. C.; Donn, K. H.; Laddu, A.; Guthrie, R. M.; Turlapaty, P.; Quon, C.Y. *J. Clin. Pharmacol.* **1988**, *28*, 1023-1032.
- <sup>4</sup> Arazaki, M.; Ishitsuka, H.; Kuruma, I.; Miwa, M.; Murasaki, C.; Shimma, N.; Umeda, I. *Eur. Patent Appl.*, **1992**, n° 92121538.0.
- <sup>5</sup> Anderson B.D. *Adv. Drug. Deliv. Rev.* 1996, *19*, 171-202
- <sup>6</sup> Kratz, F.; Müller, I.A.; Ryppa, C.; Warnecke, A. *Chem.Med.Chem.* **2008**, *3*, 20–53.
- <sup>7</sup> Ehrlich, P. *Angew. Chem.* **1910**, *23*, 2-8.
- <sup>8</sup> Matsumura, Y.; Maeda, H. *Cancer Res.* **1986**, *46*, 6387-6392.
- <sup>9</sup> a) Jaracz, S.; Chen, J.; Kuznetsova, L.V.; Ojima, I. *Bioorg. Med. Chem.* **2005**, *13*, 5043–5054; b) Allen, T. M. *Nat. Rev. Cancer* **2002**, *2*, 750–763.
- <sup>10</sup> Chari, R. V. J. *Adv. Drug Delivery Rev.* **1998**, *31*, 89–104.
- <sup>11</sup> Leamon, C.P.; Reddy, J.A. *Adv. Drug Delivery Rev.* **2004**, *56*, 1127-1141
- <sup>12</sup> a) Gupta, Y., Kohli D.V.; Jain, S.K. *Crit. Rev. Ther. Drug Carrier Syst.* **2008**, *25*, 347-379; b) Waibel, R.; Treichler, H.; Schaefer, N.G.; van Staveren, D.R.; Mundwiler, S.; Kunze, S.; Küenzi, M.; Alberto, R.; Nüesch, J.; Knuth, A.; Moch, H.; Schibli, R.; Schubiger, P.A. *Cancer Res.* **2008**, *68*, 2904-2911.
- <sup>13</sup> a) Ojima, I. *Acc. Chem. Res.* **2008**, *41*, 108-119; b) Chen, S.; Zhao, X.; Chen, J.; Chen, J.; Kuznetsova, L.; Wong, S.S.; Ojima, I. *Bioconjugate Chem.* **2010**, *21*, 979–987; c) Yang, W.; Cheng, Y.; Xu, T.; Wang, X.; Wen, L.P. *Eur. J. Med. Chem.* **2009**, *44*, 862–868; d) Chen, J.; Chen, S.; Zhao, X.; Kuznetsova, L.V.; Wong, S.S.; Ojima, I. *J. Am. Chem. Soc.* **2008**, *130*, 16778-16785.
- <sup>14</sup> a) Bareford, L.M.; Swaan, P. W. *Adv. Drug Deliv. Rev.* **2007**, *59*, 748-758; b) Foraker, A.B.; Khantwal, C.M.; Swaan, P.W. *Adv. Drug Delivery Rev.* **2003**, *55*, 1467-1483.
- <sup>15</sup> a) Xia, W.; Low, P.S. *J. Med. Chem.* **2010**, *53*, 6811–6824; b) Low, P.S.; Henne, W. A.; Doorneweerd, D. D. *Acc. Chem. Res.* **2008**, *41*, 120–129; c) Low, P.S.; Kularatne, S. A. *Curr. Opin. Chem. Biol.* **2009**, *13*, 256-262; d) Hilgenbrink, A.R.; Low, P.S. *J. Pharm. Sci.* **2005**, *94*, 2135–2146.

- 
- <sup>16</sup> Lee, J.W.; Lu, J.Y.; Low, P.S.; Fuchs, P.L. *Bioorg. Med. Chem.* **2002**, *10*, 2397-2414.
- <sup>17</sup> Wang, S.; Low, P.S. *J. Control. Release* **1998**, *53*, 39-48.
- <sup>18</sup> Leamon C.P.; Low, P.S. *Proc. Natl. Acad. Sci. U.S.A.* **1991**, *88*, 5572-5576.
- <sup>19</sup> Parker, N.; Turk, M.J.; Westrick, E.; Lewis, J.D.; Low, P.S.; Leamon, C.P. *Anal. Biochem.* **2005**, *338*, 284-293.
- <sup>20</sup> Lee, J.W.; Lu, J.Y.; Low, P.S.; Fuchs, P.L. *Bioorg. Med. Chem.* **2002**, *10*, 2397-2414.
- <sup>21</sup> Aronov, O.; Horowitz, A.T.; Gabizon, A.; Gibson, D. *Bioconjug. Chem.* **2003**, *14*, 563-574.
- <sup>22</sup> Liu, J.; Kolar, C.; Lawson, T.A.; Gmeiner, W.H. *J. Org. Chem.* **2001**, *66*, 5655-5663.
- <sup>23</sup> Kukowska Latallo, J.F.; Candido, K.A.; Cao, Z.; Nigavekar, S.S.; Majoros, I.J.; Thomas, T.P.; Balogh, L.P. Khan, M.K.; Baker, J.R. *Cancer Res.* **2005**; *65*, 5317-5324.
- <sup>24</sup> Venturoli, D.; Rippe, B. *Am. J. Physiol. Renal. Physiol.* **2005**, *288*, F605-F613.
- <sup>25</sup> Maeda, H. *Adv. Enzyme Regul.* **2001**, *41*, 189-207.
- <sup>26</sup> Pasut, G.; Veronese, F.M. *Prog. Polym. Sci.* **2007**, *32*, 933-961.
- <sup>27</sup> Feener, E. P.; Shen, W.C.; Ryser, H.J.P. *J. Biol. Chem.* **1990**, *265*, 18780-18785.
- <sup>28</sup> Devalapally, H.; Navath, R.S.; Yenamandra, V.; Akkinapally, R. R.; Devarakonda, R.K. *Arch. Pharm. Res.* **2007**, *30*, 723-732.
- <sup>29</sup> Haenseler, E.; Esswein, A.; Vitols, K.S.; Montejano, Y.; Mueller, B.M.; Reisfeld, R.A.; Huennekens, F.M. *Biochemistry* **1992**, *31*, 891-897.
- <sup>30</sup> Song, X.; Lorenzi, P.L.; Landowski, C. P.; Vig, B.S.; Hilfinger, J.M.; Amidon, G.L. *Mol. Pharm.* **2005**, *2*, 157-167
- <sup>31</sup> Sinhababu, A.K.; Thakker, D.R. *Adv. Drug Delivery Rev.* **1996**, *19*, 241-273
- <sup>32</sup> a) Panasci, L.; Paiement, J. P.; Christodouloupoulos, G.; Belenkov, A.; Malapetsa, A.; Aloyz, R. *Clin. Cancer Res.* **2001**, *7*, 454-461; b) Reux, B.; Weber, V.; Galmier, M.J.; Borel, M.; Madesclaire, M.; Madelmont, J.C.; Debiton, E. *Bioorg. Med. Chem.* **2008**, *16*, 5004-5020.

## 1.2 RESULTS AND DISCUSSION

On the basis of the results discussed in the previous section, this work is focused on the synthesis of carrier-linked prodrug systems to use in anticancer therapeutic strategies involving the active transport of drug (**Figure 1**). The tumor-specific ligand is the folic acid, the linker consists of a polyether or polyamide system and the anticancer agent, Chlorambucil, chosen from those of more modern application, is anchored to the spacer by cleavable bond that can release the drug by action of specific enzymes.

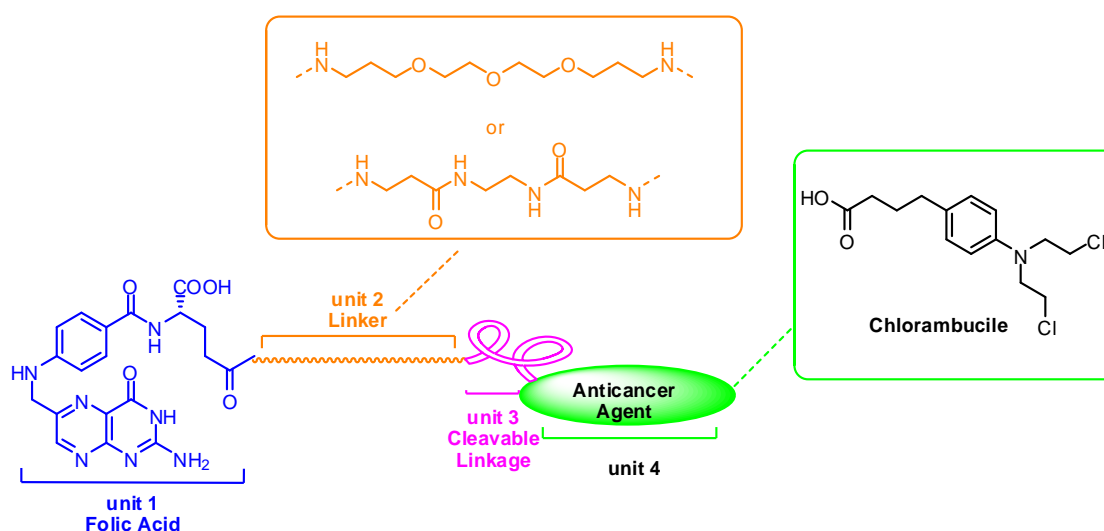


**Figure 1.** Carrier linked prodrug system.

As already mentioned, folic acid has proven to be one of the most promising ligand because its receptors are overexpressed on the surface of a large number of tumor cells, including cancer breast, lung, liver, ovaries, brain and myelogenous cells.<sup>1,2,3</sup> Objective of a part of my PhD thesis was the synthesis and biological evaluation of novel folate-conjugates **1-2** (**Figure 2**) through straightforward and versatile synthetic routes.

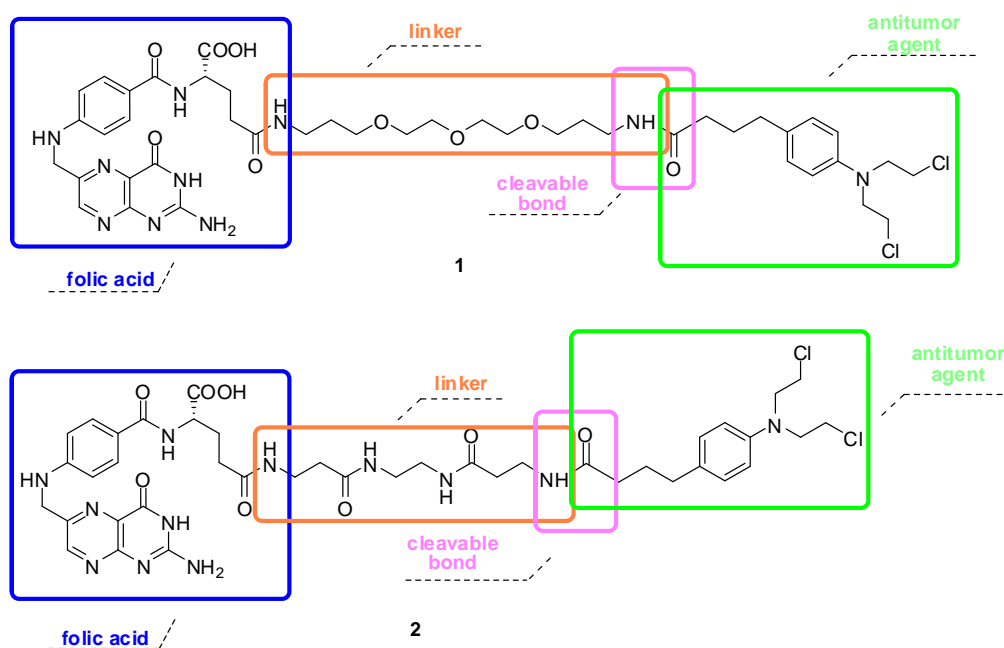


**Figure 2.** Folic acid conjugates 1-2.

It must be noted that the choice of an aminoether linker (conjugate **1**) offers a twofold advantage: a) it is biocompatible and hydrophilic as the most commonly employed polymeric linkers NH<sub>2</sub>PEG (NH<sub>2</sub>PEG2000, NH<sub>2</sub>PEG1000, etc.) and b) it's cheaper than other NH<sub>2</sub>PEG linkers.<sup>4</sup> On the other hand, the wear of a  $\beta$ -amino acid-based linker (conjugate **2**) is due of their structural characteristics. Indeed, they should ensure a good solubility and stability of our molecular systems in biological medium. It is known that  $\beta$ -amino acids systems are highly innovative alternative to the systems studied so far. They appear to be promising constituents of potential therapeutic agents, because they are appreciably more stable than their  $\alpha$ -analogues to proteolytic degradation *in vivo*.<sup>5,6</sup> The majority of  $\beta$ -peptides reported in literature is not toxic,<sup>7</sup> thus they seem to be a good compromise between solubility, biocompatibility and localized release of the drug through a prolonged systemic circulation, so they can to be interesting candidates as carriers for such strategies.

In particular we used the 4,7,10-trioxa-1,13-tridecandiamine and a linker consisting of two  $\beta$ -amino acid units separated by a ethylenediamine moiety. These linkers present amine functions at both ends so that they can bind, on the one hand folic acid via an amide bond and the other hand a cleavable unit or the drug.

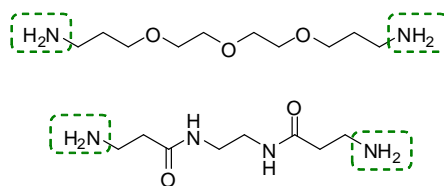


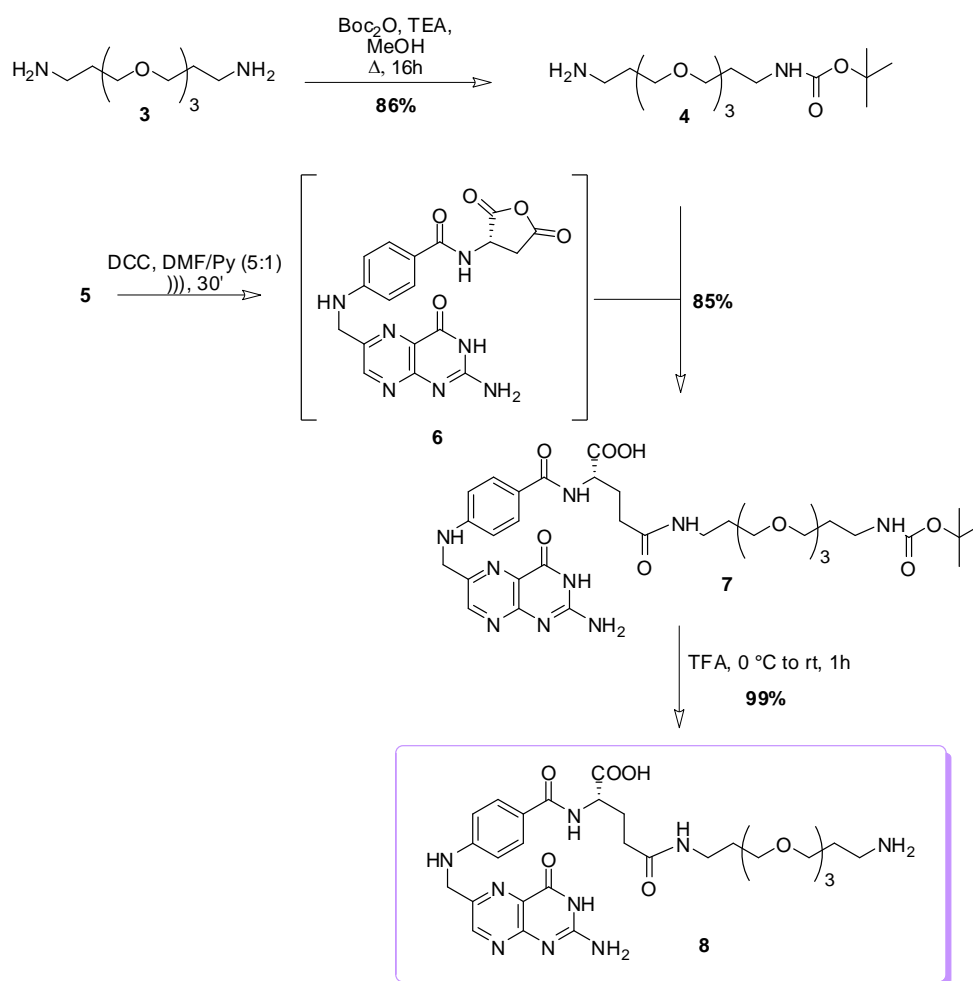
**Figure 3.** Polyether and polyamide linker.

The preparation of conjugates **1** and **2** was carried out by synthetic methodology that consists of following key steps: 1) preparation of the linkers; 2) linkers conjugation with folic acid through an amide bond formation; 3) removal of protective groups; 4) coupling reaction with the anticancer agent.

### 1.2.1 SYNTHESIS OF CLB-DELIVERY SYSTEM 1

The synthetic strategy of conjugate **1** involved the use of 4,7,10-trioxa-1,13-tridecandiamine (**3**), commercially available at low cost, and consists of a few stages. The first synthetic step (**Scheme 1**) provided *N*-Boc-monoprotection of amine **3** by reaction with Boc<sub>2</sub>O in MeOH under refluxing conditions to obtain carbamate **4** with 86% yield.

At this point, we are interested to prepare **7** by a coupling reaction of resulting carbamate **4** with folic acid (**5**). It was attempted usual synthetic routes (DCC/HOBT, DCC/NHS), but unfortunately we didn't obtained the expected product. Instead, amide **7** was successfully obtained by means of the activated folate anhydride **6**, in turn prepared *in situ* by treatment of **5** with dicyclohexylcarbodiimide (DCC) in DMF/pyridine (5:1) for 30 min in an ultrasonic bath. When it was observed formation of intermediate **6** thanks to presence of white crystals of DCU in the reaction vessel, amine **4** (1 eq) was added, smoothly leading to amide **7**. The concentrate DMF solution containing the reaction product was dropwise added to a cold mixture of acetone and diethyl ether (30:70 v/v ratio), from which the desired **7** was isolated by precipitation (85% yield).



Scheme 1. Synthesis of folic derivate 8.

In such conditions the  $\gamma$ -conjugate is the only product formed, because  $\gamma$ -position carboxyl function of folate is more reactive than the  $\alpha$ -one (Figure 4), indeed, as reported in the literature,<sup>8</sup> common amidation reactions were carried out preferably in this position, so no protections were necessary. The exclusive formation of  $\gamma$ -carboxyl-linked compound was confirmed by  $^1\text{H}$  and COSY NMR experiments.

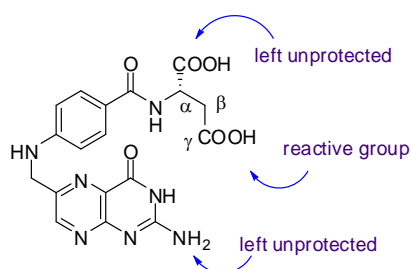
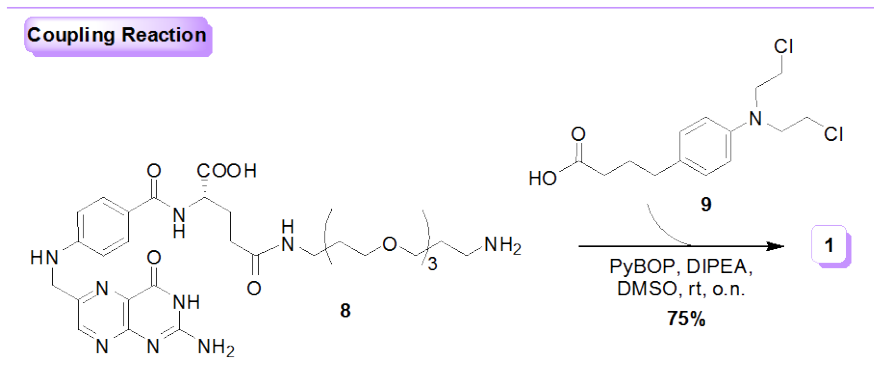


Figure 4. Folic acid.

Finally, amide **8** was quantitatively obtained via *N*-Boc group removal, by treatment of conjugate **7** with TFA in CH<sub>2</sub>Cl<sub>2</sub> (**Scheme 1**). At this point, with the product **7** in hand, our interest was focused on preparation of desired conjugate **1** by reaction with PyBOP/DIPEA and CLB (**9**) in DMSO. The crude product, purified by precipitation, gave a brownish yellow compound with 75% yield.

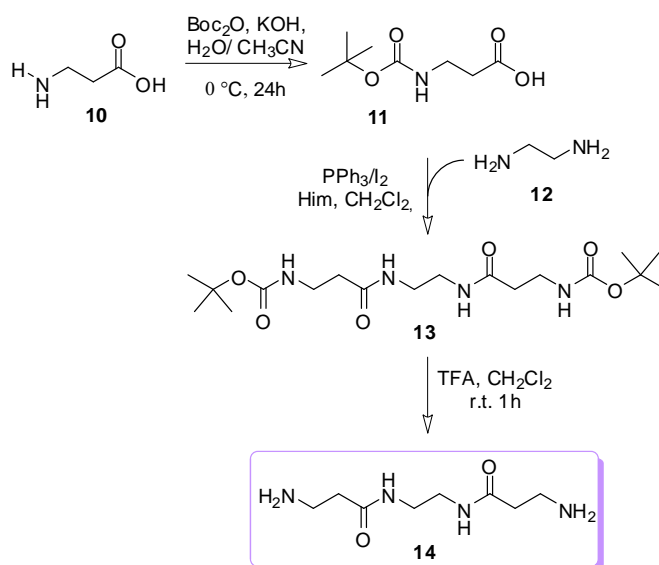


**Scheme 2.** Coupling reaction to obtain final compound **1**.

It's noteworthy that the same coupling reaction in common condition using DCC was found to be not convenient, due to difficulty to remove the resulting DCU from reaction mixture.

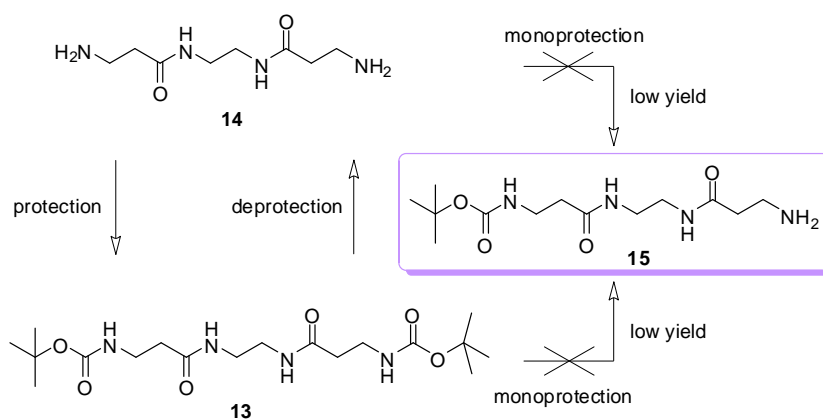
### 1.2.2 SYNTHESIS OF CLB-DELIVERY SYSTEM 2

To synthesize conjugate **2** in which a linker consisting of two  $\beta$ -alanina units bridged by ethylenediamine spacer is included, we planned to start from folic acid and a linker as **14** using the same methodology as for **1**. Linker **14** was prepared in a single step using *N*-Boc- $\beta$ -Alanine (2 eq) and free ethylenediamine. Amide bond formation was carried out activating carboxyl acid function of *N*-Boc- $\beta$ -alanine (**11**) by treatment with PPh<sub>3</sub>/I<sub>2</sub> complex and imidazole (**Scheme 3**). The use of this reagent, as widely reported in the literature<sup>9</sup> leads to formation of acyl iodide, like intermediate, which in the presence of ethylenediamine gave compound **13**. Subsequent deprotection of amino functions under usual conditions (TFA/CH<sub>2</sub>Cl<sub>2</sub>) afford diamine **14** in quantitative yield. (**Scheme 3**).



**Scheme 3.** Synthesis of pseudo- $\beta$ -dipeptide **14**.

Unfortunately, **14** coupled with folic acid did not lead to the desired conjugate but to a bis-folate derivative unsuitable for our purposes. An alternative approach was next attempted using a monoprotected linker. Both attempts to obtain **15** from **14** (by selective protection) or from **13** (by selective deprotection) failed due to the almost exclusive formation respectively of *bis*-protected (**13**) or free diamine **14**.



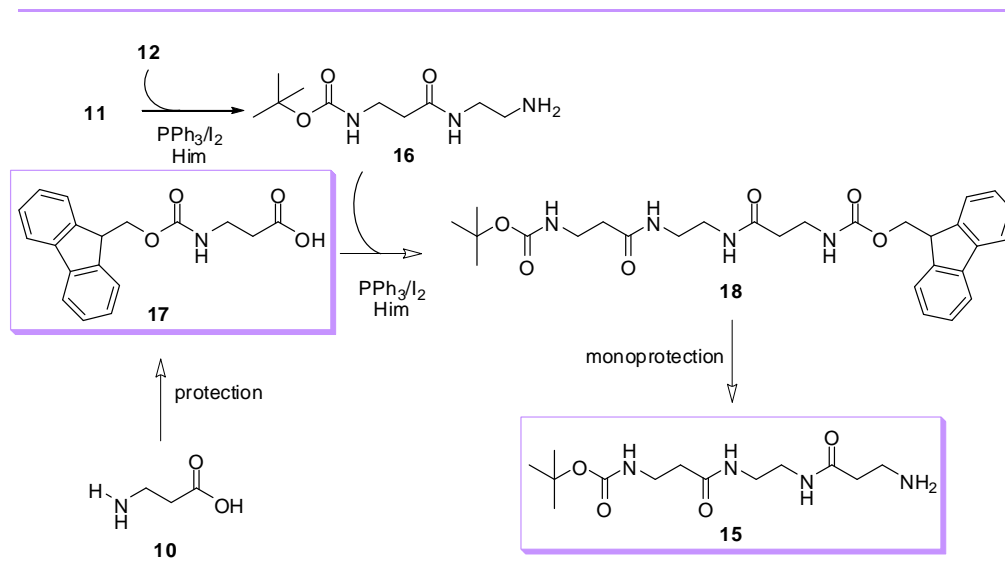
**Scheme 4.** Synthetic efforts to obtain linker **15**.

To overcome these problems, we planned to prepare an orthogonally protected diamine linker starting from *N*-Boc- $\beta$ -Ala (**11**) and *N*-Fmoc- $\beta$ -Ala (**17**). The Fmoc group is

stable under acidic conditions and may be selectively removed in basic conditions, the Boc-protecting group is acid-labile but stable under basic conditions.<sup>10</sup>

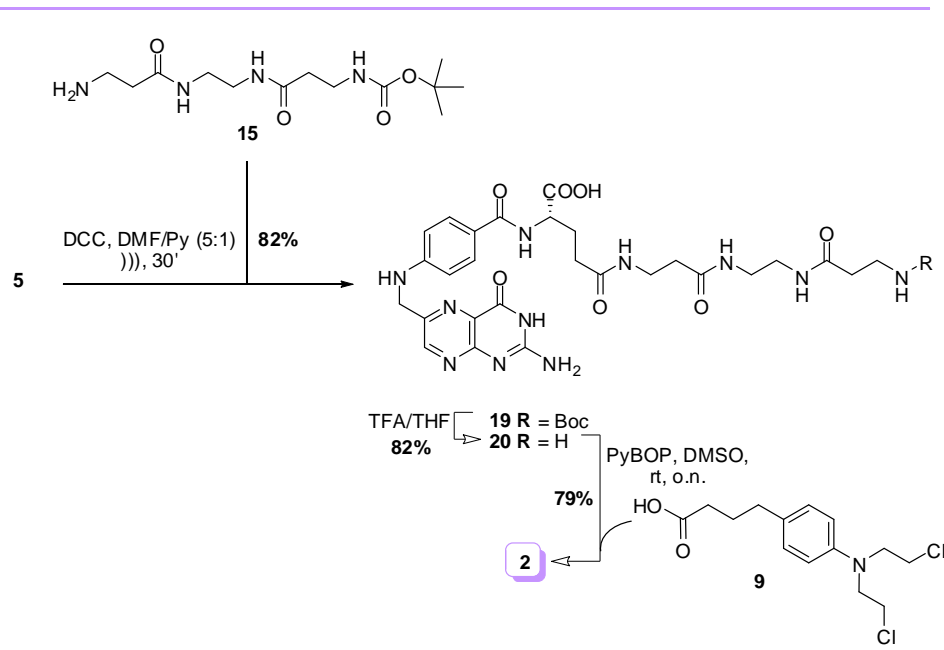
Amidation reaction of **11** with ethylenediamine (**12**) (**Scheme 5**) was carried out under the same conditions as described for **13** (carboxyl acid activation with  $\text{PPh}_3/\text{I}_2/\text{ImH}$ ), in this case, using a large excess of amine (ratio 1:15), the compound **16** was obtained in high yields (75%).

The latter was then used in the coupling reaction with *N*-Fmoc- $\beta$ -alanine (**17**) prepared through a well note procedure; the reaction was quantitative and provided orthogonally protected **18** (**Scheme 5**). Finally the selective removal of Fmoc group under common reaction conditions (5% piperidine / DMF) gave desired linker **15**.



**Scheme 5.** Synthesis of pseudo- $\beta$ -dipeptide **15** by Boc/Fmoc strategy.

Monoprotected linker **15** allowed, the preparation of folate **19**, via coupling reaction with folic acid (**Scheme 6**), in presence of DCC, Py in DMSO. Conjugate **19** was obtained with 82% of yield. *N*-Boc group removal with TFA at 0 °C gave then amine **20** that was finally coupled with CLB (**9**) using PyBOP/DIPEA in anhydrous DMSO, to allowed conjugate **2** as a brownish purple solid (79% yield).



Scheme 6. Synthesis of conjugate 2.

### 1.2.3 BIOLOGICAL ASSAYS

Following the biological assays performed on these molecular systems are reported, these assays were realized in collaboration with Prof. Giuseppe Palumbo research group (Dip. di Biologia e Patologia Cellulare e Molecolare "L. Califano).

**Cytotoxicity studies with CLB.** CLB is an alkylating agent that has been mainly used in the treatment of chronic lymphocytic leukemia (CLL).<sup>11</sup> It has been demonstrated that CLB may induce different effects in *in vitro* systems, spanning from growth arrest to cell death.<sup>12</sup> In light of these observations, our initial experiments were aimed at establishing the effective CLB concentrations against the specific cell lines used in this work. To this purpose, we incubated undifferentiated U937 and TK6 cells for 48 and 72 h with CLB at concentrations ranging from 0 to 60  $\mu\text{M}$ . As shown in **Figure 4**, metabolic activity of both cell lines was inhibited as drug concentrations and incubation times were increased. In all cases, however, changes in cell metabolic activity were less pronounced at CLB concentrations in the order of 30  $\mu\text{M}$ .

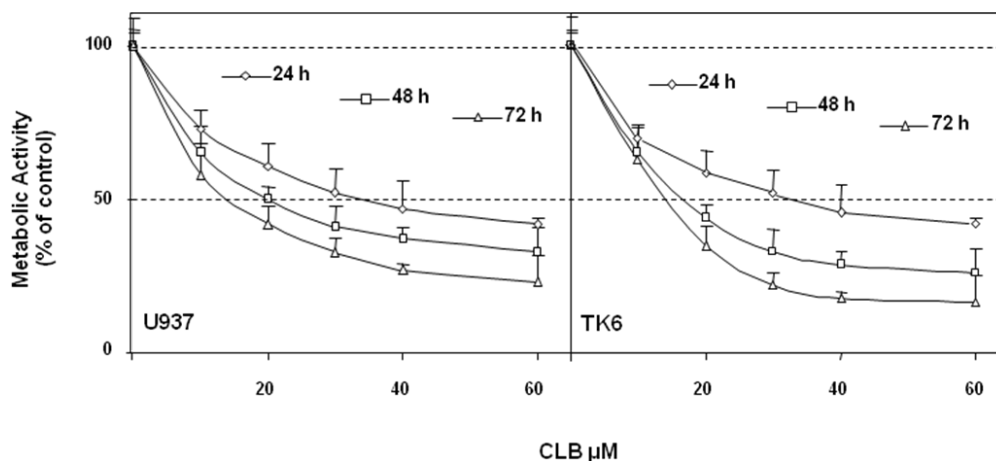


**Figure 4.** Metabolic activity of FR<sup>-</sup>-U937 (left) and FR<sup>+</sup>-TK6 cells (right) treated with increasing doses of CLB at different incubation times.

**Cytotoxicity studies with CLB conjugates 1 and 2.** A first comparison between the efficacy of CLB and our FA-conjugates was obtained by observing the presence/absence of statistically significant changes in metabolic activities of undifferentiated U937 and TK6 cells incubated for 24, 48 and 72 h with media containing 30 μM of CLB (to which both cell lines should presumably respond in a similar manner) or 30 μM FA-conjugates **1** and **2** (to which receptor positive cells should preferentially respond).

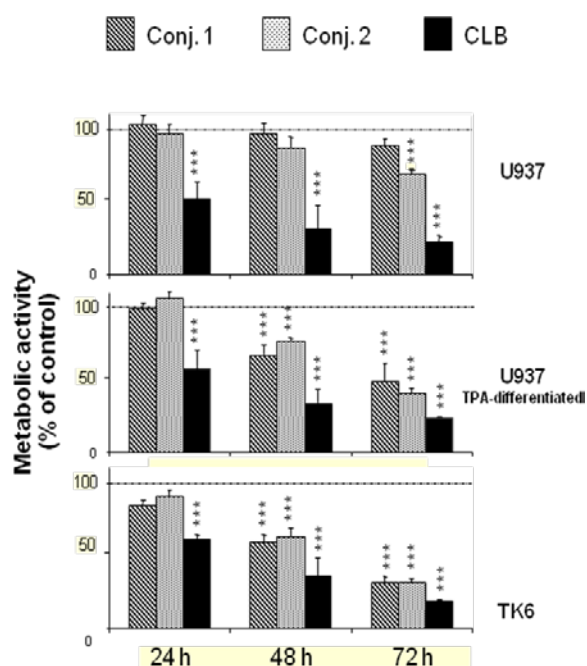


**Figure 5.** Effects of FA-CLB conjugates **1** and **2** on metabolic activity (XTT assay) of FR<sup>-</sup>-U937 (upper panel), FR<sup>+</sup>-TPA-activated U937 (middle panel) and FR<sup>+</sup>-TK6 cells

(lower panel). Significant differences ( $p < 0.0001$ , three asterisks) are referred to controls.

As shown in **Figure 4** (upper panel), the metabolic activity of undifferentiated U937 cells treated with FA-CLB conjugates did not differ appreciably from the control except for long incubation time (72 h). Conversely, we observe that the metabolic activity of TK6 cells, incubated in 30  $\mu\text{M}$  FA- conjugates **1** or **2**, decreased from nearly 50% to about 70% (as compared to controls) as the incubation time was increased from 48 to 72 h, respectively (**Figure 5**, lower panel).

We hypothesized that a different expression level of FRs may account for such a divergent behavior. Indeed, it has been demonstrated that while FR expression is restricted to only a few cell types,<sup>13</sup> Branda *et al.* reported<sup>14</sup> that this expression level in TK6 human lymphoblast cells is very high. At variance, while Antony has reported<sup>15</sup> that such receptors are essentially absent in undifferentiated U937 cells, nevertheless remarkably elevated levels have been demonstrated in macrophagic TPA-activated U937 cells.<sup>16</sup> This presence in macrophages has been largely exploited for drug targeting.<sup>17</sup> In line with these remarks, to finally proof that our folate conjugates **1** and **2** exerted antitumor activity by FR recognition and endocytosis, we differentiated the U937 FR<sup>-</sup> into FR<sup>+</sup> activated macrophages. This was achieved by incubating the U937 with 20 nM of TPA (as outlined in the experimental section). The U937 cells, which normally grow in suspension, when differentiate into macrophages become adherent to each other and to the surface of the culture vessel and cease to proliferate. We found that the metabolic activity of TPA-activated U937 incubated with **1** and **2** (30  $\mu\text{M}$ ) differed significantly from that of undifferentiated U937 cells. As shown in **Figure 4** (middle panel), cell viability of activated cells decreased significantly and progressively from 48 and 72 h. We also observed that differences in therapeutic efficacy of FA-derivatives in responsive cells were scarcely perceptible and, in any case, were similar to that of CLB at the longest incubation time (**Figure 6**).

Interesting enough, the addition of FA-conjugates to responsive cells ( $10^4$ ) pretreated for 1 h with 50 fold excess (1.5 mM) free FA, prevented appreciable changes in metabolic activities even after 72 h of incubation (**Figure 6**). At variance, the same pre-treatment resulted wholly ineffective when cells were exposed to 30  $\mu\text{M}$  CLB.

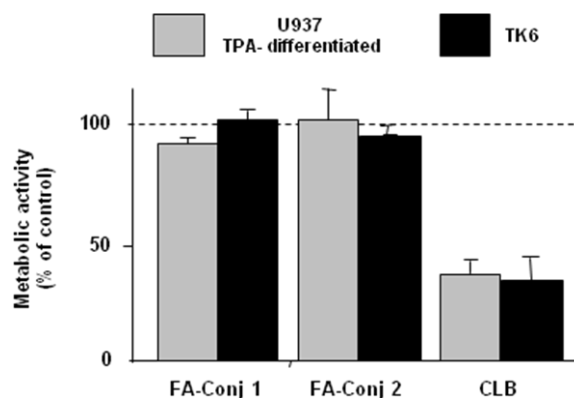


**Figure 6.** TK6 and TPA-differentiated U937 cells were pretreated with 1.5 mM free FA for 1 h and incubated with FA-conjugates **1** and **2**. The XTT assay was performed after 72 h of incubation.

#### Stability of FA-CLB conjugates **1** and **2** (shelf life and stability in human serum).

The shelf life (at 4 °C) of **1** and **2** in human serum was established *in vitro* in U937 and TK6 cell lines. Activity of our FA-CLB conjugates did not change over a 5 weeks storage period (data not shown). Similarly, when conjugates **1** and **2** were incubated in fresh human serum, their activity was preserved with negligible activity loss as determined by XTT assay.

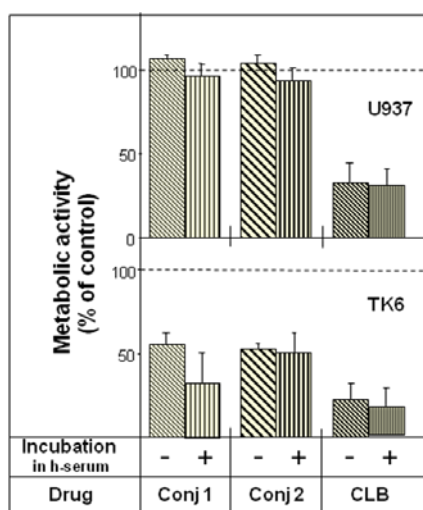


**Figure 7.** Stability studies of FA-CLB conjugates **1** and **2** pre-incubated for 12 h in fresh human serum. Details in the Methods section.

As shown in **Figure 7**, change in cell viability of both cell lines was similar to that observed by treating cells with equimolar concentrations (30  $\mu$ M) of FA-CLB conjugates **1** and **2** or CLB free form. The abatement of metabolic activity of TK6 cells

resulted similar to that observed in the absence of pre-incubation of the compounds with human serum. The U937 cells retain their unresponsiveness to both conjugates.

**Molecular studies.** Although it is generally acknowledged that the bifunctional alkylating agent chlorambucil (CLB) is not cell cycle specific, it has been demonstrated that it may induce G<sub>2</sub>/M arrest and apoptosis in several human cell lines. Clarification of the molecular mechanisms of cell cycle arrest and cell death induced by different DNA-damaging chemicals, including chlorambucil, has considerable implications for molecule-targeted cancer therapy. For this reason, it was of interest to investigate at cellular and molecular level how FA-CLB conjugates **1** and **2** exert their effects in undifferentiated U937 (FR<sup>-</sup>), TPA-U937 activated (FR<sup>+</sup>), and TK6 (FR<sup>+</sup>) cells in comparison to their parent molecule CLB. To this purpose, we studied the cell cycle distribution and apoptosis upon sublethal treatments. To this aim we analyzed the cytofluorimetric profiles and analyzed the protein expression patterns of cells incubated for 48 h with 30 μM CLB in its free form or in conjugated forms **1** and **2**. In agreement with general literature data, we confirmed in both FR<sup>+</sup> cell lines two major aspects: first, CLB promotes visible cell accumulation in G<sub>2</sub> phase and, as also suggested by the presence of a consistent sub-G1 phase, this drug induces apoptosis (**Figure 8**). The increase of the sub-G1 phase appears to be also associated to an appreciable up-regulation of the proapoptotic BAX and Clusterin (**Figure 8**). This protein has been at the core of a long-lasting debate, as conflicting data demonstrated both pro- and antiapoptotic effects. However, the controversy on Clusterin function in tumors has been clarified in that it has been demonstrated that two different *mRNA* transcripts (generated by alternative splicing) can be found in cells, one secretory and the other one coding for the a nuclear form. The activation of the latter form has proapoptotic aptitude and a regulative (negative) function in cell cycle progression.<sup>i,18</sup>

---

<sup>i</sup> However, the controversy on Clusterin function in tumors has been clarified in that it has been demonstrated that two different *mRNA* transcripts (generated by alternative splicing) can be found in cells, one secretory and the other one coding for the a nuclear form. The activation of the latter form has proapoptotic aptitude and a regulative (negative) function in cell cycle progression. See ref. 18.

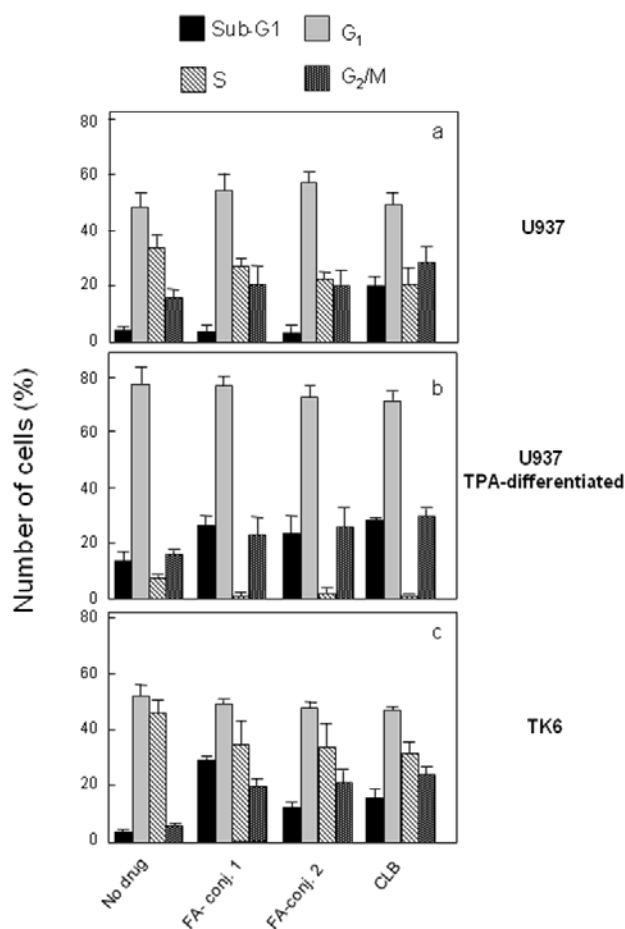


**Figure 8.** Cell cycle profiles for FR<sup>-</sup>-U937 (panel a), differentiated FR<sup>+</sup>-U937 (panel b) and FR<sup>+</sup>-TK6 cells (panel c) in response to treatments (48 h) with CLB-conjugates **1**, **2** and free CLB (30  $\mu$ M).

As the FR<sup>-</sup> cells (undifferentiated U937) are concerned, we found that treatment with FA-CLB conjugates did not roughly change the cell cycle profile and, at variance with the effect of pure CLB, it did not determine amassing of cells in the sub-G<sub>1</sub> fraction. The lack of apoptosis in cells incubated for 48 h with both conjugates was also inferred by Western blot experiments, showing no changes in the expression levels of Bax and Clusterin (**Figure 9**, left panel, lanes 2 and 3).

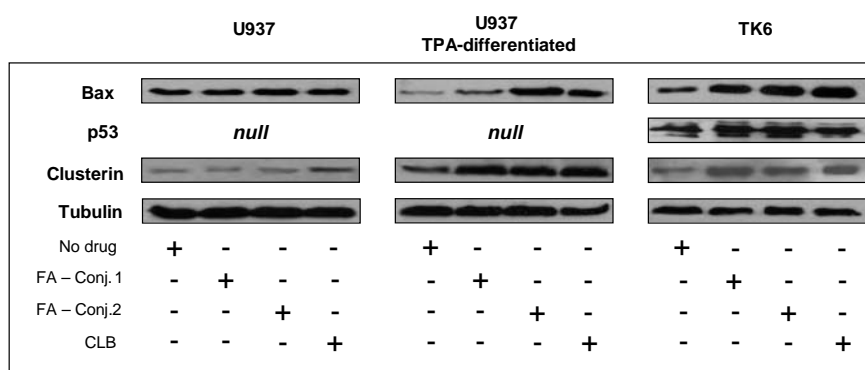


**Figure 9.** Protein expression in FR<sup>-</sup>-U937, TPA-differentiated FR<sup>+</sup>-U937 and FR<sup>+</sup>-TK6 cells in response to treatments (48 h) with CLB-conjugates **1**, **2** and free CLB (30 μM).

On the contrary, once incubated with FA-CLB conjugates (30 μM), the cell cycle profile of TK6 and TPA-differentiated U937 cells, both expressing FRs, showed a modest accumulation in G<sub>2</sub> phase while visibly activating apoptosis (**Figure 8**, panel *b* and *c*). The sub-G<sub>1</sub> fractions in fact amounted to  $\leq 20$  in TK6 cells and up to  $\geq 25\%$  of the total in TPA-treated U937 cells. The differentiation to macrophages that occurs in TPA-treated U937 cells induced synchronization in G<sub>0</sub>/G<sub>1</sub> phase and in the meanwhile proliferation was switched off. This cytofluorimetric scenario was mirrored by Western blot experiments. Apoptosis was declared by the augmented levels of BAX and of the propapoptotic form of Clusterin (**Figure 9**, middle and right panels, lanes 2 and 3) in both cell lines and, as the TK6 cells are concerned, of p53 (**Figure 9**, right panel, lanes 2 and 3). Notably, once incubated with 30 μM free CLB, TK6 cells were characterized by a time-dependent increase in the expression level of p53. This observation agrees with literature data that point to an ongoing up-regulation of p53 protein expression to explain the onset of lymphocytic cell resistance to CLB.<sup>19</sup>

- 
- <sup>1</sup> Wu, M.; Gunning, W.; Ratman, M. *Cancer Epidemiol. Biomarkers Prev.* **1999**, *8*, 775-782.
- <sup>2</sup> Sadasivan, E.; da Costa, M.; Rothenberg, S.P.; Brink, L. *Biochim. Biophys. Acta* **1987**, *925*, 36-47.
- <sup>3</sup> Toffoli, G.; Cernigoi, C.; Russo, A.; Gallo, A.; Bagnoli, M.; Boiocchi, M. *Int. J. Cancer* **1997**, *74*, 193-198.
- <sup>4</sup> Dhar, S., Liu, Z., Thomale, J., Dai, H., Lippard, S.J. *J. Am. Chem. Soc.* **2008** *130*, 11467–11476.
- <sup>5</sup> Kritzer, J.A.; Stephens, O. M.; Guarracino, D.A.; Reznik, S. K.; Schepartz, A. *Bioorg. Med. Chem.* **2004**, *13*, 11-16.
- <sup>6</sup> Koyack, M.J.; Cheng, R.P. *Methods Mol. Biol.* **2006**, *340*, 95-109.
- <sup>7</sup> Seebach, D., Beck, A. K.; Bierbaum, D.J. *Chem. Biodiv.* **2004**, *1*, 1111-1239.
- <sup>8</sup> Wang, S., Lee, R.J., Mathias, C.J., Green, M. A., Low, P. S. *Bioconjugate Chem.* **1996**, *7*, 56–62.
- <sup>9</sup> Caputo, R.; Cassano, E.; Longobardo, L.; Mastroianni, D.; Palumbo, G. *Synthesis* **1995**, *2*, 141-143.
- <sup>10</sup> Davies, J.S. *Amino Acids and Peptides*, Chapman and Hall: London 1985.
- <sup>11</sup> Rajski, S.R., Williams, R. M. *Chem. Rev.* **1998**, *98*, 2723-2796.
- <sup>12</sup> a) Secchiero, P., Voltan, R., di Iasio, M.G., Melloni, E., Tiribelli, M., Zauli, G. *Clin. Cancer Res.* **2010**, *16*, 1824–1833; b) Amrein, L, Loignon, M., Goulet, A. C., Dunn, M., Jean-Claude, B., Aloyz, R., Panasci, L. *J. Pharmacol. Exp. Ther.* **2007**, *321*, 848-855.
- <sup>13</sup> a) Sierra, E.E., Goldman, I.D. *Semin. Oncol.* **1999**, *26*, 11–23; b) Matherly, L. H., Goldman, D.I. *Vitam. Horm.* **2003**, *66*, 403–456.
- <sup>14</sup> Branda, R.F., O'Neill, J. P., Brooks E. M., Trombley L.M., Nicklas J. A. *Mutation Res.* **2001**, *473*, 51-71.
- <sup>15</sup> Antony, A.C. *Annu. Rev. Nutr.* **1996**, *16*, 501–521.
- <sup>16</sup> Antohe, F., Radulescu. L., Puchianu, E., Kennedy, M. D., Low, P.S., Simionescu, M. *Cell Tissue Res.* **2005**, *320*, 277-285.
- <sup>17</sup> Roy, E.J., Gawlick, U., Orr, B.A., Kranz D.M. *Adv. Drug Delivery Rev.* **2004**, *56*, 1219-1231.

---

<sup>18</sup> Leskov, K. S., Klokov, D. Y., Li, J., Kinsella, T. J., Boothman, D. A. Synthesis and functional analyses of nuclear clusterin, a cell death protein. *J. Biol. Chem.* **2003**, 278, 11590–11600.

<sup>19</sup> Johnston, J.B., Daeninck, P., Verburg, L., Lee, K., Williams, G., Israels, L.G., Mowat, M.R., Begleiter, A. *Leuk. Lymphoma*, **1997**, 5-6, 435–449.

### 1.3 CONCLUSION

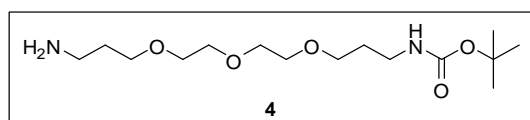
Cellular uptake of vitamin folic acid occurs via folate-receptor mediated endocytosis. Many types of cancer cells express high levels of folate receptors as they need continuous supply of this vitamin for their proliferation. With an objective to use folic acid as a ‘Trojan Horse’ to transport anticancer drugs into cancer cells, we prepared two tumor-targeted drug delivery systems **1** and **2**, which bear a FA unit as the tumor recognition moiety and the CLB as the cytotoxic agent, the two bioactive units having been jointed by aminoether (4,7,10-trioxadecane-1,13-diamine) and pseudo- $\beta$ -dipeptide ( $\beta$ -Ala-ED- $\beta$ -Ala) linkers. Preparation of the two molecular systems has been devised by a straightforward and efficient route (34-54% o.y.). When evaluated using both FR<sup>-</sup> (undifferentiated U937) and FR<sup>+</sup> (TK6 and TPA-differentiated U937) leukemic cells, both conjugates exhibited activity only against FR<sup>+</sup> cells (particularly TK6), exerting antitumor effects which are comparable to that displayed by CLB in its free form. Our *in vitro* results, then, show that the FA-derivatives specifically bind folate-receptor-positive cells, that this binding is significantly higher than in folate-receptor negative cells, and that the interaction is inhibited by free FA.

## 1.4 EXPERIMENTAL SECTION

### CHEMISTRY

All moisture-sensitive reactions were performed under nitrogen atmosphere using oven-dried glassware. Solvents were dried over standard drying agents and freshly distilled prior to use. Triethylamine (TEA) and *N,N*-diisopropylethylamine (DIPEA) were redistilled from NaOH. *N,N'*-Dicyclohexylcarbodiimide (DCC) and folic acid (FA) were purchased from Sigma-Aldrich Inc. Chlorambucil (CLB), dimethyl sulfoxide (DMSO, anhydrous) and pyridine (Py, anhydrous) were used as purchased (Fluka Chemical Co.) without further purification. Reactions were monitored by TLC (precoated silica gel plate F254, Merck). Column chromatography: Merck Kieselgel 60 (70–230 mesh); flash chromatography: Merck Kieselgel 60 (230–400 mesh). Combustion analyses were performed by using CHNS analyzer.  $^1\text{H}$  and  $^{13}\text{C}$  NMR spectra were recorded with the following instruments: Varian Gemini (200 MHz), Varian Gemini (300 MHz), Bruker DRX (400 MHz) and Varian Inova (500 MHz) spectrometers. MALDI spectra were recorded on a Voyager DE-PRO MALDI-TOF mass spectrometer.

### SYNTHETIC PROCEDURES AND CHARACTERIZATION DATA FOR INTERMEDIATES AND CONJUGATES

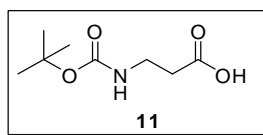


**Compound 4.** A stirring solution of 4,7,10-trioxa-1,13-tridecanediamine (**3**, 2.0 g, 9.1 mmol) in anhydrous  $\text{CH}_3\text{OH}$  (152 mL) was treated with  $\text{Boc}_2\text{O}$  (2.0 g, 9.1 mmol) and TEA (2.9 mL, 21 mmol). The reaction mixture was left at reflux for 16 h. The solvent was removed under reduced pressure and the resulting yellow oil was purified by silica gel chromatography ( $\text{CHCl}_3/\text{CH}_3\text{OH}/\text{NH}_4\text{OH} = 89:10:1$ ) to give the pure **4** (2.5 g, 86% yield). Oily;  $^1\text{H}$  NMR (300 MHz,  $\text{CD}_3\text{OD}$ )  $\delta$ : 1.44 (s, 9H), 1.73-1.78 (m, 2H), 1.90-1.96 (m, 2H), 2.03 (bs, 2H), 2.90 (t, 2H,  $J = 6.7$  Hz), 3.12 (t, 2H,  $J = 6.0$  Hz), 3.52 (t, 2H,  $J = 6.0$  Hz), 3.56-3.68 (m, 10H), 5.1 (bs, 1H).  $^{13}\text{C}$  NMR (100 MHz,  $\text{CDCl}_3$ ) ppm: 28.2,

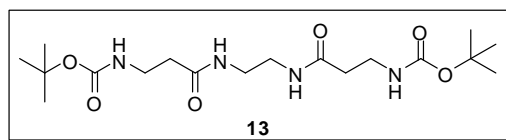




yield).  $^1\text{H}$  NMR (500 MHz,  $\text{DMSO-}d_6$ )  $\delta$ : 1.48-1.63 (m, 4H), 1.63-1.78 (m, 2H), 1.79-1.98 (m, 2H), 2.05 (appt, 2H,  $J = 7.3$  Hz), 2.30 (t, 2H,  $J = 6.7$  Hz), 2.36-2.45 (m, 2H), 2.99-3.09 (m, 2H), 3.15-3.50 (m, 14H), 3.78 (bs, 4H), 4.21-4.35 (m, 1H), 4.46 (bs, 2H), 6.63 (m, 4H), 6.93 (m, 1H), 6.98 (d, 2H,  $J = 7.0$  Hz), 7.65 (d, 2H,  $J = 8.0$  Hz), 7.76-7.87 (m, 2H), 7.93 (bd, 1H,  $J = 6.6$  Hz), 8.02-8.23 (m, 1H), 8.63 (s, 1H), 11.43 (bs, 1H).  $^{13}\text{C}$  NMR (100 MHz,  $\text{DMSO-}d_6$ ): ppm 27.0, 29.4, 30.6, 32.0, 33.8, 34.8, 35.6, 35.9, 40.4, 45.8, 52.2, 53.6, 58.5, 67.3, 68.0, 69.5, 69.7, 111.1, 111.9, 121.4, 127.9, 128.9, 129.5, 138.4, 144.4, 148.4, 150.7, 153.4, 155.1, 159.0, 160.9, 166.3, 171.8, 173.8, 174.0. MALDI-TOF MS:  $m/z$  928.38 (calcd); 951.03  $[\text{M}+\text{Na}]^+$ , 967.04  $[\text{M}+\text{K}]^+$  (found). Anal. calcd for  $\text{C}_{43}\text{H}_{58}\text{Cl}_2\text{N}_{10}\text{O}_9$ : C, 55.54; H, 6.29; Cl, 7.63; N, 15.06. Found: C, 55.75; H, 6.25; Cl, 7.57; N, 14.98.

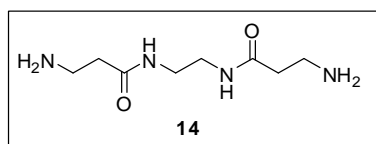


**Compound 11.** To a stirring solution of  $\beta$ -alanina (2.5 g, 28 mmol) in  $\text{H}_2\text{O}$  (55 mL) was added KOH (3.2 g, 57 mmol) in one portion and  $\text{Boc}_2\text{O}$  (2.0 g, 9.1 mmol) dissolved in  $\text{CH}_3\text{CN}$  (10 mL) at  $0^\circ\text{C}$ . After 24 h at room temperature to the mixture of reaction HCl (1M) was added until to obtained a pH  $\sim 4$  and then the reaction was extracted with  $\text{EtOAc}_2$ . The organic layer was washed with  $\text{H}_2\text{O}$  until neutrality and dried over  $\text{Na}_2\text{SO}_4$ . The solvent was removed under reduced pressure to give the pure product **11** (5.0 g, 95% yield): p.f.  $76\text{--}77^\circ\text{C}$ ;  $^1\text{H}$  NMR (200 MHz,  $\text{CDCl}_3$ )  $\delta$ : 1.43 (s, 9H), 2.50 (bt, 2H,  $J = 5.4$ ), 3.32 (bd, 2H,  $J = 6.0$ ,  $J = 11.8$ ), 5.18 (bs, 1H), 10.95 (bs, 1H).  $^{13}\text{C}$  NMR (50 MHz,  $\text{CDCl}_3$ ) ppm: 28.0, 34.1, 35.6 ( $\text{CH}_2\text{NH}$ ), 84.8, 155.8, 175.9. ESI-MS:  $m/z$  189.10 (calcd); 190.1  $[\text{M}+\text{H}]^+$  (found). Anal. calcd for  $\text{C}_8\text{H}_{15}\text{NO}_4$ : C, 50.91; H, 7.96; N, 7.37. Found: C, 50.78; H, 7.99; N, 7.40.

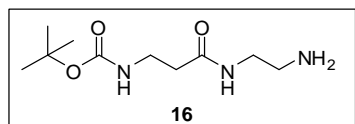


**Compound 13.** To magnetically stirred solution of  $\text{I}_2$  (503 mg, 1.98 mmol) in dry  $\text{CH}_2\text{Cl}_2$  (15 mL), under nitrose atmosphere at room temperature a solution of triphenylphosphine dissolved in the same solvent (15 mL) was added dropwise (520 mg, 1.98 mmol). After 15 min, imidazole (273 mg, 4.0 mmol) was added and after a

few min *N*-protected  $\beta$ -amino acid **11** (300 mg, 1.6 mmol) in  $\text{CH}_2\text{Cl}_2$  (5 mL) was added to the mixture of reaction. The reaction was kept at room temperature until starting material was consumed to form acyl iodide (TLC:  $\text{CHCl}_3:\text{CH}_3\text{OH} = 8/2$ ). After 3 h, ethylenediamine (0.053 mL, 0.8 mmol) was added in one portion; the resulting mixture was left at room temperature until TLC analysis indicates complete formation of compound **13** (TLC:  $\text{CHCl}_3:\text{CH}_3\text{OH} = 8/2$ ). The solution was diluted with  $\text{CH}_2\text{Cl}_2$  (20 mL), washed with a solution of sodium thiosulfate 5 N and neutralized with brine. The organic phase reunited and dried over dry  $\text{Na}_2\text{SO}_4$  was evaporated under reduced pressure to give the pure **13** (450 mg, 75% yield): pf. 182.8-184.4 °C,  $^1\text{H}$  NMR (200 MHz,  $\text{CD}_3\text{OD}$ )  $\delta$ : 1.43 (s, 18H), 2.34 (t, 4H,  $J = 6.7$ ), 3.22-3.38 (m, 8H), 5.22 (bs, 2H,  $\text{NH}_{\text{uret}}$ ), 6.63 (bs, 2H).  $^{13}\text{C}$  NMR (50 MHz,  $\text{CD}_3\text{OD}$ ) ppm: 25.0, 33.8, 34.3, 36.3, 76.3, 152.8, 172.9. ESI-MS:  $m/z$  402.25 (calcd); 403.01  $[\text{M}+\text{H}]^+$  (found). Anal. calcd for  $\text{C}_{18}\text{H}_{34}\text{N}_4\text{O}_6$ : C, 53.71; H, 8.51; N, 13.92. Found: C, 53.90; H, 8.47; N, 13.87.

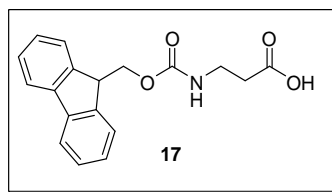


**Compound 14.** To a magnetically stirred solution of dry  $\text{CH}_2\text{Cl}_2$  (3 mL) and TFA (1.5 mL) at room temperature compound **15** (500 mg, 1.2 mmol) was added. After 1 h starting material was completely consumed (TLC,  $\text{CHCl}_3/\text{CH}_3\text{OH}=8:2$ ) and the solvent was evaporated under vacuum to give the pure compound **14** (230 mg, 95% yield):p.f. 182.8-184.4 °C,  $^1\text{H}$  NMR (200 MHz,  $\text{CD}_3\text{OD}$ )  $\delta$ : 2.63 (t, 4H,  $J=6.5$ ), 3.21 (t, 4H,  $J = 6.5$ ), 3.31 (s, 4H).  $^{13}\text{C}$  NMR (50 MHz,  $\text{CD}_3\text{OD}$ ) ppm: 29.2, 33.4, 36.2, 168.9. Anal. calcd for  $\text{C}_8\text{H}_{18}\text{N}_4\text{O}_2$ : C, 47.51; H, 8.97; N, 27.70;. Found: C, 47.68; H, 8.93; N, 27.61.

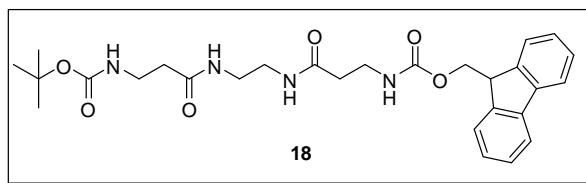


**Compound 16.** To a solution of  $\text{I}_2$  (990 mg, 3.9 mmol) in dry  $\text{CH}_2\text{Cl}_2$  (10 mL), under dry nitrogen atmosphere at room temperature, triphenylphosphine (1.1 g, 3.9 mmol) was added dropwise in the same solvent (10 mL). After 15 min imidazole (708 mg, 10.4 mmol) was added in one portion. Then, compound **11** (500 mg, 2.6 mmol), in  $\text{CH}_2\text{Cl}_2$  (5 mL) was added to the mixture. The reaction was kept at room temperature for 3 h (TLC monitoring:  $\text{CHCl}_3:\text{CH}_3\text{OH} = 8/2$ ) until all the starting amino acid was completely consumed in favor of acyl iodine. After 3 h, ethylenediamine (2.6 mL, 39

mmol) was added in one portion; the resulting mixture of reaction was kept at room temperature. When acyl iodine was consumed (TLC:  $\text{CHCl}_3:\text{CH}_3\text{OH} = 8/2$ ) the solution was diluted with  $\text{CH}_2\text{Cl}_2$  (20 mL), washed with a solution of sodium thiosulfate 5 N and brine. The organic layer was extracted with a mixture of  $\text{CHCl}_3/\text{MeOH}$  (95/5, 3 x 75 mL) and dried ( $\text{Na}_2\text{SO}_4$ ) and evaporated under vacuum to give the pure **16** (450 mg, 75% yield):  $^1\text{H}$  NMR (200 MHz  $\text{CD}_3\text{OD}$ )  $\delta$ : 1.38 (s, 9H), 1.62 (bs, 2H), 2.32 (t, 2H,  $J = 6.0$ ), 2.76 (t, 2H,  $J = 6.0$ ), 3.15-3.42(m, 4H), 5.52 (bs, 1H), 6.78 (bs, 1H).  $^{13}\text{C}$  NMR (50 MHz,  $\text{CH}_3\text{OD}$ ) ppm: 28.2, 36.2, 41.2, 41.9, 79.2, 156.2, 171.9. ESI-MS:  $m/z$ : 231.16 (calcd); 232.37  $[\text{M}+\text{H}]^+$  (found). Anal. calcd for  $\text{C}_{10}\text{H}_{21}\text{N}_3\text{O}_3$ : C, 51.93; H, 9.15; N, 18.17. Found: C, 51.72; H, 9.19; N, 18.25.

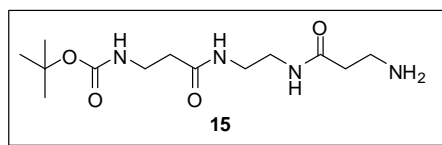


**Compound 17.** To a stirring solution of  $\beta$ -alanina (2.5 g, 13.3 mmol) in  $\text{H}_2\text{O}$  (8 mL), at  $0^\circ\text{C}$ , a 10 mL of a mixture of sodium carbonate (9%) was added slowly and then Fmoc-*O*-Su (2.69 g, 7.9 mmol) dissolved in DMF (25 mL) was added in one portion. After 30 min the reaction was diluted with  $\text{H}_2\text{O}$  (400 mL) and extracted with EtOAc (100 mL). The aqueous phase was acidified (pH  $\sim$  2) with a cold solution of HCl 1M and extracted several times with EtOAc. The organic phase reunited was washed with brine, dried on dry  $\text{Na}_2\text{SO}_4$  and evaporated under vacuum to obtain the pure **17** (3 g, 9.7 mmol, 73% yield):  $^1\text{H}$  NMR (200 MHz,  $\text{CD}_3\text{OD}$ )  $\delta$ : 2.62 (bt, 2H,  $J = 5.7$ ), 3.18-3.40 (m, 2H), 4.22 (t, 1H,  $J = 6.4$ ), 4.42 (d, 2H,  $J = 6.6$ ), 5.32 (bt, 1H,  $J = 5.6$ ), 7.20-7.46 (m, 4H), 7.58 (d, 2H,  $J = 7.3$ ), 7.76 (d, 2H,  $J = 7.1$ ), 9.54 (bs, 1H).  $^{13}\text{C}$  NMR (50 MHz) ppm: 34.2, 36.4, 47.2, 66.8, 120.0, 125.0, 127.1, 127.7, 141.3, 143.8, 156.4, 176.7. Anal. calcd for  $\text{C}_{18}\text{H}_{17}\text{NO}_4$ : C, 69.44; H, 5.50; N, 4.50. Found: C, 69.57; H, 5.48; N, 4.48.

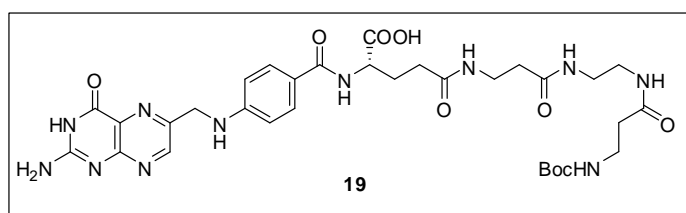


**Compound 18.** To a solution of  $\text{PPh}_3/\text{I}_2/\text{Him}$  complex in dry  $\text{CH}_2\text{Cl}_2$  anidro (30 mL), prepared with the same procedure used to prepare 13, Fmoc- $\beta$ -Ala **17** (150 mg, 0.65

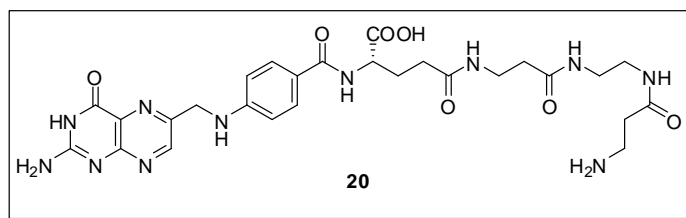
mmol, 1 eq) was added at room temperature and under nitrogen atmosphere. When it was observed the formation of acyl iodide (TLC:  $\text{CH}_2\text{Cl}_2/\text{MeOH} = 8:2$ ), to mixture of reaction the compound **13** (450 mg, 1.94 mmol) in  $\text{CH}_2\text{Cl}_2$  anidro (5 mL), was added in one portion. After 24 h, the mixture was treated with a solution of sodium thiosulfate 5N (25 mL) e brine (25 mL) and extracted with  $\text{CHCl}_3:\text{CH}_3\text{OH} = 95/5$ . The organic phases were reunited, dried over  $\text{Na}_2\text{SO}_4$  and evaporated under reduced pressure. The crude product (350 mg) was purified by crystallization (EtOAc) to give the pure **18** as white crystals (230 mg, resa 88%):  $^1\text{H}$  NMR (200 MHz, DMSO- $d_6$ )  $\delta$ : 1.38 (s, 9H), 2.11-2.29 (m, 4H), 2.99-3.26 (m, 8H), 4.14-4.32 (m, 5H.), 6.75 (bt, 2H,  $J = 5.5$ ), 7.22-7.42 (m, 4H), 7.67 (d, 2H,  $J = 7.1$ ), 7.87 (d, 2H,  $J = 6.8$ ).  $^{13}\text{C}$  NMR (50 MHz, DMSO- $d_6$ ) ppm: 28.2, 35.8, 36.7, 38.6, 39.5, 40.2, 40.7, 77.6, 40.7, 109.7, 120.0, 121.4, 127.2, 128.9, 137.4, 139.4, 155.4, 157.2, 170.5, 171.5. ESI-MS:  $m/z$  524.26 (calcd); 525.44  $[\text{M}+\text{H}]^+$  (found). Anal. calcd for  $\text{C}_{28}\text{H}_{36}\text{N}_4\text{O}_6$ : C, 64.10; H, 6.92; N, 10.68. Found: C, 64.25; H, 6.89; N, 10.64.



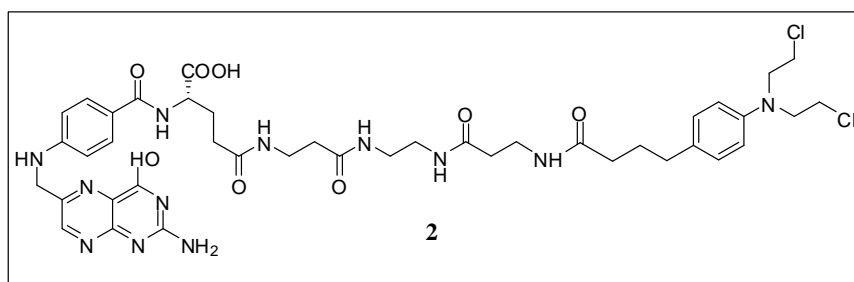
**Compound 15.** To a magnetically stirred solution of Py in DMF (5%) product **12** (230 mg, 0.44 mmol) was added at room temperature. After 2h starting material was consumed (TLC:  $\text{CHCl}_3:\text{CH}_3\text{OH} = 7/3$ ) and the solvent was evaporated under vacuum. Purification of the crude product by crystallization ( $\text{Et}_2\text{O}/\text{AcOEt}$ ) gave the pure **15** as white crystals (126 mg, yield 95%):  $^1\text{H}$  NMR (200 MHz,  $\text{CH}_3\text{OD}$ )  $\delta$ : 1.40 (s, 9H), 2.10-2.30 (m, 6H), 2.32-2.47 (m, 2H), 3.20-3.45 (m, 6H), 4.30-4.60 (m, 1H), 5.45 (bs, 1H), 6.78 (bs, 1H).  $^{13}\text{C}$  NMR (50 MHz,  $\text{CH}_3\text{OD}$ ) ppm: 28.3, 34.0, 34.2, 36.4, 39.8, 41.1, 41.7, 79.0, 156.0, 171.8. ESI-MS:  $m/z$  302.20 (calcd); 303.19  $[\text{M}+\text{H}]^+$  (found). Anal. calcd for  $\text{C}_{13}\text{H}_{26}\text{N}_4\text{O}_4$ : C, 51.64; H, 8.67; N, 18.53. Found: C, 51.82; H, 8.63; N, 18.47.



**Compound 19.** Conjugate **15** was obtained (82% yield) under the same conditions reported for the synthesis of compound **7** from folic acid and amine **15**.<sup>1</sup> Yellow solid, M.p. 207-209 °C; <sup>1</sup>H NMR (200 MHz, DMSO-*d*<sub>6</sub>) δ: 1.38 (s, 9H), 1.82-2.01 (m, 2H), 2.08-2.32 (m, 6H), 2.98-3.18 (m, 4H), 3.21-3.42 (m, 4H), 4.22-4.38 (m, 1H), 4.52 (bs, 2H), 6.62 (d, 2H, *J* = 7.5 Hz), 6.68-6.78 (m, 1H), 6.82-7.05 (m, 3H), 7.65 (d, 2H, *J* = 7.5 Hz), 7.81 (bs, 2H), 7.91-8.02 (m, 1H), 8.69 (s, 1H), 11.42 (bs, 1H). <sup>13</sup>C NMR (100 MHz, DMSO-*d*<sub>6</sub>): ppm 28.3, 30.7, 31.8, 35.4, 36.0, 36.6, 39.0, 39.1, 46.0, 51.8, 77.6, 111.2, 121.4, 128.0, 129.0, 148.5, 148.7, 150.8, 153.7, 155.5, 156.6, 160.9, 166.4, 170.5, 171.7, 173.8, 174.1. MALDI-TOF MS: *m/z* 725.32 (calcd); 748.66 [M+Na]<sup>+</sup>, 764.68 [M+K]<sup>+</sup> (found). Anal. calcd for C<sub>32</sub>H<sub>43</sub>N<sub>11</sub>O<sub>9</sub>: C, 52.96; H, 5.97; N, 21.23. Found: C, 52.84; H, 5.96; N, 21.31.



**Compound 20.** Folate conjugate **20** was obtained (82%) under the same conditions reported for the preparation of compound **8**. Yellow solid, M.p. 204-207 °C; <sup>1</sup>H NMR (500 MHz) (DMSO-*d*<sub>6</sub>) δ: 1.79-2.15 (m, 2H), 2.18-2.30 (m, 6H), 2.99-3.32 (m, 8H), 4.38 (bs, 1H), 4.50 (bd, 2H, *J* = 5.0 Hz), 4.52 (bs, 2H), 6.58 (d, 2H, *J* = 7.3 Hz), 6.78-7.02 (m, 4H), 7.62 (d, 2H, *J* = 7.3 Hz), 7.78-7.98 (m, 1H), 8.02-8.08 (m, 1H), 8.65 (s, 1H), 11.40 (bs, 1H). <sup>13</sup>C NMR (100 MHz, DMSO-*d*<sub>6</sub>): ppm 31.6, 32.1, 36.0, 36.8, 37.0, 38.8, 39.1, 46.5, 52.4, 111.7, 121.4, 128.0, 129.6, 148.2, 148.4, 151.8, 156.0, 157.5, 161.6, 167.1, 171.0, 172.6, 173.6, 174.0. MALDI-TOF MS: *m/z* 625.45 (calcd); 648.49 [M+Na]<sup>+</sup>, 664.45 [M+K]<sup>+</sup> (found). Anal. calcd for C<sub>27</sub>H<sub>35</sub>N<sub>11</sub>O<sub>7</sub>: C, 51.83; H, 5.64; N, 24.63. Found: C, 51.96; H, 5.62; N, 24.57.



**Compound 2.** Folate-CLB conjugate **2** was obtained (79% yield) under the same conditions reported for the synthesis of compound **1**. Brownish purple solid, M.p. 220 °C (dec.); <sup>1</sup>H NMR (400 MHz) (DMSO-*d*<sub>6</sub>) δ: 1.65-1.69 (m, 2H), 1.79-1.98 (m, 2H), 2.03 (appt, 2H, *J* = 7.2 Hz), 2.14-2.26 (m, 5H), 2.30 (t, 1H, *J* = 6.4 Hz), 2.32-2.42 (m, 2H), 2.97-3.18 (m, 4H), 3.19-3.37 (m, 4H), 3.60 (t, 2H, *J* = 6.3), 3.67 (s, 2H), 4.23-4.38 (m, 1H), 4.48 (bd, 2H, *J* = 5.9 Hz), 6.57-6.69 (m, 4H), 6.78-7.02 (m, 4H), 7.58-7.62 (d, 2H, *J* = 7.3), 7.82-7.94 (m, 2H), 7.98 (t, 1H, *J* = 7.6), 8.10 (d, 1H, *J* = 7.8), 8.60 (bs, 1H), 11.41 (bs, 1H). <sup>13</sup>C NMR (100 MHz, DMSO-*d*<sub>6</sub>): ppm 26.4, 30.9, 31.8, 33.5, 35.2, 35.6, 35.7, 39.0, 39.1, 40.1, 46.2, 52.6, 53.8, 111.5, 112.2, 121.7, 128.3, 129.4, 129.6, 148.9, 149.0, 151.0, 153.8, 154.1, 156.9, 161.1, 166.7, 169.9, 170.8, 172.0, 174.2. MALDI-TOF MS: *m/z* 910.34 (calcd); 933.11 [M+Na]<sup>+</sup>, 949.13 [M+K]<sup>+</sup> (found). Anal. calcd for C<sub>41</sub>H<sub>52</sub>Cl<sub>2</sub>N<sub>12</sub>O<sub>8</sub>: C, 54.01; H, 5.75; Cl, 7.78; N, 18.43. Found: C, 54.19; H, 5.73; Cl, 7.75; N, 18.35.

## BIOLOGY

**Cell lines.** The p53-null U937 human leukemic monocyte lymphoma and the p53-positive isogenic human lymphoblast TK6 cell lines were obtained from American Type Culture Collection (Rockville, MD). Both cells were grown in Dulbecco's Modified Eagle Medium, 2 mM L-glutamine, 100 µg/mL streptomycin, 100 units/mL penicillin, and 10% Foetal Calf Serum (FCS). All media and cell culture reagents were purchased from Life Technologies (San Giuliano Milanese, Italy).

**Cell differentiation.** Differentiation of the promyelocytic cell line U937 cells into macrophages was achieved according to Sordet *et al.*<sup>2</sup> by treating the cells with 20 nM 12-*O*-tetradecanoylphorbol-13-acetate (TPA) for 24 h. At the end of this time the differentiation process was considered complete as indicated by the massive attachment of cells to the plate. TPA was obtained by Sigma Aldrich. A 100 µM stock solution was prepared in 100% DMSO.

**CLB and CLB-folate conjugates stock solutions.** CLB was dissolved in 100% DMSO to obtain a concentrated (75 mM) stock solution. Before measurements, appropriate aliquots of this solution were diluted to the desired concentration.

Stock solutions of the same concentration (75 mM) of folate-trioxa-CLB and folate-(βAla-ED-βAla)-CLB stock solutions (both) were also obtained by dissolving the

powders in 100% DMSO under continuous stirring at room temperature overnight in the dark. These concentrated solutions were stored at 4 °C wrapped in aluminium foil. Before use, appropriate amounts of each stock solution were diluted to the desired concentration.

**Cell viability.** Cell viability was assayed by using the Cell Proliferation Kit II (XTT, Roche, Milan Italy). The assay is based on the cleavage of the yellow tetrazolium salt XTT to form an orange formazan dye by metabolic active cells.<sup>3</sup> Therefore, this conversion only occurs in viable cells.

Normally  $1 \times 10^4$  cells/well were seeded into 96-well plates and incubated for 24, 48 and 72 h with CLB, folate-trioxa-CLB or folate-( $\beta$ Ala-ED- $\beta$ Ala)-CLB at established concentrations and then analyzed in triplicate.

**Stability of CLB-folate conjugates in DMSO solutions.** To assess the time-stability of CLB-folate derivatives stock solutions we evaluated their biological effects on cell viability immediately after their preparation or after several weeks of storage. The changes in cytotoxic activity on U937 and TK6 cells of freshly-prepared or long stored (5 weeks) stock solutions (both 75 mM) were evaluated by comparing the residual viability of these cells (XTT assay) following 48 h treatment with scalar doses (normally 0-50  $\mu$ M) of each compound. As concentrated solutions are normally more stable than the diluted ones, the check of stability and full retention of cytotoxic activity was also performed starting from stock solutions 100 times more diluted (i.e. 0.75 mM in 33% DMSO). Even in this case, the assays were performed immediately after their preparation or after several weeks of storage at 4 °C (5 weeks).

**Stability of CLB-folate conjugates in human serum.** To test the stability of CLB-folate-conjugates in human serum, we have diluted appropriate amounts of stock solutions of folate-trioxa-CLB or folate-( $\beta$ Ala-ED- $\beta$ Ala)-CLB in human serum so that the final concentrations of the drugs were in both cases 0.5 mmol/L. These CLB-containing solutions, used as drug sources, were then incubated at 37 °C for 12 h and finally used to treat undifferentiated U937 and TK6 cells. The analysis of cell viability by XTT assay was performed 48 h later. In these experiments, CLB in free (control) or conjugated forms was 30  $\mu$ M.

**Flow cytometry.** The undifferentiated or TPA-activated U937 cells and TK6 cells were incubated individually for 48 h with CLB or with its folate conjugated forms (30  $\mu$ M). After incubation, cells were washed twice with 1 mL phosphate saline buffer pH

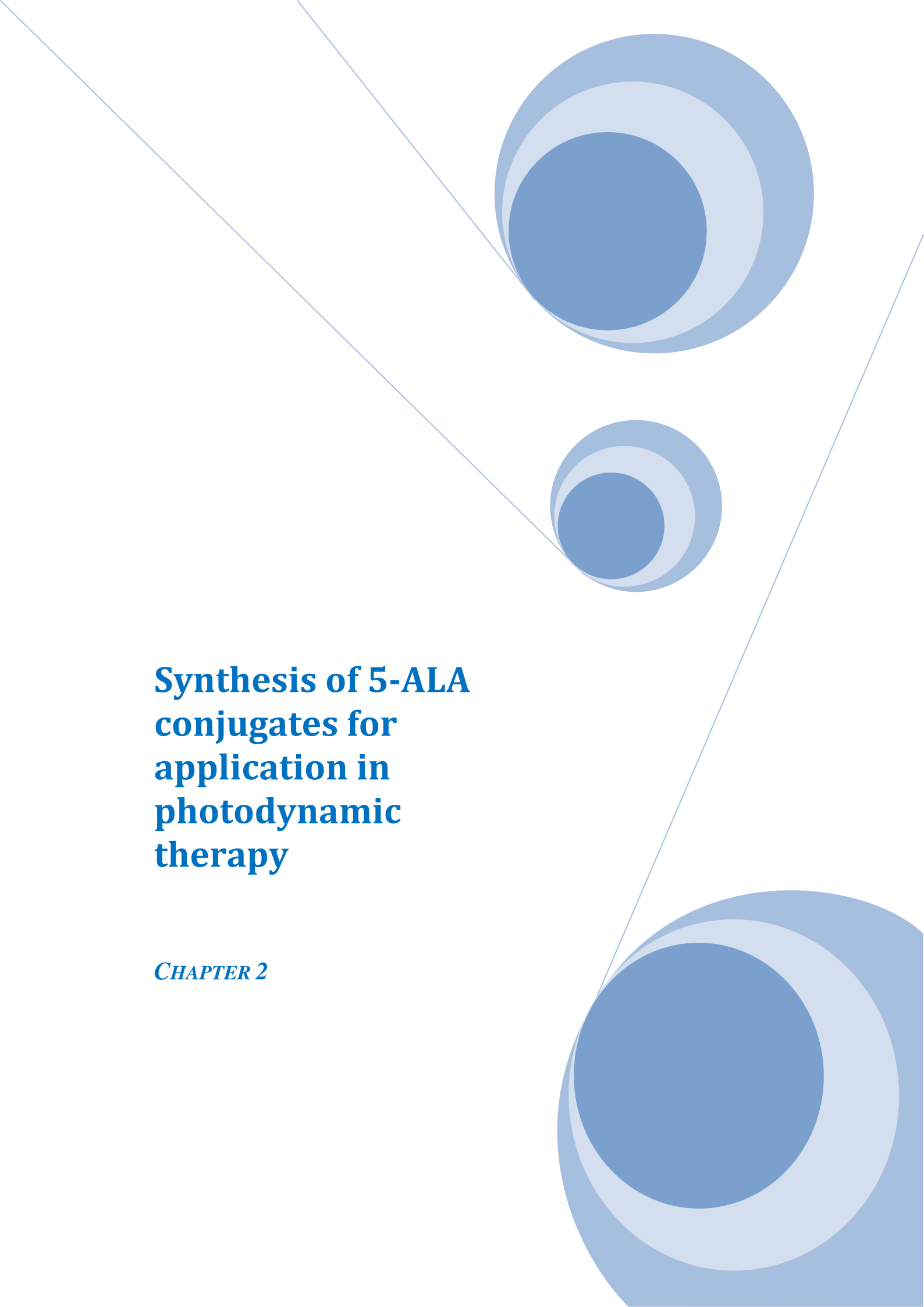
7.4 (PBS), and re-suspended and fixed in 70% ethanol. Before analysis, fixed cells were washed, centrifuged, and re-suspended in 1 mL PBS containing 1 µg RNase and 100 µg propidium iodide.<sup>4</sup> Samples were stored in the dark for 20 min at room temperature before final readings. The cellular orange fluorescence of propidium iodide was detected in a linear scale using a CyAn ADP Flow Cytometer (DAKOCytomation, Ely, UK) and analyzed by using ModFit/LT Software (Verity Software, Topsham, ME). About 30,000 events (i.e., fluorescence readings, corresponding to not less than 20,000 cells) were recorded for each sample.

**Electrophoresis and Western blot analysis.** Total cellular protein extracts were obtained by lysing cells in 50 mM Tris (pH 7.5), 100 mM NaCl, 1% NP40, 0.1% Triton X 100, 2 mM EDTA, 10 µg/mL aprotinin, and 100 µg/mL phenylmethylsulfonyl fluoride. Protein concentration was routinely measured with the Bio-Rad protein assay.<sup>5</sup> Polyacrylamide gels (10 or 15%) were prepared essentially as described by Laemmli.<sup>6</sup> Molecular weight standards were from New England Biolabs (Beverly, MA, USA). Proteins separated on the polyacrylamide gels were blotted onto nitrocellulose filters (Hybond-C pure, Amersham Italia, Milan, Italy). Filters were washed and stained with specific primary antibodies and then with secondary antisera conjugated with horseradish peroxidase (Bio-Rad; diluted 1:2,000). Filters were developed using an electro-chemiluminescent Western blotting detection reagent (Amersham Italia, Milan, Italy); profiles were acquired and grossly quantified by scanning with a Discover Pharmacia scanner equipped with a Sun Spark Classic Workstation. The anti-p53 (DO1), anti-BAX (P-19) and anti-Clusterin (N-18) were from Santa Cruz Biotechnology (Santa Cruz, CA, USA). Anti-tubulin (MCA77G) was from Serotec (Kidlington, UK).

**Statistical analysis.** All data are expressed as mean ± SD. Significance was assessed by the Student's t test for unpaired data for comparisons between two means. Statistical significance was defined as \*, p<0.01; \*\*, p< 0.001; \*\*\*, p<0.0001.

- 
- <sup>1</sup> Guaragna, A., Amoresano, A., Pinto, V., Monti, G., Mastrobuoni, G., Marino, G., Palumbo, G. *Bioconjugate Chem.* **2008**, *19*, 1095-1104.
- <sup>2</sup> Sordet, O.; Rébé, C.; Leroy, I.; Bruey, J.M.; Garrido, C.; Miguet, C.; Lizard, G.; Plenchette, S.; Corcos, L.; Solary, E. *Blood* **2002**, *100*, 4446-4453.
- <sup>3</sup> Sun, J.; Wang, L.; Waring, M.A.; Wang, C.; Woodman, K.K.; Sheil, A. G. *Artif. Organs* **1997**, *21*, 408-413.
- <sup>4</sup> Crescenzi, E.; Chiaviello, A.; Canti, G.; Reddi, E.; Veneziani, B.M.; Palumbo, G. *Mol. Cancer Ther.* **2006**, *5*, 776-785.
- <sup>5</sup> Bradford, M.A. *Anal. Biochem.* **1976**, *72*, 248-254.
- <sup>6</sup> Laemmli, U.K. *Nature* **1971**, *227*, 680-685.



The background features a decorative graphic consisting of three blue circles of varying sizes, each with a darker blue center and a lighter blue outer ring. These circles are arranged in a vertical line, with the largest at the top and bottom, and a smaller one in the middle. Two thin blue lines intersect at the top left and extend diagonally across the page, framing the central text area.

# **Synthesis of 5-ALA conjugates for application in photodynamic therapy**

*CHAPTER 2*

## 2.1 INTRODUCTION

As reported in Chapter 1 traditional cancer therapies such as surgical treatment, radiation therapy and chemotherapy lack selectivity in removing or destroying diseased tissue and sparing normal healthy cells. These conventional treatments result in serious side effects caused by the loss of normal cell functions as a result of having relatively indiscriminate cytotoxic properties. Thus it is necessary the development of new therapeutic approach that display more accurate and effective discrimination of normal and diseased tissue. Currently, one of the most widely used cancer therapies is photodynamic therapy (PDT). The PDT is a minimally invasive therapeutic modality used in the cure of various cancerous and pre-malignant diseases<sup>1</sup> because it involves the systemic administration of a non-toxic photosensitizing drug (PS), which preferentially accumulates in host and tumor cells and then gets activated by the exposure of light in presence of oxygen to generate very reactive cytotoxic species. Furthermore, PDT is a cold photochemical process, which can be applied before, or after chemotherapy, ionizing radiation or surgery, without compromising these treatments or being compromised itself. Unlike other modalities like radiotherapy and surgery it can be applied repeatedly many times at the same site without risking the integrity of surrounding tissues. Response rates and its durability are better than other traditional therapeutic tools and it has better functional outcome. The possibility of interstitial light delivery where light is fed directly into solid tumors allows PDT to be used for large tumors and in treating residual microscopic disease left behind by other treatment modalities like surgery. Hence in many ways this treatment modality is superior to thermal laser techniques, chemotherapy and surgery.

### 2.1.1 HISTORY OF PHOTODYNAMIC THERAPY

Utility of light in the medical field as a therapeutic tool traces its origin back to several thousand years. For example it's know that ancient Egyptian, Indian and Chinese civilization used light to treat various diseases such as psoriasis, rickets, vitiligo and skin cancer.<sup>2</sup> Indeed in one of India's sacred books *Atharva-veda* (1400 BC) the use of seeds of the plant *Psoralea corylifolia* for the treatment of vitiligo is described.

Psoralens are photoactive components of these seeds, just as in the extracts of the plant *Ammi majus*, which grows on the banks of the Nile, and was used by Egyptians to treat vitiligo.<sup>3</sup>

In the 18<sup>th</sup> and 19<sup>th</sup> centuries sunlight was used for treating various disease like tuberculosis or rheumatism paralysis. In 1903 a Danish scientist named N. Finsen was awarded a Nobel Prize for his work in phototherapy,<sup>4</sup> he used the red light treatment for small pox<sup>5</sup> and also ultraviolet light to treat tuberculosis.

In those years Hermann von Tappeiner, director of the Institute of Pharmacology at the University of Munich, coined the term 'photodynamic reaction'. According to the observations of Oscar Raab, his doctoral student, the reaction was characterized as an oxygen-dependent tissue reaction following photosensitization and irradiation with light.<sup>6</sup> Oscar Raab could show in his experiments that in the presence of daylight the organic photosensitizer Acridine orange was cytotoxic for paramecia.<sup>6b</sup> The assays displayed that its toxicity was not only dependent on the concentration of the dye but also on the intensity of illumination. Furthermore in collaboration with the dermatologist Jesionek, von Tappeiner successfully treated patients suffering from lupus vulgaris, stage II syphilis and superficial skin cancer with topical Eosin red solution (1–5%) (**Figure 1**).

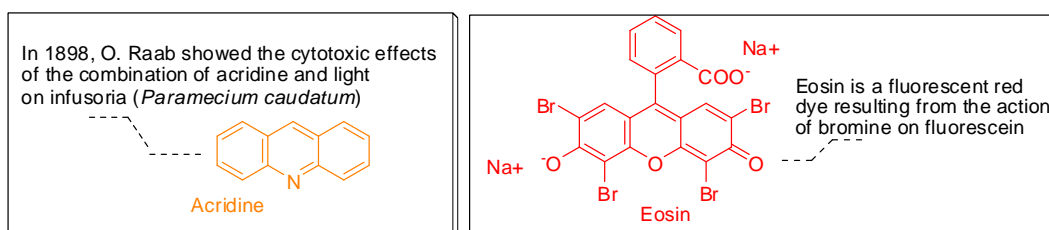


**Figure 1:** Acridine and Eosin: promoters of photodynamic reactions.

In 1913, F. Meyer-Betz investigated the porphyrins, class of compounds most often used today for their application in photodynamic therapy. He studied the accumulation of hematoporphyrin (HP) and its derivatives in rat tumors and PDT effects following systemic administration.<sup>7</sup> The fluorescence from these compounds was further studied for diagnostic and tumor margin delineation between 1940 and 1950 by F.H.J. Figgie and colleagues.<sup>8</sup> Modern photodynamic therapy was initiated by R.L. Lipson and E.J. Blades. They established that an impurity in HP was the tumor-localizing agent, and not the parent compound. This led to the synthesis of hematoporphyrin derivative (HPD), a

mixture of porphyrins produced by the acid treatment of HP.<sup>9</sup> The exact chemical composition and structure of this mixture remains unclear, although there is general consensus that the active portions consist of porphyrin oligomers with ether and ester linkages along with monomeric porphyrins. HPD was further developed for laboratory and clinical investigations through the efforts of T. J. Dougherty and colleagues in 1970s and 1980s.<sup>10</sup>

Tumors in virtually every anatomic site have been treated with PDT, and most are responsive to this therapy to some extent. Although, to date, several thousand patients have been treated with PDT for a variety of neoplasms, randomized clinical trials of this mode of cancer treatment were initiated only in 1987, using a purified form of HPD, called porfirmer sodium (Photofrin®)<sup>11</sup> (**Figure 2**). Currently, PDT with Photofrin® is approved in 10 countries.

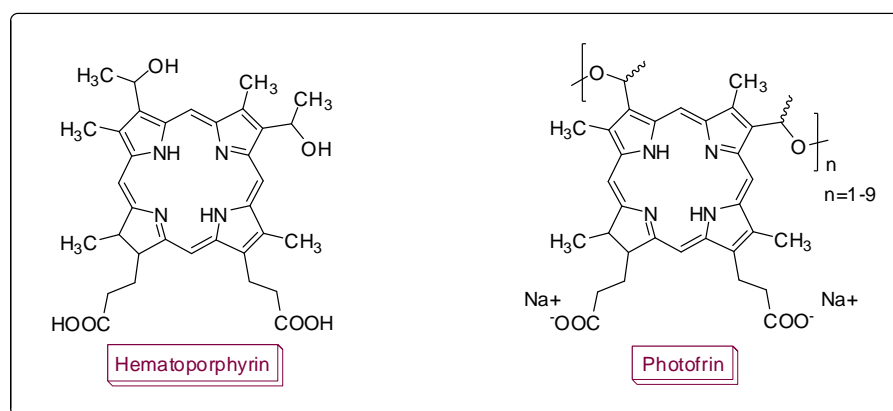


**Figure 2:** First generation photosensitizers.

The understanding of the biology of PDT has advanced, and efficient, convenient, and inexpensive systems of light delivery are now available. Moreover, encouraging results from randomized phase III trials are becoming published, and improved photosensitizing drugs are under development. Besides, porfirmer sodium (Photofrin®), temoporfin (meso-tetra (hydroxyphenyl) porphyrin (m -THPP) (Foscan®) has now been approved for systemic administration, and aminolevulinic acid and ethyl aminolevulinate have been approved for topical use.

3000 B.C.	Phototherapy is traced back to Egypt, India and Greece.
1900	O. Raab (Zeitschrift fuer Biologie, Munich, Germany) The cytotoxic effects of the combination of acridine and light on infusoria ( <i>Paramecium caudatum</i> ).
1901	N. Finsen (University of Copenhagen, Denmark) Light treatment of smallpox and cutaneous tuberculosis H. von Tappeiner and A. Jesionek (Zeitschrift für Biologie, Munich, Germany) Topical eosin application and white light treatment of malignant melanomas.
1903	N. Finsen (University of Copenhagen, Denmark) Nobel Prize for his work on phototherapy.
1907	H. von Tappeiner (Director, Pharmacological institute of the Ludwig-Maximilian University, Munich) and A. Jodlbauer introduction of the term 'photodynamic'.
1911	W. Hausmann (Physiol. Inst., Hochschule für Bodenkultur, Vienna, Austria) Phototoxic effects of haematoporphyrin on the skin of mice.
1913	F. Meyer-Betz (Chief Physician in Königsberg, Germany) First human tests. PDT using porphyrins. Self-experiment using his own hands.
1955	S. Schwartz (University of Minnesota, Minneapolis, USA) Development of haematoporphyrin derivative (HPD) by acetylation and reduction of haematoporphyrin.
1960	R. L. Lipson and E. J. Baldes (Mayo clinic / University of Vermont College of Medicine, U.S.A) Accumulation of HPD in tumors and its use in the photodetection of tumors.
1972	I. Diamond (University of California, U.S.A) Demonstration of the phototoxicity of haematoporphyrin against gliomas in vivo and in vitro T.J. Dougherty (Photodynamic Therapy Center, Roswell Park Cancer Institute, New York, U.S.A) Successful treatment of skin cancer in patients.
1975	J. F. Kelly (St. Mary's Hospital Medical School, London, United Kingdom) Treatment of bladder cancer in humans ; using HPD tumor regression is observed.
1978	T.J. Dougherty (Photodynamic Therapy Center, Roswell Park Cancer Institute, New York, U.S.A) First controlled clinical study in humans of PDT for the treatment of skin tumor.
1999	QLT Phototherapeutics, Vancouver, Canada and American Cyanamid Co. Pearl River, New York, Approval of the first PDT drug in Canada.
2001	PDT gains its first approval as a frontline therapy, using Visudyne to treat AMD.
2009	Approved PS: Photofrin, Foscan, Visudyne, Levulan, Metvix and Hexvix.

**Figure 3.** Historical development of photodynamic therapy.

### 2.1.2 MECHANISM OF PHOTODYNAMIC THERAPY

The photochemical and photophysical principles of PDT have been schematically represented in a modified Jablonski diagram (**Figure 4**).<sup>12</sup> PDT is the result of combination of three non-toxic elements namely light, oxygen and photosensitizer. A photosensitizer is administered, usually intravenously; after a period of time the sensitizer accumulates in tumor tissue. It remain inactive until exposed to light. Visible light, most relevant to PDT, covers the limited range of 400–700 nm. Sensitizer molecule exposed to light, gets excited from its singlet state  $S_0$  to short-lived (~10–6

seconds) electronically excited singlet state  $S_1$ , which can undergo radiative (fluorescence **2**) and nonradiative (internal conversion **3**) decay to come back to the ground state ( $S_0$ ). A good photosensitizer will at this stage undergo a spin forbidden inter system crossing (ISC **4**) which requires a spin inversion, converting the photosensitizer to a triplet state  $T_1$  (10-2 seconds) with high efficiency. Triplet state relaxes back to ground state *via* spin forbidden radiative pathway (phosphorescence **5**) which imposes relatively long life time for triplet state or by internal conversion, radiationless transitions during collisions with other molecules. In oxygenated environments chromophores can undergo Type II photochemical process **6** which involves an energy transfer between excited triplet state of photosensitizer and stable triplet oxygen  $^3O_2$  producing short lived and highly reactive excited singlet oxygen  $^1O_2$ . Singlet oxygen is actually a highly polarized zwitterion and is considered to be a proficient cytotoxic agent. Type I process involves electron or hydrogen transfer process where the triplet state of photosensitizer interacts with biological substrates resulting in the formation of radicals and radical ions which on interaction with molecular oxygen gives rise to cytotoxic species like superoxide ion ( $O_2^-$ ) **7**.<sup>13</sup> It is generally thought that Type II mechanism predominates during PDT but it was found that Type I mechanism plays an important role at low oxygen concentrations and in more polar environments.<sup>13</sup> The short lifetime of singlet oxygen (100-250 ns) limits the range of propagation to approximately 45 nm in cellular medium and hence cannot diffuse more than a single cell length (diameter of human cell ranges from 10-100  $\mu$ m).<sup>13,14</sup> Hence, the primary generation of  $^1O_2$  warrants for the subcellular structures that can be accessed and destroyed. The photosensitizer is usually administered using an aqueous buffer solution or liposomes, the activating light is often generated by simple and economical lasers, which produce a coherent monochromatic light. Localization and biodistribution of photosensitizer in tissue and tumors depend on various factors such as hydrophobicity, pH, lymphatic drainage and lipoprotein binding. Other possible mechanisms which contributes to the tumor localization include aggregation, molecular charge and membrane potential of tumor cells. Many subcellular targets can be attacked during PDT, including mitochondria, lysosomes, plasma membrane and nuclei and it is the exact target, which decides whether cell death occurs by necrosis or apoptosis.<sup>15</sup>

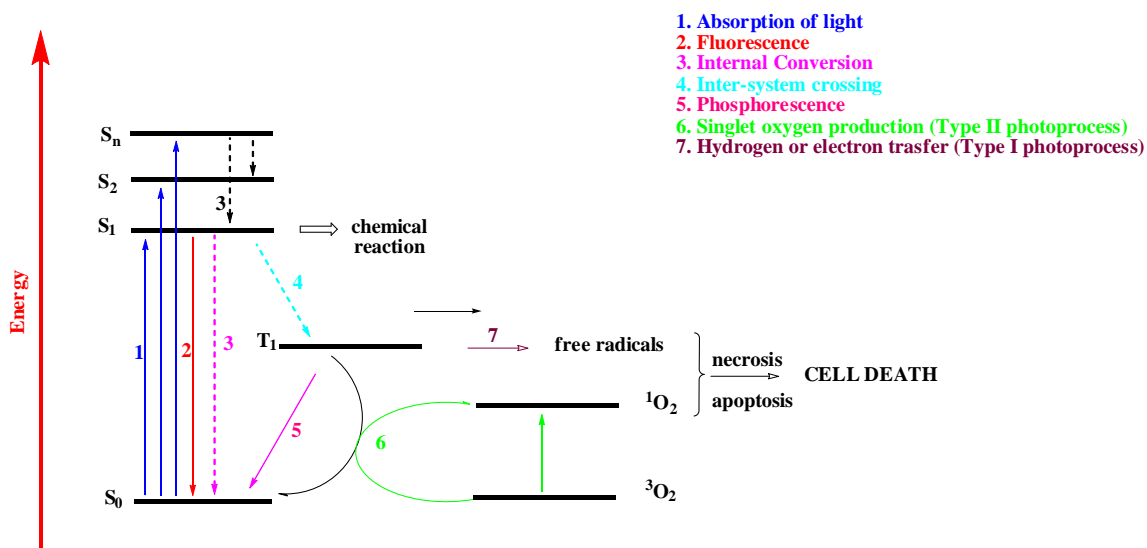


**Figure 4.** Jablonski energy level diagram for photodynamic therapy.

Thus in treating cancer with PDT (**Figure 5**), first step is the drug administration, followed by a period of incubation depending on the nature of photosensitizer used and is extremely necessary for the normal cells to get rid of the drug and the tumor cells to accumulate it. Third step is the illumination using laser which bring about the therapeutic effect. Finally, the exact method of PDT induced cell death relies primarily on the nature of the photosensitizer used and on the condition being treated and the light dose used.

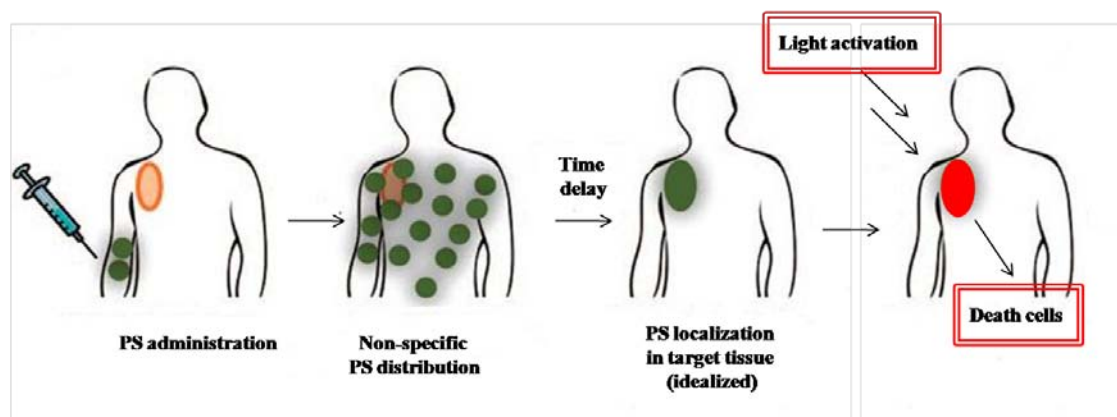


**Figure 5.** Schematic representation for PDT.<sup>i</sup>

<sup>i</sup> Figure adapted from “Imaging and Photodynamic Therapy: Mechanisms, Monitoring, and Optimization”, *Chem Rev.* **2010**, *110*, 2795–2838.

### 2.1.3 PHOTOSENSITIZERS

Among the several photosensitizers available, very few have been selected for clinical trials owing to many important factors. They include selectivity in terms of target cells against healthy cells, suitable extinction coefficients and accumulation rates in target tissues, stable composition and a chemical nature that may facilitate the entrance in the cell avoiding precipitation in aqueous environments.<sup>16</sup> The recent introduction of nanocarriers has partially modified this view, in that the properties of the PS may be not so important and that specificity toward target tissues may be improved using specific drug delivery strategies.<sup>19</sup> Photosensitizers are generally classified as porphyrins or non-porphyrins. Porphyrin-derived PS, in turn are classified as first, second or third generation PS.

#### 2.1.3.1 FIRST AND SECOND GENERATION PHOTOSENSITIZERS

First-generation PS are hematoporphyrin, its derivative HpD, and the purified, commercially available and yet largely employed Photofrin. This molecule originally approved for use in humans in 1993 in Canada, is now the PS most commonly used for the treatment of advanced stage lung, oesophageal, gastric and cervical cancer.<sup>17</sup> Beside the absence of intrinsic toxicity, other advantages offered by Photofrin include the possibility of using small drug doses, the good clearance from normal tissue and possibility of repeated administrations without serious consequences, but prolonged photosensitivity, for the neoplastic patient.<sup>18</sup>

Second generation PS include benzoporphyrin derivative, chlorins, phthalocyanines and texaphrins, as well as, naturally occurring compounds, such as hypericin, and substances that promote the production of the endogenous protoporphyrin IX (PpIX) as 5-aminolevulinic acid (5-ALA) and some ester derivatives.<sup>19</sup> 5-Aminolevulinic acid is a stable molecule<sup>20</sup> that behaves as a prodrug, since it is metabolically converted to the photo-sensitizable protoporphyrin IX.

An extremely potent second generation PS approved in Europe for the palliative treatment of neck and head cancers is Foscan. This compound, which has been shown to have a short plasma half-life in humans, is an hydrophobic molecule, is strongly

photoactivable (652 nm) with very high singlet oxygen yield while appearing to preferentially accumulate in tumor cells.<sup>21</sup> In addition, beside a direct damage to tumor cells, the curative effect of this drug is also attributed to its pharmacokinetic behavior that causes intense and sustained vascular damage.<sup>22</sup> Another PS that deserves particular mention is Talaporfin sodium (TS) a second-generation PS with a core chlorin structure containing a highly aromatic system. Its high water solubility and shorter half-life make it an attractive drug.<sup>23</sup> In preclinical experiments, activation of Talaporfin sodium with laser light (664 nm) generated singlet oxygen in a drug dose-dependent fashion. The depth of treatment is dependent on the ability of light to penetrate the target tissue with enough photons to activate the drug. Singlet oxygen causes significant alteration of macromolecules *via* oxidation of biological substrates such as DNA, membrane lipids, cholesterol and solvated molecules.<sup>24</sup> Preclinical studies have demonstrated that TS activation induces also systemic, tumor-specific immuno-modulation mediated by CD8+ T cells which involves up-regulation of both cytolytic and memory cells<sup>25</sup> and microvessels closure that may help in overcoming tumor resistance.<sup>26</sup>

### 5-AMINOLEVULINIC ACID

A new approach to PDT based on the use of endogenous photosensitizer protoporphyrin IX (**Scheme 1**), precursor in the biosynthesis of heme, was introduced in 1990. It made use of the above mentioned 5-aminolevulinic acid (**Figure 6**), which represent the first intermediate for the biosynthesis of heme.

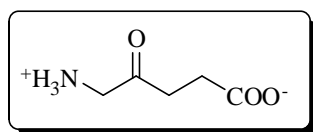
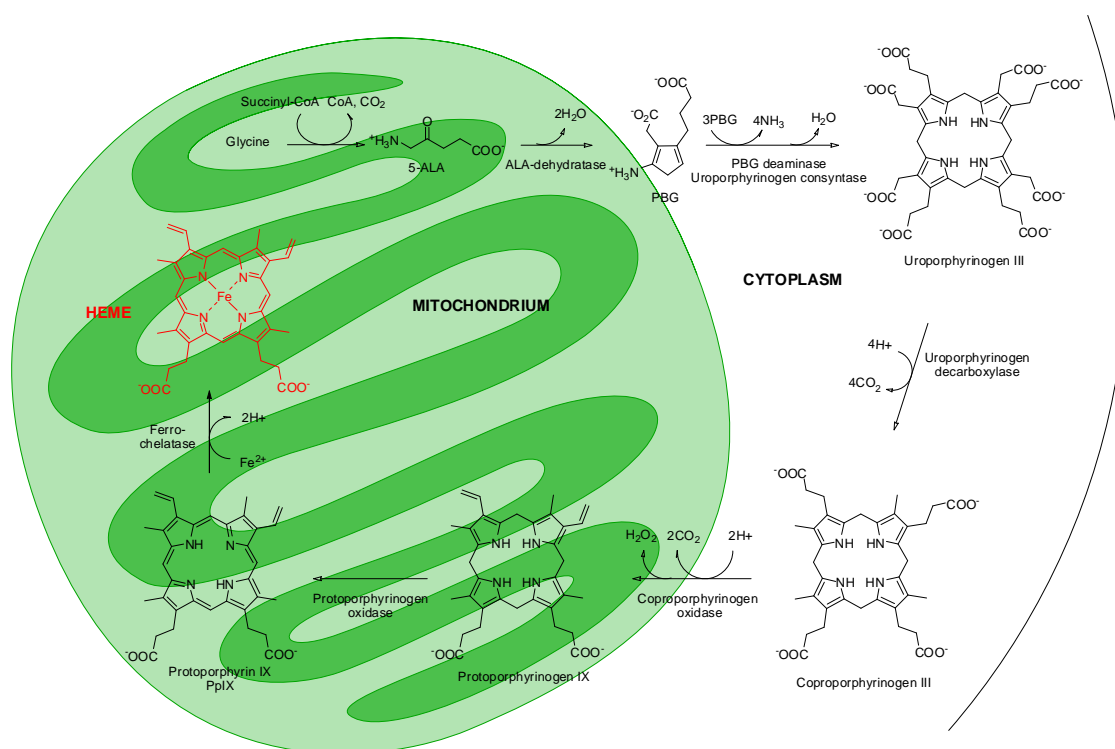


**Figure 6.** 5-Aminolevulinic acid.

### HEME BIOSYNTHESIS

It's important to note that almost all cells in the body have a requirement for heme, because it forms the reactive centre of a number of enzymes and proteins. These cells

must preserve a capacity for heme biosynthesis that occurs by the porphyrin biosynthetic pathway shown in **Scheme 1**. The synthesis of ALA is the first and rate-limiting step in the biosynthesis of heme. ALA is normally synthesized in mitochondria in the condensation reaction between glycine and succinyl-CoA<sup>27</sup> (**Scheme 1**), in presence of ALA synthase (ALAS) and pyridoxal-5-phosphate (PLP) as cofactor.<sup>28</sup> ALA so synthesized achieves cytosol, where it undergoes a condensation reaction with aminolevulinatase (ALAD), a zinc-dependent enzyme, and leads to the formation of porphobilinogen (PBG). The next step in heme biosynthesis involves combining four molecules of PBG to form an unstable tetrapyrrole (hydroxymethylbilane HMB), catalyzed by porphobilinogen deaminase (PBGD), which is covalently linked a cofactor, dipyrromethane, that consist of two PBG molecules. Four additional molecules of PBG attach to dipyrromethane leading to the formation of hexapyrrole. Afterwards, in the hydrolytic reaction, cleavage of the distal tetrapyrrole occurs, resulting in the release of HMB.<sup>29</sup> Uroporphyrinogen III synthase (URO3S) close HMB macrocycle leading to conversion of tetrapyrrole to uroporphyrinogen III.<sup>30</sup>



**Scheme 1.** Most important steps in the heme biosynthesis.

Uroporphyrinogen decarboxylase (UROD) catalyzes decarboxylation of all four acetate side chains of uroporphyrinogen III to methyl groups.<sup>31</sup> Coproporphyrinogen III so

formed, is transported into the membrane of mitochondria probably by peripheral-type benzodiazepine receptors (PBR).<sup>32</sup> Coproporphyrinogen oxidase (CPO) then catalyzes the conversion of coproporphyrinogen III to protoporphyrinogen IX with the release of H<sub>2</sub>O<sub>2</sub> and CO<sub>2</sub>, the reaction provides vinyl groups by oxidative decarboxylation of propionate groups.<sup>33</sup> The next intermediate in heme biosynthesis, protoporphyrin IX (PpIX), is synthesized in the mitochondria and requires FAD-containing protoporphyrinogen oxidase (PPO),<sup>34</sup> that catalyzes the conversion of protoporphyrinogen IX to PpIX in the six-electron oxidation. Ferrochelatase (FECH), another rate-limiting enzyme, is responsible for insertion of Fe<sup>2+</sup> into PpIX. The reaction occurs on the internal surface of the mitochondrial membrane.<sup>35</sup> This stage leads to the formation of the final product so completing the heme biosynthetic pathway.

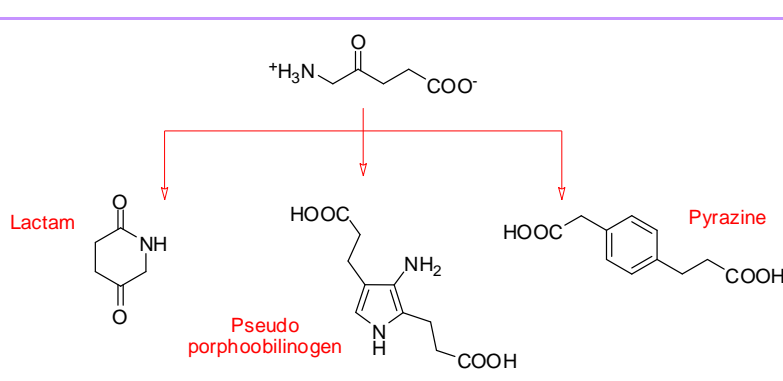
At present, knowledge about the mechanisms involved in ALA-based PDT is limited, particularly it is not clear the reason for preferential ALA uptake and conversion by tumors and dysplastic tissue. Various theories have been put forward to account for this selectivity, one of these suggested that tumors contain lower levels of ferrochelatase than the surrounding normal tissue, resulting in less efficient conversion of PpIX into heme within tumor cells and hence the build-up of PpIX. Moreover it is well established that tumors have a lower pH than normal cells and this may result in more PpIX retention in the tumor cells due to the various protonated species which may be formed from PpIX.

## **ADVANTAGES AND DISADVANTAGES OF 5-ALA**

The use of 5-ALA in PDT take the advantage of the fact that these compound is a small, in contrast to porphyrins, soluble molecule able to penetrate the abnormal stratum corneum overlying skin tumors. For this reasons, it can be applied topically unlike other photosensitizers. Moreover, in contrast to most tetrapyrrole photosensitizers, ALA-PpIX localizes in cells during the biosynthesis, rather than in the tumor vasculature. ALA and ALA-PpIX are rapidly cleared from the system, which results in an acceptably short period compared to HpD and Photofrin® of cutaneous photosensitivity or skin phototoxicity. This is viewed as an advantage over some of the other photosensitizers

where light protection may be required for several weeks. This allows multiple treatment regimens and thereby increases the efficacy of PpIX. Furthermore ALA can be easily synthesized unlike other porphyrin based photosensitizers, and the technique ALA-PDT is noninvasive, can be used to treat multiple lesions by short treatment sessions, produces excellent cosmetic results by not causing damage to surrounding tissue, has no side effects beyond slight pain during irradiation, and is well accepted by patients.<sup>36</sup>

On the contrary a significant shortcoming of ALA is its limited ability to cross certain biological barriers, such as cellular membranes due to its low lipid solubility.<sup>37</sup> PpIX is active at 630 nm, which should give adequate depth penetration; when topically administered, ALA does not penetrate thoroughly; it has limited input. The drawback associated with PDT is that, when ALA was administered systemically, patients have reported mild nausea.<sup>38</sup> Though multiple treatment regimens are possible, the efficacy of PpIX generation is decreased in the subsequent regimen if taken within 24 hours.<sup>39</sup> ALA is stable at acidic pH. In aqueous solutions buffered to a physiological pH, ALA dimerises to give pyrazine derivatives while at higher pH pseudo-porphobilinogen may be formed<sup>40</sup> and conversion to ester derivatives appears to worsen these problems. Esters are known to increase the potential for formation of lactam type derivatives (Scheme 2).



**Scheme 2:** ALA degradation products.

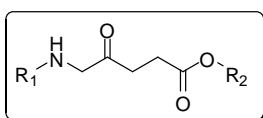
## 5-ALA DERIVATIVES: ESTERS

In order to overcome the shortcomings of ALA and improve its bioavailability, ALA can be derivatized. ALA has two principal functional groups, a carboxylic acid and an

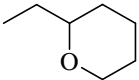
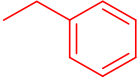
amino moiety which are both easily accessible for derivatization. The simplest way to alter the lipophilicity of ALA is via esterification of carboxylic function. The use of ALA derivatives as good candidates for the treatment of skin cancer has been extensively reviewed.<sup>41</sup>

Amongst ALA-derivatives that may have improved pharmacological properties compared with ALA, ALA esters were widely studied. They are more hydrophobic/lipophilic than ALA, and it was believed that they might be taken up into cells by different mechanisms, which might improve the efficiency of the therapy. The rationale was, that once inside cells ALA esters may be hydrolysed to ALA, which could then enter the heme biosynthetic pathway. Esters with various chain lengths<sup>42,43</sup> (**Table 1**) have indeed proved to be effective in both phototherapy and photodetection.<sup>44</sup> However, the mechanisms involved in the production of PpIX from ALA esters may not be as simple as first thought. Certainly the uptake is different from that of ALA itself.<sup>45</sup> Increased cellular uptake of lipophilic ALA esters resulting in enhanced PpIX concentrations has been demonstrated in a number of *in vitro* and *in vivo* systems.<sup>46</sup> Though these esters are incorporated into the cells at higher rate than ALA, studies conducted show that they also efflux at an increased rate mediated by passive diffusion.<sup>47</sup>

**Table1.** ALA derivatives.



ALA-derivatives	R <sub>1</sub>	R <sub>2</sub>
ALA-methyl (Metvixia <sup>®</sup> )	-H	-CH <sub>3</sub>
ALA-ethyl	-H	-C <sub>2</sub> H <sub>5</sub>
ALA-propyl	-H	-C <sub>3</sub> H <sub>7</sub>
ALA-butyl	-H	-C <sub>4</sub> H <sub>9</sub>
ALA-pentyl	-H	-C <sub>5</sub> H <sub>11</sub>
ALA-hexyl (Hexvix <sup>®</sup> )	-H	-C <sub>6</sub> H <sub>13</sub>
ALA-octyl	-H	-C <sub>8</sub> H <sub>17</sub>
R-S-ALA-2-(hydroxymethyl) hydrofuranyl	-H tetra-	

<i>R-S</i> -ALA-2-(hydroxymethyl) tetrahydropyranyl	-H	
ALA-benzyl (Benzvix <sup>®</sup> )	-H	
<i>N</i> -acetyl-ALA	CH <sub>3</sub> CO	-H
<i>N</i> -acetyl-ALA-ethyl	CH <sub>3</sub> CO	-C <sub>2</sub> H <sub>5</sub>
<i>N</i> -acetyl-ALA-butyl	CH <sub>3</sub> CO	-C <sub>4</sub> H <sub>9</sub>
<i>N</i> -butanoyl-ALA	CH <sub>3</sub> (CH <sub>2</sub> ) <sub>2</sub> CO-	-H
<i>N</i> -pentyl-ALA	CH <sub>3</sub> (CH <sub>2</sub> ) <sub>3</sub> CO-	-H
<i>N</i> -hexanoyl-ALA	CH <sub>3</sub> (CH <sub>2</sub> ) <sub>4</sub> CO-	-H
<i>N</i> -heptanoyl-ALA	CH <sub>3</sub> (CH <sub>2</sub> ) <sub>5</sub> CO-	-H

The most widely used ALA ester for in vitro work is ALA-hexyl ester.<sup>48</sup> Under the commercial name of Hexvix, it has been successfully used in the detection of bladder cancer and has already been approved in most countries of the European Union and European Economic Area countries. In addition, the new European guidelines recommended recently the use of blue light cystoscopy and Hexvix, for the diagnosis of bladder cancer.<sup>49</sup> On the other hand, it was shown that ALA methyl ester (Me-ALA) is very useful in the treatment of highly keratinised human lesions such as solar keratoses, reaching a higher ratio of porphyrins against normal skin after topical application.<sup>50</sup> A highly selective and homogeneous distribution of Me-ALA-induced porphyrin fluorescence was seen in human malignant lesions such as thick basal cell carcinomas.<sup>51</sup> Me-ALA, under the commercial name of Metvix is an approved drug for most of the European countries, USA, New Zealand, Australia and Brazil for certain non melanoma skin cancers such as superficial and nodular basal cell carcinomas, and actinic keratoses. Instead Benzvix is undergoing clinical trials for gastrointestinal cancers.

### 2.1.3.2 THIRD GENERATION PHOTOSENSITIZERS

Most therapeutic drugs distribute through the whole body, which results in general toxicity and poor acceptance of the treatments by patients. The targeted delivery of

chemotherapeutics to defined cancer cells is one of the main challenges and a very active field of research in the development of treatment strategies to minimize side-effects of drugs. Disease-associated cells express molecules, including proteases, receptors, or adhesion molecules, that are different or differently expressed than their normal counterparts. Therefore one goal in the field of targeted therapies is to develop chemically derivatized drugs or drug vectors able to target defined cells through specific recognition mechanisms.<sup>52</sup> This approach should also be able to overcome biological barriers.

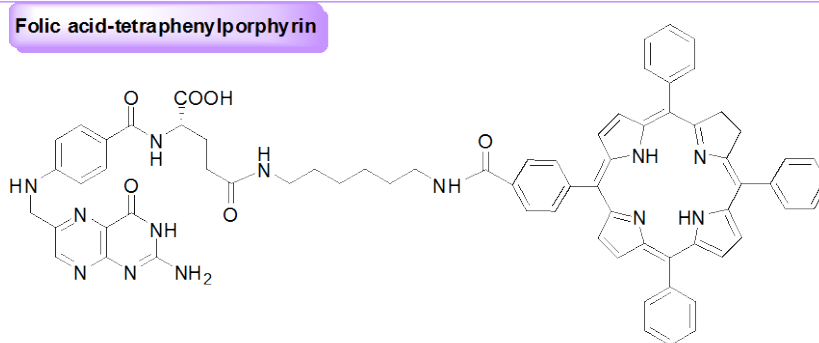
Four different strategies of improving selectivity (targeting) in PDT have been practiced so far.<sup>53</sup> First strategy for selective photosensitizer (PS) delivery utilizes targeting moieties, such as monoclonal antibodies (MAbs),<sup>54</sup> directed against antigens or ligands that are specifically overexpressed on cancer cells.

A second strategy which is commonly used, to improve the delivery of PS to target tissue involves their encapsulation in colloidal carriers, such as liposomes, oil-dispersions, polymeric particles, and polymers to facilitate drug delivery.<sup>55</sup>

Third strategy to selectively enhance PS levels in a disease site is to facilitate PS uptake more in the target tissue than the surrounding normal areas, through, for example several modification of PS taking advantage of certain properties of these cells, which either distinguish them from other cell or tissue types, or differentiate, malignant from normal cells. An note approach, is based on the altered sugar metabolism of cancer cells.<sup>56</sup> Rapidly growing tumors are able to maintain high glucose catabolic rate by upregulation of the enzyme hexokinase. This enzyme phosphorylates glucose to glucose-6-phosphate, which is then retained in the cell. Photosensitizers have been also functionalized with a large quantity of different sugars. Saccharides-porphyrin or –chlorin conjugates are probably the most active field of research in the targeting of photosensitizers.<sup>57</sup> The efficiency of the saccharide composition has been evaluated using xylosyl, arabinosyl, glucosyl, galactosyl or 2-aminoglucosamide groups.<sup>38</sup> When linked to a photosensitizer, uptake and accumulation in the endoplasmic reticulum and phototoxicity were increased in cancer cells. The length of the oligosaccharide is also an important factor for the membrane penetration.<sup>58</sup>

Fourth strategy is to conjugate photosensitizer (PS) with specific receptors which are over expressed in cancer cells. This helps in receptor mediated endocytosis. One ligand suited for this purpose is folic acid thanks to the features reported in the Chapter

1. For example tetraphenylporphyrin (TPP) has been conjugated to folic acid (**Scheme 3**) to target tumor cells overexpressing its receptors.<sup>59</sup> Cellular uptake and photodynamic activity of the conjugate on human nasopharyngeal cell line were greatly increased compared to free TPP and competitive assays using free folic acid demonstrated folate-receptor dependent uptake of the conjugate.



**Scheme 3:** Tetraphenylporphyrin (TPP) has been conjugated to folic acid.

On the contrary of this conjugated with tetraphenylporphyrin, on the basis of what just described, our attention has been concerned in the synthesis of folate-conjugated (reported in the next section) with 5-ALA and its methyl ester derivative precursors of porphyrin.

- 
- <sup>1</sup> a) Henderson, B.W.; Dougherty, T.J. *Photodynamic Therapy: Basic Principles and Clinical Applications*, Marcel Dekker: New York, **1992**. b) MacDonald, I.J.; Dougherty, T.J. *J. Porphyrins Phthalocyanines.*, **2001**, 5, 105.
- <sup>2</sup> Spikes, J.D. *Life Sciences*, **1985**. (Primary Photo-Processes Biol. Med.), 209-27.
- <sup>3</sup> Raab, O., *Zeitschrift fuer Biologie* (Munich), **1900**, 39, 524-546.
- <sup>4</sup> a) Finsen, N.R. *Lancet*, **1904**, 2, 1272.  
b) Finsen, N.R. *Journal of the American Medical Association*, **1903**, 41, 1207-1208.
- <sup>5</sup> a) Finsen, N.R. *British Medical Journal*, **1903**, 1297-1298. b). von Tappeiner, H.; Jodlbauer, A.; Lehmann, H. *Arch. klin. Med.* 82, 217-22.
- <sup>6</sup> Szeimies, R.M.; Dräger, J.; Abels, C.; Landthaler, M. *History of photodynamic therapy in dermatology. Photodynamic therapy and fluorescence diagnosis in dermatology*. Amsterdam: Elsevier, **2001**, 3-16.
- <sup>7</sup> Meyer-Betz, F. *Dtsch Arch Klin Med*, **1913**, 112, 476–503.
- <sup>8</sup> Figge, F.H.J., G.S. Weiland, and L.O.J. Manganiello, *Proceedings of the Society for Experimental Biology and Medicine*, **1948**, 68, 640-41.
- <sup>9</sup> Lipson, R.L. and E.J. Baldes, *Archives of Dermatology*, **1960**, 82, 508-516.
- <sup>10</sup> Dougherty, T.J., Kaufman, J.H.; Goldfarb, A.; *Cancer Res.*, **1978**, 38(8), 2628-2635.
- <sup>11</sup> Dougherty, T.J., Gomer, C.J.; Henderson, B.W.; Jori, G.; Kessel, D.; Korbélik, M.; Moan, J.; Peng, Q. *J. Natl. Cancer Inst.*, **1998**, 90, 889-905.
- <sup>12</sup> Sternberg, E.D.; Dolphin, D.; Brückner, C. *Tetrahedron*, **1998**, 54, 4151.
- <sup>13</sup> a) Ochsner, M. *J. Photochem. Photobiol. B.*, **1997**, 39, 1. b) Rosenthal, L.; Ben-Hur, E. *Int. J. Radiat. Biol.*, **1995**, 67, 85.
- <sup>14</sup> Moan, J. *J. Photochem. Photobiol. B.*, **1990**, 6, 343.
- <sup>15</sup> a) Zamzami, N.; Susin, S. A.; Marchetti, P.; Hirsch, T.; Gomez-Monterrey, I.; Castedo, Kroemer, G. *J. Exp. Med.*, **1996**, 183, 1533. b) Gomer, C. J.; Luna, M.; Ferrario, A.; Wong, S.; Fischer, A. M. R.; Rucker, N. *J. Clinical Laser Med. Surgery.*; **1996**, 14, 315. c) Hamblin, M.; Newman, E. L. *J. Photochem. Photobiol. B.*, **1994**, 23, 3.
- <sup>16</sup> Bechet, D.; Couleaud, P.; Frochot, C.; Viriot, M.L.; Guillemin, F.; Barberi-Heyob M. *Trends Biotechnol.* **2008**, 26, 612-621.

- 
- <sup>17</sup> a) Almeida, R.D.; Manadas, B.J.; Carvalho, A.P.; Duarte, C.B. *Biochim. Biophys. Acta* **2004**, *1704*, 59-86.
- b) Dougherty, T.J. *J. Clin. Laser Med. Surg.* **2002**, *20*, 3-7.
- <sup>18</sup> a) Mäky, P.; Messmann, H.; Regula, J.; Conio, M.; Pauer, M.; Millson, C.E.; MacRobert, A.J.; Bown, S.G. *Neoplasma* **1998**, *3*, 157-161. b) Sibata, C.H.; Colussi, V.C.; Oleinick, N.L.; Kinsella, T.J. *Expert Opin. Pharmacother.* **2001**, *2*, 917-927.
- <sup>19</sup> Agostinis, P.; Buytaert, E.; Breyskens, H.; Hendrickx, N. *Photochem. Photobiol. Sci.* **2004**, *3*, 721-729.
- <sup>20</sup> Elfsson, B.; Wallin, I.; Eksborg, S.; Rudaeus, K.; Ros, A.M.; Ehrsson, H. *Eur. J. Pharm. Sci.* **1998**, *7*, 87-91.
- <sup>21</sup> a) Ronn, A.M.; Nouri, M.; Lofgren, L.A.; Steinberg, B.M.; Westerborn, A.; Windahl, T.; Shikowitz, M.J.; Abramson A.L. *Lasers Med. Sci.* **1993**, *11*, 267-272. a) Mitra, S.; Foster, T.H. *Photochem. Photobiol.* **2005**, *81*, 849-859. c) Molinari, A.; Bombelli, C.; Mannino, S.; Stringaro, A.; Toccaceli, L.; Calcabrini, A.; Colone, M.; Mangiola, A.; Maira, G.; Luciani, P.; Mancini, G.; Arancia, G. *Int. J. Cancer* **2007**, *121*, 1149-1155.
- <sup>22</sup> Triesscheijn, M.; Ruevekamp, M.; Out, R.; Van Berkel, T.J.; Schellens, J.; Baas, P.; Stewart, F.A. *Cancer Chemother. Pharmacol.* **2007**, *60*, 113-122.
- <sup>23</sup> Wang, S.; Bromley, E.; Xu, L.; Chen, J.C.; Keltner, L. Talaporfin Sodium. *Expert Opin. Pharmacother.* **2010**, *11*, 133-140.
- <sup>24</sup> Wright, A.; Bubb, W.A.; Hawkins, C.L.; Davies, M. *J. Photochem. Photobiol.* **2002**, *76*, 35-46.
- <sup>25</sup> Bromley, E.; Owczarczak, B.; Keltner, L.; Wang, S.; Gollnick, O. *J. Clin. Oncol.* **2009**, *27*, 3052.
- <sup>26</sup> a) McMahan, K.S.; Wieman, T.J.; Moore, P.H.; Fingar, V.H. *Cancer Res.* **1994**, *54*, 5374-5379. b) Shibuya, H.; Aizawa, K.; Okunaka, T., Konaka, C.; Saito, K.; Kato H. *J. Tokyo Med. Univ.* **1999**, *57*, 136-144.
- <sup>27</sup> a) Ajioka, R.S.; Phillips, J.D.; Kushner, J.P. *Biochim. Biophys. Acta* **2006**, *1763*, 723-736. b) Fukuda, H.; Casas, A.; Battle, A. *Int. J. Biochem. Cell. Biol.* **2005**, *37*, 272-276. c) Ishizuka, M.; Abe, F.; Sano, Y.; Takahashi, K.; Inoue, K.; Nakajima, M.; Kohda, T.; Komatsu, N.; Ogura, S.I.; Tanaka, T. *Int. Immunopharmacol.* **2011**, *11*, 358-365.
- <sup>28</sup> Riddle, R.D.; Yamamoto, M.; Engel, J.D. *Proc. Natl. Acad. Sci. USA* **1989**, *86*, 792-796.

- 
- <sup>29</sup> Shoolingin-Jordan, P.M.; Al-Dbass, A.; McNeill, L.A.; Sarwar, M.; Butler, D. *Biochem. Soc. Trans.* **2003**, *31*, 731-735.
- <sup>30</sup> Jordan, P.M.; Seehra, J.S. *FEBS Lett.* **1979**, *104*, 364-366.
- <sup>31</sup> Straka, J.G.; Kushner, J.P. *Biochem.* **1983**, *22*, 4664-4672.
- <sup>32</sup> a) Taketani, S.; Kohno, H.; Furukawa, T.; Tokunaga, R. *J. Biochem.* **1995**, *117*, 875-880. b) Taketani, S.; Kohno, H.; Okuda, M.; Furukawa, T.; Tokunaga, R. *J. Biol. Chem.* **1994**, *269*, 7527-7531.
- <sup>33</sup> Yoshinaga, T.; Sano, S. Coproporphyrinogen oxidase. II. *J. Biol. Chem.* **1980**, *255*, 4727-4731.
- <sup>34</sup> a) Dailey, T.A.; Dailey, H.A. *J. Biol. Chem.* **1998**, *273*, 13658-13662.
- <sup>35</sup> Wu, C.K.; Dailey, H.A.; Rose, J.P.; Burden, A.; Sellers, V.M.; Wang, B.C. *Nat. Struct. Biol.* **2001**, *8*, 156-160.
- <sup>36</sup> Wolf, P. Kerl, H. *Dermatology*, **1995**, *190*, 183-5.
- <sup>37</sup> Kloek, J. Beijersbergen v.H. *J. Photochem. Photobiol.*, **1996**, *64*, 994-1000.
- <sup>38</sup> Peng, Q.; Warloe, T.; Berg, K.; Moan, J.; Kongshaug, M.; Giercksky, K.E.; Nesland, J.M. *Cancer*, **1997**, *79*, 2282-2308.
- <sup>39</sup> Gibson, S.L., Havens, J.J.; Foster, T.H.; Hilf, R. *Br. J. Cancer*, **1999**, *80*, 998-1004.
- <sup>40</sup> a) Butler, A.R. and S. George, *Tetrahedron*, **1992**, *48*, 7879-86. b) Jaffe, E.K. and J.S. Rajagopalan, *Bioorg. Chem.*, **1990**, *18*, 381-94. c) Gadmar, O.B., et al., *J. Photochem. Photobiol. B.* **2002**, *67*, 187-193. d) Bunke, A., et al., *J. Pharm. Sci.*, **2000**, *89*, 1335-1341. e) Elfsson, B., et al., *Eur. J. Pharm. Sci.*, **1999**, *7*, 87-91.
- <sup>41</sup> a) Lopez, R.F.V., et al., *Adv. Drug Deliv. Rev.*, **2004**, *56*, 77-94. b) Brown, S.B., E.A. Brown, and I. Walker, *Lancet Oncology*, **2004**, *5*, 497-508.
- <sup>42</sup> a) Peng, Q., et al., *J. Photochem. Photobiol. B.*, **1996**, *34*, 95-6. b) Peng, Q., et al., *J. Photochem. Photobiol.*, **1995**, *62*, 906-13.
- <sup>43</sup> a) Kloek, J. and H. Beijersbergen van, *J. Photochem. Photobiol.*, **1996**, *64*, 994-1000. b) Kloek, J., W. Akkermans, and G.M. Beijersbergen van Henegouwen, *J. Photochem. Photobiol.*, **1998**, *67*, 150-4.
- <sup>44</sup> a) Gerscher, S., et al., *J. Photochem. Photobiol. B.*, **2000**, *72*, 569-574. b) Lange, N., et al., *British Journal of Cancer*, **1999**, *80*, 185-193.
- <sup>45</sup> Rud, E.; Gederaas, O.; Hogset, A.; Berg, K. *J. Photochem. Photobiol. B.*, **2000**, *71*, 640-647.

- 
- <sup>46</sup> a) Peng, Q., et al., *J. Photochem. Photobiol. B.*, **1996**, *34*, 95-96. B) b) Kloek, J., W. Akkermans, and G.M. Beijersbergen van Henegouwen, *J. Photochem. Photobiol.*, **1998**, *67*, 150-154. c) Gaullier, J.M., et al., *Cancer Res.*, **1997**, *57*, 1481-1486.
- <sup>47</sup> Di Venosa, G.; Fukuda, H.; Batlle, A.; MacRobert, A.; Casas, A. *J. Photochem. Photobiol.B.*, **2006**, *83*, 129-136.
- <sup>48</sup> A. Casas, A.M. Batlle, A.R. Butler, D. Robertson, E.H. Brown, A. MacRobert, P.A.Riley, *Br. J. Cancer* **1999**, *80*, 1525–1532.
- <sup>49</sup> van der Meijden, A.P.; Sylvester, R.; Oosterlinck, W.; Solsona, E.; Boehle, A.; Lobel, B.; Rintala, E. *Eur. Urol.* **2005**, *48*, 363–371.
- <sup>50</sup> Fritsch, C.; Homey, B.; Stahl, W.; Lehmann, P.; Ruzicka, T.; H. Sies, *J. Photochem. Photobiol.*, **1998** *68*, 218–221.
- <sup>51</sup> Peng, Q.; Soler, A.; Warloe, T.; Nesland, J.; Giercksky, K.J.; *J. Photochem. Photobiol. B.* **2001**, *62*, 140–145.
- <sup>52</sup> a) Demidova, T.N.; Hamblin, M.R. *Int. J. Immuno. Pharm.*, **2004**, *17*, 117-126. b) Sharman, W.M., J.E. van Lier, and C.M. Allen, *Adv. Drug Deliv. Rev.*, **2004**, *56*, 53-76. c) Hamblin, M.R. **2002**, *9*, 1-24.
- <sup>53</sup> Solban, N.; Rizvi, I.; Hasan, T. *Lasers Surg Med*, **2006**, *38*, 522-31.
- <sup>54</sup> van Dongen, G.A.M.S.; Visser, G.W.M.; Vrouenraets, M.B. *Adv. Drug Deliv. Rev.*, **2004**, *56*, 31-52.
- <sup>55</sup> b) Konan, Y.N.; Gurny, R., Allemann, E.; *J. Photochem. Photobiol.B.*, **2002**, *66*(2), 89-106.
- <sup>56</sup> Zhang, M.; Zhang Z.H.; Blessington, D.; Li, H.; Busch, T.M.; Madrak, V.; Miles, J.; Chance, B.; Glickson, J.D.; Zheng, G. *Bioconjug. Chem.*, **2003**, *14*, 709-714.
- <sup>57</sup> Schell, C. and H.K. Hombrecher, *Bioorg. Med. Chem.*, **1999**, *7*, 1857-1865.
- <sup>58</sup> Desroches, M.C.; Kasselouri, A.; Meyniel, M.; Fontaine, P.; Goldmann, M.; Prognon, P.; Maillard, P.; Rosilio, V. *Langmuir*, **2004**, *20*, 11698-11705.
- <sup>59</sup> Schneider, R.; Schmitt, F.; Frochot, C.; Fort, Y.; Lourette, N.; Guillemin, F.; Muller, J.; Barberi Heyob, M. *Bioorg. Med. Chem.*, **2005**, *13*, 2799-2808.

## 2.2 RESULTS AND DISCUSSION

On the basis of the considerations given in the introduction and the promising results obtained for folate-conjugates described in the Chapter 1, the present work is focalized on development of new folate-based drug delivery systems for the selective transport of photosensitizers (FA-PS) in tumor cells.

These systems (as described in Chapter 1) consist of 4 modules: folic acid, a linker, a cleavable bond and a photosensitizer as 5-ALA and its methyl ester derivative (**Figure 1**). Beside the linkers already used for molecular systems previously cartooned, in this work we considered a third  $\beta$ -peptide-based linker prepared by solid phase synthesis in collaboration with Dr Giovanni Roviello (CNR of Napoli). The synthesis of this new compound are reported below.

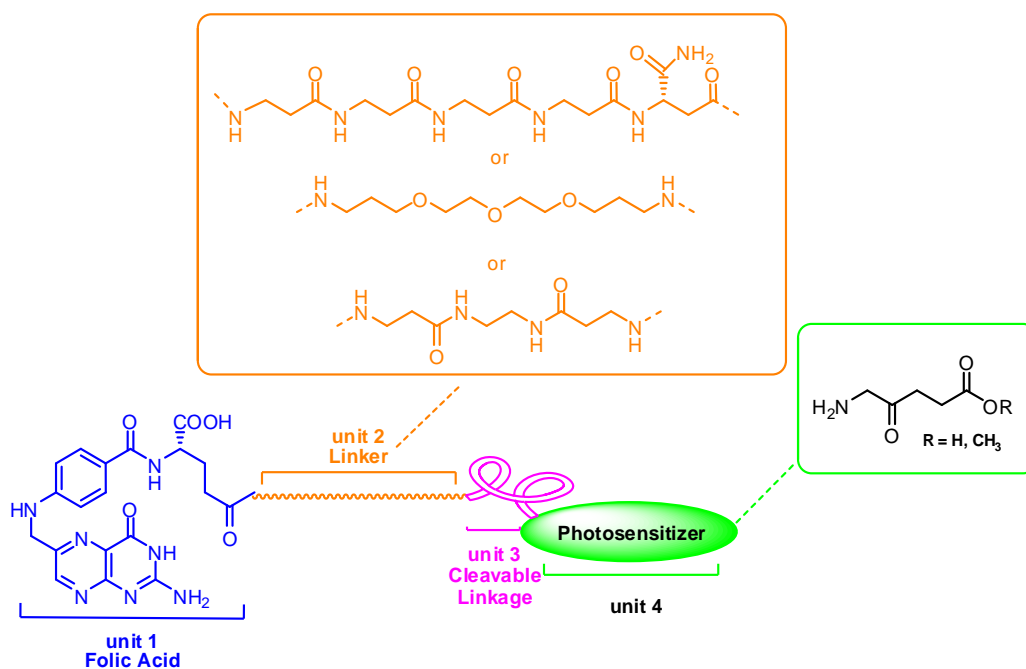


**Figure 1.** Carrier linked prodrug system for photodynamic therapy.

### 2.2.1 SYNTHESIS OF FA-5-ALA CONJUGATES 1 AND 2.

The synthesis of conjugates **1** and **2** (Figure 2) was carried out through an easy procedure starting from folate derivatives **4** and **5** prepared as previously described in Chapter 1, and 5-ALA suitably protected by reaction with  $\text{Boc}_2\text{O}$  and  $\text{NaOH}$  in a  $\text{H}_2\text{O}/1,4$ -dioxane mixture for 24h.

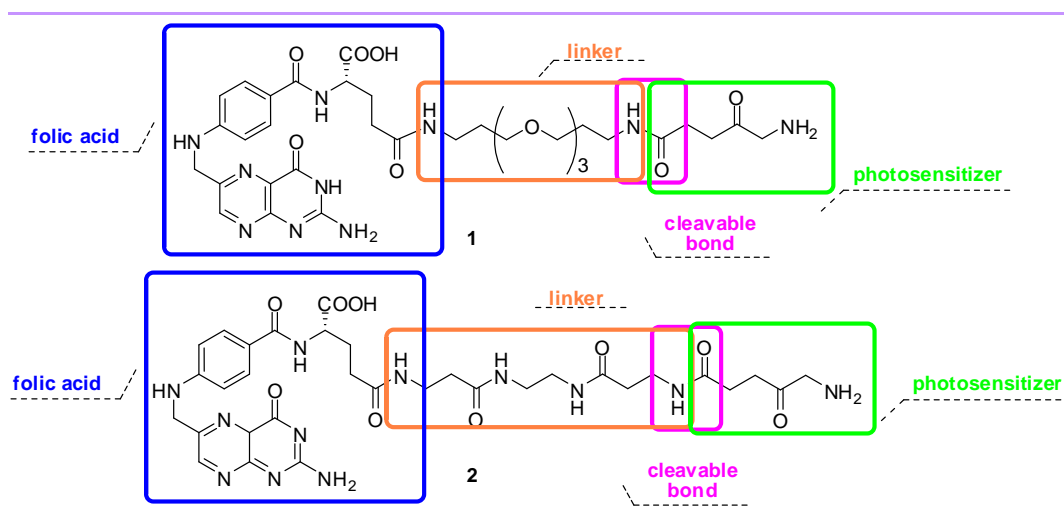
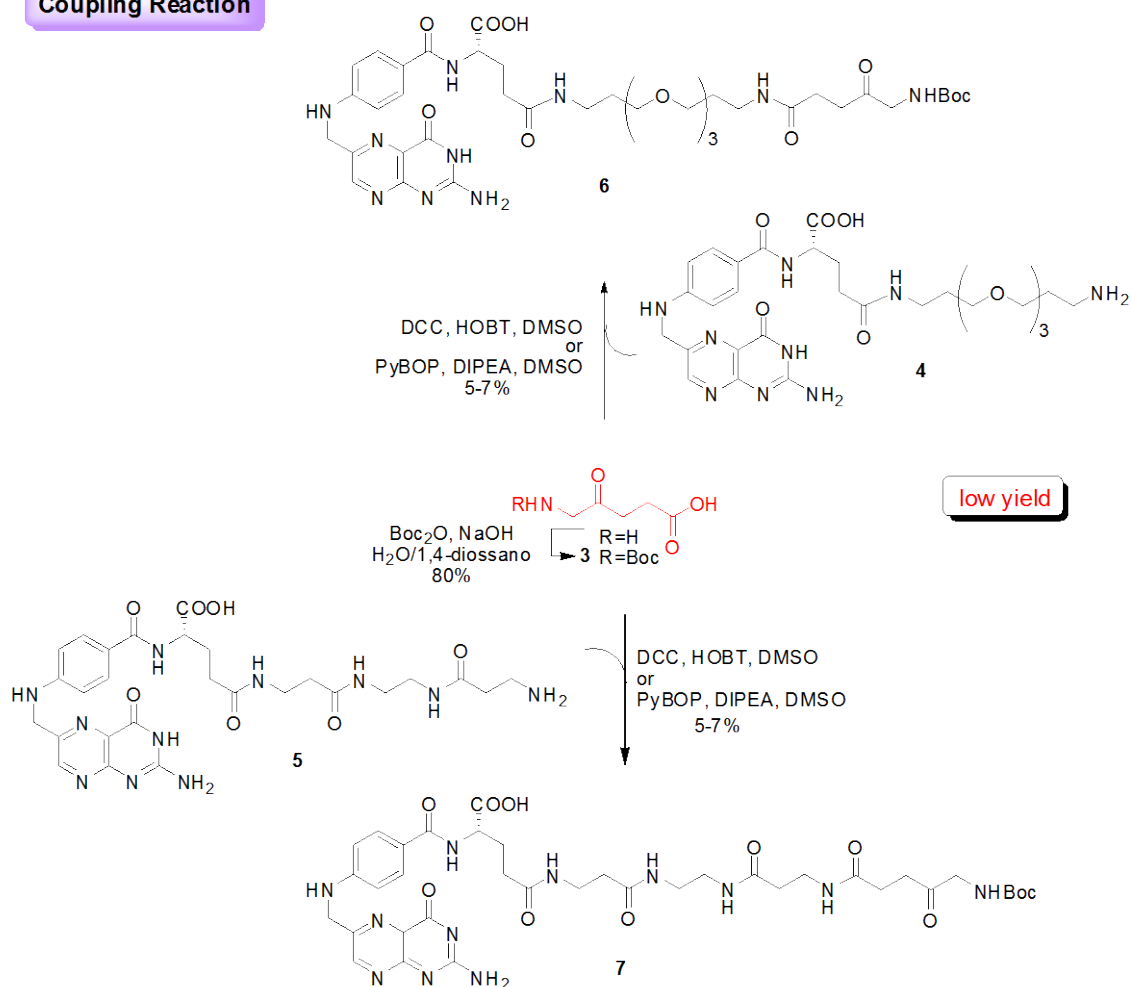


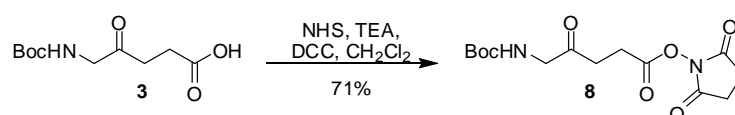
Figure 2. Folate conjugate 1-2

The omologation reaction between *N*-Boc-5ALA **3** and the compounds **4** and **5** was carried out by testing different reaction conditions including the *in situ* activation of the carboxyl function of **3** using reagents such as DCC or PyBOP. In all cases, the results were not satisfactory, indeed the conjugation products was formed only in low yield (Scheme 1).

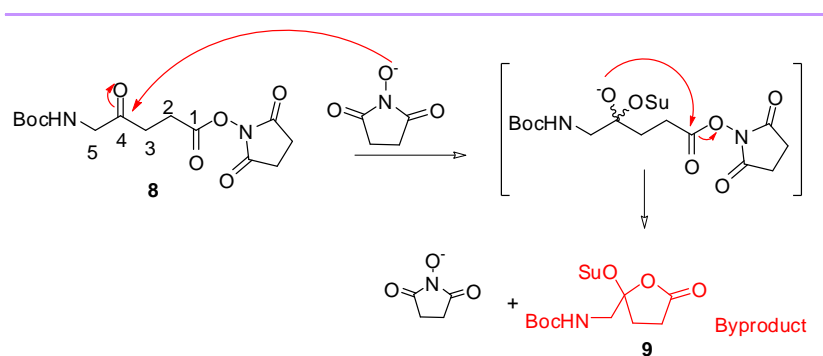
## Coupling Reaction

Scheme 1. Synthesis of folic acid-conjugates **6** and **7**.

With the aim to get the 5-ALA conjugates **6** and **7** with a better chemical yield, *N*-Boc-5-ALA was first converted in corresponding succinimidyl ester **8** by reaction of **3** with NHS, DCC and TEA in dichloromethane (71% yield, **Scheme 2**). It's interesting to note that in presence of a slight excess of NHS (1.2 eq) and extended reaction times (3h), the desired product *N*-Boc-5-ALA-OSu (**8**) was transformed quantitatively in the lactone compound (**9**).

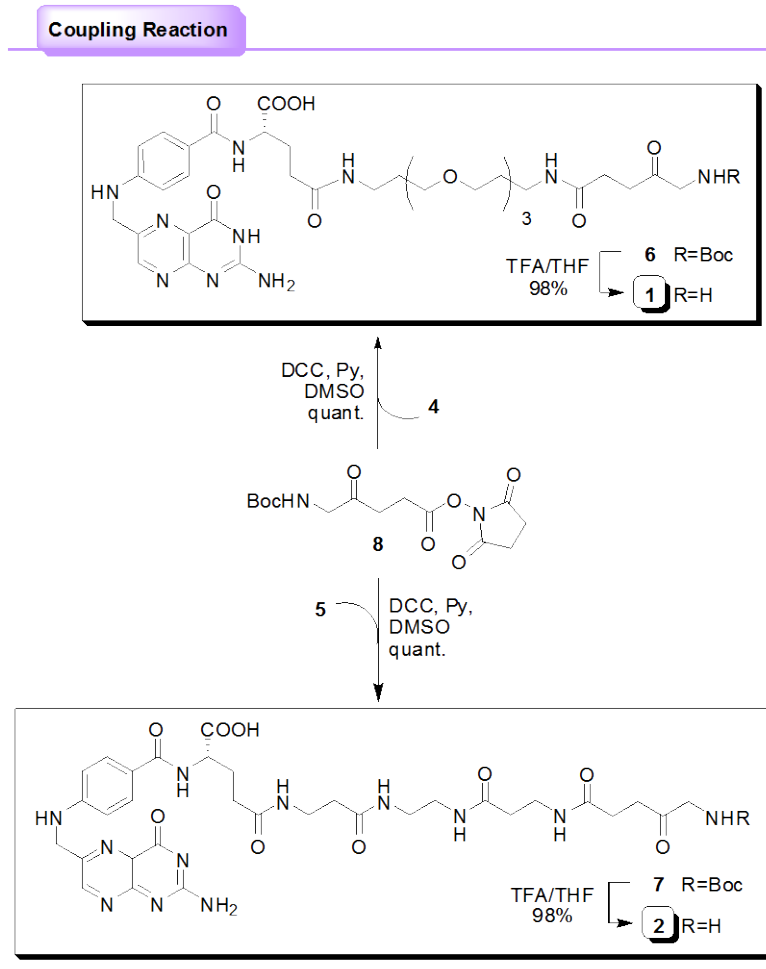
Scheme 2. Formation of *N*-Boc-5-ALA-OSu.

In **Scheme 3** the hypothesized mechanism for the formation of this product is shown: the *N*-hydroxysuccinimide, present in the reaction mixture, lead nucleophilic attack on ketone function at C-4 position. The generated anion can provide an intramolecular lactonization, entropically favored, leading to the formation of  $\gamma$ -lactone **9** and *N*-hydroxysuccinimide that can afford even to the complete conversion of **8**.



**Scheme 3.** Hypothesized mechanism for formation of byproduct **9**.

Finally, the 5-ALA so activated was used in the coupling reaction with derivatives **4** and **5** in presence of DCC and Py in DMSO (**Scheme 4**). In this case, the reaction provided the desired FA-5ALA conjugates in quantitative yield.



**Scheme 4.** Synthesis of folate-5ALA 1-2.

Finally treatment of compound **6** and **7** with TFA in THF gave FA-PS **1** and **2** with high yield (98%).

### 2.2.2 SYNTHESIS OF CONJUGATE 3

Folate conjugate **3** contain a pentapeptide linker, consisting of  $\beta$ -Alanine (four units) and aspartic acid (one unit) linked 5-ALA methyl ester as photosensitizer agent (**Figure 3**). The preparation of FA-PS conjugated was accomplished by solid-phase synthesis and involved the main following synthetic steps:

- ✚ preparation of the linker
- ✚ subsequent conjugation of the latter with folic acid
- ✚ detachment from resin and coupling with the photosensitizer.

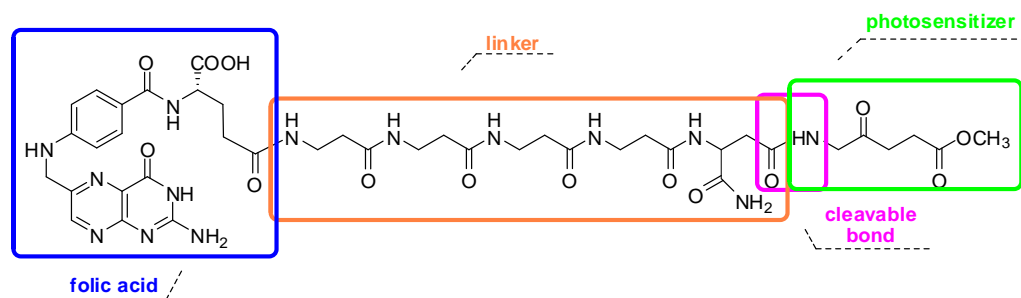


**Figure 3.** Folate-conjugate 3.

The peptide sequence has been synthesized starting from *C*-terminal carboxyl group of aspartic acid in  $\alpha$ -position which was used for anchoring to the solid phase, then the amino group was coupled to the group of the first  $\beta$ -alanine unit.  $\beta$ -Carboxyl group of aspartic acid was protected as *t*-butyl ester, an acid-labile group, stable in alkaline conditions. Fmoc group was used to protect the  $\beta$ -alanine amino function. Protected aspartic acid **10**, commercially available at low cost, has been linked to Rink Amide-MBHA resin (**Figure 4**) after removal of *N*-Fmoc protection, as reported in the literature.<sup>1</sup>

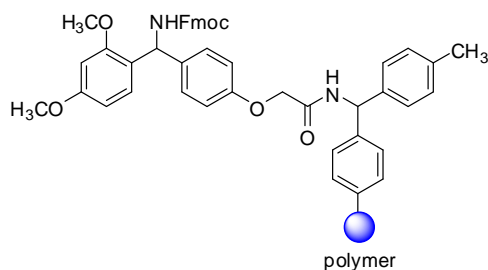
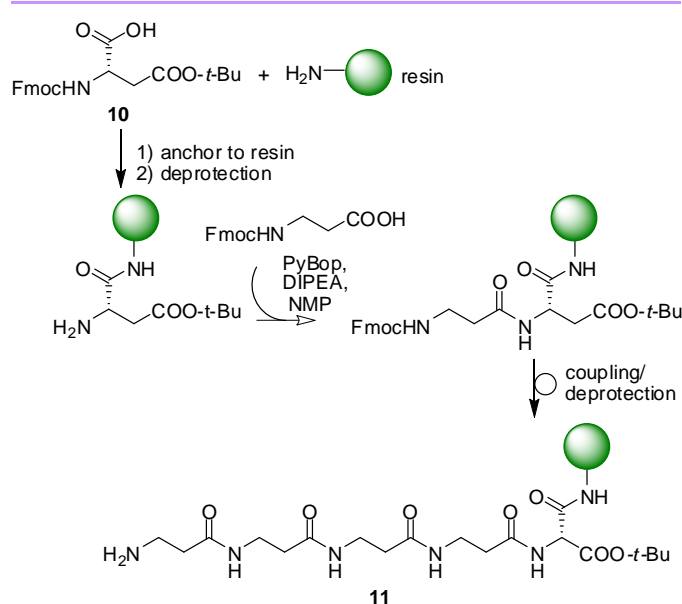


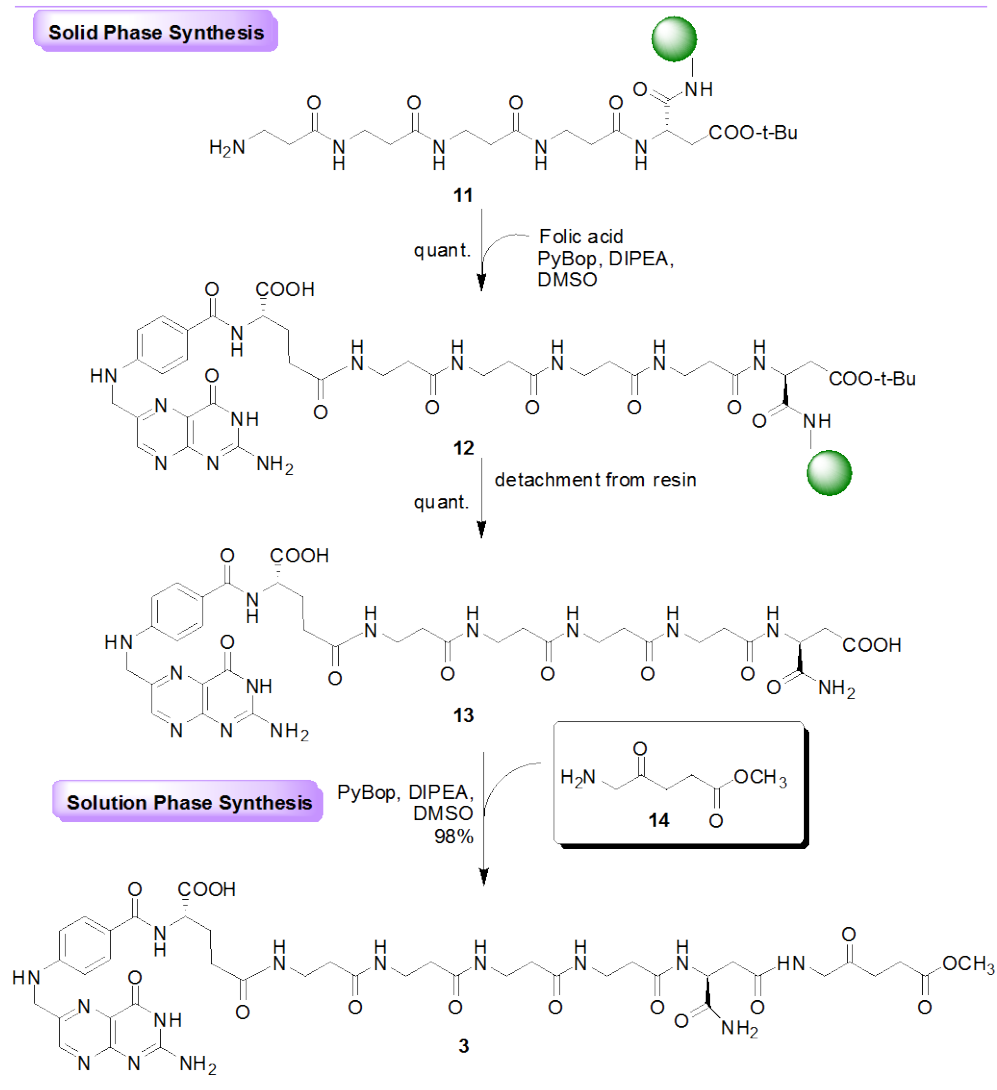
**Figure 4.** Rink Amide-MBHA resin.

Subsequently a Fmoc  $\beta$ -alanine unit was added by a coupling reaction in presence of PyBop and DIPEA in NMP. Iterating this technique three more units of  $\beta$ -alanine were then added to afford the product **11** in quantitative yield (**Scheme 5**). Reaction monitoring was possible thanks to the presence of  $\beta$ -alanine Fmoc protecting group.



**Scheme 5.** Solid-phase synthesis of polyamide linker **11**.

Linker **11** anchored to the resin, was then coupled with FA unit under the same reaction conditions allowing to prepare the compound **3**. The product **12** so obtained was detached from resin by acid hydrolysis (TFA/H<sub>2</sub>O/TIS) to provide the folate conjugate **13** with 97% yield (**Scheme 6**).



**Scheme 6.** Synthesis of folate conjugate **3**.

The last step of this synthesis consisted in the conjugation of folate-derivative **13** to 5-ALA methyl ester **14**. This reaction was carried out by treatment with PyBop and DIPEA in DMSO to give the desired compound **3** with 98% yield (**Scheme 6**).

<sup>1</sup> Boussard, C.; Doyle, V. E.; Mahmood, N.; Klimkait, T.; Pritchard, M.; Gilbert, I. H. *Eur. J. Med. Chem.* **2002**, *37*, 883-890.

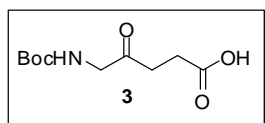
## 2.3 CONCLUSION

Photodynamic therapy is a minimally invasive treatment for the cure of malignant diseases. As clearing of the photosensitizer is often a limiting factor in PDT, the study of 5-aminolevulinic acid and its derivatives, has been receiving increasing attention. In an attempt to improve cell selectivity of ALA and its derivatives, in this work we realized an easy methodology to synthesize new folate-based carrier linked prodrugs (**1-3**) that will be subjected, in the laboratory of Prof. Giuseppe Palumbo (Department of Biology, Cellular and Molecular Pathology “L. Califano” University of Napoli Federico II), to experiments of fluorescence spectroscopy on different cell lines in order to obtain useful information on the biocompatibility and on cellular internalization of our molecular systems. In addition, further studies will be conducted to demonstrate the actual release of 5-ALA and of 5-ALA methyl ester in the tumor site, verifying the possible application of the derivatives in photodynamic therapy.

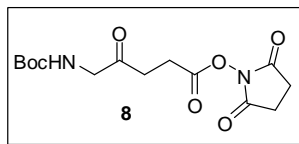
## 2.4 EXPERIMENTAL SECTION

All moisture-sensitive reactions were performed under a nitrogen atmosphere using oven-dried glassware. Solvents were dried over standard drying agents and freshly distilled prior to use. Reactions were monitored by TLC (precoated silica gel plate F254, Merck). Column chromatography: Merck Kieselgel 60 (70-230 mesh); flash chromatography: Merck Kieselgel 60 (230-400 mesh).  $^1\text{H}$  and  $^{13}\text{C}$  NMR spectra were recorded on NMR spectrometers operating on Varian VXR (200 MHz), Bruker DRX (400 MHz) or Varian Inova Marker (500 MHz), using  $\text{CDCl}_3$  solutions unless otherwise specified. In all cases, tetramethylsilane (TMS) was used as internal standard for calibrating chemical shifts ( $\delta$ ). Coupling constant values ( $J$ ) were reported in Hz. Combustion analyses were performed by using CHNS analyzer.

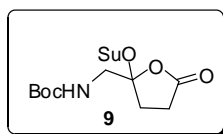
### 2.4.1 SOLUTION-PHASE SYNTHESIS



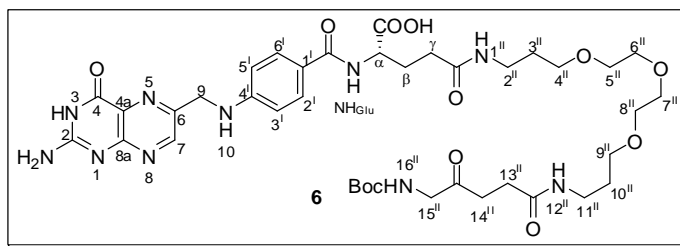
**Compound 3.** To a stirring solution of 5-aminolevulinic acid (200 mg, 1.53 mmol) in  $\text{H}_2\text{O}$  (2.4 mL), at  $0\text{ }^\circ\text{C}$ , a solution of NaOH (0.1 N) was added dropwise until pH 8-10. After a few minutes  $\text{Boc}_2\text{O}$  (6.2 g, 8.07 mmol) in 1,4-dioxane (2.4 mL) was added. The mixture was stirred at room temperature for 24h, and then was acidified with a solution of HCl 1M until pH  $\sim$  4. The solution was extracted with EtOAc and washed with  $\text{H}_2\text{O}$ . The organic phase was dried on  $\text{Na}_2\text{SO}_4$  and the solvent evaporated under reduced pressure, to offer the pure **9** (278 mg, 80% yield) without further purification:  $^1\text{H}$  NMR (500 MHz,  $\text{CDCl}_3$ )  $\delta$ : 1.43 (s, 9H,  $\text{C}(\text{CH}_3)_3$ ), 2.71 (bs, 4H, H-2, H-3), 4.11 (bs, 2H, H-5).  $^{13}\text{C}$  NMR (50 MHz,  $\text{CDCl}_3$ ) ppm: 27.4, 28.7, 34.0, 50.1, 79.9, 84.8, 155.6, 176.9, 204.0. Anal. calcd for  $\text{C}_{10}\text{H}_{17}\text{NO}_5$ : C, 51.94; H, 7.41; N, 6.06. Found: C, 51.78; H, 7.44; N, 6.08.



**Compound 8.** At a stirring solution of **3** (200 mg, 0.87 mmol) and TEA (0.18 mL, 1.3 mmol) in dry  $\text{CH}_2\text{Cl}_2$  (7.7 mL) at room temperature, NHS (200 mg, 1.74 mmol) and DCC (359 mg, 1.74 mmol) was added. After 16 h a white precipitate was formed due to the formation of dicyclohexylurea. After filtration the solvent was evaporated under reduced pressure and the crude residue purified by precipitation with cold  $\text{Et}_2\text{O}$  to provide the pure **8** (203 mg, 71% yield):  $^1\text{H}$  NMR (400 MHz  $\text{CDCl}_3$ )  $\delta$ : 1.44 (s, 9H,  $\text{C}(\text{CH}_3)_3$ ), 1.90-1.96 (m, 4H,  $\text{CH}_2$  OSu), 2.84 (t, 2H,  $J = 6.4$  Hz, H-2), 2.97 (t, 2H,  $J = 6.4$ , H-3), 4.02 (bd, 2H,  $J = 4.4$  Hz, H-5).  $^{13}\text{C}$  NMR (50 MHz): ppm 24.8, 25.5, 28.2, 33.8, 49.1, 80.2, 157.1, 168.1, 169.1, 203.0. Anal. calcd for  $\text{C}_{14}\text{H}_{20}\text{N}_2\text{O}_7$ : C, 51.22; H, 6.14; N, 8.53. Found: C, 51.38; H, 6.12; N, 8.50.



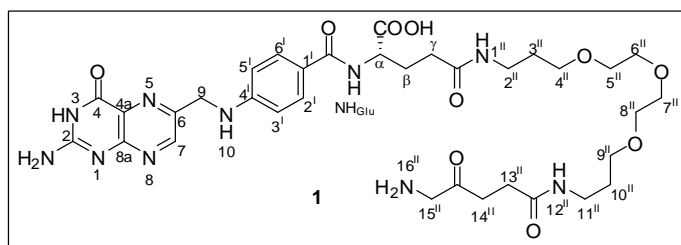
**Compound 9.** The lactone **9** was prepared under the same conditions for preparation of **8**, but for prolonged reaction time (3h) with 97% yield.  $^1\text{H}$  NMR (400 MHz,  $\text{CDCl}_3$ )  $\delta$ : 1.44 (s, 9H,  $\text{C}(\text{CH}_3)_3$ ), 2.42-2.52 (m, 2H, H-2), 2.51-2.62 (m, 1H, H-3), 2.72-2.84 (m, 4H,  $\text{CH}_2\text{OSu}$ ), 2.93-3.05 (m, 1H, H-3) 3.22 (dd, 1H,  $J = 4.4$ ,  $J = 15.6$ , H-5), 3.80 (dd, 1H,  $J = 9.3$ ,  $J = 15.6$ , H-5), 5.78 (bd, 1H,  $J = 5.3$ , NH).  $^{13}\text{C}$  NMR (100 MHz): ppm 25.3, 27.1, 28.2, 29.2, 43.1, 79.9, 113.1, 156.0, 172.0, 174.3. Anal. calcd for  $\text{C}_{10}\text{H}_{16}\text{NO}_4$ : C, 56.06; H, 7.53; N, 6.54. Found: C, 56.21; H, 7.50; N, 6.52.



**Compound 6.** To stirred solution of derivate **4** (19 mg, 0.023 mmol) in DMSO (1.2 mL) Boc-5-ALA-OSu (15mg, 0.046 mmol) and DIPEA (4  $\mu\text{L}$ , 0.023 mmol) was added. After 16h at room temperature, cold  $\text{Et}_2\text{O}$  (4 mL) was added dropwise to the mixture, after a few minutes acetone (2 mL) was added until the desired product was precipitated

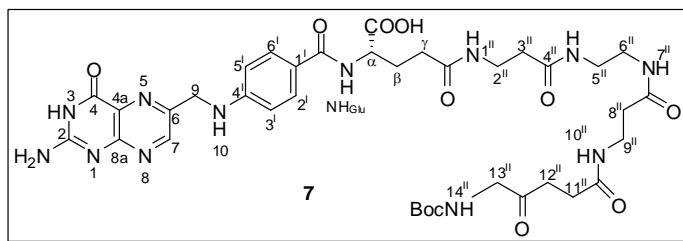
as yellow crystals, which were recovered and dried under vacuum (98% yield): pf. 210-214°C,  $^1\text{H NMR}$  (200 MHz, DMSO- $d_6$ )  $\delta$ : 1.36 (s, 9 H,  $\text{C}(\text{CH}_3)_3$ ), 1.51-1.72 (m, 4H, H-3<sup>II</sup>, H-10<sup>II</sup>), 1.80-2.10 (m, 2H, H- $\beta$ ), 2.15-2.40 (m, 6H, H-13<sup>II</sup>, H-14<sup>II</sup>, H- $\gamma$ ), 3.00-3.20 (m, 4H, H-2<sup>II</sup>, H-11<sup>II</sup>), 3.25-3.40 (m, 4H, H-4<sup>II</sup>, H-9<sup>II</sup>), 3.41-3.52 (m, 8H, H-5<sup>II</sup>, H-6<sup>II</sup>, H-7<sup>II</sup>, H-8<sup>II</sup>), 3.70-3.80 (m, 2H, H-15<sup>II</sup>), 4.20-4.42 (m, 1H, H- $\alpha$ ), 4.45 (bd, 2H,  $J = 5.4$ , H-9), 6.63 (d, 2H,  $J = 7.6$ , H-2<sup>I</sup>, H-5<sup>I</sup>), 6.75-7.00 (m, 2H, H-3, H-10), 7.63 (d, 2H,  $J = 7.6$ , H-3<sup>I</sup>, H-6<sup>I</sup>), 7.72-7.84 (m, 2H, H-1<sup>II</sup>, H-2<sup>II</sup>), 7.90-8.00 (m, 1H,  $J = 8.4$ , H-16<sup>II</sup>), 8.02-8.10 (m, 1H,  $\text{NH}_{\text{Glu}}$ ), 8.30 (s, 2H,  $\text{NH}_2$ ) 8.62 (s, 1H, H-7), 11.4 (s, 1H,  $\text{COOH}$ ).

**MALDI-TOF MS:**  $m/z$  856.41 (calcd); 880.22  $[\text{M}+\text{Na}]^+$ , 896.20  $[\text{M}+\text{K}]^+$  (found).  
Anal. calcd for  $\text{C}_{39}\text{H}_{56}\text{N}_{10}\text{O}_{12}$ : C, 54.66; H, 6.59; N, 16.35. Found: C, 54.52; 6.61; N, 16.40.



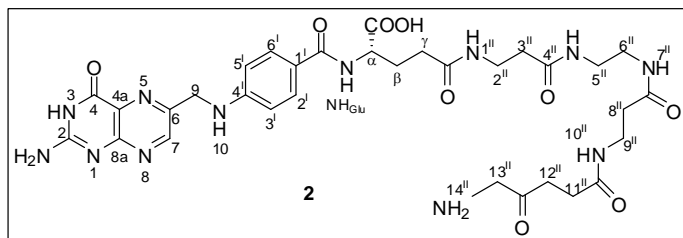
**Compound 1.** Compound **1** was prepared starting **6** with the same procedure reported in Chapter 1 for compound **8** (97% yield).  $^1\text{H NMR}$  (200 MHz, DMSO- $d_6$ )  $\delta$ : 1.80-2.00 (m, 2H, H- $\beta$ ), 2.18-2.38 (m, 10H, H-3<sup>II</sup>, H-6<sup>II</sup>, H-9<sup>II</sup>, H-12<sup>II</sup>, H- $\gamma$ ), 2.44 (dd, 1H,  $J = 7.7$ ,  $J = 16.2$ , H-14<sup>II</sup>), 2.69 (dd, 1H,  $J = 6.1$ ,  $J = 16.2$ , H-14<sup>II</sup>), 3.15-3.32 (m, 8H, H-2<sup>II</sup>, H-5<sup>II</sup>, H-8<sup>II</sup>, H-11<sup>II</sup>), 4.24-4.38 (m, 1H, H- $\alpha$ ), 4.45-4.58 (m, 2H, H-13<sup>II</sup>, H-9), 6.64 (d, 2H,  $J = 8.7$ , H-3<sup>I</sup>, H-5<sup>I</sup>), 7.08 (bs, 1H, H-10), 7.25 (bs, 1H, H-3), 7.63 (d, 2H, H-2<sup>I</sup>, H-6<sup>I</sup>), 7.80-7.95 (m, 6H, H-1<sup>II</sup>, H-4<sup>II</sup>, H-7<sup>II</sup>, H-11<sup>II</sup>,  $\text{NH}_2\text{C}=\text{O}$ ), 8.12 (d, 1H,  $\text{NH}_{\text{Glu}}$ ), 8.12 (d, 1H,  $J = 8.2$ ,  $\text{NH}_{\text{Glu}}$ ) 8.73 (s, 1H, H-7), 11.98-12.30 (m, 2H,  $2\times\text{COOH}$ ).

**MALDI-TOF MS:**  $m/z$  756.36 (Calcd); 757.19  $[\text{M}+\text{H}]^+$ , 780.21  $[\text{M}+\text{Na}]^+$ , 796.23  $[\text{M}+\text{K}]^+$  (Found). Anal. calcd for  $\text{C}_{34}\text{H}_{48}\text{N}_{10}\text{O}_{10}$ : C, 53.96; H, 6.39; N, 18.51. Found: C, 54.12; H, 6.37; N, 18.45



**Compound 7.** Under the same conditions used for compound **6**, the compound **7** was obtained with 98% yield.  $^1\text{H}$  NMR (200 MHz, DMSO- $d_6$ )  $\delta$ : 1.36 (s, 9H,  $\text{CH}_{3t\text{-Bu}}$ ), 1.82-2.08 (m, 2H, H- $\beta$ ), 2.12-2.32 (m, 10H, H-3 $^{\text{II}}$ , H-8 $^{\text{II}}$ , H- $\gamma$ , H-11 $^{\text{II}}$ , H-12 $^{\text{II}}$ ), 2.98-3.18 (m, 4H, H-2 $^{\text{II}}$ , H-9 $^{\text{II}}$ ), 3.21-3.42 (m, 4H, H-5 $^{\text{II}}$ , H-6 $^{\text{II}}$ ), 3.75 (bd, 2H,  $J = 5.4$ , H-13 $^{\text{II}}$ ), 4.31 (bs, 1H, H- $\alpha$ ), 4.52 (bd, 2H,  $J = 5.9$ , H-9), 6.62 (d, 2H,  $J = 7.5$ , H-3 $^{\text{I}}$ , H-5 $^{\text{I}}$ ), 6.88-6.96 (m, 3H, H-4 $^{\text{II}}$ , H-7 $^{\text{II}}$ , H-10), 7.65 (d, 2H,  $J = 7.5$ , H-2 $^{\text{I}}$ , H-6 $^{\text{I}}$ ), 7.81 (bs, 2H, H-1 $^{\text{II}}$ , H-10 $^{\text{II}}$ ), 7.95 (m, 2H,  $\text{NH}_{\text{Glu}}$ , H-14 $^{\text{II}}$ ), 8.12 (m, 1H, H-3), 8.69 (s, 1H, H-7), 11.42 (bs, 1H, COOH).

**MALDI-TOF MS:**  $m/z$  737.37 (calcd); 760.31  $[\text{M}+\text{Na}]^+$ , 776.29  $[\text{M}+\text{K}]^+$  (found). Anal. calcd for  $\text{C}_{33}\text{H}_{43}\text{N}_{11}\text{O}_9$ : C, 52.98; H, 6.01; N, 20.04; O, 20.98. Found: C, 52.79; H, 6.03; N, 20.10.

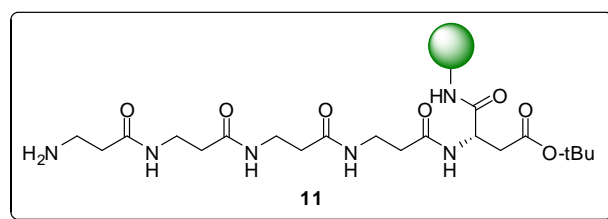


**Compound 2.** Under the same conditions used for compound **1**, the compound **2** was obtained from **7** with 98% yield.

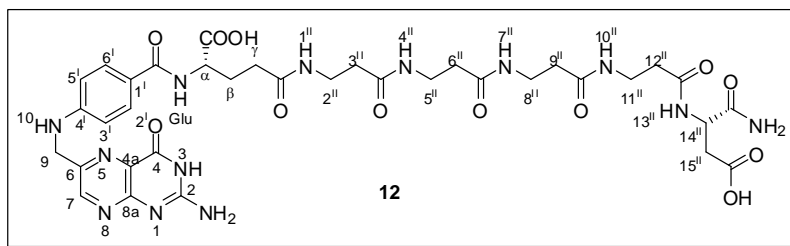
$^1\text{H}$  NMR (200 MHz, DMSO- $d_6$ )  $\delta$ : 1.82-2.08 (m, 2H, H- $\beta$ ), 2.12-2.32 (m, 10H, H-3 $^{\text{II}}$ , H-8 $^{\text{II}}$ , H- $\gamma$ , H-11 $^{\text{II}}$ , H-12 $^{\text{II}}$ ), 2.98-3.18 (m, 4H, H-2 $^{\text{II}}$ , H-9 $^{\text{II}}$ ), 3.21-3.42 (m, 4H, H-5 $^{\text{II}}$ , H-6 $^{\text{II}}$ ), 3.75 (bd, 2H,  $J = 5.4$ , H-13 $^{\text{II}}$ ), 4.31 (bs, 1H, H- $\alpha$ ), 4.52 (bd, 2H,  $J = 5.9$ , H-9), 6.62 (d, 2H,  $J = 7.5$ , H-3 $^{\text{I}}$ , H-5 $^{\text{I}}$ ), 6.88-6.96 (m, 3H, H-4 $^{\text{II}}$ , H-7 $^{\text{II}}$ , H-10), 7.65 (d, 2H,  $J = 7.5$ , H-2 $^{\text{I}}$ , H-6 $^{\text{I}}$ ), 7.81 (bs, 2H, H-1 $^{\text{II}}$ , H-10 $^{\text{II}}$ ), 7.95 (m, 3H,  $\text{NH}_{\text{Glu}}$ , H-14 $^{\text{II}}$ ), 8.12 (m, 1H, H-3), 8.69 (s, 1H, H-7), 11.42 (bs, 1H, COOH). Anal. calcd for  $\text{C}_{32}\text{H}_{42}\text{N}_{12}\text{O}_9$ : C, 52.03; H, 5.73; N, 22.75. Found: C, 52.18; H, 5.71; N, 22.68.

## 2.4.2 SOLID-PHASE SYNTHESIS

The synthesis of the pentapeptide **11** and the subsequent coupling reaction with folic acid were carried out in a reactor equipped with a plastic filter, PTFE (Teflon), a stopcock and a cap. The resin (MBHA-Rink Amide) was deprotected from Fmoc group by treatment with piperidine (30%) in DMF for 30 min. The efficiency of coupling of monomers was monitored by UV Fmoc test (absorbance of the Fmoc group:  $7800 = \epsilon_{301}$ ), so as to estimate the yield of incorporation of each residue. During the solid-phase synthesis, the *capping* of unreacted amino acid is achieved with  $\text{Ac}_2\text{O}$  (20%)/DIPEA (5%) in DMF, while the efficiency of coupling was monitored by measuring the absorbance of the released Fmoc group ( $7800 = \epsilon_{301}$ ).

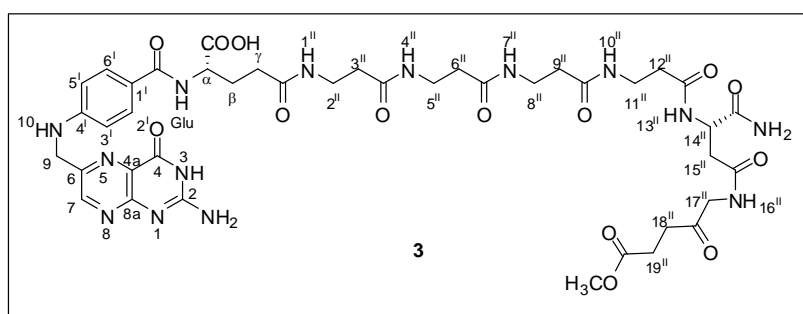


**Compound 11.** To the resin (0.5 mmol, 300 mg), previously deprotected by Fmoc group and washed with NMP, an acid solution of aspartic acid **10** (1 mL of a 0.5 M in NMP solution, 2.69 mmol, 358 mg) PyBOP (1 mL of a 0.5 M solution in NMP, 0.85 mmol) and DIPEA (295  $\mu\text{L}$ , 1.69 mmol) were added in to the reactor. After 20 min the mixture was removed from resin that was washed with NMP. To ensure peptide homogeneity the capping of unreacted amino acid was achieved using  $\text{Ac}_2\text{O}$  (20%)/DIPEA (5%) in NMP for 15 min. Deprotection of Fmoc group was achieved with piperidine (30%) in DMF (15 min). After that, a mixture of Fmoc- $\beta$ -alanine (1 mL of a 0.5 M solution in NMP, 0.88 mmol) and PyBOP (1 mL of 0.5 M solution in NMP, 0.85 mmol) and DIPEA (295  $\mu\text{L}$ , 1.69 mmol) were added into the reactor. Iterating this technique, three more units of  $\beta$ -alanine were then added to give the compound **11** in quantitative yield (calculated by UV detector).



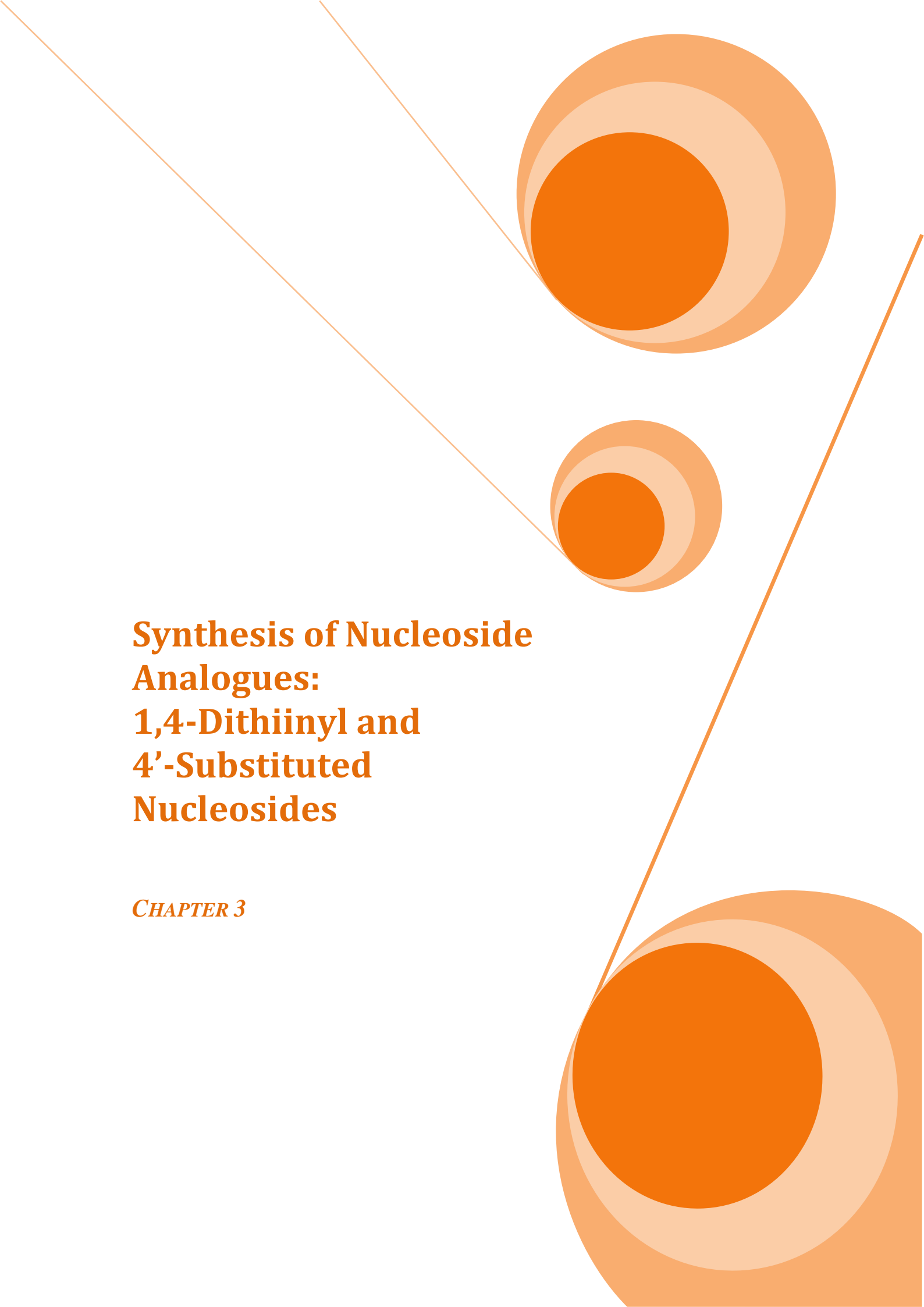
**Compound 12.** To the linker **11**, anchored to the resin, folic acid (1 mL of a 0.5 M solution in DMSO, 0.91 mmol, 400 mg), PyBOP (1 mL of a 0.5 M solution in DMSO, 0.90 mmol) and DIPEA (158  $\mu$ L, 0.91 mmol) were added. After 16h the product **12** was detached from the resin with a solution of TFA/TIS/H<sub>2</sub>O (95%:2.5%:2.5%) (1.5 mL) for 2h. TFA was removed under nitrogen atmosphere. The pure **12** (0.88 mmol, 741 mg, 97% yield) was obtained by precipitation with cold Et<sub>2</sub>O, centrifugation and subsequent lyophilization. <sup>1</sup>H NMR (300 MHz DMSO-d<sub>6</sub>)  $\delta$ : 1.82-2.00 (m, 2H, H- $\beta$ ), 2.18-2.25 (m, 10H, H-3<sup>II</sup>, H-6<sup>II</sup>, H-9<sup>II</sup>, H-12<sup>II</sup> H- $\gamma$ ), 2.39 (dd, 1H, H-14<sup>II</sup>); 2.67 (dd, 1H, H-14<sup>II</sup>); 3.18-3.25 (m, 8H, H-2<sup>II</sup>, H-5<sup>II</sup>, H-8<sup>II</sup>, H-11<sup>II</sup>), 4.30 (bs, 1H, H- $\alpha$ ); 4.58 (bs, 2H, H-9), 6.62 (d, 2H, H-3<sup>I</sup>, H-5<sup>I</sup>), 7.15-7.22 (m, 3H, H-4<sup>II</sup>, H-7<sup>II</sup>, H-10), 7.65 (d, 2H, H-2<sup>I</sup>, H-6<sup>I</sup>), 7.00-7.22 (m, 2H, H-1<sup>II</sup>, H-3), 8.10 (m, 1H, NH<sub>Glu</sub>), 8.65 (m, 1H, H-7).

**ESI-MS:**  $m/z$  839.33 (calcd); 841.03 [M+H]<sup>+</sup>, 864.34 [M+Na]<sup>+</sup>, 881.91 [M+K]<sup>+</sup> (found). Anal. calcd for C<sub>35</sub>H<sub>45</sub>N<sub>13</sub>O<sub>12</sub>: C, 50.06; H, 5.40; N, 21.68. Found: C, 50.22; H, 5.38; N, 21.59.



**Compound 3.** The compound **3** was obtained with 96% yield under the same conditions used for compound **1** described in Chapter 1, starting from **14**. <sup>1</sup>H NMR (500 MHz DMSO-d<sub>6</sub>)  $\delta$ : 1.82-2.00 (m, 2H, H- $\beta$ ), 2.18-2.25 (m, 10H, H-3<sup>II</sup>, H-6<sup>II</sup>, H-9<sup>II</sup>, H-12<sup>II</sup> H- $\gamma$ ), 2.39 (dd, 1H, H-14<sup>II</sup>); 2.67 (dd, 1H, H-14<sup>II</sup>); 2.76-2.79 (bt, 1H, H-19<sup>II</sup>), 3.12, (m, 1H, H-18<sup>II</sup>), 3.18-3.25 (m, 8H, H-2<sup>II</sup>, H-5<sup>II</sup>, H-8<sup>II</sup>, H-11<sup>II</sup>), 3.56-3.58 (m, 3H, OCH<sub>3</sub>) 4.30 (bs, 1H, H- $\alpha$ ); 4.58 (bs, 2H, H-9), 6.62 (d, 2H, H-3<sup>I</sup>, H-5<sup>I</sup>), 7.15-7.22 (m, 3H, H-4<sup>II</sup>, H-7<sup>II</sup>, H-10), 7.65 (d, 2H, H-2<sup>I</sup>, H-6<sup>I</sup>), 7.00-7.22 (m, 2H, H-1<sup>II</sup>, H-3), 8.10 (m, 1H, NH<sub>Glu</sub>),

8.46 (s, 1H, H-16<sup>II</sup>), 8.65 (m, 1H, H-7). Anal. calcd for C<sub>41</sub>H<sub>54</sub>N<sub>14</sub>O<sub>14</sub>: C, 50.93; H, 5.63; N, 20.28; O, 23.16. Found: C, 50.75; H, 5.64; N, 20.36.

The background features several abstract orange geometric shapes and lines. There are three large, overlapping circles of varying shades of orange, arranged in a roughly triangular pattern. Two thin orange lines intersect at a point, forming an 'X' shape that divides the page. The overall aesthetic is clean and modern, with a focus on warm tones and simple geometry.

# **Synthesis of Nucleoside Analogues: 1,4-Dithiinylnyl and 4'-Substituted Nucleosides**

*CHAPTER 3*

### 3.1 INTRODUCTION

Acquired immunodeficiency syndrome (AIDS) is a disease of the human immune system caused by the human immunodeficiency virus (HIV).<sup>1</sup> The disease interferes with the immune system making AIDS infected individuals much more likely to get infections, including opportunistic infections and tumors that do not affect people with working immune systems.

HIV-1 and HIV-2 are RNA viruses belonging to the retroviruses family<sup>2</sup> and so they are duplicated in a host cell by reverse transcriptase enzyme to produce DNA from its RNA genome.<sup>3</sup> The human immunodeficiency virus has a spherical shape with a diameter of about 100 nm and is composed by a capsid (glycoproteins membrane) on which *gp41* trans-membrane protein, and *gp120* surface glycoproteins are present. Within the membrane there is an nucleocapsid (protein envelope) which encloses the genetic material (two copies of single strand RNA) and enzymes necessary for virus replication: protease, integrase, reverse transcriptase and ribonuclease.

As shown in **Figure 1**, the life cycle of HIV consists of following steps:

1. HIV binds to a CD4 receptor and then fuses with the host cell;
2. after fusion, the virus releases its genetic material into the host cell (*uncoating*);
3. the reverse transcriptase enzyme converts the single-stranded viral RNA to double-stranded viral DNA;
4. the newly formed viral DNA is transported in the cellular nucleus and integrates into the host DNA by integrase enzyme (*integration*);
5. new viral RNA and viral proteins are formed (*transcription* and *trasduction*);
6. new viral RNA and proteins move to cell surface to form a new mature HIV.<sup>4</sup>

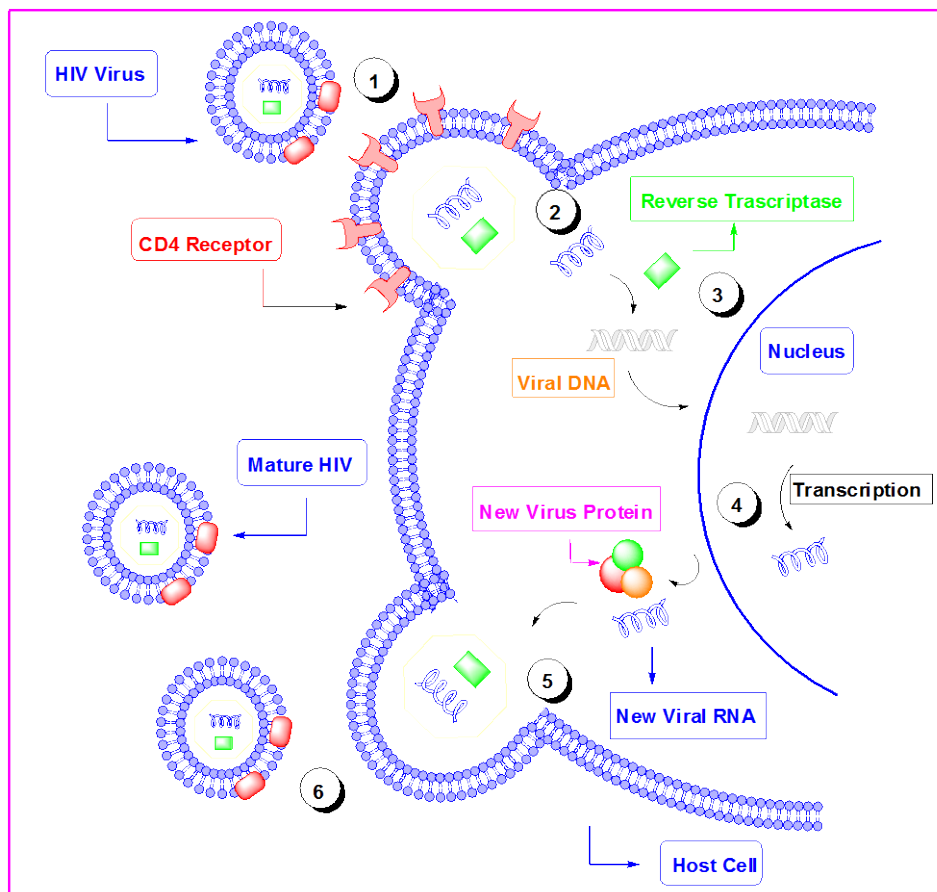


**Figure 1.** HIV life cycle.

### 3.1.1 ANTI-HIV CHEMOTHERAPY

The gained knowledge about HIV replication cycle has led to the development of several classes of chemotherapeutic agents<sup>5</sup> like, for example, nucleoside and nucleotide reverse transcriptase inhibitors (NRTIs, NtRTIs), non-nucleosides reverse transcriptase inhibitors (NNRTIs), co-receptor inhibitors (CRIs), fusion inhibitors (FIs), integrase inhibitors (INIs), protease inhibitors (PIs).<sup>6</sup> In particular, nucleosides reverse transcriptase inhibitors (NRTIs) received over the years the greater attention. The reverse transcriptase is an asymmetric heterodimer consisting of two subunits of 66 kDa (*p66*) molecular mass and 51 kDa (*p51*), with identical residues in their first 428 amino acid positions. The *p66* subunit is 560 residues in length, with its DNA polymerase and RNase H domains in the amino and carboxylterminal portions, respectively. Based on an examination of crystal forms of HIV-1 RT, the anthropomorphic shape of a hand has been used to describe the polymerase domain, with subdomains made up of the fingers,

palm, thumb, and connection to the RNase H domain. The p51 subunit comprises the same subdomains, but lacks the RNase H portion. The fingers, thumb, palm, and connection of the two subunits can be approximately superpositioned, pairwise, between *p66* and *p51*. However, the tertiary packing of the subdomains within the subunits differs: *p66* is described as an open hand, with a large cleft for binding double-stranded nucleic acids between the thumb and fingers subdomains, while *p51* is considerably more compact, with no nucleic acid binding cleft.

### 3.1.1.1 NUCLEOSIDE REVERSE TRANSCRIPTASE INHIBITORS

NRTIs, analogues of natural nucleosides, explicate their pharmacological action after phosphorylation steps<sup>7</sup> by host cell kinases and phosphotransferases to form deoxynucleoside triphosphate<sup>8,9</sup> analogues capable of viral inhibition.<sup>10</sup> In particular, they act on the process of virus replication by blocking the transcription of viral RNA into DNA, as once incorporated, the lack of OH prevents the formation of the bond 3',5'-phosphodiester bond with the next nucleotide in crescent DNA chain, thus blocking its growth.

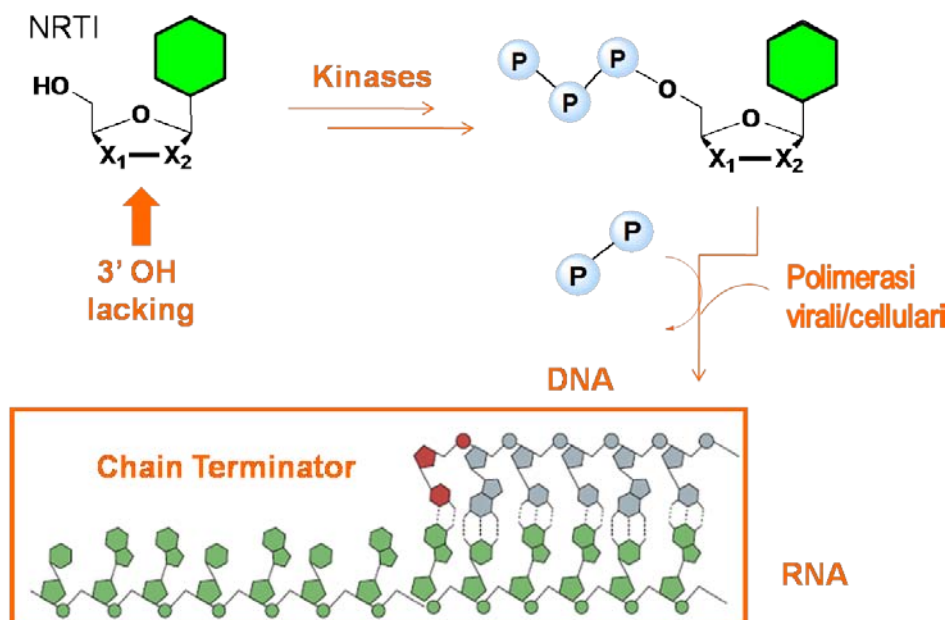


**Figure 2.** Chain termination mechanism.

Currently, there are eight NRTIs approved for HIV treatment by Food and Drug Administration (**Figure 3**).<sup>5</sup> As cartooned in **Figure 3** these drugs have as common feature the lack of 3'-OH group, even if they present different structures. Indeed, in the case of nucleosides ddI and ddC the OH-group is substituted by an H-atom, in the case of AZT, instead there is a 3'-azido function. In Abacavir drug the saccharide unit is replaced by a carbocyclic ring with a double bond, while 3TC and FTC present a sulfur atom in C3'. It's also important to note a particular saccharide portion modification of drugs 3TC, FTC, and TFV. Indeed regarding 3TC and FTC, in addition to the oxathiolane ring, they have the unnatural L-enantiomeric ribose form. Note that L-nucleoside analogues are often privileged anti-HIV agents because their activity is often associated to minor toxicity.<sup>11</sup> TFV, instead, is the only nucleotide analogue among approved NRTIs that has an acyclic linker attached to a modified phosphate. Furthermore, some of currently approved NRTIs present a modified nucleobase such as FTC that contains a fluorine at C5 position of cytosine and ABC has a modified diaminopurine ring.<sup>12</sup>

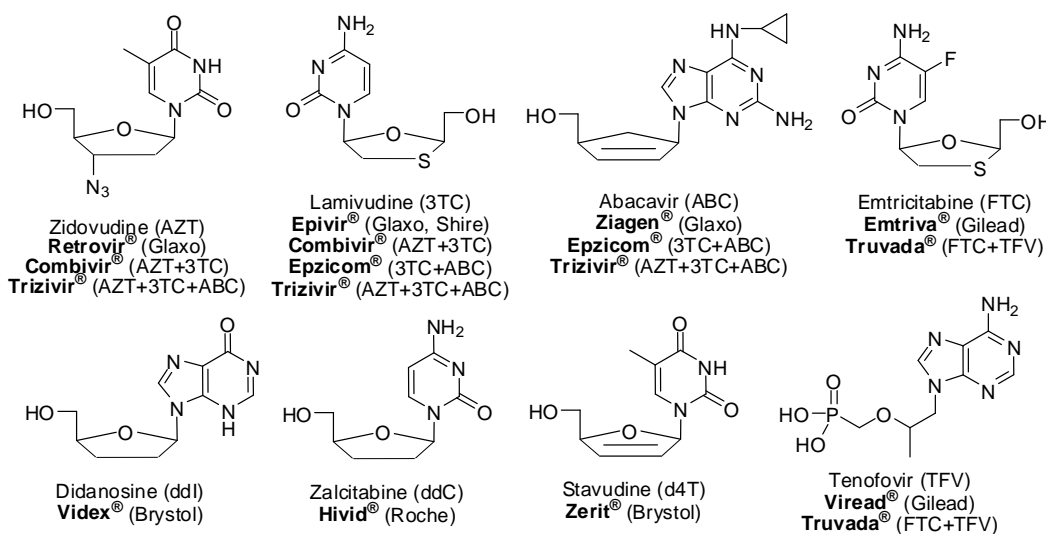


**Figure 3.** NRTIs currently used in HIV-1 and HIV-2 treatment.

### 3.1.1.2 ANTIVIRAL AND ANTITUMOR NUCLEOSIDES

The structural requirements of antiviral and antitumor nucleosides to be recognized by cellular/viral enzymes rely on three key elements:

- a) the hydroxymethyl group, necessary for nucleoside phosphorylation,
- b) the heterocyclic base moiety, involved in the main recognition processes through specific hydrogen bonds, and
- c) the sugar moiety, which can be considered as a spacer to connect the hydroxymethyl group and the nucleobase in the correct orientation.

A wide number of structural modifications at the carbohydrate moiety have been devised, with the aim to replace the furanose ring with units resembling the conformational features of natural nucleosides. Particularly, replacement of the sugar skeleton with acyclic moieties, n-membered rings (with n=3,4,5,6,7), equipped in some cases with exo- or endocyclic double bonds, has been reported. Such systems quite often contain carbon, one or more heteroatoms in place of/or along with endocyclic oxygen, resulting in major functional changes in the nucleoside subunits. Such a wide structural diversity in nucleoside architectures has led, over the years, to the development and approval of several molecules on the antiviral market in both racemic or enantiomerically pure form.

### 3.1.2 HIV DRUG RESISTANCE

In the last years, combination chemotherapy or highly active antiretroviral therapy (HAART) (**Figure 3**) using two or more NRTIs has improved the life quality of HIV-infected patients. Unfortunately the application of these compounds is clinically limited due to their cytotoxicity through inhibition of the host DNA polymerases and the rapid development of drug-resistant HIV variants. Two basic types of NRTI-resistance mechanisms known for HIV-1 reverse transcriptase are: NRTI exclusion and NRTI excision.

*NRTI exclusion.* This resistance mechanism involves enhanced discrimination when triphosphate form of a NRTI is incorporated. The M184V/I mutations are a clear example of the exclusion mechanism because it selectively reduce the incorporation of 3TC and FTC by steric hindrance.<sup>13</sup> Also the mutations L74V (ddI resistance),<sup>14</sup> K65R (TFV and ddI resistance)<sup>15</sup> and several variants that involved Q151M (resistance to most NRTIs)<sup>16</sup> cause resistance by the exclusion mechanism.

**NRTI excision.** The excision mechanism involves the selective removal of the NRTI from the end of the viral DNA after its incorporation by RT. For example the combinations of mutations M41L, D67N, K70R, L210W, T215F/Y, K219E/Q<sup>17</sup> adduce high levels of resistance to AZT and to much lower levels of resistance to some other NRTIs.

Therefore, the development of new compounds with reduced cytotoxicity and that are active against drug resistant HIV-1 variants and that prevent or delay the emergence of resistant HIV-1 variants is urgently needed.

### 3.1.2.1 4'-SUBSTITUTED NUCLEOSIDE ANALOGUES

Among new classes of nucleoside analogues endowed of the above mentioned features 4'-substituted nucleosides are currently under investigation. Some candidates for chemotherapeutic treatment of drug-resistant HIV strains and selected results of their antiviral assays are reported below.<sup>18</sup>

The first discovered 4'-substituted deoxynucleoside provided with potent anti-HIV activity is 4'-azido-thymidine.<sup>19</sup> This compound showed better antiviral potency than AZT, but also higher cytotoxicity. Among a wide range of subsequently synthesized 4'-substituted NRTIs,<sup>20</sup> 2'-deoxy-4'-C-ethynyl-2-fluoroadenosine (EFdA) (**Figure 4**) stands out as one of the most potent NRTIs.<sup>21</sup> It is up to 100-fold more potent than AZT, reaching even better *in vitro* activity than some HIV protease inhibitors.

The 4'-substituted nucleosides (4'-SdNs) in **Figure 4** are characterized by presence of 3'-OH which makes them acceptable by RT, therefore, they are incorporated into the proviral DNA chains. As reported in literature,<sup>22</sup> the 4'-substituents cause severe steric hindrance<sup>16,23</sup> to the neighbouring *cis* 3'-OH group due to restricted rotation around the C3'-C4' single bond. For this reasons 3'-OH results less reactive and it was expected that enzymatic chain elongation of DNA proceed slowly. Consequently, 4'-substituted nucleosides could be considered kinetic chain terminators<sup>24</sup> for proviral DNA biosynthesis. Furthermore 4'-SdNs would be more stable than 2'-deoxynucleosides and 2',3'-dideoxynucleosides against catabolism because of the steric repulsion between 3'-OH and 4'-substituents changes the conformation of their furanose ring, preferably to

C3'-endo conformation; this results in 4'-SdNs being less susceptible to enzymatic degradation.<sup>25</sup>

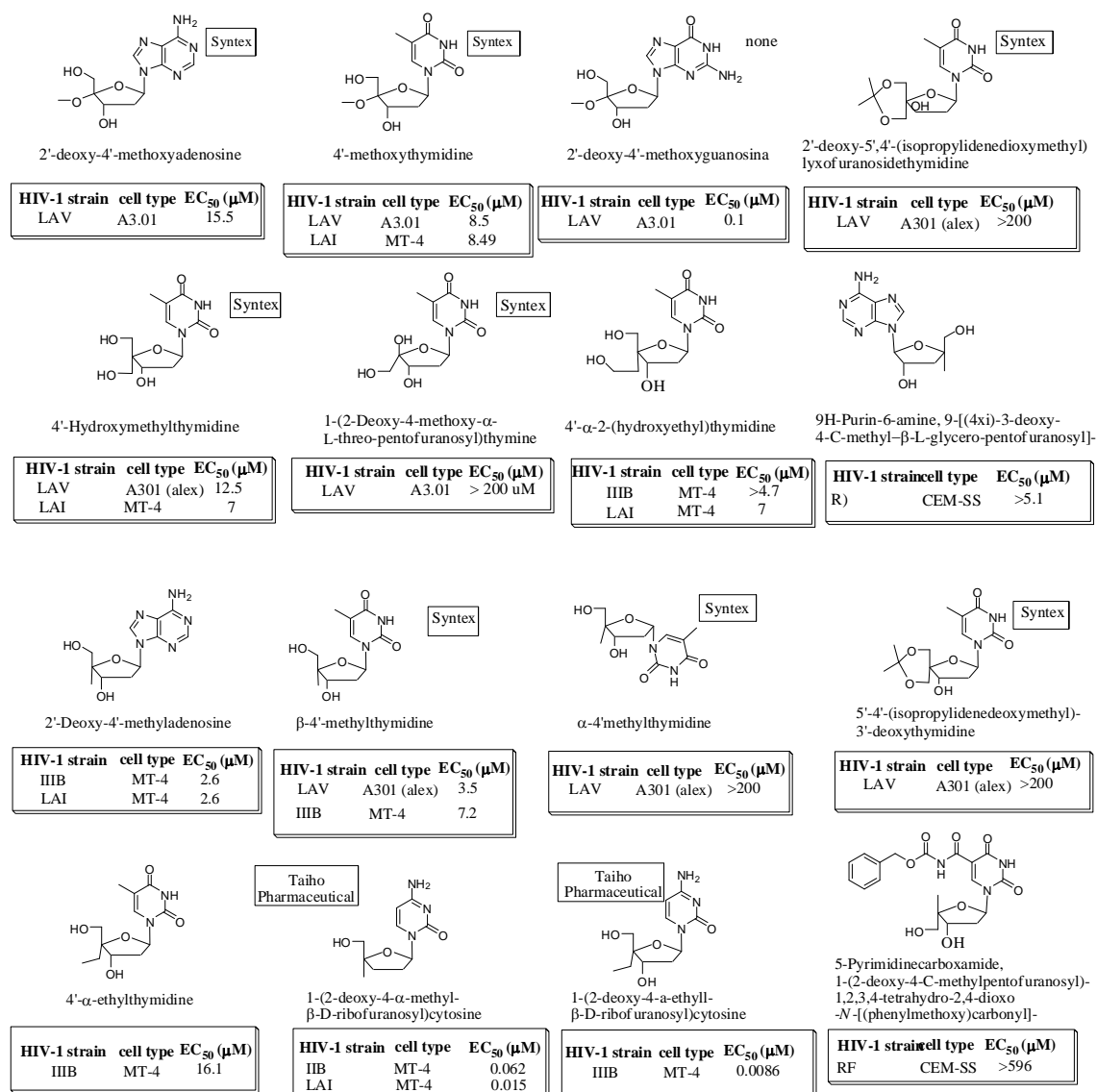


**Figure 4.** Anti-HIV-1 Activity of Nucleoside Analogues: 4'-Substituted-D- and L-nucleosides.

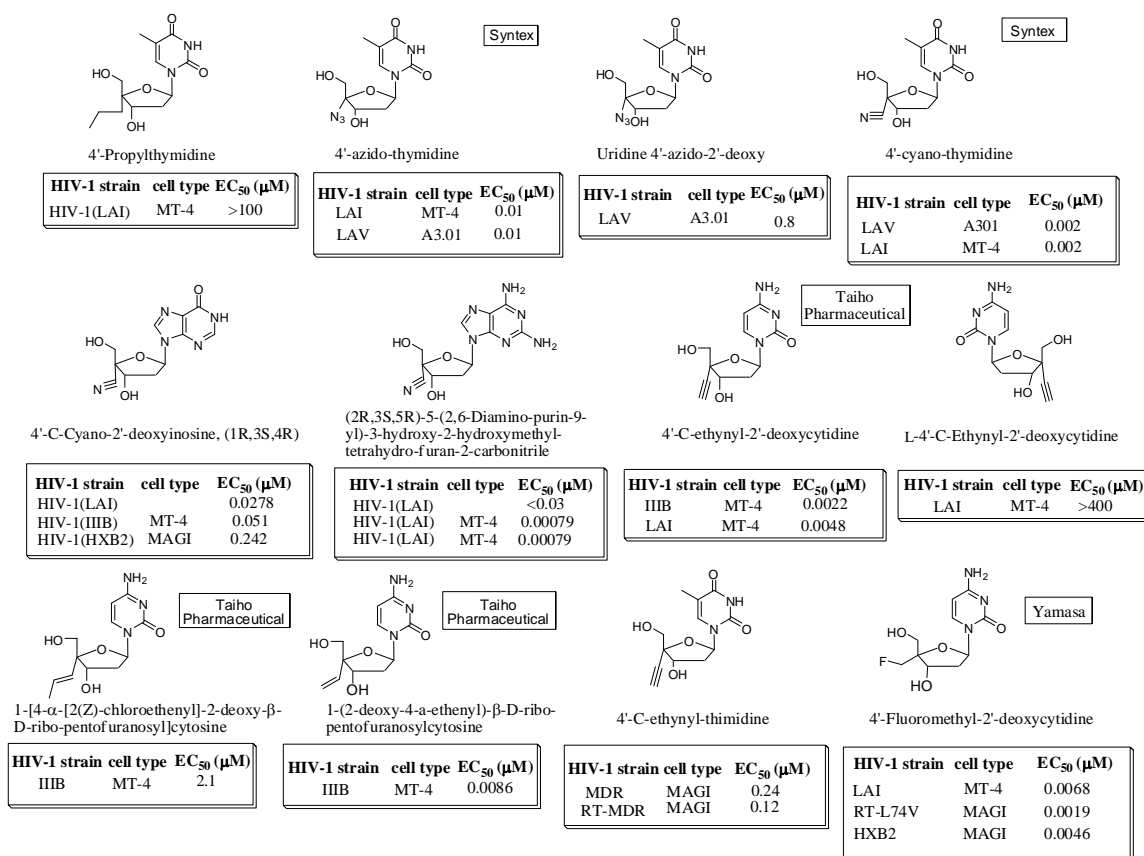


**Figure 4.** Anti-HIV-1 Activity of Nucleoside Analogues: 4'-Substituted-D- and L-nucleosides (continued).

Among the 4'-substituted nucleosides under investigation at present, an important class of this biologically active compounds are nucleosides possessing an unsaturated<sup>26</sup> or saturated sugar moiety.

The novel derivatives of d4T, like 2',3'-didehydro-3'-deoxy-4'-ethynylthymidine (4'-Ed4T) represent an interesting example (**Figure 5**).<sup>27</sup> Compared with its parental compound d4T, 4'-Ed4T is fivefold more potent against HIV-1 replication. It also showed much less cytotoxicity than d4T in cell culture studies because triphosphate 4'-Ed4T had no or only a weak inhibitory effect on major host DNA polymerases. Moreover, 4'-Ed4T was found to be active against many drug-resistant HIV-1 strains. Drug susceptibility studies showed that HIV-1 strains with the M184V single mutation and the P119S/T165A/M184V triple mutations in RT conferred three- to fivefold and 130-fold resistance to 4'-Ed4T, respectively.<sup>28</sup>

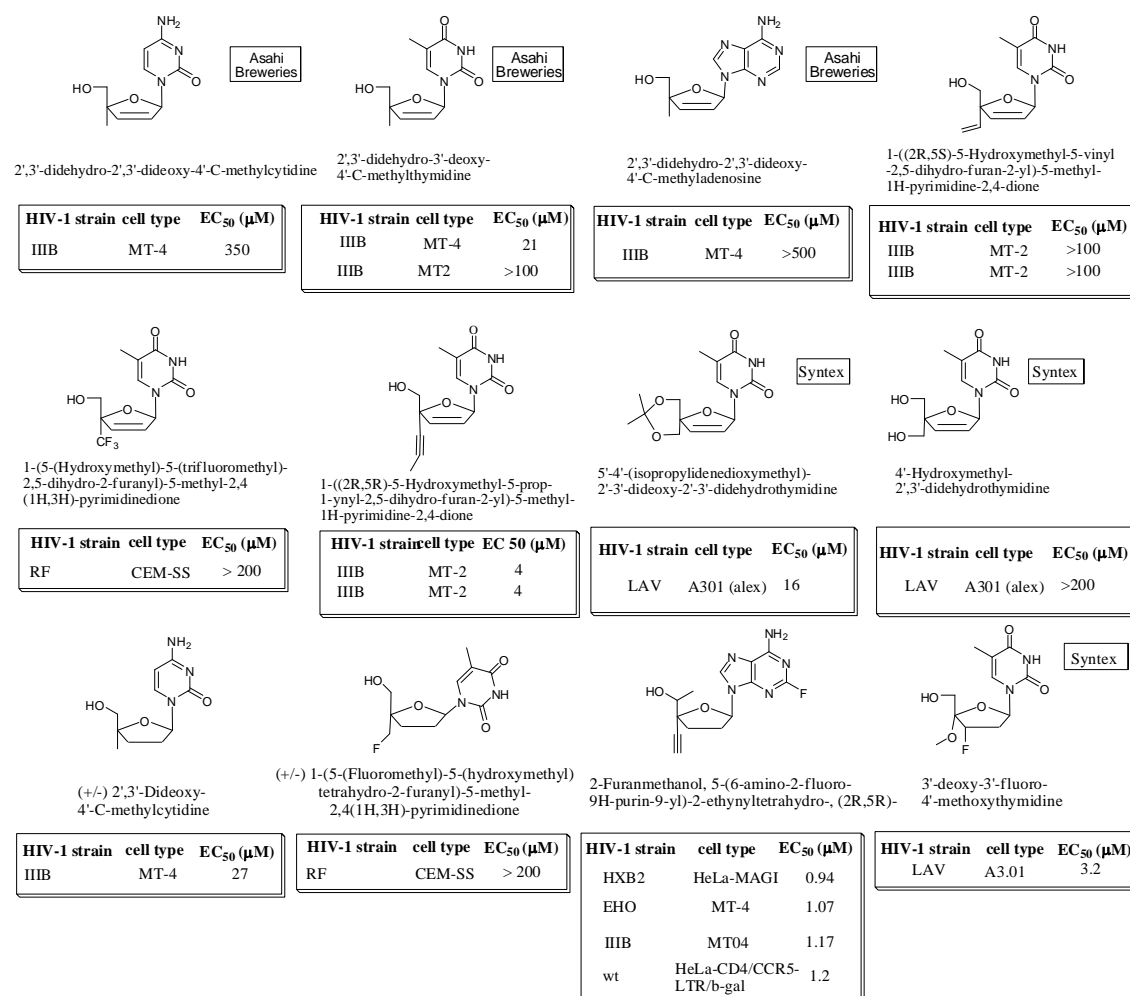


**Figure 5.** Anti-HIV-1 activity of nucleoside analogues: 2',3'-dideoxy-2',3'-dideoxy-4'-substituted-D and L-nucleosides, 2',3'-dideoxy-4'-substituted-D and L-nucleosides

Great attention in this field also received the exploration of new 4'-substituted nucleosides containing a sulfur atom sugar ring yielded potent inhibitors of HIV with EC<sub>50</sub> values ranging from 0.37 to 100 µM (**Figure 6**). In this series, 4'-azido- and 4'-cyanothionucleosides were approximately 10-fold more potent than the 4'-ethynyl-containing compounds. Unlike most of the other 4'-substituted NRTIs, the thiothymidine series appeared to maintain potent activity against viruses with the M184V mutation.<sup>29</sup>

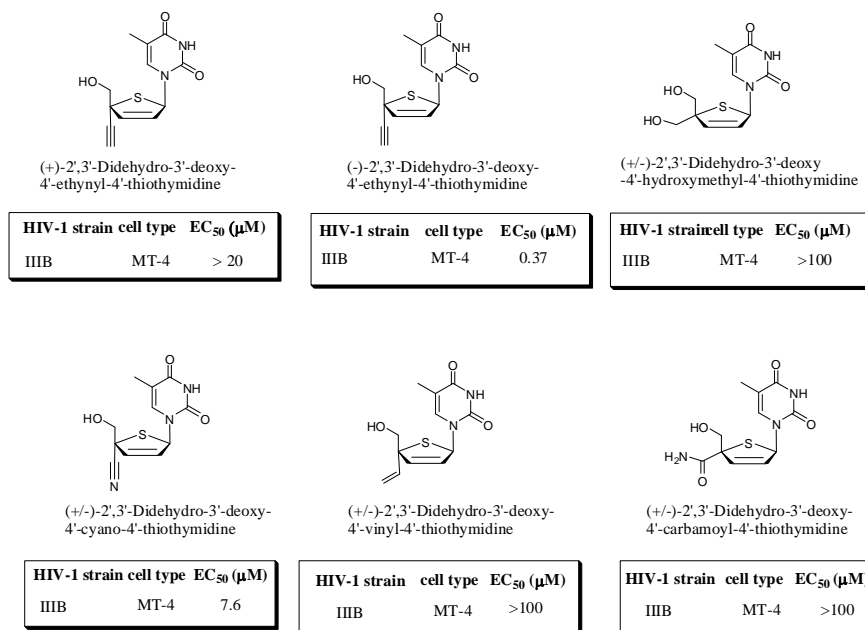


**Figure 6.** Anti-HIV-1 activity of nucleoside analogues: 2',3'-dideoxy-2'3'-dideohydro-4'-substituted-D and L-nucleosides

With the aim to prepare new compound able to overcome drug resistance, in the next section, it will be described a novel synthetic strategy to design more specific and selective antiviral agents. In particular, our attention was focused on the synthesis of sulfur-containing six-membered nucleosides<sup>30</sup> with structural similarity with natural nucleosides and 4'-substituted nucleosides to be tested as antiviral agents for treatment of HIV-infected individuals.

- 
- <sup>1</sup> Sepkowitz K.A. *N. Engl. J. Med.* **2001**, *23*, 1764–72.
- <sup>2</sup> Carter, J.; Saunders, V. *Virology - Principles and Applications*; John Wiley & Sons Ltd, West Sussex: England, **2007**.
- <sup>3</sup> De Clercq, E. *Antiviral Res.* **2005**, *67*, 56.
- <sup>4</sup> De Clercq, E. *Nat. Rev. Microbiol.* **2004**, *2*, 704-720.
- <sup>5</sup> Mehellou, Y.; De Clercq, E. *J. Med. Chem.* **2009**, *53*, 521. 538.
- <sup>6</sup> Richman, D. D. *Nature* **2001**, *410*, 995-1001.
- <sup>7</sup> Eriksson, S.; Munch-Petersen, B.; Johansson, K.; Eklund, H. *Cell. Mol. Life Sci.* **2002**, *59*, 1327-1346.
- <sup>8</sup> Pasti, C.; Gallois-Montbrun, S.; Munier-Lehmann, H.; Veron, M.; Gilles, A. M.; Deville-Bonne, D. *Eur. J. Biochem.* **2003**, *270*, 1784-1790.
- <sup>9</sup> Krishnan, P.; Gullen, E. A.; Lam, W.; Dutschman, G. E.; Grill, S. P.; Cheng, Y. C. *J. Biol. Chem.* **2003**, *278*, 36726-36732.
- <sup>10</sup> Arts, E. J.; Wainberg, M. A. *Antimicrob. Agents Chemother.* **1996**, *40*, 527-540.
- <sup>11</sup> Mathè, C.; Gosselin, G. *Antiviral Res.* **2006**, *71*, 276-28.1
- <sup>12</sup> Cihlar, T.; Ray, A.S. *Antiviral Res.* **2010**, *85*, 39-58.
- <sup>13</sup> Sarafianos, S.G.; Das, K.; Clark, Jr. A.D.; Ding, J.; Boyer, P.L.; Hughes, S.H.; Arnold, E.; *Proc. Natl. Acad. Sci. U S A* **1999**, *96*, 10027-10032.
- <sup>14</sup> Martin, J.L.; Wilson, J.E.; Haynes, R.L.; Furman, P.A. *Proc. Natl. Acad. Sci. U S A* **1993**, *90*, 6135-6139.
- <sup>15</sup> Margot, N.A.; Lu, B.; Cheng, A.; Miller, M.D. *HIV Med.* **2006**, *7*, 442-450.
- <sup>16</sup> Ueno, T.; Shirasaka, T.; Mitsuya, H. *J. Biol. Chem.* **1995**, *270*, 23605-23611.
- <sup>17</sup> Sarafianos, S. G.; Marchand, B.; Das, K.; Himmel, D. M.; Parniak, M. A.; Hughes, S. H.; Arnold, E. *J. Mol. Biol.* **2009**, *385*, 693-713.
- <sup>18</sup> Meyer, P. R.; Matsuura, S. E.; So, A. G.; Scott, W. A. *Proc. Natl. Acad. Sci. USA* **1998**, *95*, 13471-13476.
- <sup>19</sup> Maag, H.; Rydzewski, R.M.; McRoberts, M.J.; Crawford-Ruth, D.; Verheyden, J.P.; Prisbe, E.J. *J. Med. Chem.* **1992**, *35*, 1440-1451.
- <sup>20</sup> Hayakawa, H.; Kohgo, S.; Kitano, K.; Ashida, N.; Kodama, E.; Mitsuya, H.; Ohri, H. *Antiviral Chem. Chemother.* **2004**, *15*, 169-187.

- 
- <sup>21</sup> Nakata, H.; Amano, M.; Koh, Y.; Kodama, E.; Yang, G.; Bailey, C.M.; Kohgo, S.; Hayakawa, H., Matsuoka, M.; Anderson, K.S.; Cheng, Y.C.; Mitsuya, H. *Antimicrob. Agents Chemother.* **2007**, *51*, 2701-2708.
- <sup>22</sup> Ohru, H.; Mitsuya, H. *Curr. Drug Targets-Infectious Disorders* **2001**, *1*, 1-10.
- <sup>23</sup> Boyer, P. L.; Julias, J. G.; Ambrose, Z.; Siddiqui, M. A.; Marquez, V. E.; Hughes, S. H. *J. Mol. Biol.* **2007**, *371*, 873-882; Nakata, H.; Amano, M.; Koh, Y.; Kodama, E.; Yang, G.; Bailey, C. M. et al. *Antimicrob. Agents Chemother.* **2007**, *51*, 2701-2708.
- <sup>24</sup> Boyer, P. L.; Julias, J. G.; Marquez, V. E.; Hughes, S. H. *J. Mol. Biol.* **2005**, *345*, 441-450.
- <sup>25</sup> Hayakawa, H.; Kohgo, S.; Kitano, K.; Ashida, N.; Kodama, E.; Mitsuya, H.; Ohru, H. *Antiviral Chem. Chemother.* **2004**, *15*, 169-187.
- <sup>26</sup> Komoiotis, D.; Manta, S.; Tsoukala, E.; Tzioumaki, N. *Antiviral Infect. Agents Med. Chem.* **2008**, *7*, 219-244.
- <sup>27</sup> a) Nitanda, T.; Wang, H.; Kumamoto, X.; Haraguchi, K.; Tanaka, H.; Cheng, Y. C.; Baba M. *Antimicrob. Agents Chemother.* **2005**, *49*, 3355-3360. b) Dutschman, G. E.; Grill, S.P.; Gullen, E. A.; Haraguchi, K.; Takeda, S.; Tanaka, H.; Baba, M.; Cheng, Y. C. *Antimicrob. Agents Chemother.* **2004**, *48*, 1640-1646.
- <sup>28</sup> Yang, G.; Wang, J.; Cheng, Y.; Dutschman, G. E.; Tanaka, H.; Baba, M.; Cheng, Y.C. *Antimicrob. Agents Chemother.* **2008**, *52*, 2035-2042.
- <sup>29</sup> Haraguchi, K., Shimada, H., Tanaka, H., Hamasaki, T., Baba, M., Gullen, E.A., Dutschman, G.E., Cheng, Y.C. *J. Med. Chem.* **2008**, *51*, 1885-1893.
- <sup>30</sup> a) Caputo, R.; Guaragna, A.; Palumbo, G.; Pedatella, S. *Eur. J. Org. Chem.* **2003**, 346-350; b) Caputo, R.; Guaragna, A.; Palumbo, G.; Pedatella, S. *Eur. J. Org. Chem.* **1999**, 1455-1458.

## 3.2. RESULTS AND DISCUSSION

On the basis of considerations and data reported in the previous section, this work concerns the synthesis of novel nucleoside analogues endowed with potential antiviral property. In particular a novel class of nucleosides in which the sugar moiety that usually acts as a spacer between the two other unit ( $\text{CH}_2\text{OH}$  group and heterocyclic base) have been replaced by a dithiynyl one. Moreover a new methodology for the synthesis of 4'-substituted nucleosides has been realized. Both synthetic approach made use of the same starting material 5,6-dihydro-1,4-dithiin compound depicted in the square of **Figure 1**.

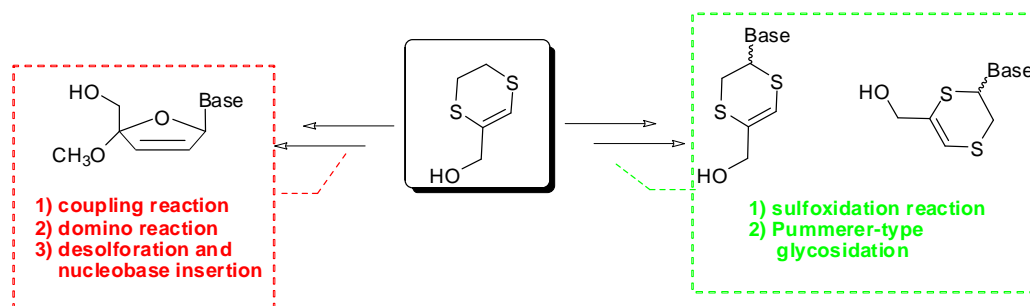


**Figure 1.** 1,4-Dithiynyl and 4'-Substituted Nucleosides.

### 3.2.1 SYNTHESIS OF 2,3-DIHYDRO-1,4-DITHIANYL NUCLEOSIDES

In this context, our interest in sulfur-containing nucleosides<sup>1</sup> and six-membered nucleoside analogues<sup>2</sup> took us to open up a synthetic study on the preparation of heterocyclic nucleosides **1** and **2**, in which the sugar moiety is substituted by a 5,6-dihydro-1,4-dithiin ring (**Figure 2**). Such a system has long been at the centre of our investigations regarding the development of novel *de novo* synthetic methodologies for the preparation of natural and unnatural compounds by three-carbon homologation of various electrophiles.<sup>3</sup> Differently from its common employ as elongating system,<sup>31,4</sup> herein we report the use of dithiynyl moiety as sugar scaffold in place of the furan ring of natural nucleosides to produce novel analogues endowed with potential antiviral activity.

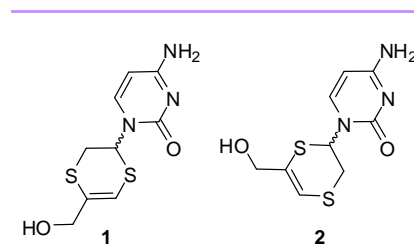


**Figure 2.** Dithiin nucleoside analogues **1** and **2**.

In spite of the unusual shape of the dithiine skeleton, we evaluated its capacity to work as a good spacer to place the nucleobase and the hydroxymethyl group in the appropriate orientation and distance for recognition by viral/cellular enzymes. With this aim, some preliminary Hyperchem calculations<sup>i</sup> were carried out, overlapping the structures of nucleosides **1** and **2** with those of natural nucleosides, as well as of other potent antiviral agents. The 1,4-dithiinyne system demonstrated to possess fairly good structural features, showing the best superimposition of both the hydroxymethyl group and the nucleobase when cytosine analogue (*S*)-**2** was overlapped with the potent antiretroviral agent Lamivudine (3TC, **3**) frozen in its bioactive *N* conformation<sup>5</sup> (**Figure 3**).

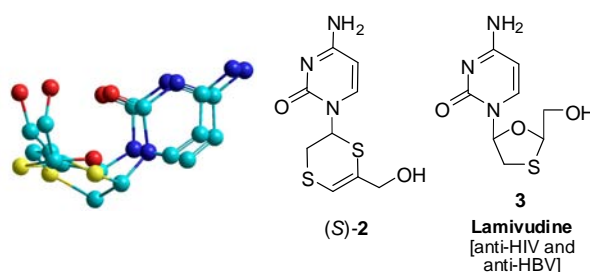


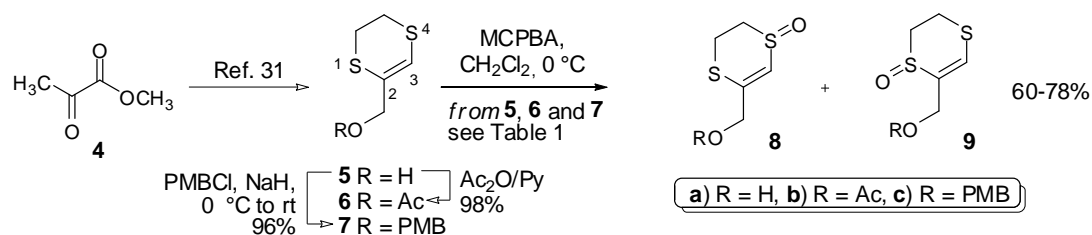
**Figure 3.** Superimposed structures of analogue (*S*)-**2** and Lamivudine (**3**).

Such studies prompted us to evaluate the biological properties of such nucleoside and to develop an expeditious procedure for its preparation as well as that of its regioisomer **1** (**Figure 3**). Moreover, given the relaxed enantioselectivity displayed by of some key enzymes involved in the activation of deoxycytidine analogues,<sup>6</sup> a comparable activity of both enantiomers should be expected. In this communication, the synthesis of target

<sup>i</sup> The models were generated by energy minimization with the Amber force field of the structures using the HYPERCHEM 8.0 software package (Hypercube Inc.)

compounds **1** and **2** as *R/S* mixture has been performed, as the antiviral evaluation of the racemic nucleosides would give results regarding both enantiomers in one procedure.

Synthesis of dithiynyl nucleosides **1** and **2** was envisioned to be carried out through a Pummerer-type glycosylation reaction on sulfoxides **8** and **9**, in turn obtained from our *bis*-thioenol ether **5** (**Scheme 1**). As already documented,<sup>31</sup> preparation of the 5,6-dihydro-1,4-dithiin ring was easily carried out in four steps from methyl pyruvate **4** (**Scheme 1**).



**Scheme 1.** Synthesis of sulfoxides **8-9**.

The synthesis began with the protection of free alcohol **5** ( $\text{Ac}_2\text{O}$ , pyridine) and subsequent thioether oxidation of the acetate **6** with *m*-CPBA in  $\text{CH}_2\text{Cl}_2$  to give a 55:45 mixture of two regioisomers **8b** and **9b** in 78% yield.

Sulfoxidation reaction was also attempted using dithiyn **5** and its derivative **7** in presence of various oxidizing agents.<sup>ii,7</sup> As shown in **Table 1**, use of *m*-CPBA gave similar results on all substrates, affording the two regioisomeric sulfoxides **8a** and **9a** in approximately 1:1 mixture ( $\text{R}=\text{H}$ ) with a slight prevalence for **8** over **9** when  $\text{R}=\text{Ac}$  or PMB. The preference for the oxidation at *S*-4 of the dithiine ring was observed in most cases; only the use of a bulkier oxidizing agent, such as pyridinium dichromate (PDC), in the oxidation of dithiyn **7**, led to a greater excess of regioisomer **8c** (entry 2). Even the use of Kagan-Modena sulfoxidation conditions<sup>8</sup> (L-DET or D-DET/*t*BuOOH/ $\text{Ti}(\text{O-}i\text{Pr})_4$ ) did not affect the reaction outcome (entries 4 and 5). Sulfoxidation reaction seemed to be essentially driven by steric hindrance reasons at allylic position, even though an additional electronic contribute was found.

<sup>ii</sup> All substrates did not exhibit any reactivity when *in situ* generated TFDO [methyl (trifluoromethyl)dioxirane] was used.

**Table 1.** Sulfoxidation of dithiins **5-7**.

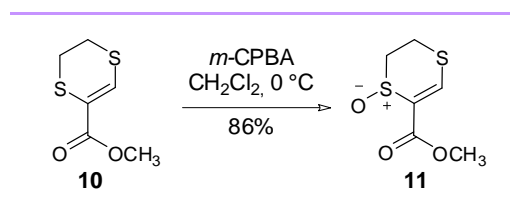
Entry	Conditions <sup>a</sup>	8/9 ratio (% yield)		
		R = H	R = Ac	R = PMB
1	<i>m</i> -CPBA (1.0 equiv), -20°C	50:50 (60)	55:45 (78)	60:40 (74)
2	PDC (1.0 equiv), -20°C	ND <sup>b</sup>	65:35 (82)	85:15 (84)
3	PDC (1.0 equiv), rt	ND <sup>b</sup>	65:35 (80)	-- <sup>c</sup> (41)
4	L-DET/ <i>t</i> BuOOH/Ti( <i>O</i> - <i>i</i> Pr) <sub>4</sub> , (2:1.2:1.0 equiv), -20 °C	50:50 (87)	60:40 (90)	65:35 (85)
5	D-DET/ <i>t</i> BuOOH/Ti( <i>O</i> - <i>i</i> Pr) <sub>4</sub> , (2:1.2:1.0 equiv), -20 °C	50:50 (89)	57:43 (91)	68:32 (86)

<sup>a</sup> CH<sub>2</sub>Cl<sub>2</sub> used as solvent in all reactions.

<sup>b</sup> ND: not determined (concurrent oxidation of primary hydroxyl group occurred).

<sup>c</sup> Further *S*-4 oxidation led to formation of a sulfone as the only product of the reaction.

It is worthy to note that a full electronic contribution has been observed when the sulfoxidation reaction was performed on methyl ester derivative **10**, in which the electron withdrawing group at *C*-2 position made *S*-4 atom a weak nucleophile (**Scheme 2**).

**Scheme 2.** Synthesis of sulfoxide **11**.

However **10** could not be used for providing nucleoside **2**, owing to fair instability of sulfoxide **11** to subsequent reaction conditions.

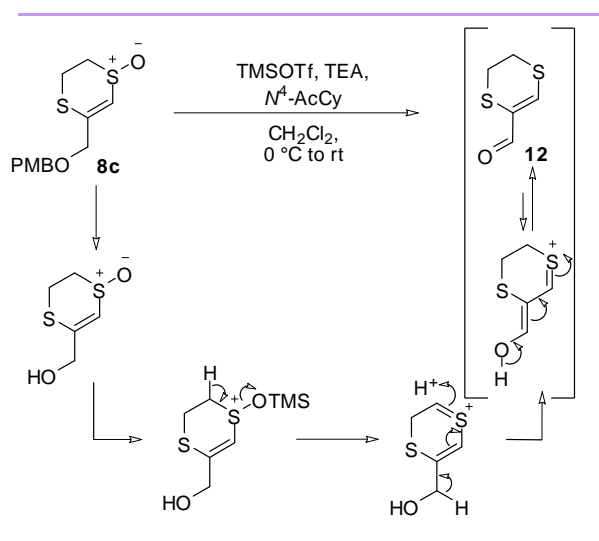
Indeed, energy calculation (B3LYP/6-31G\*)<sup>iii</sup> performed on **6** and **7** provided consistent explanation for the greater oxidability of *S*-4 compared to *S*-1. For both **6** and **7**, the HOMO molecular orbital is more localized on *S*-4 rather than on *S*-1, and coefficient value difference is grater in **7** (**Table 2**).

<sup>iii</sup> Theoretical calculations were performed by SPARTAN '08 Quantum Mechanics Program.

**Table 2.** Homo coefficients in **6** and **7**

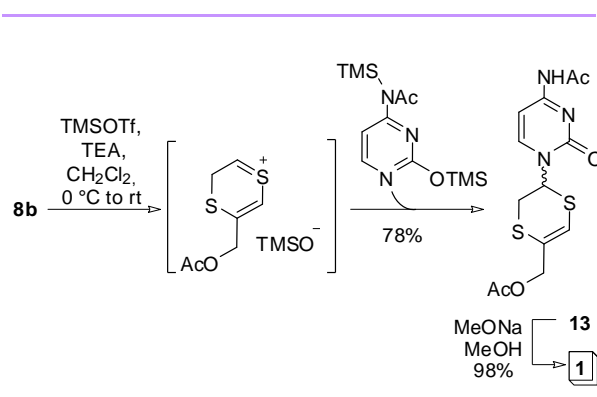
Atom	dithiin <b>6</b>	dithiin <b>7</b>
S-1	0.36824	0.28018
S-4	0.44799	0.40612

As sulfoxides **8** and **9** were obtained, preparation of target nucleoside analogues was carried out by a Pummerer-type glycosidation reaction.<sup>9</sup> First attempts carried out on sulfoxide **8c**, under the same conditions previously reported<sup>29</sup> with *N*<sup>4</sup>-acetylcytosine, TMSOTf and TEA in CH<sub>2</sub>Cl<sub>2</sub>, led as the only product of the reaction to the unexpected  $\alpha,\beta$ -unsaturated aldehyde **12**. This is probably the result of an intramolecular oxido-reduction process and, as depicted in **Scheme 3**, it can be conjectured to occur after PMB protecting group removal, sulfoxide trimethylsilylation, thionium ion formation by TEA-mediated elimination, and concurred oxidation of free hydroxyl group, to give aldehyde **12**.

**Scheme 3.**  $\alpha,\beta$ -unsaturated aldehyde **12** formation.

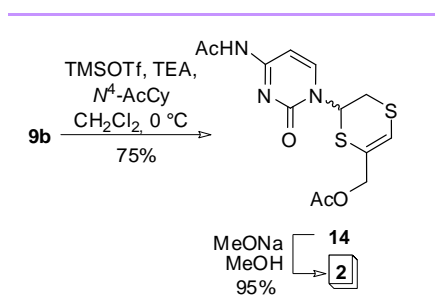
On the other hand, as depicted in **Scheme 4**, under the same conditions the use of the more stable acetylated sulfoxide **8b** allowed to obtain the desired dihydrodithiin nucleoside derivative **13** as a racemic mixture and in good yield (78%). Similarly to what observed in **Scheme 3**, the reaction proceeds through thionium ion intermediate mediated by TMSOTf and TEA and subsequent attack of silylated nucleobase on

thionum ion. Replacement of  $\text{CH}_2\text{Cl}_2$  with  $\text{CH}_3\text{CN}$  led to the final product with approximately the same yield, but prolonged reaction times were required.



**Scheme 4.** Dihydrodithiynyl nucleoside **1** via Pummerer-type glycosidation of **8b**.

Deprotection under common Zemplén conditions ( $\text{MeONa}/\text{MeOH}$ ) afforded the final target compound **1** in 98% yield. Analogously the same reactions, carried out starting from sulfoxide **9b**, led to desired nucleoside analogue **2** in 71% o.y. (**Scheme 5**).



**Scheme 5.** Dihydrodithiynyl nucleoside **2** via Pummerer-type glycosidation of **9b**.

---

<sup>1</sup> a) Caputo, R.; Guaragna, A.; Palumbo, G.; Pedatella, S. *Eur. J. Org. Chem.* **2003**, 346-350; b) Caputo, R.; Guaragna, A.; Palumbo, G.; Pedatella, S. *Eur. J. Org. Chem.* **1999**, 1455-1458.

<sup>2</sup> a) D'Alonzo, D.; Guaragna, A.; Van Aerschot, A.; Herdewijn, P.; Palumbo, G. *J. Org. Chem.* **2010**, 75, 6402-6410. b) D'Alonzo D.; Van Aerschot A.; Guaragna A.; Palumbo G.; Schepers G.; Capone, S.; Rozenski, J.; Herdewijn, P. *Chem. Eur. J.* **2009**, 15, 10121-10131; c) D'Alonzo, D.; Guaragna, A.; Van Aerschot, A.; Herdewijn, P.; Palumbo, G. *Tetrahedron Lett.* **2008**, 49, 6068-6070.

<sup>3</sup> Guaragna, A.; Pedatella, S.; Palumbo, G In: *e-Encyclopedia of Reagents for Organic Synthesis (e-EROS)*, L.A. Paquette, Editor, John Wiley & Sons, New York, US, **2008**.

<sup>4</sup> Guaragna, A.; D'Alonzo, D.; Paoella, C.; Napolitano, C.; Palumbo, G. *J. Org. Chem.* **2010**, 75, 3558-3568.

<sup>5</sup> a) Huang, H.; Chopra, R.; Verdine, G.L.; Harrison, S.C. *Science* **1998**, 282, 1669-1675; b) Marquez, V.E.; Ben-Kasus, T.; Barchi, J.J.Jr.; Green, K.M.; Nicklaus, M.C.; Agbaria, R. *J. Am. Chem. Soc.* **2004**, 126, 543-549.

<sup>6</sup> Eriksson, S.; Munch-Petersen, B.; Johansson, K.; Eklund, H. *Cell. Mol. Life Sci.* **2002**, 59, 1327-1346.

<sup>7</sup> Cermola, F.; Guaragna, A.; Iesce, M. R.; Palumbo, G.; Purcaro, R.; Rubino, M.; Tuzi, A. *J. Org. Chem.* **2007**, 72, 10075-10080.

<sup>8</sup> Wojaczyńska, E.; Wojaczyński, J. *Chem. Rev.* **2010**, 110, 4303-4356.

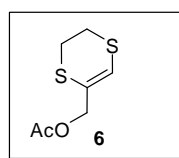
<sup>9</sup> Smith, L. H. S.; Coote, S. C.; Sneddon, H. F.; Procter, D. J. *Angew. Chem. Int. Ed.* **2010**, 49, 5832-5844.

### 3.2.1.1 CONCLUSION

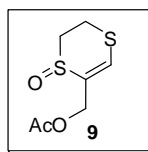
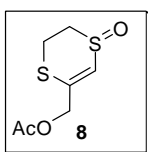
In this context a straightforward procedure for the preparation of dithiinylnucleoside **1** and **2** has been accomplished in four steps by our readily available heterocyclic system **5**. Regioselectivity of sulfoxidation reaction of *bis*-thioenoethers **6-7** was rationalized on the basis of both steric and electronic effects. Nucleobase insertion was carried out by direct addition of *N*<sup>4</sup>-acetylcytosine to sulfoxide **8b-9b** via Pummerer-type glycosidation reaction. Evaluation of racemic **1** and **2** as potential antiviral agents is currently in progress. In case, further development of asymmetric Pummerer rearrangements<sup>19</sup> and/or enantiomeric resolution of our mixtures by chiral HPLC will be considered to provide enantiopure (*S*)- and (*R*)-**1**, as well as their regioisomers (*S*)- and (*R*)-**2**.

### 3.2.1.2 EXPERIMENTAL SECTION

All moisture-sensitive reactions were performed under a nitrogen atmosphere using oven-dried glassware. Solvents were dried over standard drying agents and freshly distilled prior to use. Reactions were monitored by TLC (precoated silica gel plate F254, Merck). Column chromatography: Merck Kieselgel 60 (70-230 mesh); flash chromatography: Merck Kieselgel 60 (230-400 mesh).  $^1\text{H}$  and  $^{13}\text{C}$  NMR spectra were recorded on NMR spectrometers operating on Varian VXR (200 MHz), Bruker DRX (400 MHz) or Varian Inova Marker (500 MHz), using  $\text{CDCl}_3$  solutions unless otherwise specified. In all cases, tetramethylsilane (TMS) was used as internal standard for calibrating chemical shifts ( $\delta$ ). Coupling constant values ( $J$ ) were reported in Hz. Combustion analyses were performed by using CHNS analyzer.



**Compound 6.** To a stirring solution of alcohol **5** (0.71 g, 4.8 mmol) in dry pyridine, acetic anhydride was added at room temperature. After 3h TLC (hexane/EtOAc = 8/2) analysis showed the complete formation of final compound. The solvent was evaporated under reduced pressure and the crude residue purified by chromatography on silica gel (hexane/EtOAc = 9/1) to give the pure **6** (0.834 g, 98% yield). Oily;  $^1\text{H}$  NMR (400 MHz): ppm 2 (s, 3H,  $\text{CH}_3$ )  $\delta$  3.08-3.20 (m, 4H,  $\text{CH}_2\text{S}$ ), 4.49 (s, 2H,  $\text{CH}_2\text{O}$ ), 6.22 (s, 1H,  $\text{CH}=\text{}$ ).  $^{13}\text{C}$  NMR (200 MHz): ppm 20.63, 25.91, 26.42, 68.09, 115.89, 122.41, 170.31. Anal. calcd for  $\text{C}_7\text{H}_{10}\text{O}_2\text{S}_2$ : C, 44.18; H, 5.30; S, 33.70. Found: C, 44.34; H, 5.28; S, 33.61.

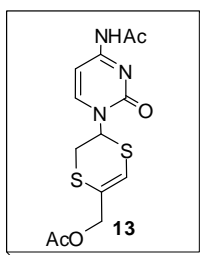


**Compound 8 and 9.** To a stirred solution of compound **6** (0.8 g, 4.2 mmol) in dry  $\text{CH}_2\text{Cl}_2$  (18 mL), at  $0^\circ\text{C}$ , *m*-chloroperoxybenzoic acid (0.361 g, 2.1 mmol) was added in one portion. After 3h the mixture was neutralized with aq  $\text{NaHCO}_3$ , and then extracted with  $\text{CH}_2\text{Cl}_2$ . Organic phase was dried on  $\text{Na}_2\text{SO}_4$  and the solvent evaporated

under vacuum. The crude residue obtained purified by chromatography on silica gel (EtOAc/CH<sub>3</sub>OH) gave the pure compounds **8** and **9** (in 6/4 ratio, 98%).

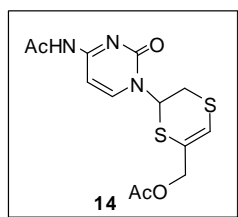
*Data for compound 8.* Oily; <sup>1</sup>H NMR (300 MHz, CDCl<sub>3</sub>): ppm 2.00 (s, 3H, CH<sub>3</sub>) 2.60 (ddd, 1H, CHS), 2.91-3.02 (d, 1H, CHS), 3.31-3.42 (d, 1H, CHS), δ 3.43-3.62 (t, 1H, CHS), 4.70 (s, 2H, CH<sub>2</sub>O), 6.80 (s, 1H, CH=). <sup>13</sup>C NMR (50 MHz, CDCl<sub>3</sub>): ppm 16.20, 20.62, 42.49, 65.64, 118.28, 143.39, 170.42. Anal. calcd for C<sub>7</sub>H<sub>10</sub>O<sub>3</sub>S<sub>2</sub>: C, 40.76; H, 4.89; O, 23.27; S, 31.09. Found: C, 40.92; H, 4.87; S, 31.00.

*Data for compound 9.* Oily; <sup>1</sup>H NMR (300 MHz, CDCl<sub>3</sub>): ppm 2.00 (s, 3H, CH<sub>3</sub>) 2.52-2.68 (t, 1H, CHS), 2.75-2.90 (d, 1H, CHS), 3.31-3.50 (m, 2H, CHS), 4.80 (s, 2H, CH<sub>2</sub>O), 7.00 (s, 1H, CH=). <sup>13</sup>C NMR (50 MHz, CDCl<sub>3</sub>): ppm 13.71, 20.73, 42.65, 65.39, 128.87, 133.50, 170.44. Anal. calcd for C<sub>7</sub>H<sub>10</sub>O<sub>3</sub>S<sub>2</sub>: C, 40.76; H, 4.89; O, 23.27; S, 31.09. Found: C, 40.90; H, 4.91; S, 30.99.

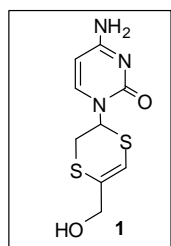


**Compound 13.** To a suspension of *N*<sup>4</sup>-acetylcytosine (0.30 g, 2.0 mmol) in CH<sub>2</sub>Cl<sub>2</sub> (10 mL) TEA (0.8 mL, 6.1 mmol) and TMSOTf (1.1 mL, 6.1 mmol) were added at 0 °C and under N<sub>2</sub> atmosphere. The mixture was left at room temperature for 30 min, after this time the mixture was cooled at 0 °C and a solution of sulfoxide **8b** (0.28 g, 1.36 mmol) was added dropwise. The reaction was warmed at room temperature for 2h, then saturated aq NaHCO<sub>3</sub> was added until neutrality. The mixture was extracted with EtOAc and washed with water; the organic layers were dried (Na<sub>2</sub>SO<sub>4</sub>) and evaporated under reduced pressure to give a crude product whose chromatography afforded the pure **11** (78% yield). <sup>1</sup>H NMR (500 MHz, CDCl<sub>3</sub>): δ 2.11 (s, 3H, OCOCH<sub>3</sub>), 2.24 (s, 3H, NHCOCH<sub>3</sub>), 3.26 (dd, *J* = 2.3, 14.6 Hz, 1H, CH<sub>a</sub>S), 3.40 (dd, *J* = 4.4, 14.6 Hz, 1H, CH<sub>b</sub>S), 4.61 (d, *J* = 12.7 Hz, 1H, CH<sub>a</sub>O), 4.65 (d, *J* = 12.7 Hz, 1H, CH<sub>b</sub>O), 6.40 (dd, *J* = 2.3, 4.4 Hz, 1H, CHS), 6.47 (s, 1H, HC=), 7.44 (d, *J* = 7.3 Hz, 1H, H-5), 7.84 (d, *J* = 7.3 Hz, 1H, H-6), 8.42 (s, 1H, NH). <sup>13</sup>C NMR (50 MHz, CDCl<sub>3</sub>): ppm 20.7 (CH<sub>3</sub>CO), 24.9, 30.6, 53.0, 67.4, 96.2, 114.1, 124.3, 147.4, 155.1, 162.5, 170.5. Anal. calcd for

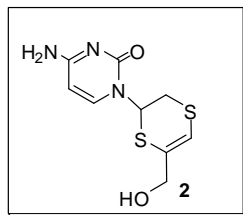
$C_{13}H_{15}N_3O_4S_2$ : C 45.73, H 4.43, N 12.31, S 18.78. Found: C 45.65, H 4.44, N 12.26, S 18.84.



**Compound 14.** Under the same conditions, starting from **9b** compound **14** was obtained (75% yield).  $^1H$  NMR (400 MHz,  $CDCl_3$ ):  $\delta$  2.13 (s, 3H,  $OCOCH_3$ ), 2.25 (s, 3H,  $NHCOCH_3$ ), 3.26 (dd, 1H,  $J = 2.0, 13.9$  Hz, 1H,  $CH_aS$ ), 3.35 (dd, 1H,  $J = 4.6, 13.9$  Hz, 1H,  $CH_bS$ ), 4.70 (d,  $J = 12.7$  Hz, 1H,  $CH_aO$ ), 4.73 (d,  $J = 12.7$  Hz, 1H,  $CH_bO$ ), 6.45 (s, 1H,  $HC=$ ), 6.48 (dd,  $J = 2.0, 4.6$  Hz, 1H,  $CHS$ ), 7.47 (d,  $J = 7.5$  Hz, 1H, H-5), 7.80 (d,  $J = 7.5$  Hz, 1H, H-6), 8.35 (s, 1H, NH).  $^{13}C$  NMR (50 MHz,  $CDCl_3$ ): ppm 20.8, 24.9, 28.8, 53.8, 67.2, 96.4, 116.0, 123.1 ( $C=CH_2$ ), 147.2 (C-6), 154.8, 162.7, 170.6. Anal. calcd for  $C_{13}H_{15}N_3O_4S_2$ : C 45.73, H 4.43, N 12.31, S 18.78. Found: C 45.80, H 4.44, N 12.28, S 18.70.



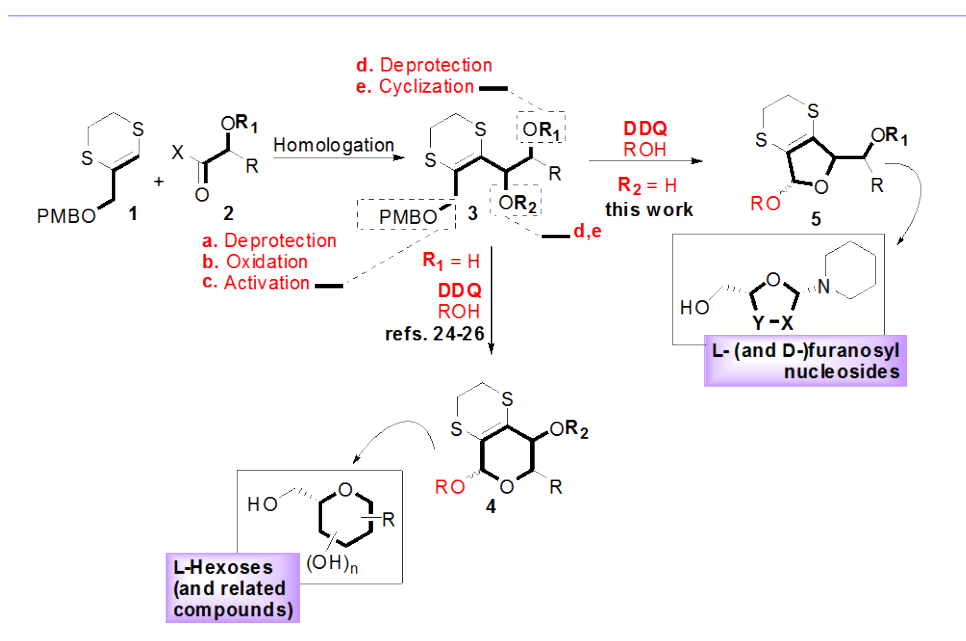
**Compound 1.** To a stirring solution of compound **13** (0.100 g, 0.4 mmol) in 10 mL of  $CH_3OH$ ,  $CH_3ONa$  (21.6 mg, 0.4 mmol) was added. After 2 h at mixture of reaction  $AcOH$  dropwise was added until neutral. The solvent was evaporated under reduced pressure to give a crude residue that purified by chromatography on silica gel ( $CHCl_3/MeOH = 9:1$ ) provided the pure **1** (98% yield).  $^1H$  NMR (200 MHz,  $CD_3OD$ ):  $\delta$  3.18-3.25 (m, 2H,  $CH_2S$ ), 4.12 (dd,  $J = 0.9, 13.0$  Hz, 1H,  $CH_aOH$ ), 4.21 (dd,  $J = 0.9, 13.1$  Hz, 1H,  $CH_bOH$ ), 5.87 (d,  $J = 7.6$  Hz, 1H, H-6), 6.34 (dd,  $J = 2.8, 3.8$  Hz, 1H,  $CHS$ ), 6.39 (d,  $J = 0.9$  Hz, 1H,  $HC=$ ), 7.66 (d,  $J = 7.6$  Hz, 1H, H-5).  $^{13}C$  NMR (50 MHz,  $CD_3OD$ ): ppm 30.6, 55.2, 67.2, 95.5, 113.1, 130.6, 145.2, 157.8, 167.8. Anal. calcd for  $C_9H_{11}N_3O_2S_2$ : C 42.01, H 4.31, N 16.33, S 24.92. Found: C 41.94, H 4.30, N 16.28, S 25.00.



**Compound 2.** Under the same conditions, starting from **14** compound **2** was obtained (97% yield).  $^1\text{H}$  NMR (200 MHz,  $\text{CD}_3\text{OD}$ ):  $\delta$  3.15-3.34 (*m*, 2H,  $\text{CH}_2\text{S}$ ), 4.05 (d,  $J = 13.1$  Hz, 1H,  $\text{CH}_a\text{OH}$ ), 4.07 (d,  $J = 13.1$  Hz, 1H,  $\text{CH}_b\text{OH}$ ), 5.84 (d,  $J = 7.6$  Hz, 1H, H-6), 6.25 (dd,  $J = 2.5, 4.8$  Hz, 1H, CHS), 6.46 (d,  $J = 0.9$  Hz, 1H,  $\text{HC}=\text{C}$ ), 7.63 (d,  $J = 7.6$  Hz, 1H, H-5).  $^{13}\text{C}$  NMR (75 MHz,  $\text{CD}_3\text{OD}$ ): ppm 31.8, 54.0, 67.2, 95.3, 112.0, 130.5, 145.4, 157.6, 167.4. Anal. calcd for  $\text{C}_9\text{H}_{11}\text{N}_3\text{O}_2\text{S}_2$ : C 42.01, H 4.31, N 16.33, S 24.92. Found: C 41.90, H 4.32, N 16.37, S 24.99.

### 3.2.2 SYNTHESIS OF 2',3'-DIDEHYDRO-2',3'-DIDEOXY-4'-METHOXY NUCLEOSIDES

Current status of organic synthesis is hampered by time-consuming, costly protecting group-based strategies and lengthy purification procedures after each synthetic step. To circumvent these inconveniences, the potential of multistep protocols including domino<sup>1</sup> or cascade<sup>2</sup> reactions has been exploited for the efficient and elegant construction of complex molecules from simple precursors in a single process. In this context, our ongoing efforts working toward the *de novo* synthesis of novel molecular systems with pharmacological potential took us to explore the versatile reactivity profile of our 1,2-*bis* thioenol ether synthon **1** in combination with 2,3-dichloro-5,6-dicyanobenzoquinone (DDQ) (Scheme 1).

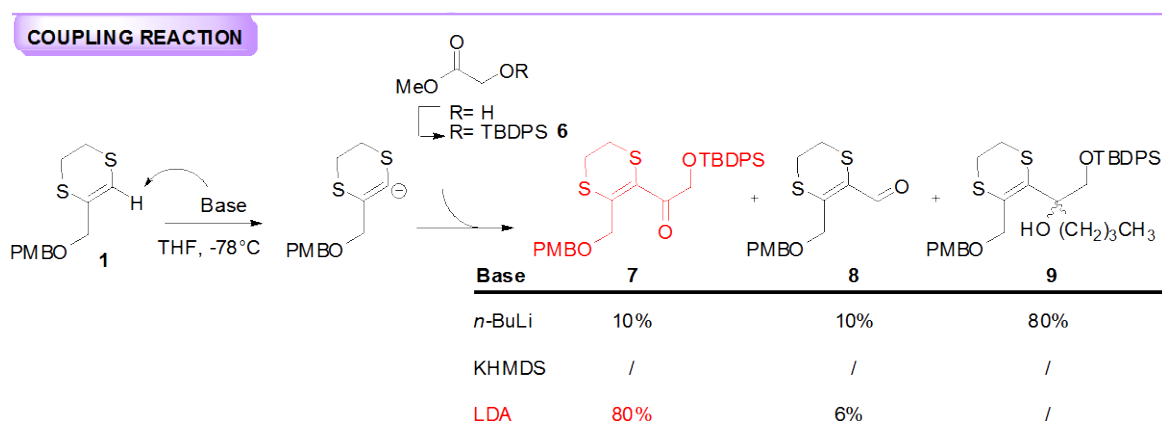


**Scheme 1.** *De novo* synthetic strategy to bicyclic furans **5**.

Whereas heterocyclic system **1** brought on C<sub>3</sub>-homologation of various electrophiles<sup>3</sup> **2**, in many cases in stereoselective fashion,<sup>3,4</sup> use of the resulting homologation products **3** with DDQ laid the ground for new efficient domino reactions for further elaboration of the carbon skeletons. As proof-of-concept of this methodology, we successfully developed an expeditious procedure for the synthesis of the whole series of rare L-hexoses<sup>4,5</sup> as well as other structurally related compounds.<sup>6</sup> In all cases, rapid assembly of pyranosyl scaffolds **4** was found a consequence of the combined electron-transfer,

oxidative and acidic properties of DDQ, which enabled sequentially PMB group deprotection of allyl ethers **3**, oxidation of the resulting primary alcohols and formyl groups activation, finally leading to six-membered cyclization by a suitably unprotected hydroxyl function (**Scheme 1**).

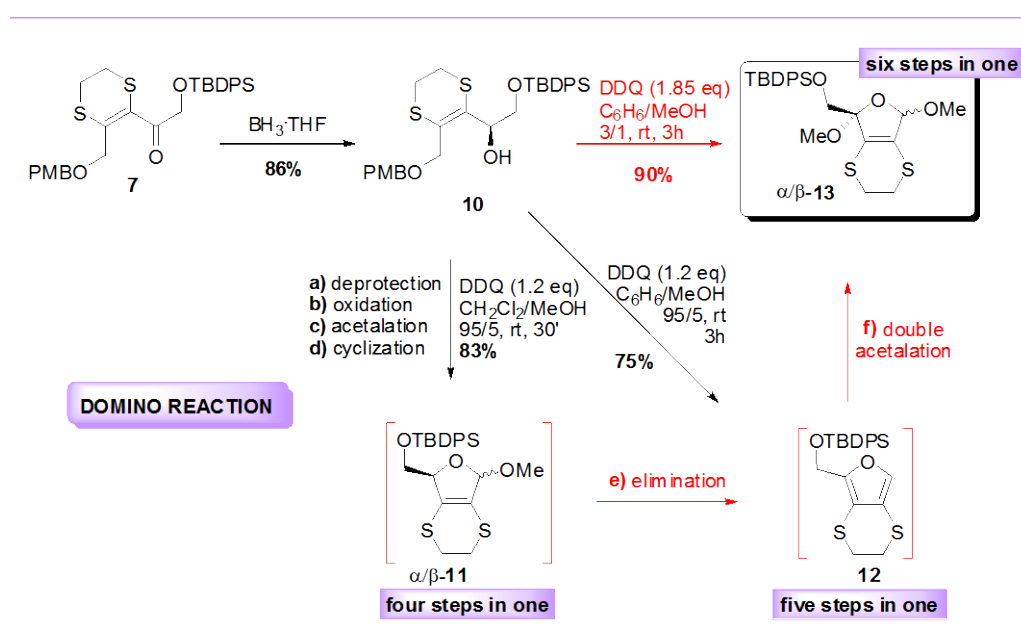
Along this line, synthetic access to dihydrofurans **5** has been herein explored (**Scheme 1**), mainly in view of their potential application in the synthesis of bioactive D- and L-(didehydro)furanosyl nucleosides.<sup>7</sup> The synthesis starts from coupling reaction of thioenol ether **1** with synthetically available methyl glycolate **6**, previously protected with a TBDPS-group. Under known conditions reported for comparable electrophile<sup>23</sup> unfortunately we didn't obtained the expected product with highly yields (**scheme 2**).



**Scheme 2.** Synthesis of coupling compound **7** using several conditions.

Particularly, treatment of heterocyclic homologating agent **1** with *n*-butyl lithium in anhydrous THF at  $-78\text{ }^{\circ}\text{C}$ , followed by addition at the same temperature of electrophile **6**, provided, along with small amounts of ketone **7** (10%), almost exclusive formation of tertiary alcohol **9** (80%) resulting from the further nucleophilic addition by the *n*-butyl lithium on C-4 position. The aldehyde **8** was also isolated as another byproduct of the reaction (10%), which seem to be formed by consumption of the coupling product **7**. This byproduct was already obtained in our laboratories, as previously reported, under same reaction conditions, during the synthesis of L-hexoses<sup>5</sup>, however the mechanism of such reaction in the current synthesis is still under investigation. On the basis of these findings, we decided to prove different basis, poor nucleophiles, like potassium hexamethyldisilazide (KHMDS) and lithium diisopropylamide (LDA). While the use of KHMDS was unsuccessful, LDA, led to more satisfactory results. This reagent was prepared *in situ* from a solution of diisopropylamine (DIPA) and *n*-BuLi, in dry THF,

at  $-78\text{ }^{\circ}\text{C}$ . The subsequent addition of **1** and then **6** at the same temperature, finally provided the ketone **7** as main product (80%), instead aldehyde **8**, under these conditions, was isolated only in small amounts (6%) (**Scheme 2**). With the product **7** in hand, our interest was focused on the achievement of key intermediate **13** by carbon skeleton cyclization *via* domino reaction (**Scheme 3**). After reduction<sup>i</sup> of **7** to the corresponding *sec*-alcohol **10** ( $\text{BH}_3\cdot\text{THF}$ , 86%), direct conversion of the latter into methyl glycosides **11** was achieved treating **10** with DDQ (1.2 equiv) in a 95/5  $\text{CH}_2\text{Cl}_2/\text{MeOH}$  solution to afford, already after only 30', a mixture of isomers  $\alpha$ -**11** and  $\beta$ -**11** in moderate selectivity ( $\alpha:\beta = 1:3.3$ ) and fairly good overall yield (83%).

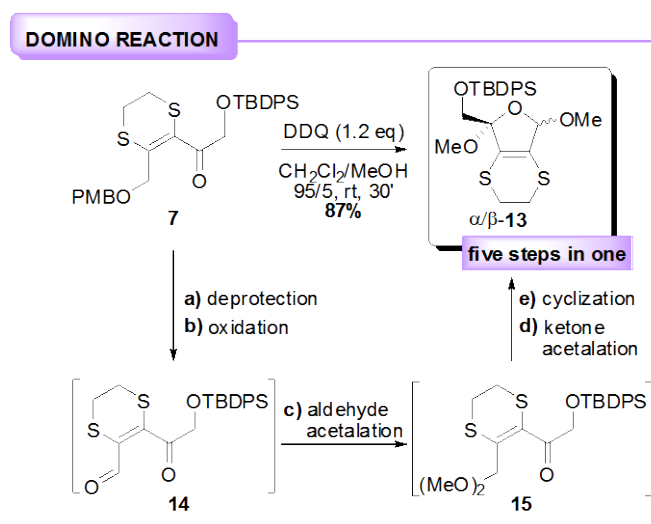


**Scheme 3.** Domino approach to (dihydro)furans **11-13**.

Surprisingly, minimal changes of reaction conditions provided a number of other synthetically relevant *in situ* transformations (**Schemes 3** and **4**). Under optimized conditions, treatment of **10** with DDQ (1.85 eq) in a 3/1  $\text{C}_6\text{H}_6/\text{MeOH}$  mixture directly led, overall after 3h at rt, to the formation of *bis*-acetals **13** ( $\alpha:\beta = 1:4$ ) in an excellent 90% o.y. (**Scheme 3**). This process was amenable to be considered a domino reaction, as it proceeded across the following six sequential transformations, carried out in a single step: a) PMB group removal, b) oxidation of the resulting primary alcohol, c)

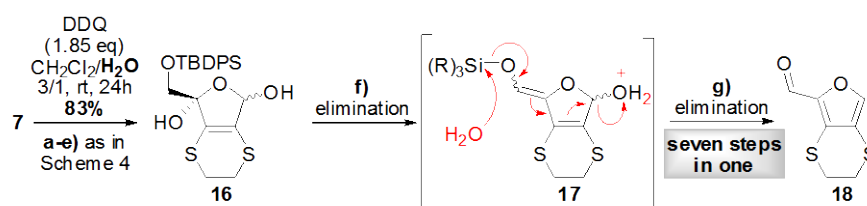
<sup>i</sup> As we were first interested to explore reactivity profile of our compounds, rather than their preparation as pure enantiomers, starting alcohol **10** was achieved in racemic form. Study of the reaction conditions enabling synthesis of **10** in both enantiomeric forms is currently ongoing.

aldehyde acetalation, **d**) ring closure, **e**) MeOH elimination, and **f**) double acetalation (**Scheme 3**). It's worth noting that, although furan **12** acted as simple intermediate under these conditions, it could be also smoothly isolated as the main product (75% yield) by further appropriate tuning of the amount of DDQ and MeOH [DDQ (1.2 eq), C<sub>6</sub>H<sub>6</sub>/MeOH 3/1, rt, 3h].



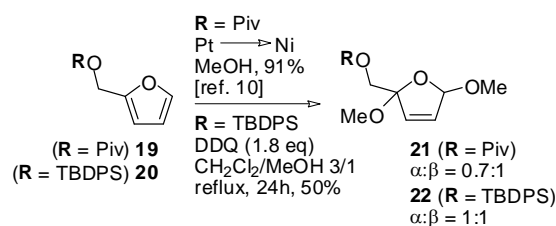
Not fully unexpected, *bis*-acetals **13** could be obtained in a single process, albeit by a different sequence of synthetic transformations, even starting directly from ketone **7** (**Scheme 4**). As a matter of fact, after addition of DDQ (1.2 eq) to a CH<sub>2</sub>Cl<sub>2</sub>/MeOH solution of **7**, acetals **13** ( $\alpha:\beta = 1:4$ ) were produced after 3h in a very good 87% yield. Although none of the synthetic intermediates could be isolated, we reasonably assumed that **13** was the result of five sequential transformations, including oxidative deprotection of **7** leading to aldehyde **14**, its double acetalation and concurrent cyclization (**Scheme 4**).

It's worth mentioning that replacement of MeOH with H<sub>2</sub>O under the above conditions provided even more unexpected reactivity, as it led to furfural derivative **18** (83%). Analogously to **Scheme 4**, reaction was supposed to proceed through formation of *bis*-hemiacetal **16**, then undergoing H<sub>3</sub>O<sup>+</sup>-mediated double elimination affording **18** even after seven synthetic steps. However, **18** was not enough stable for further synthetic manipulations.



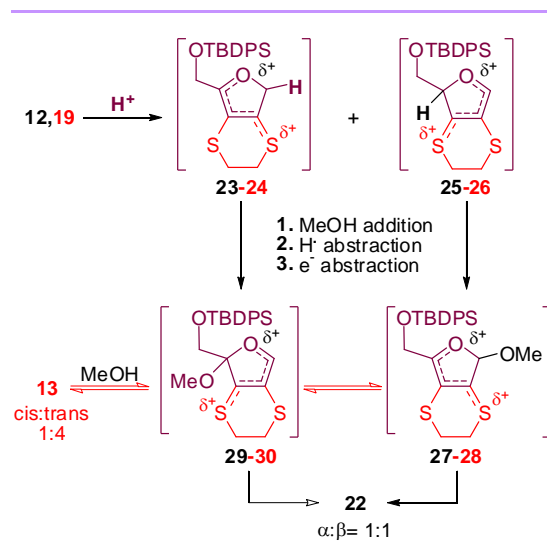
**Scheme 5.** Synthesis of furfural derivatives **18**.

Excellent synthetic potential of the above processes rely on a combination of versatility of DDQ and intriguing chemical properties of the 1,4-dithiopyran scaffold. Given the apparent synthetic applications of the domino products, their formation and especially that of *bis*-acetals **13** was investigated in greater detail. We started observing that last step of the domino process depicted in **Scheme 3** closely resembles the well known Clauson-Kaas reaction,<sup>8</sup> providing substituted 2,5-dialkoxy-2,5-dihydrofurans **21** from corresponding furans **19** under electrochemical conditions (**Scheme 5**).



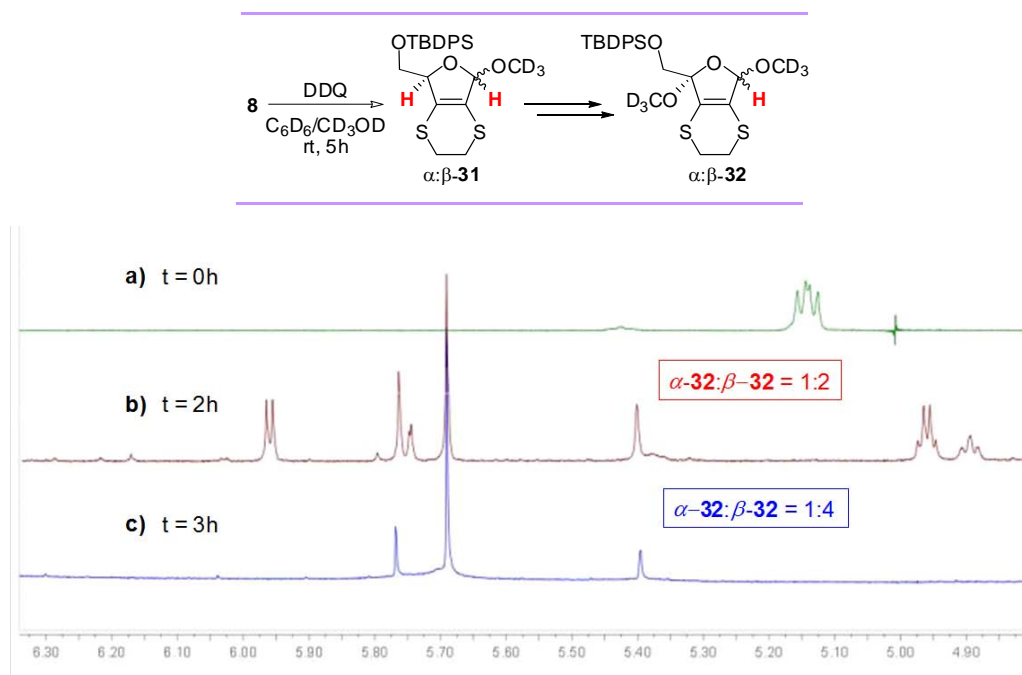
**Scheme 6.** (Modified) Clauson-Kaas approach to acetals **21-22**.

Herein, we established that the same transformation could be analogously carried out by DDQ (**Scheme 5**). However, compared to the above domino process, reaction of **Scheme 6** was less efficient (50%), requiring harder conditions (24h at reflux) and even resulting in a worst stereoselectivity ( $\alpha:\beta = 1:1$ ). Therefore, a crucial influence of the dithiodimethylene bridge on reaction rate and stereoselectivity became apparent.



**Scheme 7.** Conversion of furans **12** and **19** into *bis*-acetals **13** and **22**: hypothesized reaction mechanism.

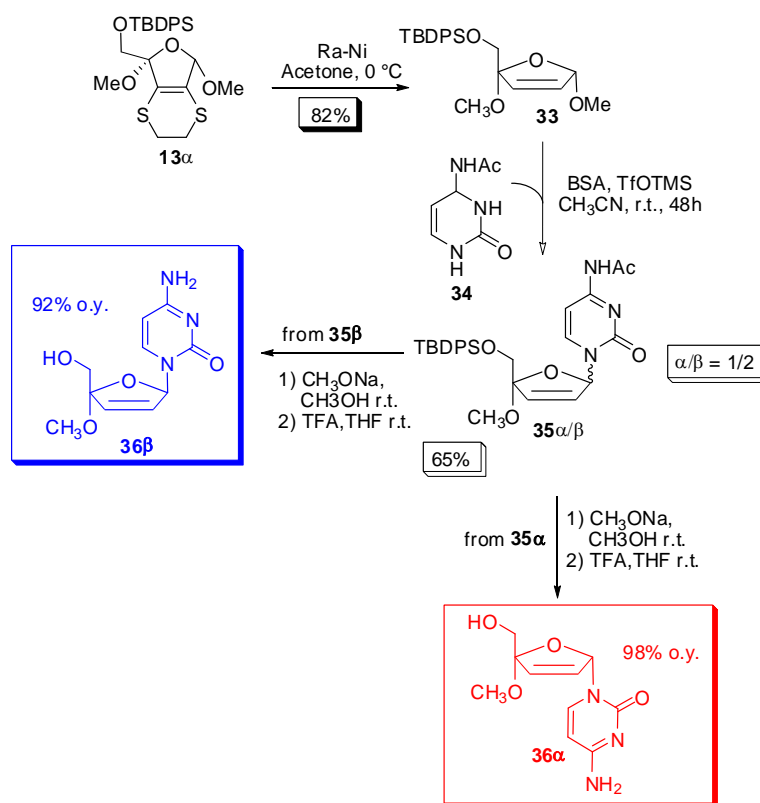
We hypothesized that reaction mechanism underlying conversion of both furans **12** and **19** into corresponding *bis*-acetals **13** and **22** follow a common path (**Scheme 7**). However, in case of furan **12**, we reasoned that unusual stability of oxocarbenium ions **28** and **30**, owing to deep delocalization of the positive charge by sulfur atoms at both C2 and C3-positions, significantly contributed to speed reaction up. In addition, since identical mechanistic paths involving furans **12** and **19** must be postulated, we assumed that, in case of **12**, stabilization of oxocarbenium ions **28** and **30** also influenced the stereochemical outcome of the reaction, due to a concurrent thermodynamic equilibrium between α:β-**13** and **28** and **30**, not occurring with acetals α:β-**22** (**Scheme 7**). To proof the above assumptions, domino reaction converting alcohol **10** into acetal **13** was carried out using C<sub>6</sub>D<sub>6</sub>/CD<sub>3</sub>OD as solvent mixture (**Scheme 8**). As primarily expected, reaction monitoring via <sup>1</sup>H NMR enabled us to reasonably exclude any mechanistic path other than that described in **Scheme 2**, by recognizing disappearance of distinctive <sup>1</sup>H NMR signals belonging to **10** (5.14 ppm, **Scheme 8a**) with those of furan **12** and especially the deuterated forms of acetals **11** and **13** (i.e. compounds α:β-**31**, 5.73 and 5.96 ppm, and α:β-**32**, 5.68 and 5.75 ppm; **Scheme 8b-c**). Most importantly, occurrence of an equilibrium between α and β isomers of **13** was proved by changes in α:β ratio of acetals **32** (**Scheme 8b-c**).



**Scheme 8.**  $^1\text{H}$  NMR monitoring of domino reaction.

A practical experimental evidence was also produced by simply treating pure  $\beta$ -**13** with DDQ in a 3/1  $\text{CDCl}_3/\text{CD}_3\text{OD}$  solution: complete conversion (>99% by  $^1\text{H}$  NMR) after 16h at rt of the latter into corresponding *bis*-trideuteromethoxy acetal **32** as a  $\alpha:\beta = 1:4$  mixture of isomers further confirmed, on one hand, existence of a thermodynamic equilibrium between the two isomers. On the other hand, it demonstrated that *bis*-thioenol ether moiety enabled effective activation of neighboring acetal functions, even under extremely mild acidic conditions. As expected, the same reaction did not proceed using acetal **22**.

Finally, the double bond of **13 $\alpha$**  was easily unmasked by dithioethylene bridge removal treating the most abundant  $\alpha$ -anomer, previously separated from  $\beta$ -anomer by crystallization from methanol, with raney-Ni in acetone at 0 °C affording the saturated furanosides **31** in good yield (82%) (**Scheme 9**).



**Scheme 9.** *N*-glycosidation reaction: Vorbrüggen one-pot protocol.

Then, the key intermediate **33** was coupled with the heterocyclic bases **34**, using the well-known Vorbrüggen one-pot protocol, in which the glycosidic bond was achieved by Lewis acid-catalyzed *N*-glycosidation reaction of **33** with *in situ* silylated bases by BSA. In fact, treatment of compound **33** with cytosine **34**, trimethylsilyl trifluoromethanesulfonate (TfOMTS) and *N,O*-bis[trimethylsilyl]acetamide (BSA) in acetonitrile, at room temperature for 48h, allowed to obtain a mixture of α- and β-nucleoside derivatives **35α/β** (1/2) which were easily separated by silica gel column chromatography (65% yield) (**Scheme 9**).

At last simple removal *O*-silyl and *N*-acetyl-protected groups, respectively with TBAF in THF and 6M NH<sub>3</sub>/CH<sub>3</sub>OH at room temperature, offered the final target compounds **36α** and **36β**, with high overall yields (98% and 92% respectively). Evaluation of racemic **36α** and **36β** as potential antiviral agents is currently in progress. In case, further development of asymmetric reaction will be considered to provide enantiopure nucleosides.

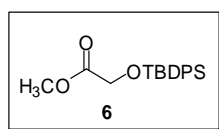
- 
- <sup>1</sup> Ruiz, M.; Lopez-Alvarado, P.; Giorgi, G.; Menendez, J.C. *Chem. Soc. Rev.* **2011**, *40*, 3445-3454.
- <sup>2</sup> Grondal, C.; Jeanty, M.; Enders, D. *Nat. Chem.* **2010**, *2*, 167-178.
- <sup>3</sup> Guaragna, A.; D'Errico, S.; D'Alonzo, D.; Pedatella S.; Palumbo, G. *Org. Lett.* **2007**, *9*, 3473-3476.
- <sup>4</sup> Guaragna, A.; D'Alonzo, D.; Paoletta, C.; Napolitano, C.; Palumbo, G. *J. Org. Chem.* **2010**, *75*, 3558-3568.
- <sup>5</sup> a) Guaragna, A.; Napolitano, C.; D'Alonzo, D.; Pedatella, S.; Palumbo, G. *Org. Lett.* **2006**, *8*, 4863-4866; b) D'Alonzo, D.; Guaragna, A.; Napolitano, C.; Palumbo, G. *J. Org. Chem.* **2008**, *73*, 5636-5639.
- <sup>6</sup> a) D'Alonzo, D.; Van Aerschot, A.; Guaragna, A.; Palumbo, G.; Schepers, G.; Capone, S.; Rozenski, J.; Herdewijn, P. *Chem. Eur. J.* **2009**, *15*, 10121-10131; b) D'Alonzo, D.; Guaragna, A.; Van Aerschot, A.; Herdewijn, P.; Palumbo, G. *J. Org. Chem.* **2010**, *75*, 6402-6410.
- <sup>7</sup> Len, C.; Mackenzie, G. *Tetrahedron* **2006**, *62*, 9085-9107.
- <sup>8</sup> Albert, M.; De Souza, D.; Feiertag, P.; Hönig, H. *Org. Lett.* **2002**, *4*, 3251-3254.

### 3.2.2.1 CONCLUSION

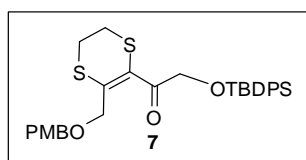
A DDQ-mediated domino reaction, enabling synthesis of a number of substituted furans and 2,3-dihydrofurans from a common acyclic starting material containing the 5,6-dihydro-1,4-dithiin moiety, has been developed. Analysis of reaction mechanism highlighted a crucial role of the heterocyclic unit in influencing rate and stereoselectivity of the process. This domino approach represents the key step of the straightforward synthesis of novel D- and L-4'-substituted nucleosides.

### 3.2.2.2 EXPERIMENTAL SECTION

All moisture-sensitive reactions were performed under a nitrogen atmosphere using oven-dried glassware. Solvents were dried over standard drying agents and freshly distilled prior to use. Reactions were monitored by TLC (precoated silica gel plate F254, Merck). Column chromatography: Merck Kieselgel 60 (70-230 mesh); flash chromatography: Merck Kieselgel 60 (230-400 mesh).  $^1\text{H}$  and  $^{13}\text{C}$  NMR spectra were recorded on NMR spectrometers operating on Varian VXR (200 MHz), Bruker DRX (400 MHz) or Varian Inova Marker (500 MHz), using  $\text{CDCl}_3$  solutions unless otherwise specified. In all cases, tetramethylsilane (TMS) was used as internal standard for calibrating chemical shifts ( $\delta$ ). Coupling constant values ( $J$ ) were reported in Hz. Combustion analyses were performed by using CHNS analyzer.

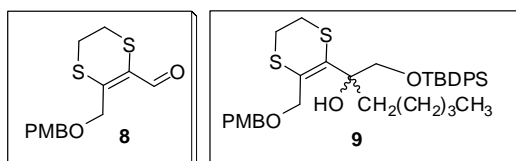


**Compound 6.** To a stirred solution of methyl glycolate (0.500 g, 5.5 mmol) in dry DMF (8 mL), imidazole (0.453 g, 6.66 mmol) and TBDPSCl (1.7 mL, 6.6 mmol) was added at room temperature. After 3h (TLC: Hexane/EtOAc 9:1) the solvent was evaporated under reduced pressure at room temperature; the residue was transferred in a separatory flask with  $\text{CHCl}_3$  and washed with ice-cold water. The organic layer was dried on  $\text{Na}_2\text{SO}_4$  and the solvent was evaporated under vacuum. The crude residue was purified by silica gel column chromatography to give the pure **6** (1.76 g, yield 98%): oily.  $^1\text{H}$  NMR (200 MHz,  $\text{CDCl}_3$ ):  $\delta$  1.09 (s, 9H,  $\text{C}(\text{CH}_3)_3$ ), 3.68 (s, 3H,  $\text{OCH}_3$ ), 4.25 (s, 2H,  $\text{CH}_2$ ), 7.38-7.42 (m, 6H, Arom-H), 7.66-7.71 (m, 4H, Arom-H).  $^{13}\text{C}$  NMR (50 MHz,  $\text{CDCl}_3$ ): ppm 19.5, 26.9, 51.8, 62.4, 128.0, 130.2, 133.01, 135.8, 171.9. Anal. calcd for  $\text{C}_{19}\text{H}_{24}\text{O}_3\text{Si}$ : C 69.47, H 7.36, Si 8.55. Found: C 69.67, H 7.33.



**Compound 7.** To a stirring solution of DIPA (0.32 mL, 2.23 mmol) in dry THF (4 mL), at  $-78\text{ }^\circ\text{C}$  under nitrogen atmosphere, *n*-BuLi (1.6 M, 0.21 mL, 2.23 mmol) was added to generate lithium diisopropylamide *in situ*. After 10 min, to the mixture a solution of **1**

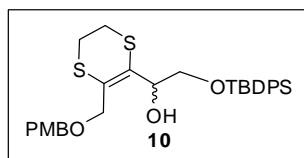
(0.50 g, 1.86 mmol) in dry THF (2 mL). The solution was stirred for 30 min at  $-78\text{ }^{\circ}\text{C}$ , then a solution of electrophile **6** (0.612 g, 1.86 mmol) in THF (2 mL) was added. After 20 min TLC (hexane/EtOAc 9:1) showed the complete formation of final product and the reaction mixture was carefully quenched with 10% aq  $\text{NH}_4\text{Cl}$ . The mixture was extracted with EtOAc, and the combined organic phases were washed with brine, dried ( $\text{Na}_2\text{SO}_4$ ) and evaporated under reduced pressure to give a crude residue from which chromatography over silica gel column (hexane/AcOEt=8:2) gave the pure **7** (0.840 g, yield 80%): oily.  $^1\text{H}$  NMR (200 MHz,  $\text{CDCl}_3$ ):  $\delta$  1.09 (s, 9H,  $\text{C}(\text{CH}_3)_3$ ), 2.99-3.05 (m, 2H,  $\text{CH}_2\text{S}$ ), 3.19-3.22 (m, 2H,  $\text{CH}_2\text{S}$ ), 3.79 (s, 3H,  $\text{OCH}_3$ ), 4.34 (s, 2H,  $\text{PhCH}_2\text{O}$ ), 4.38 (s, 2H,  $\text{CH}_2\text{OSi}$ ), 4.57 (s, 2H,  $\text{OCH}_2\text{C}=\text{C}$ ), 6.85 (d, 2H,  $\text{PMB-H}_{\text{ortho}}$ ), 7.25 (d, 2H,  $\text{PMB-H}_{\text{meta}}$ ), 7.34-7.43 (m, 6H, Arom-H), 7.65-7.71 (m, 4H, Arom-H).  $^{13}\text{C}$  NMR (50 MHz,  $\text{CDCl}_3$ ): ppm 19.2, 26.4, 28.2, 29.6, 55.1, 68.6, 71.1, 72.2, 113.6, 122.6, 127.6, 129.5, 129.7, 132.9, 135.5, 140.5, 159.2, 195.4. Anal. calcd for  $\text{C}_{31}\text{H}_{36}\text{O}_4\text{S}_2\text{Si}$ : C 65.92, H 6.42, S 11.35, Si 4.97. Found: C 66.11, H 6.40, S 11.30.



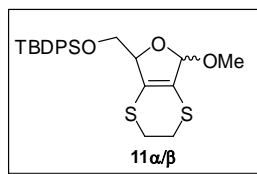
**Compound 8 and 9.** BuLi (1.6 M in hexane, 0.35 mL) was added dropwise to a stirred solution of **1** (0.1 g, 0.37 mmol) in anhydrous THF (0.5 mL) at  $-78\text{ }^{\circ}\text{C}$  and under nitrogen atmosphere. After 10 min a solution of electrophile **6** (0.122 g, 0.37 mmol) in the same solvent (0.5 mL) was added. The reaction mixture was stirred for 2h at  $-78\text{ }^{\circ}\text{C}$ , then carefully quenched with 10% aq  $\text{NH}_4\text{Cl}$ . The mixture was extracted with EtOAc, the combined organic phases washed with brine, dried ( $\text{Na}_2\text{SO}_4$ ) and evaporated under reduced pressure. Chromatography of the crude residue over silica gel (hexane/EtOAc = 9:1) gave the two separated product **8** (10% yield) and **9** (80% yield).

*Data for compound 8.* Oily;  $^1\text{H}$  NMR (500 MHz,  $\text{CDCl}_3$ ):  $\delta$  3.10-3.18 (m, 2H,  $\text{CH}_2\text{S}$ ), 3.28-3.32 (m, 2H,  $\text{CH}_2\text{S}$ ), 3.81 (s, 3H,  $\text{OCH}_3$ ), 4.41 (s, 2H,  $\text{PhCH}_2\text{O}$ ), 4.52 (s, 2H,  $\text{OCH}_2\text{C}=\text{C}$ ), 6.89 (d,  $J = 8.3$  Hz, 2H,  $\text{PMB-H}_{\text{ortho}}$ ), 7.26 (d,  $J = 8.3$  Hz, 2H,  $\text{PMB-H}_{\text{meta}}$ ), 9.82 (s, 1H,  $\text{CH}=\text{O}$ ).  $^{13}\text{C}$  NMR (125 MHz,  $\text{CDCl}_3$ ):  $\delta$  25.5, 30.2, 55.3, 68.9, 72.2, 114.0, 129.0, 129.6, 148.8, 159.6, 183.5. Anal. calcd for  $\text{C}_{14}\text{H}_{16}\text{O}_3\text{S}_2$ : C, 56.73; H, 5.44. Found: C, 56.90; H, 5.42.

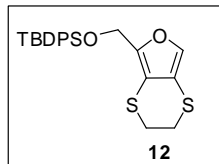
**Data for compound 9.** Oily;  $^1\text{H}$  NMR (200 MHz,  $\text{CDCl}_3$ ):  $\delta$  1.07 (s, 9H,  $\text{C}(\text{CH}_3)_3$ ), 1.24-1.55 (m, 5H,  $\text{CH}_2\text{CH}_3$ ), 1.61-1.82 (m, 2H,  $\text{CH}_2$ ), 2.95-3.05 (m, 2H,  $\text{CH}_2\text{S}$ ), 3.18-3.24 (m, 2H,  $\text{CH}_2\text{S}$ ) 3.56 (d,  $J_{a-b} = 10$ , 1H,  $\text{CHH}_a\text{OSi}$ ), 3.78 (s, 3H,  $\text{OCH}_3$ ), 4.05 (d,  $J_{b-a} = 10$ , 1H,  $\text{CHH}_b\text{OSi}$ ) 4.23 (d,  $J_{a-b} = 11.2$ , 1H,  $\text{CHH}_a\text{COH}$ ) 4.50 (s, 2H,  $\text{CH}_2\text{Ph}$ ), 4.62 (d,  $J_{a-b} = 11.2$ , 1H,  $\text{CHH}_a\text{COH}$ ), 6.84 (d,  $J = 8.6$ , 2H,  $\text{PMB-H}_{\text{orto}}$ ), 7.25 (d,  $J = 8.6$ , 2H,  $\text{PMB-H}_{\text{meta}}$ ), 7.36-7.52 (m, 6H, Arom-H), 7.63-7.81 (m, 4H, Arom-H).  $^{13}\text{C}$  NMR (50 MHz,  $\text{CDCl}_3$ ): ppm 14.3, 19.25, 19.64, 23.28, 25.7, 26.8, 27.1, 29.6, 32.5, 36.8, 55.5, 71.1, 72.1, 72.4, 77.5, 82.8, 116.9, 124.3, 127.6, 128.8, 129.5, 129.6, 132.8, 135.3, 159.0. Anal. calcd for  $\text{C}_{36}\text{H}_{48}\text{O}_4\text{S}_2\text{Si}$ : C 67.88, H 7.60, S 10.07, Si 4.41. Found: C 67.90, H 7.58, S 10.05.



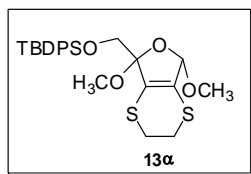
**Compound 10.** To a stirring solution of ketone **7** (0.50 g, 0.89 mmol) in dry THF (15.5 mL) at room temperature, under nitrogen atmosphere, a 1M solution of  $\text{BH}_3\text{-THF}$  (2.2 mL, 2.2 mmol) was added dropwise. After 5h to the mixture of reaction  $\text{CH}_3\text{OH}$  (5 mL) was slowly added, then the solvent was evaporated under reduced pressure. Column chromatography of crude residue over silica gel (hexane/EtOAc 9/1) gave the pure **10** (0.43 g 86% yield): oily.  $^1\text{H}$  NMR (400 MHz,  $\text{CDCl}_3$ ):  $\delta$  1.11 (s, 9H,  $\text{C}(\text{CH}_3)_3$ ), 2.94-3.29 (m, 4H,  $\text{CH}_2\text{S}$ ), 3.70-3.89 (m, 5H,  $\text{CH}_2\text{OSi}$ ,  $\text{OCH}_3$ ), 3.92 (d,  $J_{a-b} = 12.2$ , 1H,  $\text{CHH}_a\text{O}$ ), 3.96 (d,  $J_{b-a} = 12.2$ , 1H,  $\text{CHH}_b\text{O}$ ), 4.31 (d,  $J_{a-b} = 11.6$ , 1H,  $\text{CHH}_a\text{Ph}$ ), 4.36 (d,  $J_{b-a} = 11.6$ , 1H,  $\text{CHH}_b\text{Ph}$ ), 4.86 (dd,  $J = 5.0$ ,  $J = 7.8$ , 1H, CH), 6.87 (d,  $J = 8.6$ , 2H,  $\text{PMB-H}_{\text{orto}}$ ), 7.25 (d,  $J = 8.6$ , 2H,  $\text{PMB-H}_{\text{meta}}$ ), 7.36-7.52 (m, 6H, Arom-H), 7.63-7.81 (m, 4H, Arom-H).  $^{13}\text{C}$  NMR (50 MHz,  $\text{CDCl}_3$ ): ppm 19.0, 26.6, 27.0, 29.1, 54.9, 64.6, 66.4, 69.4, 71.4, 113.5, 124.3, 127.6, 128.8, 129.5, 129.6, 132.8, 135.3, 159.0. Anal. calcd for  $\text{C}_{31}\text{H}_{38}\text{O}_4\text{S}_2\text{Si}$ : C 65.68, H 6.76, S 11.31, Si 4.41. Found: C 65.72, H 6.80, S 11.25.



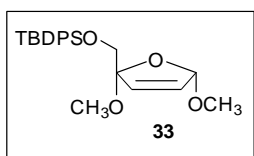
**Compound 11 $\alpha$  e 11 $\beta$ .** To a stirred  $\text{CH}_2\text{Cl}_2/\text{CH}_3\text{OH}$  (95/5) solution (8.75 mL) containing the alcohol **10** (0.50 g, 0.88 mmol) DDQ (0.28 g, 1.06 mmol) was added in one portion at room temperature. After 30 min the reaction was stopped,  $\text{H}_2\text{O}$  was added, and the mixture extracted with  $\text{CH}_2\text{Cl}_2$ . The organic layer was dried ( $\text{Na}_2\text{SO}_4$ ), and the solvent evaporated under reduced pressure. Chromatography of the crude residue over silica gel (hexane/EtOAc:95/5) gave a mixture of anomers  $\alpha/\beta$ :3.3/1 (0.335 g, 83% yield). Data for major isomer **11 $\alpha$** :  $^1\text{H}$  NMR (200 MHz,  $\text{CDCl}_3$ ):  $\delta$  1.04 (s, 9H,  $\text{C}(\text{CH}_3)_3$ ), 3.17-3.26 (m, 4H), 3.27 (s, 3H), 3.55 (s, 3H), 3.70 (d,  $J=10.5$ , 1H), 3.80 (d,  $J=10.25$ , 1H) 5.46 (s, 1H), 7.34-7.42 (m, 5H), 7.66-7.72 (m, 5H).  $^{13}\text{C}$  NMR (100 MHz,  $\text{CDCl}_3$ ): ppm 19.2, 25.9, 26.0, 26.5, 49.7, 55.7, 65.6, 99.4, 107.4, 113.9, 127.4, 129.4, 135.4, 135.5. Anal. calcd for  $\text{C}_{24}\text{H}_{30}\text{O}_3\text{S}_2\text{Si}$ : C 62.84, H 6.59, S 13.98, Si 6.12. Found: C 62.68, H 6.56, S 14.03.



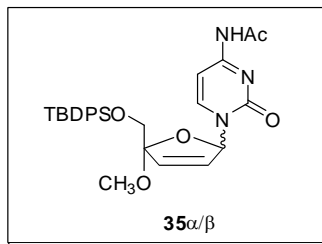
**Compound 12.** To a stirred  $\text{C}_6\text{H}_6/\text{CH}_3\text{OH}$  (95/5) solution (8.75 mL) containing the alcohol **10** (0.50 g, 0.88 mmol) DDQ (0.28 g, 1.06 mmol) was added in one portion at room temperature. After 3h the reaction was stopped,  $\text{H}_2\text{O}$  was added, and the mixture extracted with EtOAc. The organic layer was dried ( $\text{Na}_2\text{SO}_4$ ), and the solvent evaporated under reduced pressure. Chromatography of the crude residue over silica gel (hexane/EtOAc:98/2) gave the pure compound **12** (0.285 g, 75% yield).  $^1\text{H}$  NMR (200 MHz,  $\text{C}_6\text{D}_6$ ):  $\delta$  1.12 (s, 9H,  $\text{C}(\text{CH}_3)_3$ ), 2.34 (s, 4H,  $\text{CH}_2\text{S}$ ), 4.56 (s, 2H,  $\text{CH}_2\text{OSi}$ ), 6.77 (s, 1H, H-4), 7.17-7.21 (m, 5H, Arom-H), 7.74-7.80 (m, 5H, Arom-H).  $^{13}\text{C}$  NMR (100 MHz,  $\text{C}_6\text{D}_6$ ): ppm 19.2, 25.8, 26.1, 26.3, 26.6, 29.7, 57.0, 128.1, 129.4, 129.6, 133.2, 134.9, 135.7, 136.3. Anal. calcd for  $\text{C}_{23}\text{H}_{26}\text{O}_2\text{S}_2\text{Si}$ : C 64.75, H 6.14, S 15.03, Si 6.58. Found: C 65.00, H 6.12, S 15.08.



**Compound 13 $\alpha$ .** To a stirred C<sub>6</sub>H<sub>6</sub>/CH<sub>3</sub>OH (3/1) solution (8.75 mL) containing the alcohol **10** (0.50 g, 0.89 mmol) DDQ (0.37 g, 1.65 mmol) was added in one portion at room temperature. After 3h the reaction was complete, H<sub>2</sub>O was added, and the mixture was extracted with CH<sub>2</sub>Cl<sub>2</sub>. The organic layer was dried (Na<sub>2</sub>SO<sub>4</sub>), and the solvent was evaporated under reduced pressure. Chromatography of the crude residue over silica gel (hexane/EtOAc:95/5) gave a mixture of anomers  $\alpha/\beta=4/1$  (0.39 g, 90% yield). The  $\alpha$ -anomer was separated from  $\beta$ -anomer by crystallization from CH<sub>3</sub>OH. Data for major anomer **13 $\alpha$**  <sup>1</sup>H NMR (200 MHz, C<sub>6</sub>D<sub>6</sub>):  $\delta$  1.16 (s, 9H, C(CH<sub>3</sub>)<sub>3</sub>), 2.31-2.54 (m, 4H, CH<sub>2</sub>S), 3.24 (s, 3H, OCH<sub>3</sub>), 3.37 (s, 3H, OCH<sub>3</sub>), 4.04 (d,  $J_{a,b} = 9.7$ , 1H, 5-H<sub>a</sub>), 4.15 (d,  $J_{b,a} = 9.7$ , 1H, 5-H<sub>b</sub>) 5.61 (s, 1H, 1-H), 7.01-7.27 (m, 6H, Arom-H), 7.74-7.87 (m, 4H, Arom-H). <sup>13</sup>C NMR (100 MHz, CDCl<sub>3</sub>): ppm 19.2, 25.9, 26.0, 26.5, 49.7, 55.7, 65.6, 99.4, 107.4, 114.0, 127.4, 129.4, 133.5, 135.4, 135.5. Anal. calcd for C<sub>25</sub>H<sub>32</sub>O<sub>4</sub>S<sub>2</sub>Si: C 61.44, H 6.60, S 13.12, Si 5.75. Found: C 61.20, H 6.63, S 13.16.



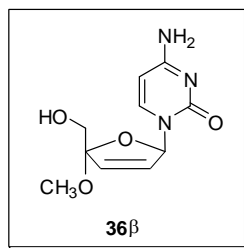
**Compound 33.** A solution of **13 $\alpha$**  (0.30 g, 0.61 mmol) in acetone (7 mL) was added in one portion to a stirred suspension of Raney-Ni (W2) (2.25 g, wet) in the same solvent (7 mL) at 0 °C. The suspension was stirred for 5h, then the solid was filtered off and washed with EtOAc. The filtrate was evaporated under reduced pressure to afford a crude residue which chromatography over silica gel (hexane/EtOAc = 98/2) gave the pure **33** (0.20 g, 82% yield) white crystals (from CH<sub>3</sub>OH). <sup>1</sup>H NMR (400 MHz, C<sub>6</sub>D<sub>6</sub>):  $\delta$  1.25 (s, 9H C(CH<sub>3</sub>)<sub>3</sub>), 3.35 (s, 3H, OCH<sub>3</sub>), 3.38 (s, 3H, OCH<sub>3</sub>), 4.09 (d,  $J_{a-b} = 10.3$ , 1H, 5-H<sub>a</sub>), 4.13 (d,  $J_{b-a} = 10.3$ , 1H, 5-H<sub>b</sub>) 5.52 (dd,  $J_{1,2}=J_{1,3} = 0.8$ , 1H, 1-H), 5.77 (dd,  $J_{2,1} 1.0$ ,  $J_{2,3} 5.8$ , 1H, 2-H), 5.88 (dd,  $J_{3,1} = 0.8$ ,  $J_{3,2} = 5.8$ , 1H, 3-H), 7.21-7.30 (m, 5H, Arom-H) 7.78-7.88 (m, 5H, Arom-H). <sup>13</sup>C NMR (50 MHz, C<sub>6</sub>H<sub>6</sub>): ppm 19.3, 26.8, 50.3, 56.2, 67.0, 107.5, 113.7, 127.6, 129.6, 132.0, 133.4, 134.8, 135.6, 135.7, 135.8. Anal. calcd for C<sub>22</sub>H<sub>30</sub>O<sub>4</sub>Si: C 69.31, H 7.59, Si 7.05. Found: C 69.52, H 7.56.



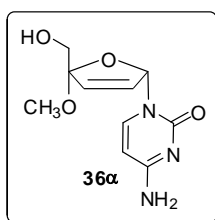
**Compound 35 $\alpha$  e 35 $\beta$ .** Cytosine (0.22 g, 1.4 mmol) and glycosyl donor **33** (0.5 g, 1.3 mmol) was dried by coevaporation with anhydrous toluene, and resuspended in anhydrous CH<sub>3</sub>CN (5 mL). To this *N,O*-bis(trimethylsilyl)acetamide (BSA, 1.25 mL, 5.0 mmol) was added and the reaction mixture was kept at room temperature for 20 min under nitrogen atmosphere. When a homogenous solution was observed TMSOTf (0.05 mL, 0.13 mmol) was added. After 24h at room temperature, to reaction mixture NaHCO<sub>3</sub> aq was added. After 10 min the solution was extracted with EtOAc and washed with brine. Organic phase was dried (Na<sub>2</sub>SO<sub>4</sub>) and evaporated under reduced pressure; chromatography (hexane/EtOAc : 1/1) of the crude residue over silica gel afforded protected nucleosides **34 $\alpha$**  e **34 $\beta$**  (0.439 g, 65%) as a 1:2 anomeric mixture. Anal. calcd for C<sub>25</sub>H<sub>33</sub>N<sub>3</sub>O<sub>5</sub>Si: C 64.71, H 6.40, N 8.09, Si 5.40. Found: C 64.99, H 6.38, N 8.06.

*Data for 35 $\alpha$ :* white crystals; <sup>1</sup>H NMR (400 MHz, CDCl<sub>3</sub>):  $\delta$  1.06 (s, 9H, C(CH<sub>3</sub>)<sub>3</sub>), 2.27 (s, 3H, COOCH<sub>3</sub>), 3.28 (s, 3H, OCH<sub>3</sub>), 3.76 (d,  $J_{a-b} = 10.9$ , 1H, 5'-H<sub>a</sub>), 3.93 (d,  $J_{b-a} = 10.9$ , 1H, 5'-H<sub>b</sub>), 6.22 (dd,  $J_{2',1'} = 1.2$ ,  $J_{2',3'} = 5.9$ , 1H, 2'-H), 6.26 (d,  $J_{3',2'} = 5.9$ , 1H, 3'-H), 6.89 (s, 1H, 1'-H), 7.37-7.46 (m, 7H, 5-H, Arom-H), 7.64-7.66 (m, 4H, Arom-H), 7.86 (d,  $J = 7.5$ , 1H, 6-H), 9.76 (bs, 1H, NH). <sup>13</sup>C NMR (125 MHz, CDCl<sub>3</sub>): ppm 19.2, 24.9, 26.8, 51.0, 64.8, 89.9, 97.1, 114.7, 127.8, 129.8, 129.9, 130.3, 132.9, 133.9, 135.5, 135.6, 144.6, 155.3, 162.9, 171.0.

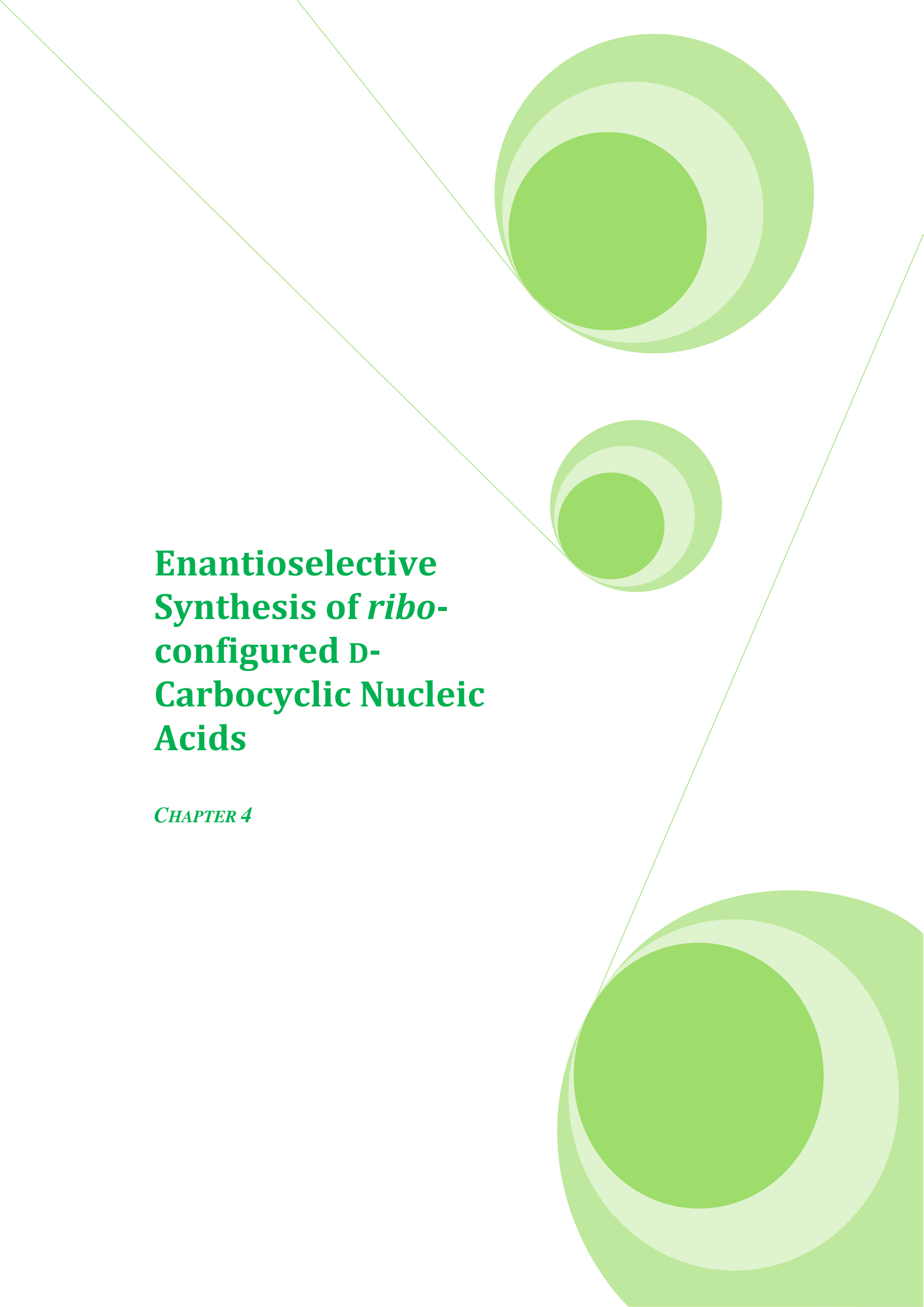
*Data for 35 $\beta$ :* white crystals; <sup>1</sup>H NMR (200 MHz, CDCl<sub>3</sub>):  $\delta$  1.09 (s, 9H, C(CH<sub>3</sub>)<sub>3</sub>), 2.23 (s, 3H, COOCH<sub>3</sub>), 3.18 (s, 3H, OCH<sub>3</sub>), 3.92 (d,  $J_{a-b} = 11.2$ , 1H, 5'-H<sub>a</sub>), 4.05 (d,  $J_{b-a} = 11.2$ , 1H, 5'-H<sub>b</sub>), 5.92 (dd,  $J_{2,1} = 1.8$ ,  $J_{2',3'} = 5.8$ , 1H, 2'-H), 6.37 (dd,  $J_{1',2'} = 0.7$ ,  $J_{2',3'} = 5.8$ , 1H, 3'-H), 7.15 (s, 1H, 1'-H), 7.37-7.48 (m, 7H, 5-H, Arom-H), 7.55-7.64 (m, 4H, Arom-H), 8.23 (d,  $J = 7.5$ , 1H, 6-H), 9.0 (bs, 1H, NH). <sup>13</sup>C NMR (125 MHz, CDCl<sub>3</sub>): ppm 19.3, 25.0, 26.9, 27.0, 29.7, 49.7, 66.7, 90.7, 116.2, 127.8, 127.9, 130.0, 130.1, 132.0, 132.3, 135.4, 135.6, 145.2, 156.2, 162.6, 170.6.



**Compound 36β.** To a stirred solution of **35β** (0.05 g, 0.10 mmol) in THF (670 μL) TBAF (11 μL, 1 M solution in THF, 0.11 mmol) was added at room temperature. The reaction was stirred for 18h, then the solvent was evaporated under vacuum. The crude residue was treated with 1 mL of NH<sub>3</sub>/CH<sub>3</sub>OH 6M at room temperature. After 2h the solvent was evaporated and the crude residue purified by chromatography on silica gel (CHCl<sub>3</sub>/CH<sub>3</sub>OH 8/2) affording the unprotected nucleoside **36β** as white crystals (0.023 g, 97 % o.y.). <sup>1</sup>H NMR (400 MHz, CD<sub>3</sub>OD): 3.26 (s, 3H, OCH<sub>3</sub>), 3.58 (d,  $J_{a-b} = 11.8$ , 1H, 5-H<sub>a</sub>), 3.74 (d,  $J_{b-a} = 11.8$ , 1H, 5-H<sub>b</sub>), 5.90 (d,  $J = 7.5$ , 1H, 5-H), 6.26 (dd,  $J_{2',1'} = 1.3$ ,  $J_{2',3'} = 5.9$ , 1H, 2'-H), 6.32 (d,  $J_{3',2'} = 5.9$ , 1H, 3'-H), 6.83 (bs, 1H, 1'-H), 7.59 (d,  $J = 7.5$ , 1H, 6-H). <sup>13</sup>C NMR (100 MHz, CD<sub>3</sub>OD): ppm 55.0, 65.2, 90.1, 96.6, 115.5, 131.8, 135.3, 142.8, 158.6, 167.9. Anal. calcd for C<sub>10</sub>H<sub>13</sub>N<sub>3</sub>O<sub>4</sub>: C 50.39, H 5.46, N 17.50. Found: C 50.39, H 5.46, N 17.50.



**Compound 36α.** The nucleoside **36α** was obtained (92% o.y.) under the same conditions reported for the synthesis of compound **36β**. White crystals; <sup>1</sup>H NMR (400 MHz, CD<sub>3</sub>OD): 3.21 (s, 3H, OCH<sub>3</sub>), 3.59 (d,  $J_{a-b} = 11.9$ , 1H, 5-H<sub>a</sub>), 3.74 (d,  $J_{b-a} = 11.9$ , 1H, 5-H<sub>b</sub>), 5.84 (d,  $J = 7.5$ , 1H, 5-H), 6.12 (dd,  $J_{2',1'} = 1.7$ ,  $J_{2',3'} = 5.8$ , 1H, 2'-H), 6.30 (d,  $J_{3',2'} = 5.8$ , 1H, 3'-H), 7.13 (s, 1H, 1'-H), 7.88 (d,  $J = 7.5$ , 1H, 6-H). <sup>13</sup>C NMR (100 MHz, CD<sub>3</sub>OD): ppm 50.0, 65.7, 91.7, 96.3, 117.0, 133.3, 135.3, 143.1, 158.7, 167.8. Anal. calcd for C<sub>10</sub>H<sub>13</sub>N<sub>3</sub>O<sub>4</sub>: C 50.39, H 5.46, N 17.50. Found: C 50.39, H 5.46, N 17.50.



# **Enantioselective Synthesis of *ribo*- configured D- Carbocyclic Nucleic Acids**

*CHAPTER 4*

## 4.1 INTRODUCTION

Modified oligonucleotides MOs, are synthetic compounds devised to have a structural resemblance with their corresponding natural counterparts, and occupy a privileged position in antiviral and anti-tumor drug design. Compared to nucleoside analogues (NAs), which are well established lead compounds for the treatment of a large number of human diseases, on the other hand, given their more relatively recent birthdate, only a few MOs are currently undergoing advanced clinical trials as drug candidates; however, they have potentially much wider and safer therapeutic applications.

By virtue of their obvious biochemical link, NAs and MOs share a common overall pharmacological effect, as they are both able to inhibit viral/cellular replication by selectively blocking the information flow enclosed in the viral/human genome. However, they use different action mechanisms. On one side, NAs are enzymatically converted into their triphosphate forms (NA-TPs), acting as building blocks for nucleic acid biosynthesis and usually preventing further viral nucleic acid chain elongation by means of various mechanisms as reported in the chapter 3. On the other side, MOs interact with nucleic acid complements, with a subsequent involvement of enzymatic machineries, which provide the eventual pharmacological effect. The discovery by Zamecnik and Stephenson<sup>1</sup> (1978) that gene expression can be modified by exogenous nucleic acids, sets the basis for so called “gene silencing strategies” in human therapy, stimulating the development of technologies that use modified nucleic acids to manipulate gene expression.

Some of the most common approaches for gene silencing<sup>2</sup> are briefly discussed below (**Figure 1**).

**Antisense strategy.** Short MOs are designed to bind to specific sequences of a specific *mRNA* strand via Watson–Crick duplex formation, the resulting complex being recognized by hydrolytic enzymes, such as the RNase H, which cleaves the RNA strand releasing the MOs.<sup>3</sup>

**Antigene strategy.** MOs bind sequence selectively to genomic, double stranded DNA and interfere with transcription and the DNA processing machinery via triple helix formation.<sup>4</sup>

**RNA interference.** This approach is based on the use of a double helix of a short stretch of synthetic RNA (known as siRNA, small interfering RNA). siRNA is introduced into the cell and then incorporated into the RNA-induced silencing complex (RISC), resulting in the cleavage of the sense strand of RNA by argonaute 2 (AGO2). The activated RISC–siRNA complex seeks out, binds to and degrades complementary mRNA, which leads to the silencing of the target gene. The activated RISC–siRNA complex can then be recycled for the destruction of identical mRNA targets.<sup>5</sup>

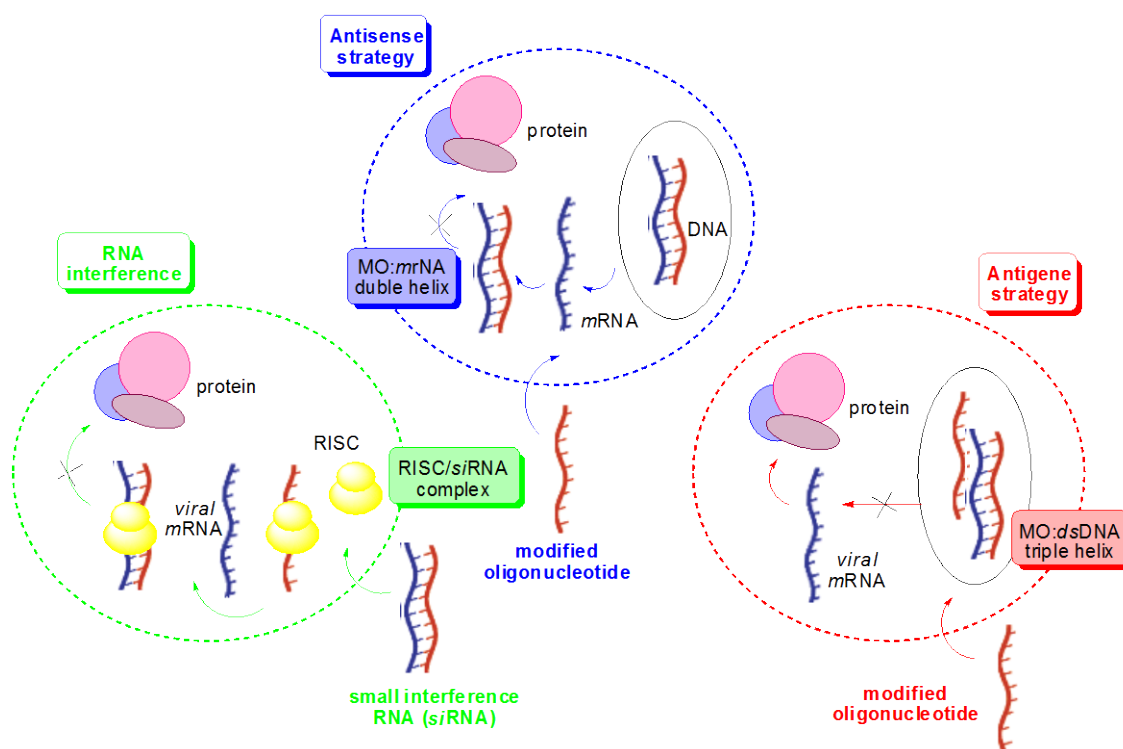


**Figure 1.** Action mechanism of MOs as therapeutic agents.

#### 4.1.1 FEATURES OF SYNTHETIC OLIGONUCLEOTIDES.

With the aim of ensuring active therapeutic efficacy *in vivo*, the MOs must have appropriate structural features.

**High affinity and specificity of an oligonucleotide to its mRNA target.** MOs consisting of 13 nucleotides have the minimum sequence of bases to form hybrids (double, triple helices, or more complex structures) with specific complementary strand mRNA/DNA, because statistically there are not two strand of this length with the same

sequence of bases. In contrast, oligomers of shorter length can theoretically form double helices with more of a complementary sequence and so they are less selective.

**Stability of the hybrid.** Synthetic MOs are designed to form stable hybrids with complementary DNA/mRNA. The stability of a hybrid, whether formed by natural and synthetic sequences, can be observed by melting temperature  $T_m$ , i.e. the temperature at which half of the DNA strands are in the double-helical state and half are in the random coil states. Obviously, the oligomer with a better specificity for the complementary treatment target is characterized by a higher  $T_m$ . It's also clear that the latter must be higher than body temperature, in order to allow his obligation to perform its therapeutic activity *in vivo*.

**Bioavailability.** Although an oligonucleotide strand too "short" could lead to a weak selectivity for the MO target, the choice to synthesize an oligomer consisting of many nucleotide units could make the molecule highly polar (due to the large number of phosphate groups), preventing an efficient across cell membranes and nuclear. The best choice for determining the length of an ON adapter must therefore represent a compromise between specific factors and bioavailability.

**Biostability.** MO units consisting of (deoxy)ribonucleotide chemically identical to natural (i.e. those studied *in vitro* by Zamenick and Stephenson) have limited applicability *in vivo* due to rapid degradation by cellular nucleases.<sup>1</sup> In the modern development of strategies for gene silencing plays, therefore, a very important role in the design of analogues of natural nucleic acids, provided with appropriate changes in the chemical structure of the nucleotide base unit in order to improve the stability of the biological medium.

#### 4.1.2 STABILITY *IN VIVO* OF SYNTHETIC OLIGONUCLEOTIDES: SUGAR-MODIFIED NUCLEIC ACIDS

Three main types of chemical modifications are under investigation in oligonucleotide antisense, antigene or RNAi experiments: a) modified nucleobase,<sup>6</sup> b) modified sugar,<sup>7</sup> c) modified phosphate group.<sup>3,8</sup>

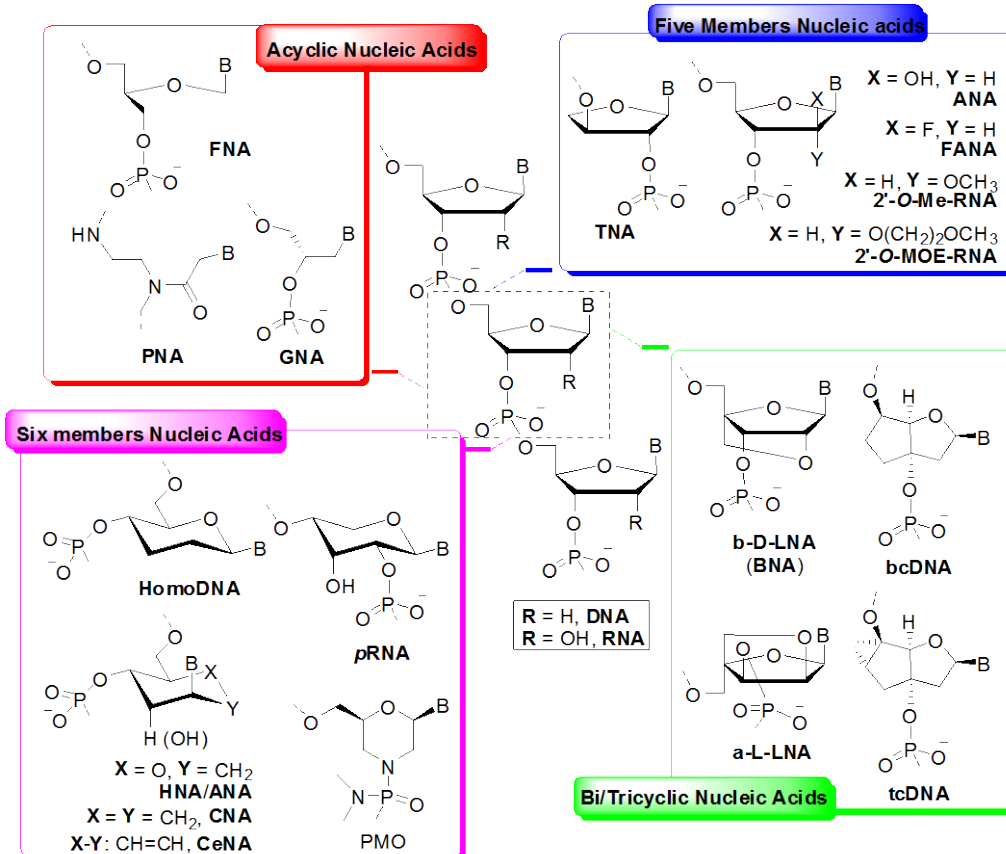


**Figure 2.** Chemically-modified nucleic acids.

In particular, the study of oligonucleotide sequences containing chemical modified sugar units is a line of research of great interest. Over the last few years an huge number of variations of the native furanoside skeleton has been achieved, like simple functionalization of the hydroxyl group on C2' of ribonucleotide ring<sup>3b</sup> or complete replacement of the latter with at six-membered rings,<sup>7c</sup> bi/tricyclic<sup>4,7a</sup> or acyclic<sup>7b</sup> structures (**Figure 2**). In many cases, the resulting nucleic acids have shown excellent potential as therapeutic agents.<sup>3</sup>

The replacement of the (deoxy) ribofuranoside unit of DNA and RNA with variously modified monosaccharides is generally devised relying on three important factors for the stability and efficacy of the resulting MO analogues: a) resistance to nucleases, b) mimicking of natural nucleic acids, c) structural preorganization of the nucleotide strand.

**Resistance to nucleases.** The replacement of furanoside ring of natural nucleic acids with other saccharide units (or their analogues) makes the resulting MOs typically more stable to nucleases because the substrate is not recognized as a natural.<sup>7c</sup> In some cases,

the ability of MOs to limit the degradative action of cellular nucleases was also obtained by replacing the more labile functional groups of natural nucleic acids with chemically more stable groups one.<sup>9</sup>

**Mimicking natural nucleic acids.** The complete definition of the conformation of a nucleoside usually involves the determination of three groups of structural parameters: a) the orientation about the glycosyl bond as *syn* or *anti*, which is more accurately defined by the value of the angle  $\chi$ , b) the orientation of the hydroxymethyl group, determined by the value of the angle  $\gamma$ , and c) the deviation from planarity of the sugar ring, measured by the angle of pseudorotation  $P$ .<sup>10</sup> Particularly, the pseudorotation angle has been introduced to describe the continuous interconversions among a (virtually) infinite number of puckered forms related to the furanose ring of natural (deoxy)ribonucleotides. Thus, furanose ring conformations (mainly envelope and twisted) can be conveniently described by the value of phase angle  $P$  in the pseudorotational cycle (**Figure 3**).

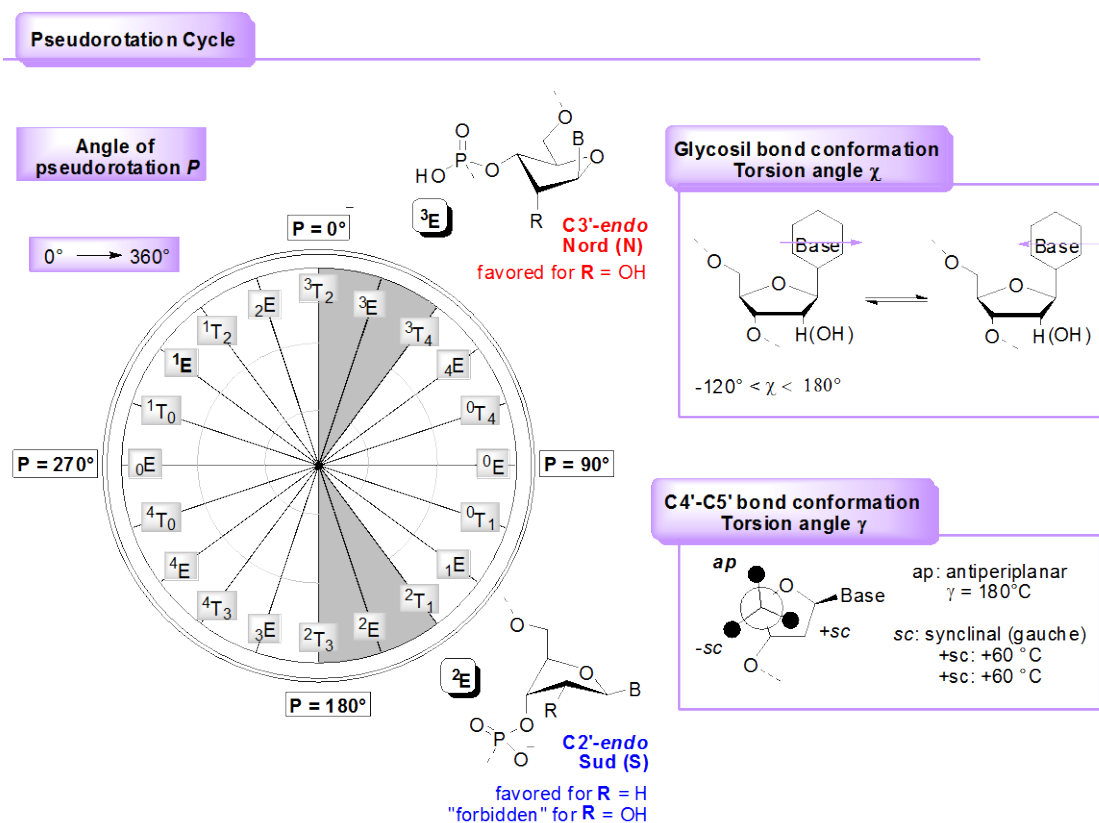


**Figure 3.** Structural parameters defining the conformation of a (deoxy)ribonucleoside.

By convention,  $P = 0^\circ$  corresponds to a *C*-3'-*endo* puckering, while  $P = 180^\circ$  corresponds to the *C*-2'-*endo* antipode; they are also generically described, respectively, as *N* (North) and *S* (South) conformations. In ribose and deoxyribose nucleosides, sugar moieties fluctuate between these two extremes, because the crossing energy barrier between *N* and *S* forms is relatively small ( $\Delta G \sim 20 \text{ kJ mol}^{-1}$ ). Crystallographic data of individual nucleosides revealed that the puckering modes of the furanose ring cluster near one of these two antipodal regions:<sup>11</sup> *N* domain between  $342^\circ$  and  $18^\circ$  ( ${}^2E \rightarrow {}^3T_2 \rightarrow {}^3E$ ) and antipodean *S* area between  $162^\circ$  and  $198^\circ$  ( ${}^2E \rightarrow {}^2T_3 \rightarrow {}^3E$ ) (Figure 3).

When the sugar rings of natural D-(deoxy)ribonucleotides occupy *N* and *S* domains in polymeric structures (e.g. RNA and DNA) they lead, respectively, to two common right-handed helices, known as A- and B-type forms.<sup>12</sup> These two different puckering modes are favored because they best alleviate the steric clashes of sugar substituents. However, the preference for one conformation or for another one seems to derive from the nature of the *C*-2' group. In the presence of a withdrawing (e.g. OH) group, the *C*-3'-*endo* (*N*) pucker is the only conformation observed (such as in *ds*RNA, A-type helix); if it is absent, the *C*-2'-*endo* (*S*) pucker is preferred (such as in *ds*DNA, B-type helix)<sup>[1]</sup> (Figure 4).

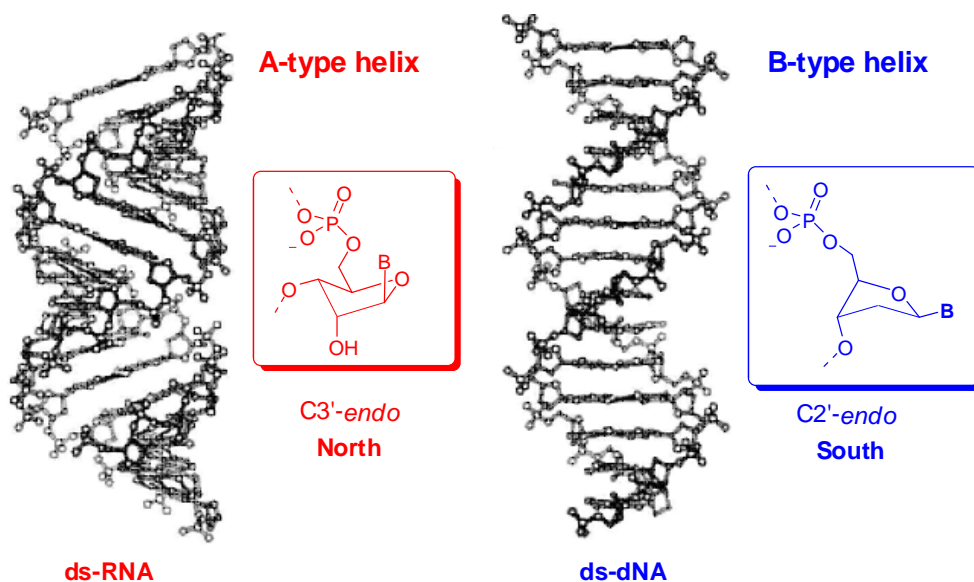


**Figure 4.** A- and B-type duplex conformations reported, respectively, for *ds*RNA and *ds*DNA.

**The structural preorganization of the nucleotide strand.** It is now well established that biological events relying on host-guest recognition processes require appropriate structural features of both components.<sup>13</sup> The formation of these kind of complexes is thermodynamically unlikely for two main reasons. First of all, three degrees of translational and rotational entropy are lost while forming a complex from two separate molecules. Moreover, if each molecule has free internal bond rotations to be locked for the complex, several degrees of freedom for each bond will be lost. Even though the first effect is mostly an unavoidable feature of molecular recognition, guest-molecular design can overcome the last one.<sup>14</sup> Particularly, if a guest molecule is designed to be “frozen” in the binding conformation before the recognition process, then any entropy cost, due to fixing bond rotations, will not be necessary in binding. This assumption introduces the concept of “preorganization”, coined by Donald Cram to explain host-guest interactions in supramolecular chemistry. In few words, reduction of all possible conformational states of a guest molecule to those fitting with the geometric and stereochemical requirements of a host molecule may lead to an entropic benefit of complex formation, and thus to enhanced complex stability. As reported below, the concept of molecular preorganization (particularly, that of sugar preorganization within nucleoside or oligonucleotide structures) has been profitably exploited to gain insight into the structural details underlying both enzyme-NAs recognition events and the hybridization properties of MOs to be efficiently annealed with natural complementary strands.

### **4.1.3 THE CRITICAL ROLE OF SUGAR CONFORMATION IN THE THERAPEUTIC POTENTIAL OF OLIGONUCLEOTIDE ANALOGUES**

To be successful, most MOs must rely on efficient hybridization with natural RNA and DNA complements. This goal is usually attained by designing structurally-preorganized MOs, able to keep the potential for communication (*via* WC or any other alternative base-pairing system) resembling the natural A-type or B-type duplexes without entropy penalty involved in the binding process.<sup>15</sup> In particular, MOs having sugar units restricted into the *N* conformation, thus forming A-type duplexes, resulted into the highest duplex stabilities.<sup>16</sup> On the other hand, examples of MOs with mononucleotide

units resembling the *S* sugar pucker, thus leading to B-type duplexes, are much more sporadic. An accurate structural similarity with natural nucleic acids is of key relevance in some strategies, such as in the antisense approach. Thus, a convincing way to improve the binding properties of a MO toward the desired duplex conformation has been to apply conformational restrictions of the furanose ring of nucleotide units toward one of the two *C3'-endo* and *C2'-endo* sugar conformations. Hereafter, the potential of the most relevant sugar modified MOs will be briefly discussed.

#### 4.1.4 SIX-MEMBERED NUCLEIC ACIDS

**1',5'-D-Anhydrohexitol Nucleic Acids (HNA).** As above discussed, replacement of a furanose ring with a pyranose one involves differences in flexibility, causing conformational preorganization of the corresponding oligonucleotide system.<sup>17</sup> This was the rationale behind the design of a great amount of (pento and hexo)-pyranosyl oligonucleotides, which have been investigated over the years to consider their potential in therapy,<sup>18</sup> diagnostics,<sup>19</sup> synthetic biology<sup>20</sup> and etiology-oriented research.<sup>21</sup> In this context, it was thought that nucleobase positioning at the axial or equatorial C2' site of an hexopyranosyl unit could bring the extra methylene group of the six-membered ring in the minor groove site, where it should not influence the conformational freedom of nucleobases in the neighboring residues. This assumption led to the design of conformationally restricted pyranose ONs such as 1',5'-anhydro-D-*ribo/arabino*-hexitol nucleic acids (respectively  $\alpha$ - and  $\beta$ -HNA).<sup>22</sup> Particularly, the  $\beta$ -isomer (corresponding to the axial orientation of the nucleobase) demonstrated most accurate mimicking of natural nucleic acids. Indeed, as already mentioned for the anhydrohexitol nucleosides, the nucleotide unit of  $\beta$ -HNA (hereafter HNA) closely resemble that found in natural nucleic acids inducing A-type duplexes, such as RNA.<sup>39</sup>

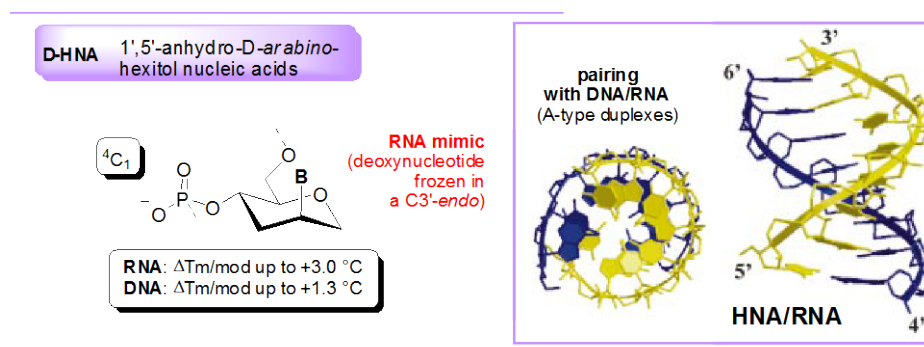


**Figure 5.** 1',5'-D-Anhydrohexitol Nucleic Acids (HNA).

Because of these features, the HNA system represented one of the most prominent examples of hexopyranose nucleic acids with capability for cross-communication with natural complements (DNA:  $\Delta T_m/\text{mod}$  up to +1.3 °C; RNA:  $\Delta T_m/\text{mod}$  up to +3 °C).<sup>24</sup> CD analysis demonstrated that HNA strands of both HNA:RNA and HNA:DNA hybrids adopted a winding very close to the A-type helix (**Figure 5**). However, this could also be the reason why HNA:RNA duplexes were resistant to RNase H activation.<sup>[39]</sup> Nonetheless, HNA could be used to control gene expression, as demonstrated by the inhibition of P-glycoprotein expression in a cell system.<sup>23</sup>

The intriguing properties of HNA stimulated the development of further analogues (**Figure 6**) based on modifications in both structure and configuration of the sugar ring.<sup>44</sup> For example, the hydroxylated versions of HNA, namely ANA (Altritol Nucleic Acids) and MNA (Mannitol Nucleic Acids) were prepared and evaluated (**Figure 6**). The complexes between ANA and RNA or DNA were reported to be even more stable than those between HNA and natural complements (e.g., RNA:  $\Delta T_m/\text{mod}$  up to +7 °C).<sup>24</sup> This was evidently due to the introduction of the axially-oriented hydroxyl group, with more accurate RNA mimicking. Hybridization ability of ANA enabled to consider it as an efficient tool in gene expression inhibition<sup>25</sup> and in nucleic acid-based diagnostics and nanotechnology.<sup>26</sup> Conversely, the diastereoisomeric MNA displayed considerably minor affinity to RNA, compared to ANA or HNA.<sup>27</sup> Molecular modelling studies identified the reason for such reduced affinity in the intrastrand inter-residue H-bond formation between the equatorial C3'-positioned OH group and the O6' of the phosphodiester group of the following nucleotide unit, tying the MNA single strand into a non-pairing conformation.<sup>28</sup>

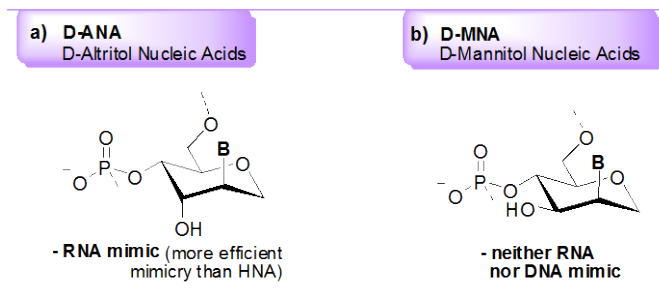


**Figure 6.** HNA derivatives.

**CNA (Cyclohexanyl Nucleic Acids).** An interesting example of saturated six-membered nucleic acids derived from HNA, is Cyclohexanyl Nucleic Acids (CNA).<sup>29</sup> The rigidity of the chair conformation of cyclohexane of CNA gives a high structural preorganization to corresponding oligonucleotide strands.

However, the CNA drew attention because they represent a first example of oligonucleotides existing in two extreme forms. In fact solution phase analysis reveals that this nucleosides adopt a) an A-type helix (corresponding to a  ${}^4C_1$  conformation of pseudosaccharide portion) superimposable to HNA structure and b) a quasi-linear structure (corresponding to a  ${}^1C_4$  conformation of pseudosaccharide portion).<sup>7c</sup> In particular, the single-strand of CNA is present in a non-helical conformation as the cyclohexane ring adopts a  ${}^1C_4$  conformation due to unfavorable 1,3-diaxial interactions between the nucleobase and the atoms of hydrogen on C1' and C3' in the  ${}^4C_1$  conformation (**Figure 7**). The presence of a complementary strand (DNA or RNA) can, however, involve a significant thermodynamic advantage by promoting the inversion of the chair ( ${}^1C_4 \rightarrow {}^4C_1$ ) in the adequate conformation for base pairing.<sup>12</sup>

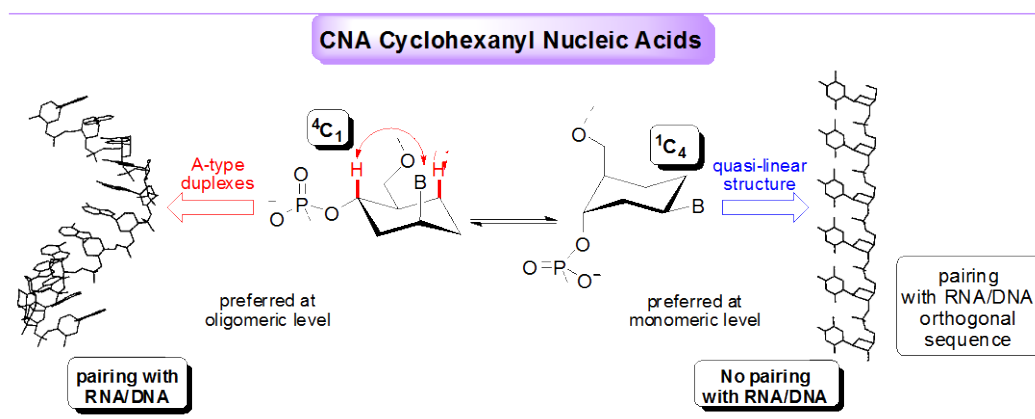


**Figure 7.** Conformation of CNA systems.

The formation of one of the two conformational states may depend on the type of sequence complementary. In fact, it was found that the CNA is able to hybridize with orthogonal complementary sequences (D- and L-oligonucleotides) using the two different conformations of the nucleotide monomer unit.<sup>30</sup> The ability of hybridization of CNA with orthogonal complement represents a rare case of modified oligonucleotide systems studied until now.<sup>7c</sup> If pairing with natural DNA and RNA showed the possible use of CNA in therapeutic systems,<sup>27</sup> its ability to hybridize with orthogonal nucleic acids to natural ones has applications in diagnostic field,<sup>7c</sup> and even in prebiotic chemical experiments.<sup>28</sup>

On the basis of the above and the study of oligonucleotide systems with limited conformational freedom, (in particular of the CNA system), the conformation of the saccharide unit of a nucleotide is very important in the development of efficient and versatile applicability oligonucleotide drugs. However, it still remains to clarify the precise reasons why structural conformational changes, such as modified saccharide unit of the CNA, may determine the pairing of a nucleotide respect to two orthogonal complements. This justifies the conformational studies currently under way in this field, in particular the studies based on nucleic acids having six-membered (pseudo-) saccharide units, carried out in order to make new oligonucleotide systems with remarkable therapeutic potential.

**Cyclohexenyl Nucleic Acids (CeNA).** One of the most effective six-membered MOs is indeed represented by cyclohexenyl nucleic acids (CeNA), a DNA mimic having the deoxyribose replaced by a cyclohexenyl moiety<sup>31</sup> (**Figure 8**). Although this system holds minor flexibility than that of a natural nucleotide (constraints are introduced by the rigid double bond within the six-membered ring), conformational equilibria and thermodynamic parameters of a cyclohexenyl nucleoside [ $\Delta E$  between  $^3H_2$  (*N*-type) and  $^2H_3$  (*S*-type) is 1.8 kJ/mol with a barrier of 10.9 kJ/mol] were very similar compared to a natural ribonucleoside ( $\Delta E$  between *N*-type and *S*-type conformers is 2 kJ/mol with a barrier of 4-20 kJ/mol).<sup>32</sup> The flexibility of the cyclohexenyl nucleotide was further demonstrated by the fast equilibrium between two conformational states adopted when the NA was incorporated in *ds*-DNA sequences.<sup>33</sup>

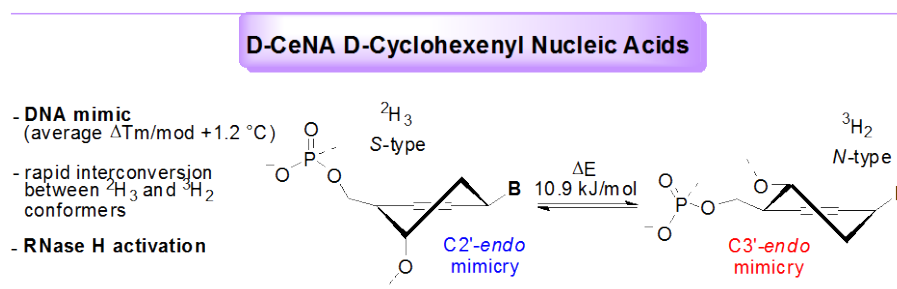


**Figure 8.** Cyclohexenyl Nucleic Acids (CeNA).

CeNA were capable of forming hybrids with natural complements (average  $\Delta T_m/\text{mod} + 1.2\text{ }^\circ\text{C}$ ), CeNA/RNA duplexes being more stable than the corresponding DNA/RNA hybrids.<sup>34</sup> In view of the selective interaction with RNA complements and the preservation of RNaseH recognition of a CeNA:RNA hybrid, CeNA currently represents one of the most promising antisense candidates. Moreover, it has recently been demonstrated that CeNA could be incorporated in siRNA duplexes, with retention of potent biological activity.<sup>35</sup>

The above results highlighted how, among the most relevant examples of conformationally restricted NAs, those bearing a six-membered moiety drew most attention, as they demonstrated to enable precise positioning of functional groups (in ways otherwise thermodynamically disfavored) in recognition events dealing with the development of both efficient NAs and MOs. This justifies the longstanding efforts in the field, as well as the still ongoing studies aimed to explore other six-membered NAs endowed with broad therapeutic activity.

- 
- <sup>1</sup> a) Zamecnik, P.C.; Stephenson, M.L. *Proc. Natl. Acad. Sci. U.S.A.* **1978**, *75*, 280. b) Stephenson, M.L.; Zamecnik, P.C. *Proc. Natl. Acad. Sci. U.S.A.* **1978**, *75*, 285.
- <sup>2</sup> Kurreck, J. "Therapeutic Oligonucleotides", Cambridge, UK: RSC Publishing, **2008**.
- <sup>3</sup> a) Crooke, S.T. Boca Raton, FL: CRC Press, **2008**. b) Bennett, C. F.; Swayze, E.E. *Annu. Rev. Pharm. Tox.* **2010**, *50*, 259-293.
- <sup>4</sup> Buchini, S.; Leumann, C.J. *Curr. Opin. Chem. Biol.* **2003**, *7*, 717-726.
- <sup>5</sup> a) Whitehead, K.A.; Langer, R.; Anderson, D.G. *Nat. Rev. Drug Discov.* **2009**, *8*, 129-138. b) Kurreck, J. *Angew. Chem. Int. Ed.* **2009**, *48*, 1378-1398.
- <sup>6</sup> Krueger, A. T.; Kool, E. T. *Chem. Biol.* **2009**, *16*, 242-248.
- <sup>7</sup> a) Veedu, R.N.; Wengel, J. *Chem. Biodiversity* **2010**, *7*, 536-542. b) Zhang, S.; Switzer, C.; Chaput, J.C. *Chem. Biodiversity* **2010**, *7*, 245-258. c) D'Alonzo, D.; Guaragna, A.; Palumbo, G. *Chem. Biodiversity* **2011**, *8*, 373-413.
- <sup>8</sup> Bell, N.M.; Micklefield, J. *ChemBioChem* **2009**, *10*, 2691-2703.
- <sup>9</sup> Nielsen, P.E. *Chem. Biodiversity* **2010**, *7*, 786-804.
- <sup>10</sup> Thibaudeau, C.; Acharya, P.; Chattopadhyaya, J. *Stereoelectronic effects in nucleosides and nucleotides and their structural implications*. Uppsala University Press; Uppsala, Sweden: **2005**.
- <sup>11</sup> Saenger, W. *Principles in Nucleic Acid Structure*; Springer-Verlag: New York, Berlin, Heidelberg, **1984**. Chapter 9.
- <sup>12</sup> Rich, A.; Zhang, S. *Nat. Rev. Genet.* **2003**, *4*, 566-572.
- <sup>13</sup> Steed, J. W.; Atwood, J. L. *Supramolecular Chemistry (Second Edition)*; John Wiley & Sons, Ltd: Chichester, UK, **2009**.
- <sup>14</sup> Kool, E. T. *Chem. Rev.* **1997**, *97*, 1473-1487.
- <sup>15</sup> Leumann, C.F. *J. Bioorg. Med. Chem.* **2002**, *10*, 841-854.
- <sup>16</sup> Bennett, C.F. Swayze, E. *Ann. Rev. Pharm. Tox.* **2010**, *50*, 259-293.
- <sup>17</sup> Lescrinier, E.; Froeyen, M.; Herdewijn, P. *Nucleic Acids Res.* **2003**, *31*, 2975-2989.
- <sup>18</sup> Herdewijn, P. *Chem. Biodiv.* **2010**, *7*, 1-59.
- <sup>19</sup> Crey-Desbiolles, C.; Ahn, D.R.; Leumann, C.J. *Nucleic Acids Res.* **2005**, *33*, e77.
- <sup>20</sup> a) Herdewijn, P.; Marlière, P. *Chem. Biodiversity* **2009**, *6*, 791-808. b) Appella, D.H. *Curr. Opin. Chem. Biol.* **2009**, *13*, 687-696.

- 
- <sup>21</sup> a) Eschenmoser, A. Chemical Etiology of Nucleic Acid Structure. *Science* **1999**, *284*, 2118-2124. b) Ebert, M.O.; Jaun, B. *Chem. Biodiversity* **2010**, *7*, 103-28.
- <sup>22</sup> a) Hendrix, C.; Rosemeyer, H.; Verheggen, I.; Seela, F.; Van Aerschot, A.; Herdewijn, P. *Chem. Eur. J.* **1997**, *3*, 110-120. b) Kerremans, K.; Schepers, G.; Rozenski, J.; Busson, R.; Van Aerschot, A.; Herdewijn P. *Org. Lett.* **2001**, *3*, 4129-4132.
- <sup>23</sup> Kang, H.; Fisher, M.H.; Xu, D.; Miyamoto, Y. J.; Marchand, A.; Van Aerschot, A.; Herdewijn, P.; Juliano, R.L. *Nucleic Acids Res.* **2004**, *32*, 4411-4419.
- <sup>24</sup> Allart, B.; Khan, K.; Rosemeyer, H.; Schepers, G.; Hendrix, C.; Rothenbacher, K.; Seela, F.; Van Aerschot, A.; Herdewijn, P. *Chem. Eur. J.* **1999**, *5*, 2424.
- <sup>25</sup> a) Fisher, M.; Abramov, M.; Van Aerschot, A.; Xu, D.; Juliano, R. L.; Herdewijn, P. *Nucleic Acids Res.* **2007**, *35*, 1064-1074. b) Fisher, M.; Abramov, M.; Van Aerschot, A.; Rozenski, J.; Dixit, V.; Juliano, R.L.; Herdewijn, P. *Eur. J. Pharmacol.* **2009**, *606*, 38-44.
- <sup>26</sup> a) Abramov, M.; Schepers, G.; Van Aerschot, A.; Van Hummelen, P.; Herdewijn, P. *Biosens. Bioelectron.* **2008**, *23*, 1728-1732. b) Wang, G.; Bobkov, G.V.; Mikhailov, S. N.; Schepers, G.; Van Aerschot, A.; Rozenski, J.; Van der Auweraer, M.; Herdewijn, P.; De Feyter, S. *ChemBioChem* **2009**, *10*, 1175-1185.
- <sup>27</sup> Hossain, N.; Wroblowski, B.; Van Aerschot, A.; Rozenski, J.; De Bruyn, A.; Herdewijn, P. *J. Org. Chem.* **1998**, *63*, 1574-1582.
- <sup>28</sup> Froeyen, M.; Wroblowski, B.; Esnouf, R.; De Winter, H.; Allart, B.; Lescrinier, E.; Herdewijn, P. *Helv. Chim. Acta* **2000**, *83*, 2153.
- <sup>29</sup> Maurinsh, Y.; Rosemeyer, H.; Esnouf, R.; Medvedovici, A.; Wang, J.; Ceulemans, G.; Lescrinier, E.; Hendrix, C.; Busson, R.; Sandra, P.; Seela, F.; Van Aerschot, A.; Herdewijn, P. *Chem. Eur. J.* **1999**, *5*, 2139.
- <sup>30</sup> Froeyen, M.; Morvan, F.; Vasseur, J.J.; Nielsen, P.; Van Aerschot, A.; Rosemeyer, H.; Herdewijn, P. *Chem. Biodivers.* **2007**, *4*, 803.
- <sup>31</sup> Wang, J.; Verbeure, B.; Luyten, I.; Lescrinier, E.; Froeyen, M.; Hendrix, C.; Rosemeyer, H.; Seela, F.; Van Aerschot, A.; Herdewijn, P. *J. Am. Chem. Soc.* **2000**, *122*, 8595-8602.
- <sup>32</sup> Nauwelaerts, K.; Lescrinier, E.; Sclep, G.; Herdewijn, P.; *Nucleic Acids Res.* **2005**, *33*, 2452-2463.

---

<sup>33</sup> Robeyns, K.; Herdewijn, P.; Van Meervelt, L. *Nucleic Acids Res.* **2008**, *36*, 1407-1414.

<sup>34</sup> Wang, J.; Verbeure, B.; Luyten, I.; Lescrinier, E.; Froeyen, M.; Hendrix, C.; Rosemeyer, H.; Seela, F.; Van Aerschot, A.; Herdewijn, P. *J. Am. Chem. Soc.* **2000**, *122*, 8595-8602.

<sup>35</sup> Nauwelaerts, K.; Fisher, M.; Froeyen, M.; Lescrinier, E.; Van Aerschot, A.; Xu, D.; DeLong, R.; Kang, H.; Juliano, R.L.; Herdewijn, P. *J. Am. Chem. Soc.* **2007**, *129*, 9340-9348.

## 4.2 RESULTS AND DISCUSSION

Considering the results discussed in the previous section, during my PhD, an efficient synthetic routes to prepare a new class of carbocyclic nucleic acid, identifiable with acronym “*ribo*-CNA” (*ribo*-configured *D*-Cyclohexanyl Nucleic Acids) has been developed. They were been designed on the basis of structural analogy with CNA and ANA modified oligonucleotides (**Figure 1a-b**). As in the case of ANA (**Figure 1a**), the sugar unit of *ribo*-CNA should be able to mimic the RNA structure locked in its bioactive conformation (*C3'*-endo or <sup>3</sup>E), in order to make MOs able to form stable double and triple helices. As in the case of CNA (**Figure 1b**), it will be evaluated the capacity of *ribo*-CNA to adopt different conformations of saccharidic unit to study the geometric relationships that exist between this latter and the ability of hybridization of corresponding nucleic acid sequences compared to their complementary sequences.

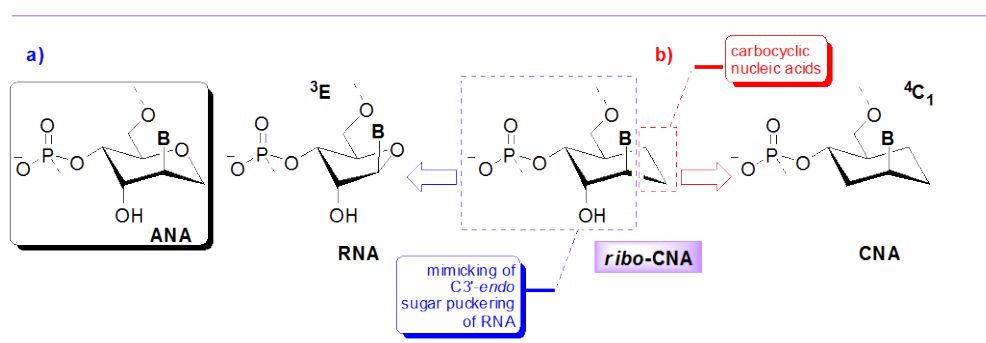
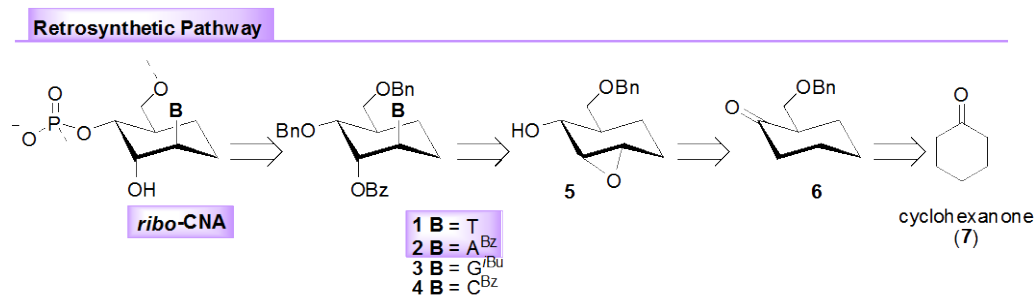


**Figure 1.** *ribo*-CNA, a new class of carbocyclic nucleic acids.

This work concerned the preparation of the nucleosides **1** and **2** (B = T, A<sup>Bz</sup>), through a versatile procedure applicable also for the preparation of the remaining nucleosides **3-4** (B = G<sup>iBu</sup>, C<sup>Bz</sup>, **Scheme 1**). Compounds **1-4** constitute the building blocks for the subsequent oligonucleotide synthesis of *ribo*-CNA, whose ability to form stable double/triple helices with complementary sequences of natural *mRNA* and *dsDNA* will be evaluate.



**Scheme 1.** Nucleoside monomers **1-4**: retrosynthetic path.

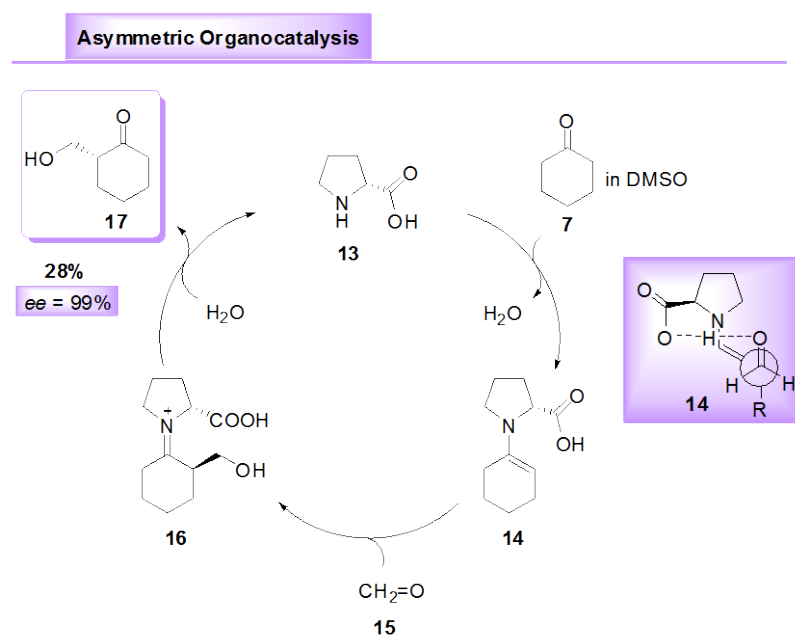
#### 4.2.1 SYNTHESIS OF NUCLEOSIDE UNITS.

The structure of nucleosides **1-4** consists of a six-membered carbocyclic skeleton whose configuration of stereogenic centers mimics the D-altrosie. As indicated by retrosynthetic analysis (**Scheme 1**), the preparation of this compounds can be achieved through an enantioselective synthetic procedure using an economical starting material cyclohexanone (**7**), *via* the intermediates **5** and **6**. The synthesis of the nucleosides **1-2** is described below.

#### SYNTHESIS OF (2*R*)-2-(HYDROXYMETHYL) CYCLOHEXAN-1-ONE (**17**)

The first step of the synthesis is represented by the enantioselective reaction of  $\alpha$ -hydroxymethylation of cyclohexanone (**7**), resulting in the formation of a new chiral center that will determine the steric series (D- or L-) of nucleoside unit target. In particular  $\alpha$ -hydroxymethylation of **7** was conducted through an organocatalytic reaction. It's know that organocatalysis<sup>1</sup> is a branch of asymmetric catalysis in which the catalytic activity, often associated with a high stereoselectivity, uses available commercially organic molecules (such as natural amino acids)<sup>2</sup> or easily synthesized molecules (modified pyrrolidines chiral or monosaccharides derivatives)<sup>3,4</sup> without the use of transition metals. For this reason, organocatalysis associates a significant eco-compatibility and low toxicity of the reagents with a high efficiency and versatility. From a synthetic point of view, organocatalysts commonly act on carbonyl compounds (mainly aldehydes and ketones), leading to generally products of  $\alpha$ -functionalization<sup>5</sup> via aldolic condensation reactions<sup>6</sup> or Mannich reactions.<sup>7</sup>

The organocatalytic procedure<sup>8</sup> used to allow the insertion of hydroxymethyl group on the cyclohexanone (**7**) (**Scheme 2**) involved the use of D-proline, enantiomer of natural L-proline.<sup>i,9</sup> A product with the (*R*) configuration required by the target nucleoside was obtained. Specifically, treatment of a solution of **7** in dimethyl sulfoxide (DMSO), with an aqueous solution of formaldehyde (**15**) and a catalytic amount (10%) of D-proline (**13**) took to the formation, after 16h at room temperature, of alcohol **17**, obtained with complete enantioselectivity (*ee* = 99%), albeit with a modest yield (28%). The mechanism of this reaction involves the initial formation of the enamine intermediate **14**, by reaction of the carbonyl group of **7** with proline **13**, with leakage of a water molecule. The reaction of **14** with the electrophile **15** led to imino intermediate **16**. Finally, the attack of H<sub>2</sub>O established again the carbonyl function, giving the  $\alpha$ -hydroxymethyl cyclohexanone (**17**) (**Scheme 2**).



**Scheme 2.**  $\alpha$ -Hydroxymethylation of cyclohexanone (**7**).

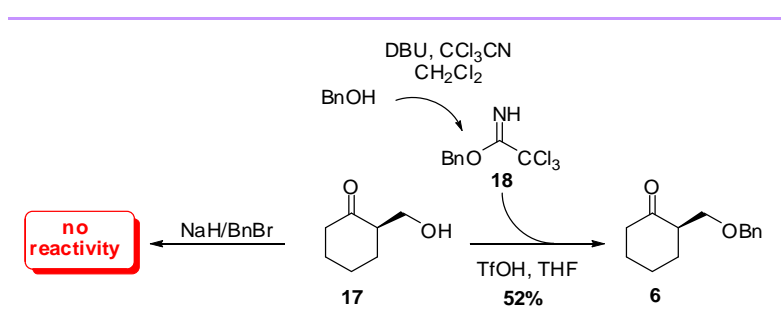
The complete stereoselectivity of this reaction is due to formation of intramolecular hydrogen interaction in enamine intermediate **14**, (**Scheme 2**), the *Re* face of **14** presents more steric hindrance that obstructs a possible nucleophilic attack. The high enantiomeric excess of reaction makes this method particularly useful for our synthetic

<sup>i</sup> Amino acids, especially proline, have taken a leading role because they have been among the best catalysts in this reactions, presenting in the same molecule, the amino group and the carboxyl function; see ref. 1.

purposes, although this reaction is characterized by a low chemical yield (this problem is not important in virtue of the large commercial availability of starting materials).

### SYNTHESIS OF (2*R*)-2-(BENZYLOXYMETHYL) CYCLOHEXAN-1-ONE (6)

The primary alcohol **17** was then protected; over a wide range of protecting groups (*t*-butyldiphenylsilyl- TBDPS; monomethoxy trityl- MMT; *p*-methoxybenzyl- PMB) tested only benzyl group proved to be sufficiently stable in subsequent synthetic transformations and it was hence selected for the protection of primary alcoholic function of **17**. Common conditions of benzylation (NaH/BnBr) did not afford the desired protected compound (**Scheme 3**). On the other hand the use of benzyl-2,2,2-trichloroacetimidate **18** (easily prepared from benzyl alcohol (BnOH), 1,8-diazabicyclo [5,4,0] undecane-7-ene (DBU) and trichloroacetonitrile)<sup>10</sup> and triflic acid (TfOH) gave the desired product **6** with a satisfactory yield (52%; **Scheme 3**).

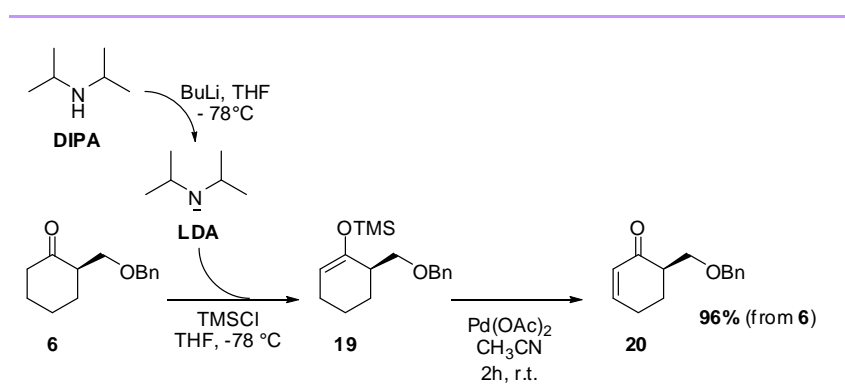


**Scheme 3.** Synthesis of (2*R*)-2-(benzyloxymethyl) cyclohexan-1-one (**6**).

### SYNTHESIS OF (6*R*)-6-(BENZYLOXYMETHYL)-2-CYCLOHEXEN-1-ONE (20)

Benzyl ether **6** was further functionalized with introduction of a double bond in not chiral  $\alpha$ -position, in view of installation of the remaining chiral centers of target nucleoside unit. The preparation of **20** proceeded through the formation of trimethylsilyl enol ether **19**, obtained by treatment of ketone **6** with lithium diisopropylamide (LDA) and trimethylsilyl chloride (TMSCl) in tetrahydrofuran at -78 °C (**Scheme 4**). The reaction was carried out using LDA generated *in situ* by treatment of diisopropylamine (DIPA) with *n*-butyllithium (Buli). The silyl enol ether **19** is not sufficiently stable to be stored, anyway it could be isolated for its <sup>1</sup>H NMR characterization, so it was used directly in subsequent reaction. In particular, treatment of **19** with palladium acetate in

anhydrous acetonitrile led, after 2 h at room temperature, with complete conversion to **20** (96% overall yield starting from **6**).

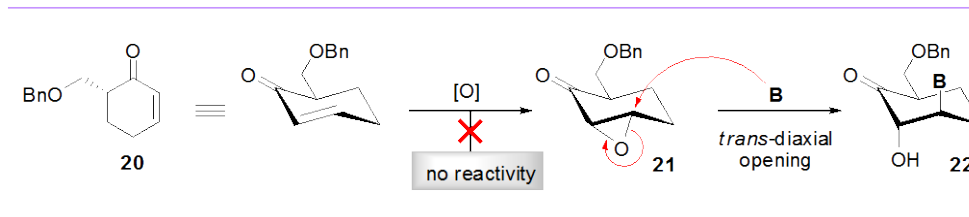


**Scheme 4.** Synthesis of (6*R*)-6-(benzyloxymethyl)-2-cyclohexen-1-one (**20**).

### SYNTHESIS OF (1*A,S*, 2*R*, 3*R*, 5*A,S*)-2-HYDROXY-3-(BENZYLOXYMETHYL)PERHYDRO-1-BENZOXIRENE [SYN-(*ANTI*-5)]

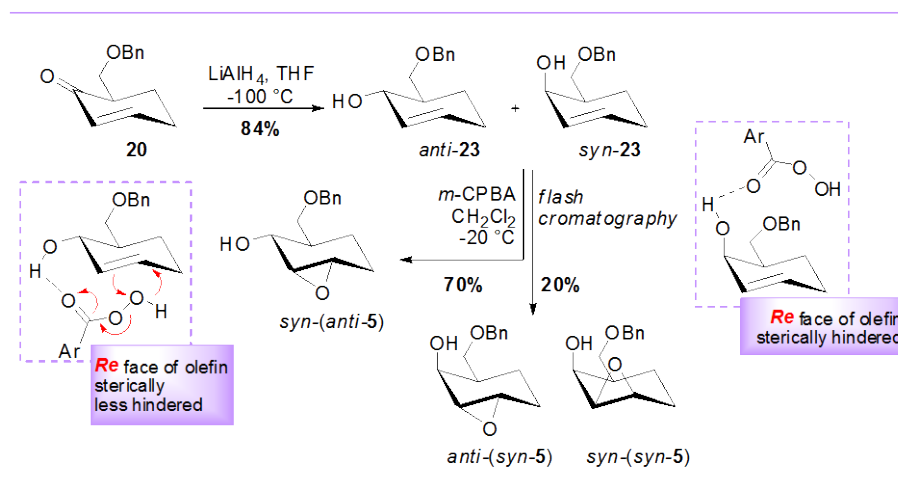
With the compound **20** in hand, the possibility to insert nucleobase exploiting the presence of an electrophilic center on the carbocyclic skeleton was then examined. As reported on similar substrates,<sup>11</sup> the electrophilic center is commonly achieved through the installation of an epoxy function (as in **21**) able to undergo nucleophilic attack by nucleobase, to obtain the desired nucleoside **22** in the right configuration (**Scheme 5**). However, a stereoselective epoxidation reaction is necessary; indeed only the epoxide with appropriate stereochemistry (*anti* to hydroxymethyl group) allow the addition of nucleobase in the desired position and with appropriate axial orientation.

Preliminary tests of epoxidation of **20** were carried out using a wide range of reagents (H<sub>2</sub>O<sub>2</sub>/NaOH, UHP/NaOH, Triton B/H<sub>2</sub>O<sub>2</sub>). However, in all conditions used no satisfactory results were obtained (**Scheme 5**) probably due to the presence of carbonyl group near the chiral center. In fact, under common basic conditions, required for the epoxidation of a  $\alpha,\beta$ -unsaturated ketone, the carbonyl function may be subject to enolization by proton removal on chiral carbon leading to racemization of the substrate and loss of stereoselectivity.



**Scheme 5.** Epoxidation for nucleobase insertion.

On the basis of these considerations, an alternative strategy was chosen. Firstly reduction of the carbonyl group was carried out, and then stereoselective epoxidation of the corresponding allyl alcohol was attempted (**Scheme 6**). The reduction of the carbonyl group of **20** was realized using a wide range of reducing agents ( $\text{NaBH}_4$ ,  $\text{LiAlH}_4$ ,  $\text{Na}(\text{AcO})_3\text{BH}$ ,  $\text{LiBH}_4$ , DIBAL-H, Red-Al,  $\text{Li}(\text{MeO})_3\text{AlH}$ ), to study the most favorable conditions for the stereoselective formation of the required *anti*-product. As recently reported in the literature on similar substrates,<sup>12</sup> best conditions were found by the use of lithium aluminum hydride ( $\text{LiAlH}_4$ ) in anhydrous THF (**Scheme 6**); indeed after 3.5h at  $-100\text{ }^\circ\text{C}$ , a mixture of *anti*-**23** and *syn*-**23** diastereomers was isolated (84% overall yield), with a satisfactory preference for the *anti*-product ( $\text{dr}_{\text{anti/syn}} = 75:25$ ).



**Scheme 6.** Reduction and epoxidation reactions.

Unfortunately, reduction products (*anti*-**23** and *syn*-**23**) were not separable by chromatography: therefore the mixture of diastereoisomers was directly used in the next epoxidation step.

It's known that epoxidation reactions on chiral allylic alcohols with peroxy acids are typically associated to high stereoselectivity of the oxidation process,<sup>13</sup> thanks to the

a hydrogen bond established between the allylic hydroxyl group and peracid, which guides the formation of a single stereoisomer predominantly. Hence, the epoxidation reaction was carried out starting from the mixture of alcohols knowing that four possible diastereoisomeric oxiranes could be obtained. In fact, treatment of alcohols *anti/syn-23* with a slight excess of *m*-chloroperoxybenzoic acid (*m*-CPBA) in anhydrous CH<sub>2</sub>Cl<sub>2</sub> gave, after 3 h at -20 °C, only three epoxides, the *syn-(anti-5)* being the most abundant (70% yield; easily purified by flash chromatography). On the other side, it is reasonable to hypothesize that treatment of *syn-23* with *m*-CPBA has not led to any stereoselectivity, leading to the formation of a 1/1 mixture of *syn-(syn-5)* and *anti-(syn-5)* epoxides (20% yield), due to the steric hindrance of the benzyl ether group on *Re* face which is typically involved in the formation of the epoxy function. (**Scheme 6**).

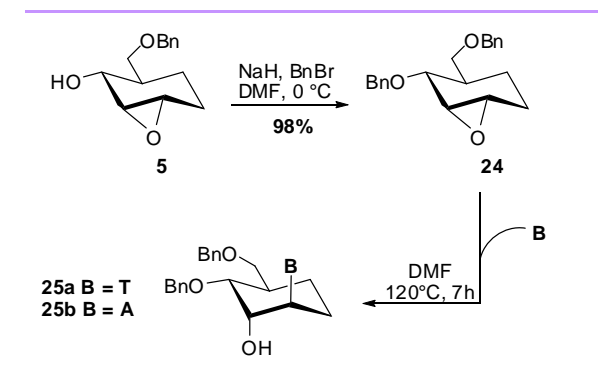
## SYNTHESIS OF CARBOCYCLIC NUCLEOSIDE ANALOGUES 1 AND 2.

At this point our attention was focalized on synthesis of the nucleosides **25a** and **25b** from the most abundant oxirane *syn-(anti-5)* through the steps shown in **Scheme 7**. The alcohol *syn-(anti-5)* was further protected with a benzyl group: in this case the most common benzylation conditions (NaH/BnBr) were suitable to achieve the desired benzyl ether **24** (98%).

The regioselective<sup>14</sup> ring opening of the epoxide **24** with nucleobases was achieved in reasonable yields in the presence of DBU,<sup>ii</sup> affording the desired carbocyclic nucleosides.<sup>15</sup> Indeed, *trans*-diaxial ring opening of **24** with thymine (**T**) and DBU in dry DMF at 120 °C for 7 h afforded protected nucleoside **25a**, in 80% yield, with “*D-altra*” configuration to the newly formed stereogenic centers (**Scheme 7**). Analogously, the reaction of **24** with adenine (**A**), under the same conditions, gave nucleoside **25b** with more satisfactory 90% yield.

---

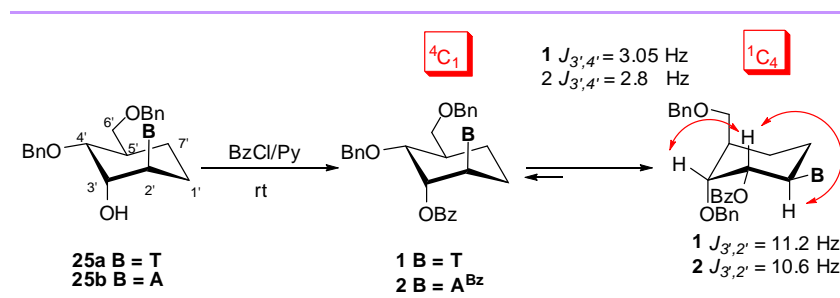
<sup>ii</sup> DBU was preferred to other commonly used bases, such as NaH or LiH, because not strictly anhydrous conditions were required.



**Scheme 7.** Synthesis of nucleosides **25a-b**: *trans*-diaxial ring opening of epoxide **24**.

Finally, protection of hydroxyl function of **25a** using a catalytic amount of 4-dimethylamino pyridine (DMAP) and benzoyl chloride in pyridine for 4h, led to the desired nucleoside **1** with 98% yield. Under the same conditions and through the subsequent *in situ* mono-*N*<sup>6</sup>-debenzoylation (by treatment of reaction mixture with concentrated ammonia) nucleoside **2** was obtained with a satisfactory 95% yield (**Scheme 8**).

It's noteworthy to note that nucleoside **1** and **2** adopt a <sup>1</sup>C<sub>4</sub>-like conformation due to the steric hindrance of 3'-OBz group and the nucleobase in axial position (**Scheme 8**).<sup>iii</sup> Inversion of conformation was verified by coupling constants analysis of <sup>1</sup>H NMR for compounds **1** and **2** which showed a  $J_{3',4'}$  ( $J = 3.05$  Hz),  $J_{3',2'}$  ( $J = 11.2$  Hz) for **1**, and  $J_{3',4'}$  ( $J = 2.8$  Hz),  $J_{3',2'}$  ( $J = 10.6$  Hz) for **2**.



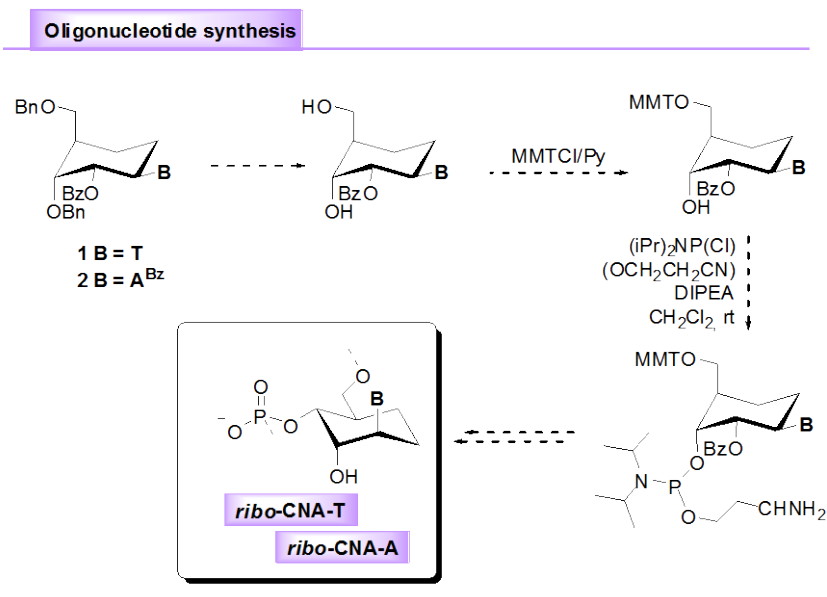
**Scheme 8.** Synthesis of nucleosides **1-2**.

Even though they adopt the <sup>1</sup>C<sub>4</sub> in the form of nucleosides, it's reasonable to hypothesize that the corresponding nucleotides will adopt the <sup>4</sup>C<sub>1</sub> one, because otherwise they should resemble the “forbidden” C2'-*endo* super pucker of RNA.

<sup>iii</sup> Starting from compounds **25a-b**, numbering was attributed on the base of analogy with natural nucleosides.

## 4.2.2 OLIGONUCLEOTIDE SYNTHESIS

Nucleosides **1** and **2** represent the building blocks for the next oligonucleotide synthesis (**Scheme 10**), which will be assembled into oligomers of different sequences, each consisting of 13 nucleotide units, containing the *ribo*-CNA-T, and *ribo*-CNA-A monomers.



**Scheme 10.** Oligonucleotide synthesis by phosphoramidite method.

The stage of nucleoside incorporation into oligomeric sequences,<sup>16</sup> after deprotection of hydroxyl groups in C-4' and C-6' position, will be accomplished by using the common phosphoramidite method<sup>17</sup> on a solid support in laboratories of Professors Piet Herdewijn and Arthur van Aerschot of the Rega Institute for Medical Research, Katholieke Universiteit Leuven (Belgium).

- 
- <sup>1</sup> a) *Chem. Rev.* **2007**, *107*, 5413-5883 (thematic issue: Organocatalysis). b) Berkessel, A.; Gröger, H. *Asymmetric Organocatalysis – From Biomimetic Concepts to Applications in Asymmetric Synthesis*, Wiley-VCH Verlag GmbH & Co. KGaA: Weinheim, **2005**. c) *Enantioselective Organocatalysis, Reactions and Experimental Procedures*, Dalco, P. I. Ed.; Wiley-VCH, Weinheim, **2007**.
- <sup>2</sup> List, B. *Acc. Chem. Res.* **2004**, *37*, 548-557.
- <sup>3</sup> Lelais, G.; MacMillan, D. W. C. *Aldrich. Acta* **2006**, *39*, 79-87.
- <sup>4</sup> Wong, A. O.; Shi, Y. *Chem. Rev.* **2008**, *108*, 3958-3987.
- <sup>5</sup> a) Dondoni, A.; Massi, A. *Angew. Chem., Int. Ed.* **2008**, *47*, 4638-4660. b) Bertelsen, S.; Jørgensen, K. A. *Chem. Soc. Rev.* **2009**, *38*, 2178-2189.
- <sup>6</sup> Northrup, A. B.; MacMillan, D. W. C. *Science* **2004**, *305*, 1752.
- <sup>7</sup> Yang, J. W.; Chandler, C.; Stadler, M.; Kampen, D.; List, B. *Nature* **2008**, *452*, 453-455.
- <sup>8</sup> a) Casas, J.; Sunden, H.; Cordova, A. *Tetrahedron Lett.* **2004**, *45*, 6117-6119; b) Chen, A.; Xu, J.; Chiang, W.; Chai, C. L. L. *Tetrahedron* **2010**, *66*, 1489-1495.
- <sup>9</sup> MacMillan, D. W. C. *Nature* **2008**, *455*, 304.
- <sup>10</sup> Patil, V. J. *Tetrahedron Lett.* **1996**, *37*, 1481-1484.
- <sup>11</sup> D'Alonzo, D.; Van Aerschot, A.; Guaragna, A.; Palumbo, G.; Schepers, G.; Capone, S.; Rozenski, J.; Herdewijn, P. *Chem. Eur. J.* **2009**, *15*, 10121-10131.
- <sup>12</sup> Shan, M.; O'Doherty, G. A. *Org. Lett.* **2010**, *12*, 2986-2989.
- <sup>13</sup> Henbest, H. B.; Wilson, R. A. L. *J. Chem. Soc.* **1957**, 1958.
- <sup>14</sup> Allart, B.; Busson, R.; Rozenski, J.; Van Aerschot, A.; Herdewijn, P. *Tetrahedron* **1999**, *55*, 6527-6546.
- <sup>15</sup> Zhan, T.R.; Ma, Y.D.; Fan, P.H.; Ji, M.; Lou, H.X. *Chemistry & biodiversity*, **2006**, *3*, 1126-1137.
- <sup>16</sup> Herdewijn, P.; Totowa, New Jersey: Humana Press, **2005**.
- <sup>17</sup> Gait, M. *Oligonucleotides: A Practical Approach*, IRL, Oxford, **1984**.

### 4.3 CONCLUSION

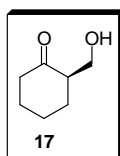
At the beginning of last century, the Nobel prize Paul Ehrlich, medical microbiologist, immunologist and pioneer of chemotherapy, theorized the existence of magic bullets capable of locked the action of toxic substances in infected organisms, reducing dramatically the occurrence of side effects. The advent of gene silencing strategies based on the development of synthetic MOs promises to achieve the specificity and efficacy that Ehrlich thought. This strategies for regulating the expression of a gene results completely selective, and of universal applicability, compared to traditional therapies.

For more than two decades, chemists have explored the chemical space in search for analogs of natural nucleic acids (NAs) endowed with certain desirable properties, such as increased stability against nucleolytic degradation and improved binding affinity toward natural complements. Strong motivations for this research have been the therapeutic promises of antisense, antigene, aptamer, and, in more recent times, RNAi and miRNA strategies. In addition, chemically modified NAs, and particularly those equipped with a sugar moiety in the backbone deviating from the natural D-(deoxy)ribose, have been considered for a plethora of other potential *in vitro* and *in vivo* applications: they have been used, *inter alia*, as chemical probes in NA diagnostics or in the analysis of protein-NA interactions; as (potential) unnatural carriers of genetic information; as building blocks for the assembly of higher-order nanostructures; as synthetic models of alternative basepairing systems, aimed at potentially yielding insights into the origin and uniqueness of DNA and RNA. Over the years, slight modifications of the original furanose moiety or replacement of the five-membered ring with six-membered, bicyclic, tricyclic, or even acyclic structures have been conceived, resulting, in many cases, in excellent candidates for cross-pairing with natural complements.

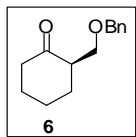
In this work an enantioselective procedure for the synthesis of *ribo*-configured cyclohexanyl nucleic acids starting from economical cyclohexanone **7**, has been conveniently reported. Further experiments aimed to incorporate nucleosides **1** and **2** in oligonucleotide strands, will determine their hybridization aptitude with natural *mRNA* and *dsDNA* sequences.

## 4.4 EXPERIMENTAL SECTION

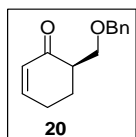
All moisture-sensitive reactions were performed under a nitrogen atmosphere using oven-dried glassware. Solvents were dried over standard drying agents and freshly distilled prior to use. Reactions were monitored by TLC (precoated silica gel plate F254, Merck). Column chromatography: Merck Kieselgel 60 (70-230 mesh); flash chromatography: Merck Kieselgel 60 (230-400 mesh).  $^1\text{H}$  and  $^{13}\text{C}$  NMR spectra were recorded on NMR spectrometers operating on Varian VXR (200 MHz), Bruker DRX (400 MHz) or Varian Inova Marker (500 MHz), using  $\text{CDCl}_3$  solutions unless otherwise specified. In all cases, tetramethylsilane (TMS) was used as internal standard for calibrating chemical shifts ( $\delta$ ). Coupling constant values ( $J$ ) were reported in Hz. Combustion analyses were performed by using CHNS analyzer.



**(2R)-2-(hydroxymethyl) cyclohexan-1-one (17)**. To a solution of cyclohexanone **7** (10.0 g, 0.10 mmol) and (D)-proline **13** (1.2 g 0.01 mmol) in DMSO (120 mL), formaldehyde **15** (4 mL, 0.05 mmol, 37% in  $\text{H}_2\text{O}$ ) was added at room temperature. After 16 h, the reaction mixture was quenched by the addition of brine and extracted with EtOAc. The combined organic extracts were concentrated and the crude product purified by silica gel column chromatography (hexane/ EtOAc 6:4) affording the pure **17** in 28% yield with >99% ee;  $[\alpha]_{\text{D}}^{25} -11.9$  ( $c$  0.41,  $\text{CHCl}_3$ ).  $^1\text{H}$  NMR (200 MHz,  $\text{CDCl}_3$ ):  $\delta$  1.39–1.50 (m, 2H, H-4); 1.56–1.73 (m, 2H, H-5); 1.86–1.92 (m, 1H, OH); 1.97–2.12 (m, 2H, H-3); 2.25–2.41 (m, 2H, H-6); 2.42–2.53 (m, 1H, H-2); 3.57 (dd,  $J_{a,b} = 11.5$ ,  $J_{a,2} = 3.8$ , 1H,  $\text{CHHaOH}$ ); 3.72 (dd,  $J_{b,a} = 11.5$ ,  $J_{b,2} = 7.5$ , 1H,  $\text{CHHbOH}$ ).  $^{13}\text{C}$  NMR (50 MHz,  $\text{CDCl}_3$ )  $\delta$ : 24.9, 27.7, 30.2; 42.4; 52.5, 63.0; 215.0. Anal. calcd for  $\text{C}_7\text{H}_{12}\text{O}_2$ : C, 65.60; H, 9.44. Found: C, 65.38; H, 9.47.

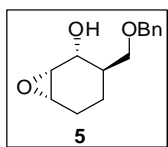


**(2R)-2-(benzyloxymethyl) cyclohexan-1-one (6).** To a solution of **17** (0.5 g, 3.9 mmol) in dry  $\text{CH}_2\text{Cl}_2$  (16 mL)  $\text{BnOC}(\text{NH})\text{CCl}_3$  **18** (1.97 g, 7.8 mmol) in dry THF (3.25 mL) and triflic acid (40  $\mu\text{l}$ , 0.39 mmol) was added at  $-10\text{ }^\circ\text{C}$ . After 2 h to the mixture of reaction  $\text{NaOH}_{\text{aq}}$  (3%) was added. The mixture was washed three times with  $\text{H}_2\text{O}$  extracted with  $\text{CH}_2\text{Cl}_2$  and the organic phase dried on dry  $\text{Na}_2\text{SO}_4$ . The solvent was evaporated under vacuum, crude product obtained was purified by chromatography on silica gel (1:30, hexane/ $\text{Et}_2\text{O}$ , 8:2) to give the pure **6** (0.4 g, 52% yield). Oily;  $^1\text{H}$  NMR (300 MHz,  $\text{CDCl}_3$ ):  $\delta$  1.48-1.52 (m, 2H, H-4), 1.66-1.71 (m, 2H, H-5), 2.07–2.08 (m, 2H, H-3), 2.32–2.38 (m, 2H, H-6), 2.65–2.70 (m, 1H, H-2), 3.46 (dd,  $J_{\text{Ha,Hb}} = 9.50$ ,  $J_{\text{Ha,H-2}} = 7.40$ , 1H,  $\text{CHaHOBn}$ ), 3.86 (dd,  $J_{a,b} = 9.50$ ,  $J_{b,2} = 5.10$ , 1H,  $\text{CHHbOBn}$ ), 4.52 (d,  $J_{a,b} = 11.9$ ,  $\text{CHHaPh}$ , 1H), 4.57 (d,  $J_{b,a} = 11.9$ ,  $\text{CHHbPh}$ , 1H), 7.35 (m, 5H, Arom-H).  $^{13}\text{C}$  NMR (75 MHz,  $\text{CDCl}_3$ ): ppm 24.7, 27.6, 31.4, 42.0, 50.8, 69.3, 73.2, 69.3, 127.4, 127.5, 128.22, 138.3, 211.5. Anal. calcd for  $\text{C}_{14}\text{H}_{18}\text{O}_2$ : C, 77.03; H, 8.31. Found: C, 76.92; H, 8.35.

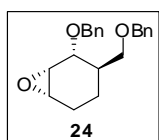


**(6R)-6-(benzyloxymethyl)-2-cyclohexen-1-one (20).** To a stirred solution of DIPA (312  $\mu\text{l}$ , 2.2 mmol) in dry THF (4 mL), at  $-78\text{ }^\circ\text{C}$ ,  $n\text{-BuLi}$  (1.6 M in hexane, 1.81 mL, 1.94 mmol) was added to prepare LDA *in situ*. After 10 min, to the mixture ketone **6** (0.4 g, 1.84 mmol) in dry THF (4 mL) was added. The mixture was stirred for further 30 min at this temperature, and then  $\text{TMSCl}$  (400  $\mu\text{l}$ , 3.13 mmol) was added. After 3 h the solvent was evaporated under reduced pressure and the crude residue was filtered on celite and washed with pentane. To a solution of Silyl enol ether **19** so obtained was in  $\text{CH}_3\text{CN}$  (20 mL)  $\text{Pd}(\text{OAc})_2$  (408 mg, 1.84 mmol) was added. After 2 h the mixture was filtered on celite and eluted with  $\text{CH}_2\text{Cl}_2$ , the eluate was washed with brine. The crude residue purified by chromatography on silica gel gave the pure compound **20** (381 mg, 96% o.y.). Oily;  $^1\text{H}$  NMR (200 MHz,  $\text{CDCl}_3$ ):  $\delta$  1.80-2.06 (m, 2H, H-5), 2.22-2.47, (m, 2H, H-4), 2.56–2.70 (m, 1H, H-6), 3.62 (dd,  $J_{a,b} = 9.52$ ,  $J_{a,2} = 7.57$ , 1H,  $\text{CHaHOBn}$ ), 3.87 (dd,  $J_{a,b} = 9.53$ ,  $J_{b,2} = 4.15$ , 1H,  $\text{CHHbOBn}$ ), 4.53 (s, 2H,  $\text{CH}_2\text{Ph}$ ), 6.52 (dt,  $J =$

1.96,  $J = 2.15$ , 1H, H-3), 6.92-7.01(m, 1H, H-2), 7.28-7.34 (m, 5H, Aromat-H).  $^{13}\text{C}$  NMR (50 MHz,  $\text{CDCl}_3$ ): ppm 23.0, 25.5, 25.9, 26.3, 38.05, 47.4, 61.1, 69.4, 73.5, 127.8, 127.9, 128.6, 130.0, 138.6, 146.7, 150.5, 200.8. Anal. calcd for  $\text{C}_{14}\text{H}_{16}\text{O}_2$ : C, 77.75; H, 7.46. Found: C, 77.65; H, 7.49.

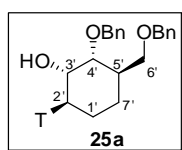


**(1a*S*, 2*R*, 3*R*, 5a*S*)-2-hydroxy-3-(benzyloxymethyl) perhydro 1-benzoxirene (5).** To a stirring solution of **20** (0.02 mg, 0.92 mmol) in dry THF (4.5 mL), at  $-100\text{ }^\circ\text{C}$  under nitrogen atmosphere  $\text{LiAlH}_4$  (9.0 mg, 0.23 mmol) was added. After 3.5h, the mixture was cooled at  $0\text{ }^\circ\text{C}$ , diluted with EtOAc and  $\text{NaHCO}_3$  aq (7.5 mL). After 15', the solution was extracted with EtOAc. The organic phase was dried on  $\text{Na}_2\text{SO}_4$  and evaporated under vacuum. The crude residue, purified by chromatography on silica gel (hexane/EtOAc = 8:2), gave a mixture of alcohols *syn*-**23** e *anti*-**23** (164 mg, 84% yield, *anti*/*syn*:75/25). To a stirred solution of olefins *syn*-**23** e *anti*-**23** (0.10 g, 0.46 mmol) e  $\text{NaHCO}_3$  (40 mg, 0.46 mmol) in dry  $\text{CH}_2\text{Cl}_2$  (3 mL), at  $-20\text{ }^\circ\text{C}$ , under nitrogen atmosphere, *m*-CPBA (0.97 g, 0.46 mmol) was added in one portion. After 3h, the mixture was extracted with  $\text{CH}_2\text{Cl}_2$  and washed with brine. The organic phase was dried on  $\text{Na}_2\text{SO}_4$  and evaporated under vacuum to give a crude residue which was purified by flash chromatography (hexane/ EtOAc = 8:2), affording the pure *syn*-(*anti*-**5**) (82 mg, 70% yield). Oily;  $^1\text{H}$  NMR (300 MHz,  $\text{CDCl}_3$ ):  $\delta$  1.02–1.19 (m, 2H, H-4), 1.35–1.49 (m, 2H, H-5), 1.89-1.90 (m, 2H, H-3, OH), 3.33 (bs, 2H,  $\text{CH}_2\text{OBn}$ ), 3.51 (m, 2H, H-1a, H-5a), 3.95 (d, 1H, H-2), 4.55 (bs, 2H,  $\text{CH}_2\text{Ph}$ ), 7.35 (m, 5H, Arom-H).  $^{13}\text{C}$  NMR (75 MHz,  $\text{CDCl}_3$ )  $\delta$ : 22.2, 23.1, 37.4, 54.7, 56.0, 72.1, 73.1, 73.5, 127.5, 127.6, 128.3, 137.7. Anal. calcd for  $\text{C}_{14}\text{H}_{16}\text{O}_2$ : C, 77.75; H, 7.46. Found: C, 77.65; H, 7.49.

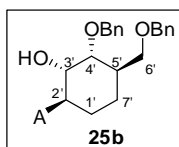


**(1a*S*, 2*R*, 3*R*, 5a*S*)-2-benzyloxy-3-(benzyloxymethyl) perhydro-1-benzoxirene (24).** To a stirred solution of alcohol **5** (0.82 g, 0.35 mmol) in dry DMF (3 mL) at  $0\text{ }^\circ\text{C}$ , under nitrogen atmosphere,  $\text{BnBr}$  (0.72 g, 0.46 mmol) and  $\text{NaH}$  (8.4 mg, 0.35 mmol) were added. After 1.5h, the mixture was extracted with AcOEt and washed with brine. The

organic phase was dried on  $\text{Na}_2\text{SO}_4$  evaporated under reduced pressure. Chromatography of crude residue over silica gel (hexane/EtOAc = 9:1) gave the pure **24** (0.11 g, 98% yield). Oily;  $^1\text{H}$  NMR (300 MHz,  $\text{CDCl}_3$ ):  $\delta$  1.28-1.35 (m, 2H, H-4), 1.58-1.69 (m, 2H, H-5), 1.85-1.95 (m, 1H, H-3), 3.33 (m, 2H, H-1a, H-5a), 3.54 (m, 2H,  $\text{CH}_2\text{OBn}$ ), 3.80 (d,  $J_{2,1a} = 9.5$  Hz, 1H, H-2), 4.46 (d,  $J_{a,b} = 11.9$  Hz, 1H,  $\text{CHaHPh}'$ ), 4.49 (d,  $J_{b,a} = 11.9$  Hz, 1H,  $\text{CHbHPh}'$ ), 4.63 (d,  $J_{a,b} = 11.7$  Hz, 1H,  $\text{CHHaPh}$ ), 4.75 (d,  $J_{b,a} = 11.7$  Hz, 1H,  $\text{CHHbPh}$ ), 7.34 (m, 10H, Arom-H).  $^{13}\text{C}$  NMR (75 MHz,  $\text{CDCl}_3$ ):  $\delta$  22.3, 24.2, 35.9, 53.4, 54.3, 70.5, 70.6, 72.7, 127.2, 127.6, 128.0, 128.1, 138.2, 138.3. Anal. calcd for  $\text{C}_{21}\text{H}_{24}\text{O}_3$ : C, 77.75; H, 7.46. Found: C, 77.64; H, 7.49.

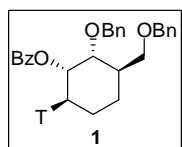


**Compound 25a.** To a solution of epoxyde **24** (0.10 g, 0.31 mmol) in dry DMF (3 mL), under nitrogen atmosphere, thymine (0.89 g, 0.71 mmol) was added at room temperature. After 15 min, to the resulting mixture DBU (0.11 g, 0.71 mmol) was added. The solution was stirred at 120 °C for 7h; after that the solution was cooled at room temperature, extracted with  $\text{CH}_2\text{Cl}_2$  and washed with  $\text{NH}_4\text{Cl}$ . The organic phase dried on  $\text{Na}_2\text{SO}_4$  was evaporated under vacuum to give a crude residue that purified on silica gel (EtOAc/hexane = 1:1) provided the pure **25** (0.12 g, 80% yield). White crystals (from EtOAc);  $^1\text{H}$  NMR (300 MHz,  $\text{CDCl}_3$ ):  $\delta$  1.45-1.99 (m, 7H,  $\text{CH}_3$ , H-1', H-7'), 2.51 (m, 1H, H-5'), 3.57-3.62 (m, 3H, H-4',  $\text{CH}_2\text{OBn}$ ), 3.85-3.95 (m, 1H, H-2'), 3.99 (bs, 1H, H-3'), 4.49-4.73 (m, 4H,  $2 \times \text{CH}_2\text{Ph}$ ), 6.77 (s, 1H, H-6), 7.36 (m, 10H, Arom-H), 8.54 (s, 1H, NH).  $^{13}\text{C}$  NMR (75 MHz,  $\text{CDCl}_3$ ):  $\delta$  12.3, 22.2, 25.9, 29.6, 36.4, 69.3, 71.0, 71.7, 73.5, 79.8, 110.5, 127.7, 127.9, 128.4, 128.5, 137.2, 137.7, 137.8, 151.4, 163.2. Anal. calcd for  $\text{C}_{26}\text{H}_{30}\text{N}_2\text{O}_5$ : C, 69.31; H, 6.71; N, 6.22. Found: C, 69.18; H, 6.74; N, 6.25.

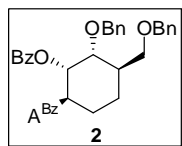


**Compound 25b.** Under the same conditions used to prepare nucleosides **25a**, compound **25b** was obtained in 90% yield. White crystals (from EtOAc);  $^1\text{H}$  NMR (300 MHz,  $\text{CD}_3\text{OD}$ ):  $\delta$  1.66-1.70 (m, 2H, H-7'), 1.83-2.11 (m, 4H,  $\text{CH}_3$ , H-1'), 2.52 (m, 1H,

H-5'), 3.65-3.78 (m, 2H, CH<sub>2</sub>OBn), 4.00 (bs, 1H, H-4'), 4.47 (dd,  $J_{3'-4'} = 3.1$ ,  $J_{3'-2'} = 10.6$ , 1H, H-3'), 4.56 (s, 2H, CH<sub>2</sub>Ph'), 4.58-4.78 (m, 3H, H-2', CH<sub>2</sub>Ph'), 7.28-7.45 (m, 10H, Arom-H), 8.05 (s, 1H, H-8), 8.14 (s, 1H, H-2). <sup>13</sup>C NMR (75 MHz, CD<sub>3</sub>OD):  $\delta$  12.1, 20.9, 22.0, 26.3, 28.7, 29.0, 31.3, 36.9, 56.9, 68.6, 69.4, 71.6, 72.4, 78.8, 118.7, 126.9, 127.0, 127.2, 127.4, 127.6, 127.7, 138.1, 138.4, 140.5, 149.3, 151.5, 155.4. Anal. calcd for C<sub>26</sub>H<sub>29</sub>N<sub>5</sub>O<sub>3</sub>: C, 67.95; H, 6.36; N, 15.24. Found: C, 67.82; H, 6.39; N, 15.30.



**Compound 1.** To a stirring solution of **25a** (0.10 g, 0.23 mmol) in dry pyridine (1 mL), benzoyl chloride (276  $\mu$ L) and a catalytic amount of DMAP (10%) were added at room temperature. After 4 h the TLC showed the complete formation of final product. The solvent was evaporated under vacuum and the crude residue was extracted with EtOAc and washed with brine. Purification by chromatography over silica gel (EtOAc/hexane = 1:1) gave the pure **1** (98% yield). White crystals (from EtOAc); <sup>1</sup>H NMR (300 MHz, CDCl<sub>3</sub>):  $\delta$  1.72 (s, 4H, CH<sub>3</sub>), 1.77-1.80 (m, 1H, H-7'), 1.86-1.90 (m, 2H, H-1'), 2.37 (bs, 1H, H-5'), 3.66-3.68 (m, 2H, CH<sub>2</sub>OBn), 4.15 (bs, 1H, H-4'), 4.55-5.58 (m, 4H, CH<sub>2</sub>Ph'), 5.16 (s, 1H, H-2'), 5.62 (dd,  $J_{3'-4'} = 3.05$ ,  $J_{3'-2'} = 11.2$ , 1H, H-3'), 6.87 (d, 1H,  $J_{6-5} = 1.15$ , H-6), 7.28-7.56 (m, 11H, Arom-H), 7.66 (d,  $J = 8.25$ , 2H, Arom-H) 7.98 (d,  $J = 8.25$ , 2H, Arom-H). <sup>13</sup>C NMR (75 MHz, CDCl<sub>3</sub>):  $\delta$  11.95, 21.9, 26.4, 38.2, 71.1, 72.1, 72.3, 73.5, 110.4, 127.2, 127.6, 127.9, 128.1, 128.2, 128.3, 129.1, 129.4, 129.8, 133.0, 133.1, 137.7, 137.9, 150.8, 163.3, 165.4. Anal. calcd for C<sub>33</sub>H<sub>34</sub>N<sub>2</sub>O<sub>6</sub>: C, 71.46; H, 6.18; N, 5.04. Found: C, 71.58; H, 6.16; N, 5.03.



**Compound 2.** To a stirring solution of **25b** (0.1 g, 0.21 mmol) in dry pyridine (1 mL), benzoyl chloride (274  $\mu$ L) and a catalytic amount of DMAP (10%) was added at room temperature. After 3h concentrated ammonia (0.1 mL), was added to afford selective N<sup>6</sup>-monodebenzoylation. After stirring for 1 h at 0 °C the solvent was removed under reduced pressure and residue coevaporated three times with toluene. Chromatography of crude residue over silica gel (EtOAc) gave the pure nucleoside **2** (95% yield). White

crystals (from EtOAc);  $^1\text{H}$  NMR (300 MHz,  $\text{CDCl}_3$ ):  $\delta$  1.12-1.43 (m, 2H), 1.44-1.85 (m, xH) 2.07-2.22 (m, xH), 2.58 (m, 1H, H-5'), 3.64-3.81 (m, xH, H-6'), 4.25 (bs, 1H, H-4'), 4.59-4.69 (m, 2H,  $\text{CH}_2\text{Ph}$ ), 5.24 (dt,  $J = 4.2$ ,  $J = 11.6$ , 1H, H-2'), 5.91 (dd,  $J_{3'-4'} = 2.8$ ,  $J_{3'-2'} = 10.6$ , 1H, H-3'), 7.16-7.25 (m, xH, Arom-H), 7.30-7.57 (m, xH, Arom-H), 7.79 (d,  $J = 8.2$ , 2H, Arom-H), 7.92 (s, 1H, H-8), 8.00 (d,  $J = 8.2$ , 2H, Arom-H), 8.78 (s, 1H, H-2), 9.05 (s, 1H, NH).  $^{13}\text{C}$  NMR (75 MHz,  $\text{CDCl}_3$ ):  $\delta$  12.3, 22.2, 25.9, 29.6, 36.4, 69.3, 71.0, 71.7, 73.5, 79.8, 110.5, 127.7, 127.9, 128.4, 128.5, 137.2, 137.7, 137.8, 151.4, 163.2. Anal. calcd for  $\text{C}_{40}\text{H}_{37}\text{N}_5\text{O}_5$ : C, 71.95; H, 5.58; N, 10.49. Found: C, 71.85; H, 5.60; N, 10.53.